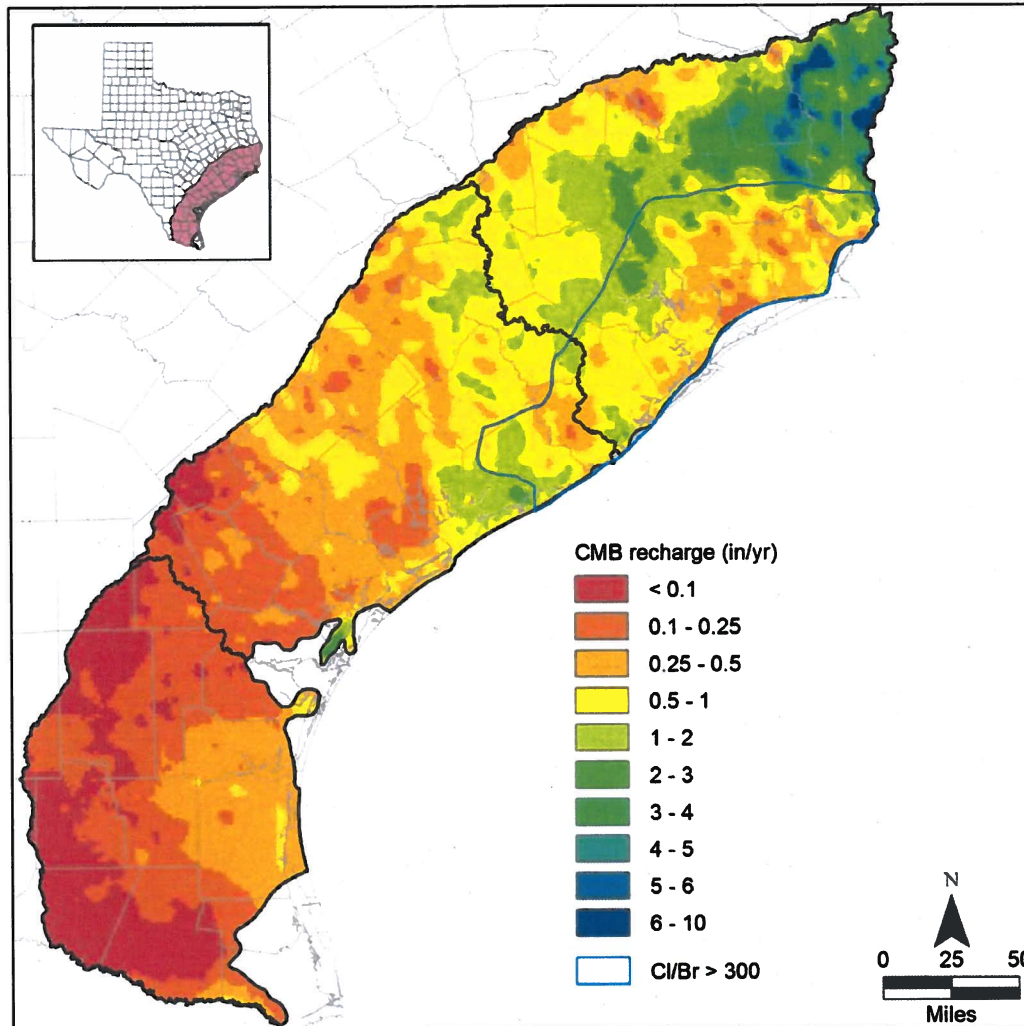


Estimation of Groundwater Recharge to the Gulf Coast Aquifer in Texas, USA



Final Contract Report
to
Texas Water Development Board

Bridget R. Scanlon, Robert Reedy, Gil Strassberg, Yun Huang, and Gabriel Senay*
Bureau of Economic Geology, Jackson School of Geosciences, University of
Texas at Austin

*US Geological Survey, Sioux Falls, South Dakota

2012 JUL 26 PM 1:56
CONTRACT ADMINISTRATION


0904831001
UT-BEG_Final Report

Geoscientist Seal

The contents of this report (including figures and tables) document the work of the following licensed Texas geoscientists:

Bridget Scanlon, Ph.D., P.G. No. 1645

Dr. Scanlon was responsible for the introductory material and parts of the methods and discussion. The seal appearing on this document was authorized October 31, 2011, by



Bridget Scanlon



Robert C. Reedy, P.G. No. 4038

Mr. Reedy was responsible for project field work, data analysis, and parts of the methods and discussion. The seal appearing on this document was authorized October 31, 2011, by



Robert C. Reedy

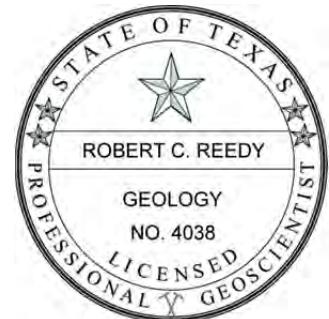


Table of Contents

| | |
|--|----|
| Executive Summary | 1 |
| Introduction | 2 |
| Materials and Methods..... | 4 |
| Study Area..... | 4 |
| General Information | 4 |
| Geology | 5 |
| Recharge Rates from Previous Studies..... | 8 |
| Methods..... | 10 |
| Estimation of Evapotranspiration | 10 |
| Theory of Recharge Estimation Approach..... | 12 |
| Estimation of Recharge Rates | 13 |
| Results and Discussion..... | 19 |
| Evapotranspiration | 19 |
| Regional Recharge Rates from Groundwater Chloride data..... | 19 |
| Relationships between Precipitation, Soil Texture, and Land Use with CMB Recharge..... | 21 |
| Regional Recharge Rates from Water Table Fluctuations | 22 |
| Local Recharge Rates from Unsaturated Zone Profiles..... | 22 |
| Regional Recharge Rates from Streamflow Hydrograph Separation..... | 24 |
| Comparison of Recharge Rates from Different Approaches | 25 |
| Summary..... | 25 |
| Acknowledgments..... | 26 |
| References..... | 28 |

List of Tables

| | |
|---|----|
| Table 1. Monthly and annual mean total PET from TexasET network..... | 31 |
| Table 2. Monthly and annual mean total PET from NSRDB network. | 31 |
| Table 3. Unsaturated zone borehole data..... | 32 |
| Table 4. Groundwater well water level hydrograph analysis results | 33 |
| Table 5. Borehole sample analysis results summary..... | 34 |
| Table 6. Borehole chloride mass balance (CMB) recharge flux results summary. | 35 |
| Table 7. Recharge estimates based on stream baseflow separation analysis | 36 |
| Table 8. Recharge estimates based on stream baseflow separation analysis | 37 |

List of Figures

| | |
|---|----|
| Figure 1. Mean annual precipitation..... | 38 |
| Figure 2. Distribution of mean monthly total precipitation | 39 |
| Figure 3. Mean annual temperature..... | 40 |
| Figure 4. Distribution of soil clay content | 41 |
| Figure 5. Distribution of land use / cover | 42 |
| Figure 6. Surface geology map..... | 43 |
| Figure 7. Stratigraphic and hydrostratigraphic classification..... | 44 |
| Figure 8. Relationship between chloride deposition and distance from coastline..... | 45 |
| Figure 9. Estimated distribution of chloride in bulk precipitation | 46 |
| Figure 10. Location of unsaturated zone boreholes..... | 47 |
| Figure 11. Mean annual actual ET | 48 |
| Figure 12. Annual actual ET | 49 |
| Figure 13. Mean monthly actual ET | 50 |
| Figure 14. Distribution of groundwater chloride concentrations..... | 51 |
| Figure 15. Distribution of groundwater Cl/Br ratios | 52 |
| Figure 16. Distribution of groundwater Cl/SO ₄ ratios | 53 |
| Figure 17. Distribution of groundwater CMB recharge rates..... | 54 |
| Figure 18. Distribution of CMB recharge as a percentage of precipitation | 55 |
| Figure 19. Distribution of groundwater NO ₃ -N | 56 |
| Figure 20. Probability of groundwater NO ₃ -N > 2 mg/L..... | 57 |
| Figure 21. Relationship between UZ chloride CMB percolation rate. | 58 |
| Figure 22. Unsaturated zone profiles..... | 59 |
| Figure 23. Unsaturated zone profiles..... | 60 |
| Figure 24. Example flow duration curves..... | 61 |
| Figure 25. Baseflow separation example..... | 62 |
| Figure 26. Distribution of BFI recharge rates | 63 |
| Figure 27. Relationship between CMB recharge and BFI recharge | 64 |

Executive Summary

Quantifying groundwater recharge is essential for managing water resources in aquifers. The objective of this study was to quantify spatial variability in recharge in the outcrop zones of the Gulf Coast aquifer in Texas. Regional recharge was estimated using the chloride mass balance approach applied to groundwater chloride data from the TWDB database in 10,530 wells, which represented the most recent samples from wells located in the region. Regional groundwater recharge was also estimated using streamflow hydrograph separation in 59 watersheds using USGS unregulated gage data. Recharge was also estimated by applying the chloride mass balance approach to unsaturated zone chloride data from 27 boreholes that represented a range of precipitation, land use, and soil texture settings in the central and southern Gulf Coast regions.

Groundwater chloride concentrations generally decrease from the southern to the northern Gulf Coast, qualitatively indicating increasing recharge in this direction with increasing precipitation. Ratios of chloride to bromide are < 150 to 200 throughout most of the Gulf Coast, suggesting a predominantly meteoric source for groundwater chloride. Recharge rates based on the chloride mass balance approach range from <0.1 in/yr in the south to 10 in/yr in the north, correlated with increasing precipitation. Stream flow ranges from ephemeral in parts of the southern Gulf Coast to perennial throughout the rest of the Gulf Coast based on flow duration curves. Hydrograph separation using Base-Flow Index (BFI) showed that recharge increased from south to north, similar to increases in recharge based on groundwater chloride data. Unsaturated zone profiles show high local variability in chloride concentrations, with mean concentrations below the root zone ranging from 7 to 10,200 mg/L. Resultant percolation rates below the root zone based on the chloride mass balance approach range from <0.1 to 6.8 in/yr. In some areas, variations in percolation rates are related to differences in soil texture whereas in other regions, they are related to differences in land use. However, there is no systematic variation in percolation rates throughout the region, unlike the trends in recharge with regional precipitation from groundwater chloride data and stream hydrograph separation.

Recharge rates based on groundwater chloride data can be considered to provide a conservative lower bound on actual recharge because many processes can add chloride to the system, resulting in lower recharge rates whereas there are no processes that can remove chloride from the system in the Gulf Coast. Stream hydrograph separation provides recharge rates in contributing basins that do not cover the entire Gulf Coast region. Recharge estimates from the chloride mass balance applied to groundwater and perennial stream hydrograph separation are highly correlated ($r = 0.96$) and differences between these two sets of recharge

estimates can be used to evaluate uncertainties in recharge rates in contributing basins to the stream gages. Recharge rates from groundwater chloride and streamflow hydrograph separation can be used to provide a range of recharge rates for future groundwater models of the Gulf Coast aquifer.

Introduction

Recharge is critical for estimating groundwater availability. Most models used to simulate groundwater availability require recharge rates as input and often calibrate the models by varying the recharge rates (Chowdhury and Mace, 2003; Chowdhury et al., 2004; Kasmarek and Robinson, 2004). The Gulf Coast aquifer is typical of dipping confined aquifers found along the Gulf Coast. Conceptual models of recharge in these aquifers generally include local and intermediate flow systems in the outcrop zones and regional flow systems into the deeper confined portions of the aquifers, based on Toth's original conceptual model (Toth, 1963). Much of the recharge occurring in local and intermediate flow systems discharges to streams, sometimes referred to as "rejected recharge". The remaining recharge moves downdip into confined aquifers and is sometimes termed "deep recharge".

Recharge can be derived from a variety of sources, including precipitation, irrigation return flow, and stream flow. In the Gulf Coast system, precipitation is the dominant source of recharge in the outcrop zones. Irrigation is mostly sourced by surface water near the Rio Grande and Colorado River, and return flow in these regions provides an additional source of groundwater recharge. Groundwater is also used for irrigation, primarily in Wharton and Matagorda counties near the Colorado River; however, return flow from groundwater-fed irrigation is simply recycling of water. Streams in the southern Gulf Coast are generally ephemeral and recharge the aquifer also.

Primary controls on recharge include precipitation, soil texture, and vegetation. To assess the maximum potential recharge in a region, Keese et al. (2005) simulated recharge using local climatic forcing (1961 – 1990 data) in sandy soil. Because finer textured soils, layering of soils, and vegetation all reduce recharge, omitting these in the simulations should result in the maximum potential recharge in response to climate forcing. Maximum recharge rates ranged from 50% of precipitation in Starr county in the south, 54% in Victoria County in the central region, and 60% in Liberty county in the north. These recharge estimates provide an upper bound on recharge in the system. Adding layered soils based on data from SSURGO reduced these recharge rates as a percentage of precipitation to 29% (Starr county), 10% (Victoria county), and 19% (Liberty county). Vegetation further reduced recharge rates to 5% (Starr

county), 3% (Victoria county), and 10% (Liberty county). These simulations provide an indication of the relative importance of different controls on recharge rates. Many studies have shown that cultivating land can exert an important control on groundwater recharge (Scanlon et al., 2007). However, reconstructing past land use is difficult because records generally only extend back to the 1950s or 1960s (National Agricultural Statistics Services, Texas Agricultural Statistics Services).

A variety of techniques are available for estimating recharge. Techniques vary in the space/time scales covered, range of recharge rates that can be estimated, and reliability of recharge (Scanlon et al., 2002). Recharge rates for assessing groundwater availability generally require techniques that cover large spatial scales and decadal timescales. The range of recharge rates that can be estimated using different approaches varies. Depending on the level of *a priori* information on recharge rates in a region, it may be difficult to match appropriate techniques to actual recharge rates and an iterative approach may be required with reconnaissance estimates initially followed by more detailed studies. Recharge estimates based on different techniques vary in the reliability of their estimates. Potential recharge rates can be derived from surface-water and unsaturated-zone techniques, whereas actual recharge rates are based on groundwater data. Techniques for estimating recharge can be categorized as physical, chemical, and modeling techniques, and according to the source of data, including surface water, unsaturated zone, and groundwater (Scanlon et al., 2002). Water budgets are widely applied to develop a conceptual understanding of recharge in a system. However, recharge rates based on water budgets may have large uncertainties. Assuming a simplified system where the components of the water budget can be estimated within $\pm 10\%$ and using the following values results in $(P (40 \pm 4 \text{ in/yr}) - \text{Roff} (4 \pm 0.4 \text{ in/yr}) - \text{ET} (33 \pm 3.3 \text{ in/yr}) = R (3 \pm 5 \text{ in/yr})$. This calculation shows that the resultant recharge estimate has an uncertainty of 170%. Groundwater recharge can also be evaluated by examining groundwater discharge as baseflow to streams through hydrograph separation, using codes such as baseflow index (BFI) (Wahl and Wahl, 1995). The reliability of recharge estimates from streamflow hydrograph separation depends on the validity of the assumption that most baseflow equates to groundwater discharge. However, groundwater also discharges through pumpage and evapotranspiration while bank storage and wetlands can also contribute additional flow to the system during low flow periods (Halford and Mayer, 2000). However, previous analyses suggest that recharge estimates based on BFI may overestimate actual recharge rates because of impacts of bank storage (Halford and Mayer, 2000). Groundwater table fluctuations are also used to quantify recharge (Healy and Cook, 2002). The most widely used environmental tracer for recharge

estimation is chloride, which can be used with groundwater or unsaturated zone chloride data. However, other stable and radioactive isotopes can also be used. Because recharge is difficult to estimate, it is important to apply as many different approaches as possible to constrain uncertainties.

There are certain issues that should be considered with respect to recharge for groundwater models. Because most groundwater models are only calibrated with hydraulic head data, these models can only estimate the ratio of recharge to hydraulic conductivity (R/K); therefore, reliability of recharge estimates from models depends on the accuracy of hydraulic conductivity data. The entire water budget is important for groundwater availability analysis. In some cases, high recharge rates are simulated during predevelopment, i.e. before large scale pumpage. Heads are matched by discharging most of the groundwater as ET and baseflow to streams. While this approach may not be a problem for predevelopment conditions, groundwater pumpage during aquifer development may capture water that was previously discharged as ET and this approach may overestimate water availability during development. Therefore, knowledge of ET is also important.

The objective of this study was to quantify spatial variability in recharge in the outcrop areas of the Gulf Coast aquifer. Unique aspects of the study include application of different approaches to estimate recharge, primarily chloride mass balance applied at regional groundwater scales and local unsaturated zone scales and streamflow hydrograph separation applied to streamflow gages, representing recharge to contributing groundwater basins. Comparison of recharge estimates from the different techniques provides information on the reliability of the recharge estimates. This study should significantly advance our understanding of recharge to the Gulf Coast aquifer. Quantitative estimates of recharge will improve reliability of future groundwater availability models of these aquifers.

Materials and Methods

Study Area

General Information

The Gulf Coast aquifer area is subdivided for the purposes of this study into three zones (southern, central, and northern) because of the large variability of climate conditions and other factors. The southern region is bounded by the Rio Grande River and the Nueces River, The central region is bounded by the Nueces River and the Brazos River, and the northern region is bounded by the Brazos River and Sabine River (Figure 1). The climate in the Gulf Coast ranges from subtropical subhumid to subtropical humid (Larkin and Bomar, 1983) with mean annual

precipitation ranging from 21 to 62 in/yr (1971 – 2000; PRISM www.prism.oregonstate.edu) (Figure 1). Median annual precipitation is 26 in/yr in the southern region, 41 in/yr in the central region, and 53 in/yr in the northern region. The seasonal distribution in precipitation is dominated by precipitation from March through October in the southern and central regions whereas precipitation remains relatively high through the winter in the northern region (Figure 2). Precipitation is double peaked in the south and central region with peaks in May-June and September, whereas precipitation in the north is dominated by a peak in June. Winters are generally drier (20-30% of annual precipitation Nov–Feb). Precipitation is derived primarily from the Gulf of Mexico in the summer. Hurricanes from the Gulf of Mexico frequently result in heavy precipitation in the summer and early fall. In the winter, Pacific and Canadian air masses bring limited to moderate precipitation. Mean annual temperature decreases from 74°F in the south to 64°F in the north (Figure 3; PRISM 1971 – 2000).

Soil clay content in the Gulf Coast ranges from < 15% to 78% (Figure 4; SSURGO, USDA 1995). Soils are generally coarser grained in the south. More clay rich soils are found in the central and northern regions, primarily near the coast. Another band of finer grained soils is found near the inland margin in the central and northern regions of the Gulf Coast aquifer.

Current land use includes grass/pasture (31%), shrubland (18%), water/wetlands (17%), forest (12%), crops (12%) and developed areas (9%) (Figure 5; USGS National Land Cover Data, 2001). The distribution of these different land use/land cover types varies, with predominantly shrubland, grassland and cropland in the southern region, cropland, forest, and water/wetlands in the central region, and urban, forest, and water in the north. EPA has also defined ecoregions for the Gulf Coast, that include the Lower Rio Grande Alluvial Floodplain, Lower Rio Grande Valley, Coastal Sand Plain, Southern Subhumid and Northern Humid Gulf Coastal Prairies, floodplains and low terraces along the rivers, and flatwoods in the north (Griffith et al., 2004).

Geology

The geology of the different aquifers is summarized in Figures 6 and 7. The Gulf Coast aquifer consists of interbedded sands, silts, and clays of fluvial and marine origin (Ashworth and Hopkins, 1995). The hydrogeologic units crop out parallel to the coast and thicken downdip. The correspondence between the hydrogeologic and stratigraphic units is derived from Baker (1979) and the ages of the formations are based on Galloway et al. (2000).

The Gulf Coast aquifer deposits are underlain by sediments deposited from shallow inland seas during the Cretaceous that formed broad continental shelves covering most of Texas. In

the Tertiary (starting 65 million years ago), the Rocky Mountains to the west started rising, and large river systems flowed toward the Gulf of Mexico, carrying abundant sediment, similar to today's Mississippi River. Most of Texas, particularly west Texas, was also uplifted, generating a local sediment source. Six major progradational events occurred where sedimentation built out into the Gulf Coast Basin. These progradational sequences include the most recent Vicksburg-Catahoula-Frio, Oakville-Fleming, and Plio-Pleistocene sand-rich wedges. Hydrostratigraphic units are defined in terms of flow (i.e., in terms of "shales" vs. "sands") and do not necessarily correspond to stratigraphic units which are defined in terms of age (Figure 7). The Gulf Coast aquifer system includes three main aquifers: the Jasper, Evangeline, and Chicot aquifers that broadly correspond to the Oakville Sandstone, the Goliad Sand, and Quaternary units, respectively. The Fleming Fm. is a confining unit between the Jasper and Evangeline aquifers and is named the Burkeville confining unit.

The component geologic units of the Gulf Coast aquifer are, from oldest to youngest, (1) Catahoula Fm., (2) Oakville Sandstone/Fleming Fm., (3) Goliad Fm., (4) Pleistocene formations (Willis Fm., Lissie Fm., and Beaumont Fm.), and (5) Quaternary terrace deposits and alluvium (Doering, 1935; Baker, 1979).

Catahoula (Gueydan) Formation is equivalent to the Catahoula Confining System. The Catahoula Fm. has a different lithology and provenance in the southwestern Gulf Coast than it does in the northeastern Gulf Coast. Baker (1979) noted that this unit is referred to as Catahoula Tuff in the southwest and Catahoula Sandstone to the northeast of the Colorado River, where it contains more sand and less volcanic material than in the southwest. In the southwest the Catahoula/Gueydan formations are unconformably overlain by either the Oakville Fm. or the Goliad Fm., whereas in the northeast they are overlain by the Fleming Fm. (Aronow et. al., 1987; Shelby et. al., 1992). Galloway (1977) described the Catahoula Fm. as being deposited by two separate fluvial systems, Gueydan in the southwest and Chita-Corrigan in the northeast parts of the Gulf Coast. The Gueydan bedload fluvial system was deposited in the Rio Grande embayment. The Chita-Corrigan mixed-load fluvial system was deposited in the Houston Embayment. Both depositional systems contain volcanic ash; however, Galloway (1977) cites differences in alteration clay minerals as evidence that Gueydan deposition occurred in an arid environment, whereas the depositional environment of Chita-Corrigan was more humid.

Oakville Sandstone/Fleming Formations – These two units are commonly grouped because they are both composed of varying amounts of interbedded sand and clay. In the central part of the Gulf Coast (Brazos River to central Duval County) they are easily recognized as

stratigraphically adjacent units because the Oakville is sand-rich and the Fleming is more clay-rich. To the northeast of the Brazos River, the two units are indistinguishable. Baker (1979, 1986) assigned the Miocene Oakville/Fleming geologic units to the Jasper aquifer, which has been best characterized along the northeastern Texas Gulf Coast, north of the Brazos River. Galloway et al. (1982) described the Oakville in the southwest Gulf Coast as a sand-rich fluvial system overlying the Catahoula Fm. They associated the Oakville Sandstone with the Jasper aquifer and stated that the Evangeline aquifer includes most of the Fleming Fm.

Goliad Formation – The Goliad Fm. is only present at surface as far as Lavaca County, just south of the Colorado River as seen on the Seguin GAT sheet (Proctor et. al., 1974) and is absent farther to the northeast (not present on the Beaumont GAT sheet (Shelby et. al., 1992)). The Goliad Fm. was deposited during the Pliocene or as recently as 5 Ma. Hoel (1982) found the Goliad Fm. to be genetically and compositionally similar to the underlying Oakville and Catahoula formations as they exist in the southwest Gulf Coast. Hoel (1982) noted a distinct change in character of the Goliad Fm. along a line perpendicular to the coast, just north of the Nueces River roughly coincident with the San Patricio-Refugio county line. Southwest of this line the Goliad Fm. was deposited by rivers carrying bed load or very coarse sediments containing a large proportion of orthoclase and plagioclase feldspar crystals and volcanic rock fragments from a “distant western source.” Northeast of this line the rivers carried finer grained sediments composed primarily of calc-lithic particles presumably derived from Edwards Plateau rocks of central Texas.

The Evangeline aquifer is composed of water-bearing zones primarily within the Goliad Sand and secondarily in underlying portions of the Fleming Fm. (Ryder and Ardis, 1991) The Goliad Sand is only identified as an aquifer unit in the TWDB well database within and to the south and west of Lavaca and Jackson counties. However, the Evangeline aquifer is present throughout the Gulf Coast aquifer in the northeast into Louisiana. Clearly there is a difference in the geologic units that compose the Evangeline aquifer in the southwest and northeast sections of the Gulf Coast aquifer. According to Baker (1979), the Evangeline aquifer was originally only defined as far west as Austin, Brazoria, Fort Bend, and Washington counties in Texas. He stated that extending the Evangeline farther west is speculative; however, in 1976 the USGS decided to extend the Evangeline to the Rio Grande.

Pleistocene and Recent Alluvial Deposits – Since Pleistocene time, packages of fluvial sediments representing successively younger progradational cycles have been deposited along the Texas Gulf Coast (Blum, 1992). The fluvial sediments range in texture from gravel to clay and are commonly poorly indurated. Decreasing dip of the strata toward the coast through time

reflects changes in relative uplift of inland areas (southern Rocky Mountains, Great Plains, and the Edwards Plateau) and subsidence in the Gulf of Mexico (Doering, 1935; Blum, 1992). The older portions of this depositional sequence are coarser grained and dip 3 to 7 m per mile (Willis Sand), whereas the younger units are finer grained and dip only approximately 2×10^{-4} (1 ft/mi) (Beaumont Fm.) (Doering, 1935). Major Pleistocene to Recent formations along the Texas Gulf Coast, listed from oldest to youngest, include Willis Fm., Lissie Fm., Beaumont Fm., and Quaternary terrace deposits and alluvium (Doering, 1935; Baker, 1979). These units plus Quaternary alluvial deposits are all assigned to the Chicot aquifer.

Northeast of the Colorado River, Miocene- to Pliocene-age Fleming Fm. clay is unconformably overlain by the Willis Sand, which is in turn unconformably overlain by the sand and clay of the Lissie Fm. South of the Colorado River, the Pliocene-age Goliad Fm. is overlain by the Lissie Fm., which consists of sand, silt, clay, and minor amounts of gravel. The Lissie Fm. is overlain by clay, silt, and fine-grained sand of the Pleistocene-age Beaumont Fm. throughout the Texas Gulf Coast. Although the Beaumont Fm. as a whole is much finer grained than directly underlying formations, it contains localized sand channel deposits. The base of the Pleistocene (thought to be Willis Fm. in the northeast Gulf Coast and Lissie Fm. in southwest Gulf Coast) is very difficult to identify on geophysical logs (Baker, 1979). Because of this the bottom of the Chicot aquifer, which has in the past been defined as the base of the Pleistocene, is ambiguously defined and is often lumped together with the Evangeline aquifer.

Recharge Rates from Previous Studies

Recharge rates for Gulf Coast aquifer have been determined in many previous studies. A variety of approaches were used to estimate recharge, including Darcy's Law, environmental tracers, hydrograph separation, and numerical modeling.

Recharge rates in the Trinity River Basin ranged from 0.0 – 7.2 in/yr (median 0.9 in/yr) based on Darcian pedotransfer functions, 0.0 – 5.6 in/yr (median 0.4 in/yr) based on the chloride mass balance approach applied to unsaturated zone samples, and 0.0 – 4.1 in/yr (median 0.8 in/yr) based on chloride mass balance applied to groundwater data (Nolan et al., 2007). The regional recharge rates based on groundwater chloride data were not as variable as those based on unsaturated zone chloride data. Recharge rates based on Darcy's Law range from 1.2 to 1.3 in/yr in the Chicot and Evangeline aquifers in Colorado, Lavaca, and Wharton Counties (Loskot et al., 1982).

Recharge rates in the Chico and Evangeline aquifers were estimated using tritium isotopes in groundwater by Noble et al. (1996). An upper bound on the average recharge rate of 6 in/yr

was estimated using the deepest penetration of tritium (80 ft) in 41 sampled wells in the Chicot and Evangeline outcrop areas.

Variations in recharge rates among groundwater models are attributed to differences in model grid size, hydraulic conductivity distribution, and degree of aquifer development. Recharge rates based on groundwater models may be biased because of scale issues (Johnston, 1997). Grid sizes in regional models are generally ≥ 1 mi². Therefore, in areas with large topographic relief with recharge discharging through streams within grid blocks, total recharge will be underestimated by the model because local and possibly intermediate flow systems are not captured in the larger grid blocks because they encompass both, and oftentimes only regional flow systems can be simulated.

Because most groundwater models of the Gulf Coast are calibrated using hydraulic head data alone, they can only simulate the ratio of recharge to hydraulic conductivity (Scanlon et al., 2002). Therefore, variations in recharge among the models are generally related to hydraulic conductivity, i.e. low recharge rates (0.0004 to 0.12 in/yr) associated with low hydraulic conductivity distribution (Hay, 1999).

Ryder (1988) estimated an average recharge rate of 0.74 in/yr in the outcrop areas of the upper Gulf Coast. Calibrated recharge rates in the southern Gulf Coast ranged from 0 – 4 in/yr for Goliad sand. A later model by Ryder and Ardis (2002) reported an average recharge rate of 0.12 in/yr. Simulated recharge rates of 0.1 to 0.4 in/yr were estimated by Dutton and Richter (1990) for the Chicot and Evangeline aquifers in Matagorda, Wharton, and Colorado counties.

Simulations of the northern Gulf Coast aquifer as part of the Groundwater Availability Modeling program resulted in predevelopment recharge rates in the aquifer outcrop zones of 0.14 in/yr in the Chicot and 0.41 in/yr in the Evangeline (Kasmarek and Robinson, 2004). Simulated transient recharge rates in the aquifer outcrop zones range from 0.4 in/yr in the Chicot and 0.12 in/yr in the Evangeline in 1977. Recharge increases to 0.55 in/yr in the Chicot in 2000 and decreases to 0.11 in/yr in the Evangeline. In the central and southern Gulf Coast GAMs, groundwater recharge was calibrated in the model as a uniform percent of distributed mean annual precipitation according to soil characteristics, which resulted in higher recharge rates in the central Gulf Coast because of higher precipitation relative to the southern Gulf Coast (Chowdhury et al., 2004, Chowdhury and Mace, 2003). Calibrated recharge rates were low in the Jasper Aquifer (≤ 0.1 in/yr) and higher in the Evangeline (0.1 – 0.2 in/yr) and Chicot (0.1 – 0.3 in/yr) aquifers based on results for 1980 1990, and 1999. Recharge in the lower Rio Grande Valley is derived from precipitation (47%) and from the Rio Grande seepage (0.53%).

Methods

Actual evapotranspiration (ET_a) was estimated to ensure that ET used in future groundwater models in this region does not exceed actual ET estimates. In addition, reference ET (ET₀) was also evaluated to compare with actual ET at station locations. Various techniques were used to estimate aquifer recharge. The primary techniques are chloride mass balance approach applied to groundwater and unsaturated zone chloride data, water table fluctuations, and streamflow hydrograph separation. Additional data were collected to further constrain recharge rates. For example, chemical data from streams were compared with those from groundwater during low flow conditions to evaluate reliability of baseflow discharge estimates from stream data.

Estimation of Evapotranspiration

Reference Evapotranspiration

Evapotranspiration is generally the second largest parameter in the water budget in most regions. Reference ET refers to ET that is not limited by water availability in the soil profile and is only controlled by meteorological parameters such as radiation, temperature, wind, and relative humidity. Reference ET was estimated using the Penman Monteith approach (Allen et al., 1998):

$$ET_0 = \frac{0.408\Delta(R_n - G) + \gamma \frac{900}{T + 273} u_2 (e_s - e_a)}{\Delta + \gamma(1 + 0.34u_2)} \quad (1)$$

where ET_0 = reference evapotranspiration [mm day⁻¹],

R_n = net radiation at the crop surface [MJ m²/ d],

G = soil heat flux density [MJ/m² d],

T = mean daily air temperature at 2 m height [°C],

u_2 = wind speed at 2 m height [m/ s],

e_s = saturation vapor pressure [kPa],

e_a = actual vapor pressure [kPa],

Δ = slope of vapor pressure curve [kPa/°C],

γ = psychrometric constant [kPa/ °C].

Reference ET was obtained for 10 stations in and surrounding the Texas Gulf Coast region from the TexasET Network (Table 1). This network is partially supported through a federal program, the “Rio Grande Basin Initiative,” and administered by the Texas Water Resources Institute of the Texas A&M University System and other groups. TexasET contains weather

information, current and average ET data, and irrigation watering recommendations. The standard Penman-Monteith method is used to calculate ET_0 from the weather station data. Reference ET was also estimated using stations from The National Solar Radiation Database (NSRDB) established by the National Renewable Energy Lab (NREL). Eight class I stations in the Gulf Coast region were selected for ET_0 estimation (Table 2). Hourly data from 1991 to 2005 for each station were extracted from the archive and hourly ET_0 was calculated using Penman-Monteith equation. Annual ET_0 by station was summarized from hourly values. Monthly and annual ET_0 were calculated for all stations (Table 2).

Atmometers (2) were installed to monitor reference ET in a riparian setting adjacent to the Colorado River at La Grange, Fayette County. One atmometer was installed in a small clearing receiving full sunlight and another was installed under the tree canopy in full shade, both separated by a distance of about 150 ft. The atmometers (Model E, ETGage, Loveland, CO, www.etgage.com) consist of a reservoir of distilled water connected to a porous ceramic evaporator through an electronic measuring device that records evaporation in 0.01-inch increments. The ceramic is covered by a canvas diffusion cover designed to simulate reference ET (ET_0). The reservoir has a capacity to supply 12 in of evaporation.

Actual Evapotranspiration

Actual ET is generally the parameter of most interest to hydrologists and is impacted by land use/land cover and soil moisture. Remote sensing is widely used to develop regional estimates of ETa. A variety of codes are available to estimate ETa including SEBAL, METRIC, SSEB (Gowda et al., 2008). In this study, SSEB was used to estimate ETa in the Gulf Coast region.

All of these approaches estimate ETa or latent heat flux as the residual term in the surface energy balance equation:

$$ETa = LE = Rn - G - H \quad (2)$$

where LE is latent heat flux (energy consumed by ET), Rn is net radiation at the surface, G is ground heat flux, and H is sensible heat flux, all in units of W/m^2 . The Simplified Surface Energy Balance (SSEB) approach was developed at USGS/Center for Earth Resources Observation and Science (EROS) for operational applications (Senay et al., 2007). The SSEB approach produces ETa estimates using a combination of ET fractions generated from thermal imagery and global reference ET over homogeneous areas with similar climate zones where differences in surface temperature are mainly caused by differences in vegetation water use rates. ETa is a product of ET fraction (ET_f) and ET_0 : ET_f is calculated from Moderate Resolution Imaging Spectroradiometer (MODIS) thermal image. Average 8 day MODIS data are used because of

problems with cloudiness for daily data. Reference ET (ET_0) is calculated globally from assimilated meteorological datasets of the Global Data Assimilation System of NOAA (Senay et al., 2008). The 8 day average temperature of hot and cold pixels are used to calculate proportional fractions of ET on a per pixel bases based on the assumption that hot pixels have ET close to 0 (Allen and Tasumi, 2005) and cold pixels represent maximum ET. Using Normalized Difference Vegetation Index (NDVI) from MODIS, hot pixels are selected from dry and bare areas and cold pixels from well-watered, vegetated areas. The ET fraction ($ET_{f,x}$) is calculated for each pixel “x” by applying the following equation to each of the 8-day MODIS land surface temperature grids.

$$ET_{f,x} = \frac{TH - T_x}{TH - TC} \quad (3)$$

where TH and TC are the averages of hot and cold pixels selected for a given scene, and T_x is the land surface T for any given pixel in the composite scene.

Theory of Recharge Estimation Approach

Chloride Mass Balance Approach

Chloride is produced naturally in the Earth’s atmosphere and has been widely used to estimate recharge rates since the late 1970s (Allison and Hughes 1978). The chloride mass balance (CMB) approach is used to estimate the recharge rate in which the chloride input to the soil profile from precipitation is balanced by chloride output in percolation below the root zone which is equated to recharge at the water table. The CMB approach can be applied to unsaturated zone profiles or to groundwater chloride data:

$$P \times Cl_P = Pe_{CMB} \times Cl_{UZ} = R_{CMB} \times Cl_{UZ} \quad (4)$$

$$P \times Cl_P = R_{CMB} \times Cl_{GW} \quad (5)$$

$$R_{CMB} = \frac{P \times Cl_P}{Cl_{UZ}} = \frac{P \times Cl_P}{Cl_{GW}} \quad (6)$$

where P is precipitation, subscripts P, UZ, and GW are precipitation, unsaturated zone, and groundwater, Pe is percolation rate (in/yr), and R is recharge rate. Percolation/recharge rates are inversely related to chloride concentrations in the unsaturated zone or groundwater; high percolation/recharge rates correspond to low chloride concentrations because chloride is flushed through the system whereas low percolation/recharge rates correspond to high chloride concentrations because chloride accumulates. Therefore, chloride concentrations can be used qualitatively to assess recharge rates. Quantitative percolation/recharge estimates require

application of equations 4 through 6. The accumulation time represented by chloride in unsaturated zone profiles can be determined by dividing the cumulative total mass of chloride for the depth interval of interest by the chloride input:

$$t = \frac{\int_0^z \theta \times Cl_{UZ} dz}{P \times Cl_p} \quad (7)$$

Chloride concentrations generally increase through the root zone as a result of evapotranspiration and then remain constant below this depth. Bulge-shaped chloride profiles in unsaturated profiles in the High Plains have been attributed to higher recharge during the Pleistocene glacial period and chloride accumulation during the drier Holocene period (Scanlon and Goldsmith, 1997).

The chloride mass balance approach assumes that precipitation is the only source of groundwater chloride. However, groundwater chloride can also be derived from underlying more saline aquifers. Mass concentration (mg/L) ratios of groundwater Cl/Br and Cl/SO₄ can be used to distinguish chloride of meteoric origin from precipitation from chloride derived from upward flow of saline groundwater from deeper aquifers, as was done in the Central High Plains (Scanlon et al., 2010).

Estimation of Recharge Rates

Chloride Deposition

Applying the chloride mass balance (CMB) approach to estimate recharge requires information on chloride input into the system. Chloride concentration data are generally obtained from the National Atmospheric Deposition Program (NADP) in the US (www.nadp.org). These data include wet chloride deposition only because the precipitation collectors are only open when it is raining. The CMB approach requires information on wet and dry chloride deposition or bulk chloride deposition. Many previous studies in the Texas High Plains doubled the wet chloride deposition as an estimate of bulk chloride deposition based on estimates of bulk chloride deposition from ³⁶Cl/Cl ratios below the root zone (Scanlon et al., 2010). There are no ³⁶Cl/Cl data available for the Gulf Coast region. We examined literature data to assess relative amounts of wet and dry deposition near coastal zones. Measurements from coastal zones in Spain showed that dry deposition accounts for up to 50% of bulk deposition.

Application of the CMB approach requires information on chloride deposition (equation 6). Many studies have indicated that chloride deposition varies markedly with distance from the coast. Blackburn and McLeod (1983) suggested exponential reduction in chloride deposition

near the coast, but attributed most of the reduction to variations in dry deposition. Keywood et al. (1997) also approximated changes in chloride deposition from the coast by exponential relationships based on a W-E and N-S transects in bulk deposition and attributed the changes in deposition to a fast portion characterized by rapid removal of chloride near the coast with a decay constant of ~ 60 km and a slow portion with a decay constant of ~700 km. They also noted that reduction in precipitation from the coast is also important. Biggs (2006) suggested that a higher correlation was obtained using mass rather than volume concentrations and indicated that reductions from the coast can penetrate to 300 to 400 km from the coast. Alcalá and Custodio (2008) noted that dry deposition only accounted for up to 50% of bulk deposition based on data from Spain.

As a result of these studies, we developed a relationship for chloride deposition with distance from the coast using 20 stations from the NADP. The stations are located within approximately 5 to 200 miles from the Gulf Coast and include stations in Texas, Louisiana, Mississippi, Alabama, Georgia, and Florida. The median annual deposition rate for the period of record for each station was used. Mass concentrations (kg/ha) rather than volume concentrations (mg/L) were used based on the findings from Biggs (2006). A high correlation ($r^2 = 0.98$) was obtained between chloride mass deposition (Cl_{PM}) and distance from the coast (x) (Figure 8). To convert wet mass deposition (Cl_{PM} , kg/ha) to concentration (Cl_p , mg/L), the following is used:

$$Cl_p = \frac{Cl_{PM}}{P} = \frac{42 - 14.6 \ln x + 1.39 (\ln x)^2}{P} \times 2450 \quad (8)$$

where the second-order equation in the numerator represents a least-squares fit to NADP median mass concentration deposition versus distance from the coast is in miles, precipitation (P) is in inches, and 2450 is a units conversion factor.

To gain insight into the relative amount of dry deposition in the study area, precipitation collectors were installed adjacent to the two NADP stations in the Gulf Coast to collect bulk chloride deposition. Additional collectors were installed at 8 other locations (Figure 9). Unlike the NADP precipitation collectors, which open mechanically during precipitation events and are closed at other times, the deployed collectors are open at all times. The open collectors located at the NADP sites are sampled on the same schedule as the NADP wet-only collectors for direct comparison to NADP results (weekly), while open collectors at the remaining sites are sampled at intervals varying approximately from weekly to monthly. However, the region has been in a

drought since installation of these collectors and there is insufficient data to modify the chloride deposition function based on the NADP data.

Unsaturated Zone Field Studies and Chemical Analysis

Field studies were designed to drill and sample boreholes in different settings to estimate percolation using the chloride mass balance approach. A total of 18 boreholes were drilled and core samples collected for analysis of texture, water content, and anion concentrations in pore water (Figure 10). In addition, results from nine boreholes drilled in a previous study in the southern Gulf Coast were used to estimate recharge in this region (Scanlon et al., 2005). Continuous soil cores were obtained using a direct push drill rig (Model 6620DT, Geoprobe, Salina, KS). Borehole depths ranged from 8.0 to 47.5 ft (Table 3). Core samples were collected in plastic sample sleeves and capped.

Subsamples of the core from depth intervals varying between 1 and 5 ft were analyzed for soil water content and texture. Chemical parameters analyzed included water-extractable anion concentrations, including chloride, sulfate, and nitrate-N in water leached from the samples. Core subsamples (25 g) were leached using 40 mL of double deionized water. The mixture was placed in a reciprocal shaker for 4 hr, centrifuged at 7,000 rpm for 20 min, and the supernatant was filtered (0.2 μ m). Core subsamples were then oven dried at 105°C for 48 hr to determine gravimetric water content. Ionic concentrations were analyzed using ion chromatography (Dionex ICS 2000, EPA Method 300.0). Water-extractable ion concentrations are expressed on a mass basis as mg ion per kg of dry soil and were calculated by multiplying ion concentrations in the supernatant by the extraction ratio (g water/g soil). Ion concentrations are also expressed as mg ion per L of soil pore water and were calculated by dividing concentrations in mg/kg by gravimetric water content and multiplying by water density. Soil texture analyses were conducted using hydrometer methods at the Soil Water and Plant Analysis Laboratory at the University of Arizona to determine percentages of sand, silt, and clay.

Chloride Mass Balance Applied to Groundwater Data

Groundwater chloride concentrations (Cl_{GW}) were used to estimate regional recharge rates on the basis of equation (6). Chloride data were obtained from 8,721 wells in the outcrop area of the Jasper, Evangeline, and Chicot aquifers from Texas Water Development Board (TWDB) database (www.twdb.state.tx.us). Chloride concentrations in precipitation were obtained from the National Atmospheric Deposition Program (NADP, <http://nadp.sws.uiuc.edu/>). Mass concentration (mg/L) ratios for subsets of the chloride data for groundwater Cl/Br (1,339 wells) and Cl/SO₄ (8,086 wells) were used to distinguish chloride of meteoric origin from precipitation

from chloride derived from upward flow of saline groundwater from deeper aquifers. The chloride and sulfate concentration data represent samples analyzed between 1913 and 2009 (median 1966). The bromide concentration data for the region represent samples analyzed between 1990 and 2009 (median 2001).

Water Table Fluctuation Method

The water table fluctuation (WTF) method (Healy and Cook, 2002) was applied to groundwater level data from the TWDB database. The WTF method is based on the premise that rises in groundwater levels in unconfined aquifers are due to recharge water arriving at the water table. Recharge is calculated as

$$R = S_y \frac{D\Delta h}{\Delta t} \quad (9)$$

where S_y is specific yield, h is water-table height, and t is time (Healy and Cook, 2002). The method has been applied to groundwater level rises that occurred over several years in the High Plains aquifer (Scanlon et al., 2010). Difficulties in applying the method are related to ensuring that fluctuations in water levels are due to recharge following precipitation and are not the result of recovery after pumping, changes in atmospheric pressure, presence of entrapped air, ET, or other phenomena. Determining a representative value for specific yield can also be problematic. The method is only applicable to unconfined aquifers and is best applied to shallow water tables that display sharp water-level changes.

Wells in the TWDB database that were deeper than 50 ft were eliminated from consideration as they are more likely to be completed in confined water-bearing units. Wells were further eliminated that have a measurement frequency of greater than about 60 days, considered a minimum required to capture water level fluctuation related to precipitation events, and that had sufficient records to span at least one full year. These criteria resulted in only 30 wells out of the approximately 16,600 wells in the database. All of the selected wells are completed in the Chicot aquifer and a uniform specific yield value of 0.05 was used.

Stream Hydrograph Separation

This section presents various estimates for shallow recharge that discharges to rivers and streams within the Gulf Coast aquifer. This discharge, which is typically called baseflow, occurs when the water table in an aquifer is at a higher elevation than the water surface of the river. Under these conditions, the river is said to be gaining, because water flows from the aquifer to the river. Flow duration curves were developed to determine whether streams are gaining or

losing. Baseflow represents the relatively steady portion of river flow that occurs between periods of surface runoff. By analyzing the portion of river flow that occurs as baseflow, it is then possible to determine the amount that discharges from the aquifer to the river system. Streamflow hydrograph separation was conducted using the Base-Flow Index (BFI) code developed by Wahl and Wahl (1995). BFI is an automated procedure for determining baseflow on a consistent basis from reach to reach, so that they may be compared. BFI is the ratio of baseflow to streamflow. Values of BFI range from 0 (for no baseflow contribution to streamflow) to 1 (for 100% streamflow as baseflow). This program has two options, the first is the Institute of Hydrology method (1990), and the other is referred to as the Modified method. These methods locate low points on the streamflow record (referred to as turning points) and interpolate daily values between these low points. The Institute of Hydrology method was used in this study. The parameter N, number of days, was set to 5 based on an initial sensitivity analysis using selected gage data. The turning point, F, was set to 0.9, which is the default value in the BFI code. Results were not very sensitive to the F parameter.

For this study, 59 unregulated stream gages with drainage areas intersecting the Gulf Coast aquifer were selected and hydrograph separation completed for all the years of record during the time the drainage area upstream of the gage was unregulated. Shallow areal recharge flux in inches was then calculated by dividing the estimated baseflow rate by the drainage area. With baseflow calculated for multiple years it was then possible to estimate the average baseflow at a given stream gage. While using the Base Flow Index code is a fairly simple task, several criteria must be satisfied when selecting gages to be analyzed. If one of these criteria is not fully met then the estimate of recharge may not be valid. The criteria used in this study are listed below:

1. The gage should be on a stream that is considered to be gaining.
2. The catchment area of the gage should be primarily in the aquifer.
3. If the contributing area is outside the aquifer then an upstream gage must be utilized in order to subtract the effects of the upstream area.
4. The majority of the contributing area must be unregulated.

The first criterion ensures that the baseflow separation calculation can be accomplished. For a river with perennial flow (gaining) most of the basin yield usually comes from baseflow, indicating that a large portion of the rainfall is infiltrated into the basin and reaches the stream as subsurface flow (Chow, 1988). However, if the gage was located on an intermittent stream then an estimate of baseflow would only be valid during times when the stream was flowing. The second and third criteria ensure that gains/losses are calculated for the aquifer being analyzed

and the fourth criteria ensures that gains to the system are due to groundwater sources instead of discharge from reservoirs. Estimates of the time periods where a stream was regulated (influenced by reservoir discharge) are available in a USGS report (Slade et al., 2002). This report lists beginning and ending years of regulation for many active and discontinued streamflow gaging stations in Texas. Calculations of baseflow were made based on the unregulated years reported by Slade (2002). Note that Slade (2002) only lists regulated years up to the year 2000, because that was the most recent data at the time of the report. For the current study, if a gage was unregulated in 2000, it was assumed that it continued to be unregulated to the present time as no reservoirs have reportedly become active in the Gulf Coast region in the last decade.

Results and Discussion

Evapotranspiration

Reference ET (ET_0) refers to the ability of the atmosphere to remove water and is controlled by meteorological forcing. Reference ET refers to the maximum possible ET for fully watered vegetation. Based on historical periods of record for TexasET network stations in the region, ET_0 ranges from 52.7 to 57.0 in/yr, with an overall trend toward higher values from north to south and also increasing inland from the coast (Table 1). Seasonal ET_0 is lowest from November through February (~20% of annual total) and highest in other months (~80% of annual total), with maximum monthly totals occurring between June and August for different locations. Values of ET_0 calculated from the NSRDB database (Table 2) and from the TexasET network generally agree within $\pm 10\%$.

Annual mean actual ET (ETa) ranges from 32 in/yr in the south to 36 in/yr in the central and 42 in/yr in the north region (2000 – 2009) (Figure 11). Although ETa might be expected to be greater in the south where temperatures are highest, ETa in this region is limited by water availability. In contrast, ETa is greatest in the north because precipitation and water availability are highest in this region. Interannual variability is greatest in the south, with annual ETa ranging from 24 to 42 in/yr with a coefficient of variance (CV, standard deviation divided by the mean) of 20% (Figure 12). ETa ranges from 27 to 44 in/yr in the central region (CV = 14%) and from 39 to 48 in/yr in the north (CV = 6%). Average monthly ETa varies systematically with the seasons in all regions, with minimum values (0.3 to 0.7 in) occurring in January and maximum values (5.0 to 6.5 in) occurring in July (Figure 13). Differences among regions are greatest in the summer and least during fall and early winter.

Regional Recharge Rates from Groundwater Chloride Data

Groundwater chloride concentrations range from 3 to 1,700 mg/L and decrease regionally from south to north (Figure 14). Chloride concentrations are generally highest within the southern region in areas that surround a lower concentration (100 – 300 mg/L) zone corresponding to a sand dune area (Figure 4). Within the central region, higher concentrations are generally limited to the southern coastal area and concentrations decrease toward the northeast. Chloride concentrations are lowest overall in the northern region, with regional higher concentrations limited to a narrow zone near the coast.

The CMB approach assumes that all chloride is derived from precipitation. To assess the validity of this assumption, ratios of Cl/Br and Cl/SO₄ were evaluated to determine the chloride contribution from possible upward movement of more saline water from underlying geologic

units (Figures 15 and 16). Mass ratios of Cl/Br typical of precipitation range from 50 to 150, and those typical of fresh groundwater range from 100 to 200, whereas ratios in groundwater impacted by salt dissolution range from 1000 to 10,000 (Davis et al., 1998). Ratios of Cl/Br throughout much of the Gulf Coast generally range from 80 to 300, mostly within the range of those typical of precipitation and fresh groundwater; however, Cl/Br ratios in the north near the coast are generally higher (300–600) and suggest an additional source of chloride input, possibly as upward cross formational flow of saline water from deeper aquifers in this region (Figure 15). The region of elevated Cl/Br ratios is ~ 7,000 mi² in area and is coincident with a large cluster of salt domes (Hamlin, 2006). The high Cl/Br ratios are attributed to low Br concentrations typical of recrystallized halite. Ratios of Cl/SO₄ greater than 20 are also characteristic of this region and are generally consistent with the high Cl/Br (>300) area (Figure 16), suggesting that groundwater throughout this region may be impacted by upward cross-formational flow. Therefore, groundwater Cl data should provide a lower bound on actual recharge rates in this region.

Estimated recharge rates based on groundwater chloride concentrations range from <0.1 to 10 in/yr throughout the Gulf Coast aquifer (Figure 17). Median recharge rates range from 0.12 in/yr in the southern region, 0.39 in/yr in the central region, to 1.26 in/yr in the northern region (excluding the region with Cl/Br >300). Most recharge in the southern region falls within the range of <0.1 to 0.25 in/yr with a zone of slightly higher recharge generally corresponding to a sand dune area (Figure 4). In the central region, recharge generally ranges from 0.25 to 0.5 in/yr in the southwest to 0.5 to 1 in/yr in the northeast and near the northeast coast. Recharge in the northern region is lowest along the inland margin and is higher along a band across the center ranging from about 1 in/yr in the southwest to a maximum of about 10 in/yr in the northeast.

Estimated recharge rates in the Gulf Coast represent <0.1 to 16% of mean annual precipitation (Figure 18). Recharge rates in the southern region range from 0.1 to 2.2% (median 0.5%, mean 0.7%) of mean precipitation. Recharge rates in the central region range from 0.1 to 9% (median 1.0%, mean 1.2%) of mean precipitation. Recharge rates in the northern region range from 0.2 to 16% (median 2.6%, mean 3.5%) of mean precipitation (excluding the Cl/Br >300 region). These recharge rates are generally lower than those predicted using the precipitation model by Keese et al. (2005), which, for texturally variable vegetated soils, predicts recharge as a percentage of precipitation of 1.9% in the southern region, 5.9% in the central region, and 11% in the northern region.

Many studies have noted high correlations between groundwater nitrate concentrations and recharge to shallow aquifers (Nolan et al., 2002; Fram and Belitz, 2011). Therefore, we examined variations in groundwater nitrate concentrations to determine if these variations are related to recharge. Nitrate concentrations were generally low throughout the Gulf Coast aquifer, ≤ 1 mg/L $\text{NO}_3\text{-N}$ in most of the northern Gulf Coast, ≤ 2 mg/L throughout much of the central Gulf Coast. Higher concentrations are restricted to the southern Gulf Coast (2- 13 mg/L) and are greatest near the Rio Grande (Figure 19). Generally low nitrate concentrations throughout most of the north and central Gulf Coast could reflect limited input from nitrate fertilizer application, denitrification associated with reducing conditions, or low recharge rates. To assess the distribution of anthropogenic input, the probability of nitrate concentrations exceeding 2 mg/L $\text{NO}_3\text{-N}$, which is considered background levels, was calculated and the data kriged. Results indicate higher probabilities in the south where recharge rates are generally low and much lower probabilities in the central and northern regions (Figure 20).

Relationships between Precipitation, Soil Texture, and Land Use with CMB Recharge

Relationships between precipitation, land use, soil texture, and groundwater CMB recharge rates were investigated using multiple linear regression. Groundwater CMB recharge rates (log-transformed) for each well were compared to long-term average annual total precipitation depth (Figure 1), soil clay content percentage (Figure 4), and land use category (Figure 5). Various combinations of these variables were modeled to characterize which, if any, might demonstrate a significant ability to predict the groundwater CMB recharge rates. The numerical values for precipitation and soil clay content at each well location were derived from the respective maps. For land use, coded variables (1's and 0's) representing the dominant land use category within 500 m of each well location were used. In this approach, the dominant land use category is assigned a value of "1" and all other categories are assigned a value of "0". Additionally, one category is implicitly omitted from the model for comparison (this is required to prevent the model from being "over-specified"). The "Pasture" category was selected for comparison as it represents the dominant land use near approximately one-third of the wells in the study area. Models were run encompassing the entire Gulf Coast region and separately for the Northern, Central, and Southern subregions. Overall model statistics including correlation (r) and standard errors of prediction were used to compare the results of the models. Results indicate that both regionally and within each subregion, precipitation has the greatest effect with $r = 0.61$ regionally and ranging from 0.37 to 0.54 for the individual subregions. The regional land use model had $r=0.40$ and ranged from 0.14 to 0.48 within subregions. The regional soil clay content model had

$r=0.01$ and ranged from 0.13 to 0.28 within subregions. Incorporating precipitation, soil clay content, and land use into the models resulted in only marginal increases in CMB recharge predictability, with $r=0.63$ regionally and ranging from 0.39 to 0.57 within subregions. In all cases, the standard errors indicate order-of-magnitude predictability at best.

Regional Recharge Rates from Water Table Fluctuations

The WTF method was applied to shallow (≤ 50 ft) wells, resulting in a total of 30 wells restricted to the central and northern regions. Most (21, 70%) wells are located in the northern region (Table 4). The median recharge rate for all wells is 2.5 in/yr (range 0.5 to 5.7 in/yr) and there is no significant difference between the results for wells located in the north and central regions. Analyzed periods range from the early 1930s to 2008, and most (26, 87%) wells have relatively short suitable records for analysis that span less than 8 years (range 1.3 to 7.9 yr, median 2.2 yr), while the remaining four wells have periods ranging from about 31 to 33 yr. However, there is no significant difference between the median recharge rate of the short-period analyses (< 8 yr, median 2.5 in/yr) and the long-period analyses (> 30 yr, median 2.4 in/yr). The apparent recharge rates are generally consistent, though slightly higher, than the groundwater CMB results. However, nine of the wells (median 2.7 in/yr, range: 1.8 to 4.9 in/yr) are located in the region with Cl/Br > 300 where the CMB method likely underestimates recharge rates. Also, there is uncertainty related to the assumed uniform specific yield value (0.05).

Local Recharge Rates from Unsaturated Zone Profiles

Unsaturated zone profiling was restricted to the central and southern regions of the Gulf Coast. The primary objective of this part of the study was to conduct a reconnaissance of unsaturated zone profiles of chloride, sulfate, and nitrate to assess local variations in recharge with soil type and land use/vegetation. The profile data can be used to make qualitative assessments of recharge. Unsaturated zone profile analytical results for water content, chloride, sulfate, and nitrate-N concentrations, and texture for all profiles are presented in Appendix 1. Mean chloride concentrations below the root zone range from 7 to 10,200 mg/L (Table 5). However, there is no systematic variation in median chloride concentrations similar to the regional variations found in groundwater chloride concentrations. Sulfate profiles also provide qualitative information on flushing through the profile, although sulfate may lag chloride because of sorption onto sediments.

Low chloride concentrations were found in 8 of the 28 profiles, with mean concentrations below the root zone ranging from 7 to 90 mg/L (median 34 mg/L) (Table 5). These low chloride concentrations result in percolation rates ranging from 1.4 to 6.8 in/yr (median 3.9 in/yr) (Figure

21) and represent from 5.7% to 20% (median 9.5%) of local mean precipitation with corresponding short chloride accumulation times ranging from 5 to 87 yr (median 27 yr) to the total depth sampled (Table 6). Sulfate concentrations were also low in these profiles (64 to 150 mg/L, median 97 mg/L), consistent with flushing. Some of the higher percolation rates may reflect recharge to shallow perched aquifers rather than to the regional system, as one profile (Fay10-04) encountered saturated conditions at a depth of 18 ft while a groundwater well approximately 300 ft distant indicated a depth to water of about 130 ft.

A total of five profiles have slightly higher chloride (90 to 190 mg/L, median 140 mg/L), with three of the profiles having low sulfate concentrations (110 to 180 mg/L) and the remaining two having elevated sulfate concentrations (430 and 660 mg/L) (Table 5). Calculated percolation rates range from 0.35 to 0.73 in/yr (median 0.52 in/yr) for these five profiles, representing from 1.1% to 3.4% (median 1.4%) of local precipitation (Table 6, Figure 21).

The remaining profiles (14) have high chloride concentrations (560 – 10,200 mg/L, median 2,400 mg/L) and high sulfate concentrations (550 – 15,300 mg/L, median 1,400 mg/L) (Table 5), with very low calculated percolation rates ranging from 0.01 to 0.16 in/yr (median 0.03 in/yr) and represent only 0.02% to 0.16% (median 0.1%) of local mean precipitation (Table 6, Figure 21). Accumulation times in this group are up to 13,000 yr, with a median accumulation time of 4,000 yr for boreholes between 20 and 37 ft deep. Chloride profiles show increasing or stable concentration at depth.

Nitrate is sometimes used to fingerprint water fluxes associated with cultivation and fertilization (Scanlon et al., 2010). Most profiles in the Gulf Coast have low nitrate concentrations (median 0.1 – 2 mg/L) (Table 5). A few profiles have slightly higher nitrate levels (3-8 mg/L). The remaining profiles with high mean nitrate concentrations (31 – 275 mg/L) have high levels in the shallow subsurface in some profiles (Bee10-01, Kar10-01) and high levels towards the base in other profiles (Hid05-01, and Liv10-02). The latter have increased nitrate levels coincident with chloride concentration increases, suggesting release of nitrate at the beginning of cultivation, similar to profiles in the High Plains (Scanlon et al., 2008). One of the profiles (Liv10-01) is unusual in that high nitrate extends to 6 m depth, although chloride concentrations are extremely high. The clay content in this profile is extremely high and deep penetration of nitrate may suggest preferential flow.

In summary, there are no regional trends in percolation with precipitation from unsaturated zone profiles, with low and high percolation rates found throughout the sampled region. There is no systematic variation in percolation rate with soil texture. Locally, soil texture may exert a dominant control, e.g. percolation is limited (0.01 in/yr) at a location in Nueces County by clayey

soils under a rainfed agricultural setting whereas percolation is much higher (4.91 in/yr) in sandy soils in Kenedy County despite heavy forest/shrub vegetation (efficient at using water) (Figure 22). Land use also plays an important role locally in determining percolation rates. In Karnes County, two boreholes separated by about 300 ft differ only in land use history (Figure 23). One borehole (Kar10-01) is located in pastureland that was cleared of trees in 1975, is currently grassland with sparse shrubs, and has high Cl and SO₄ concentrations indicating essentially no percolation (0.03 in/yr). The other borehole location (Kar10-02) was cleared in ~1910 and was under continuous cultivation until 1972 when it was allowed to revert to pastureland, is currently covered in grasses similar to Kar10-01, and has low Cl and SO₄ concentrations indicative of flushing with a percolation rate of 5.65 in/yr.

Land use history was difficult to determine accurately for many of the pasture sites sampled because current landowners are only aware of relatively recent land use. Cotton was an important regional crop in the past and much of the current pastureland may have been previously cultivated for cotton.

Regional Recharge Rates from Streamflow Hydrograph Separation

Recharge rates from previous streamflow hydrograph analyses are provided in Appendix 2. Flow duration curves were calculated to determine whether streams are ephemeral or perennial. The curves for all gages are presented in Appendix 3. Two example flow duration curves are shown in Figure 24. From the flow duration curve for gage 8115500, in the southwestern Gulf Coast, ~65% of the time the stream at this location becomes dry and has no flow. In contrast, the flow duration curve for gage 8117500, located in the more humid Brazos River basin, terminates near 100%, which is characteristic of a perennial stream.

Streamflow hydrograph separation was conducted on stream gages whose flow duration curves indicated that they are perennial. Temporal trends in baseflow were first examined prior to estimating recharge rates for contributing basins (Appendix 4). In some areas, such as in the Lower Colorado River Basin, groundwater pumping has varied dramatically through time, and the impact may be evident in the temporal trends of baseflow. Groundwater levels in the Gulf Coast aquifer reached their minimum in the area in approximately 1985-1990 (URS, 2004).

Results from the streamflow hydrograph separation analysis are presented in Tables 7 and 8. Statistics describing baseflow temporal variability are also presented to show the standard deviation and range of values calculated for each gaging station during the period of unregulated flow. Figure 26 shows the locations of the drainage areas analyzed for baseflow recharge and the associated average recharge rates in relation to groundwater CMB recharge

rates in the corresponding drainage basin areas. The results are consistent and indicate that average recharge increases from south to north with increasing precipitation, as expected. Average recharge is negligible in the south, and increases to up to 7 in/yr in the north near the Sabine River.

Comparison of Recharge Rates from Different Approaches

Regional recharge estimates from groundwater chloride data may be considered a lower bound because various processes can add chloride to groundwater whereas no process removes chloride from groundwater in the Gulf Coast. For comparison with the groundwater chloride mass balance results, the streamflow hydrograph results were grouped into four categories based on results of the hydrograph analysis, including (1) perennial streams where the flow duration curves indicate flow persisted for at least 99% of the time, (2) perennial streams as in (1) but that have BFI values below 7%, (3) perennial streams as in (1) that exhibit strong increasing temporal trends in BFI (all located in the Houston area), and (4) nonperennial streams where the flow duration curves indicate flow persisted for less than 99% of the time. Category 1 represents all hydrograph results that indicate a persistent hydraulic connection between the stream and the groundwater in the drainage area while the remaining categories indicate changing or nonpersistent connections.

The trend in groundwater CMB recharge rates is highly correlated with the 24 perennial streamflow hydrograph separations ($r = 0.96$, Figure 27) with most data pairs falling within about 25% of the 1:1 line. The high level of agreement between these two independent methods serves to reinforce the results of the recharge estimates for both methods. Within the remaining hydrograph categories, all of the perennial hydrographs showing strong temporal BFI trends plot above the 1:1 line while all but one of the nonperennial and low BFI hydrographs plot below the 1:1 line. Higher BFI recharge estimates in the former category suggests that these estimates may be impacted by increased streamflow over time in the Houston area while the lower BFI recharge estimates in the latter categories are indicative of basins with nonpersistent connections between surface water and groundwater.

Summary

A variety of approaches were used to assess recharge to the Gulf Coast aquifer. The techniques were primarily chosen to provide regional recharge estimates for input to future groundwater availability models of these aquifers. The chloride mass balance approach was applied to groundwater chloride data to estimate recharge throughout the Gulf Coast and

streamflow hydrograph separation was applied to 59 unregulated stream gages to estimate recharge in contributing groundwater basins to these gages. The chloride mass balance approach was also applied to unsaturated zone profile data in 27 boreholes in the central and southern Gulf Gulf Coast regions. Reference ET was estimated from station data and actual ET was estimated from MODIS satellite data to provide an upper bound on simulated ET in future groundwater models, because ET can be captured through pumpage during development.

Regional recharge rates from groundwater chloride data range from <0.1 in/yr in the south to 6.8 in/yr in the north. Spatial increases in recharge from south to north correlate with increases in precipitation. Calculated recharge rates range from 0.1 to 16% of precipitation. Recharge rates were based on an exponential chloride deposition model developed from NADP data. Ratios of Cl/Br in groundwater that exceed 300 were excluded from recharge estimation because high Cl/Br ratios are attributed to upward movement of saline water near the coast to the northeast. The regional recharge map indicates that precipitation is the primary driver of recharge. While there is no relationship regionally between soil texture and recharge, it is important locally, including a sand dune area in the south increasing recharge and the Beaumont clay towards the northeast decreasing recharge.

Streamflow hydrograph data indicate that streams in the south are ephemeral based on flow duration curves. Baseflow indices were calculated for the remaining perennial streams and were normalized by contributing groundwater basin area to estimate recharge rates. Calculated recharge rates range from 0.0 to 7.1 in/yr and increase from south to north.

Percolation rates below the root zone calculated from chloride data in unsaturated zone profiles are quite variable (<0.1 to 6.8 in/yr) and do not display any systematic variation with precipitation, land use, or soil texture; however, locally soil texture or land use are important. Stratification of sediments makes it difficult to project unsaturated zone results to regional groundwater recharge rates. Sulfate behaves similar to chloride and can be used as a qualitative indicator of percolation rates.

Comparison of the various recharge estimation techniques shows that recharge rates based on groundwater chloride data are in excellent agreement with perennial streamflow hydrograph separation estimates in contributing basins that do not exhibit strong temporal trends in BFI.

Acknowledgments

We appreciate the financial support for this project provided by the Texas Water Development Board. We greatly appreciate the cooperation of property owners who provided access for drilling. We thank David Van Dresar of the Fayette County GCD for monitoring

atmometers and coordinating drilling. We also thank Barbara Smith (Goliad GCD), Lonnie Stewart (Live Oak UWCD and Bee GCD), Larry Akers (Evergreen UWCD), and Charlotte Krause (Pecan Valley GCD) for coordinating drilling in their district areas. For monitoring chloride deposition, we appreciate the support of Terry Rossignol and Matthew Wepler (USFWS, Attwater Prairie Chicken NWR), and Jamie Foster and Jeff Rahmes (USDA/Texas A&M Beeville Experiment Station) of the NADP network, Kim Spring (Lavaca-Navidad River Authority), and Guy Fipps, Martin Barroso, Tim Pannkuk, Mark Hutton, and Allen Malone (Texas A&M TexasET Network). Publication authorized by the Director, Bureau of Economic Geology.

References

- Alcala, F. J., and E. Custodio (2008), Atmospheric chloride deposition in continental Spain, *Hydrological Processes*, 22(18), 3636-3650.
- Allen, R. G., L. S. Pereira, D. Raes, and M. Smith (1998), *Crop Evapotranspiration: Guidelines for Computing Crop Water Requirements*, 290 p. pp., FAO Irrigation and Drainage Paper No. 56.
- Allen, R. G., and M. Tasumi (2005), Evaporation from American Falls Reservoir in Idaho via a Combination of Bowen Ratio and Eddy Covariance, paper presented at EWRI, Anchorage, Alaska.
- Allison, G. B., and M. W. Hughes (1978), The use of environmental chloride and tritium to estimate total recharge to an unconfined aquifer, *Aust. J. Soil Res.*, 16, 181-195.
- Aronow, S., T. E. Brown, D. H. Eargle, and V. E. Barnes (1987), Beeville - Bay City Sheet, University of Texas at Austin, Bureau of Economic Geology.
- Ashworth, J. B., and J. Hopkins (1995), Aquifers of Texas, *Texas Water Development Board Report 345*, 68 p.
- Baker, R. C., and O. C. Dale (1961), Ground-water resources of the Lower Rio Grande Valley area, Texas, *Texas Board of Water Engineers, Bulletin 6014*, v. I, 88 p. v. II, 340 p. .
- Baker, E. T. (1979), Stratigraphic and hydrogeologic framework of part of the Coastal Plain of Texas, *Texas Department of Water Resources Report no. 236*, 43 p.
- Baker, E. T., Jr. (1986), Hydrology of the Jasper Aquifer in the southeast Texas Coastal Plain, *Texas Water Development Board Report 295*, 64 p.
- Biggs, A. J. W. (2006), Rainfall salt accessions in the Queensland Murray-Darling Basin, *Australian Journal of Soil Research*, 44(6), 637-645.
- Blackburn, G., and S. McLeod (1983), Salinity of Atmospheric Precipitation in the Murray-Darling Drainage Division, Australia, *Australian Journal of Soil Research*, 21(4), 411-434.
- Blum, M. D. (1992), Modern depositional environments and recent alluvial history of the lower Colorado River, gulf coastal plain of Texas, unpublished PhD. dissertation thesis, 286 p. pp, Department of Geological Sciences, University of Texas at Austin.
- Chow, V. T., D. R. Maidment, and L. W. Mays (1988), *Applied Hydrology*. McGraw Hill Professional, 624 p.
- Chowdhury, A. H., and R. E. Mace (2003), A groundwater availability model of the Gulf Coast aquifer in the Lower Rio Grande Valley, Texas: Numerical simulations through 2050, *Texas Water Development Board Report, October 2003*, 171 p.
- Chowdhury, A. H., S. Wade, R. E. Mace, and C. Ridgeway (2004), Groundwater availability model for the central part of the Gulf Coast aquifer—Numerical simulations through 1999:, *Texas Water Development Board Report*, 163 p.
- Davis, S. N., D. O. Whittemore, and J. Fabryka-Martin (1998), Uses of chloride/bromide ratios in studies of potable water, *Ground Water*, 36, 338-350.
- Doering, J. (1935), Post-Fleming surface formations of coastal southeast Texas and south Louisiana, *American Association of Petroleum Geologists Bulletin*, 19(5), 651-688.
- Dutton, A. R., and B. C. Richter (1990), Regional geohydrology of the Gulf Coast Aquifer in Matagorda and Wharton Counties, Texas: Development of a numerical model to estimate the impact of water-management strategies, *Bureau of Economic Geology, Univ. of Texas at Austin, Final Technical Report prepared for the Lower Colorado River Authority*, 116 p.
- Fram, M. S., and K. Belitz (2011), Probability of Detecting Perchlorate under Natural Conditions in Deep Groundwater in California and the Southwestern United States, *Environmental Science & Technology*, 45(4), 1271-1277.
- Galloway, W. E. (1977), Catahoula Formation of the Texas coastal plain: depositional systems, composition, structural development, ground-water flow history, and uranium deposition.,

- University of Texas at Austin, Bureau of Economic Geology Report of Investigations No. 87, 59 p.*
- Galloway, W. E., C. D. Henry, and G. E. Smith (1982), Depositional framework, hydrostratigraphy, and uranium mineralization of the Oakville sandstone (Miocene), Texas coastal plain, *The University of Texas at Austin, Bureau of Economic Geology Report of Investigations No. 113, 51 p.*
- Galloway, W. E., P. Ganey-Curry, X. X. Li, and R. T. Buffler (2000), Cenozoic depositional evolution of the Gulf of Mexico Basin, *AAPG Bulletin, 84, 1743-1774.*
- Gowda, P. H., J. L. Chavez, P. D. Colaizzi, S. R. Evett, T. A. Howell, and J. A. Tolk (2008), ET mapping for agricultural water management: present status and challenges, *Irrigation Science, 26(3), 223-237.*
- Griffith, G. E., S. A. Bryce, J. M. Omernik, J. A. Comstock, A. C. Rogers, B. Harrison, S. L. Hatch, and D. Bezanson (2004), Ecoregions of Texas (color poster with map, descriptive text, and photographs), *Reston, Virginia, USGS (map scale 1:2,500,000).*
- Halford, K. J., and G. C. Mayer (2000), Problems associated with estimating ground water discharge and recharge from stream-discharge records, *Ground Water, 38, 331-342.*
- Hamlin, H. S., (2006), Salt Domes in the Gulf Coast Aquifer, *in* Aquifers of the Gulf Coast of Texas, Mace, R. E., Davidson, S. C., Angle, E. S., and Mullican, W. F., eds., *Texas Water Development Board, Report 365, 217-230.*
- Hay, R. (1999), A numerical groundwater flow model of the Gulf Coast aquifer along the South Texas Gulf Coast, M.Sc. thesis, 47 pp, Texas A&M, Corpus Christi.
- Healy, R. W., and P. G. Cook (2002), Using ground-water levels to estimate recharge, *Hydrogeol. Journal, 10, 91-109.*
- Hoel, H. D. (1982), Goliad Formation of the south Texas gulf coastal plain: regional genetic stratigraphy and uranium mineralization, unpublished Master's Thesis thesis, 173 p. +172 plates pp, Department of Geological Sciences, University of Texas at Austin.
- Johnston, R. H. (1997), Sources of water supplying pumpage from regional aquifer systems of the United States, *Hydrogeol. J., 5(2), 54-63.*
- Kasmarek, M. C., and J. L. Robinson (2004), Hydrogeology and simulation of Groundwater flow and land surface subsidence in the Northern part of the Gulf Coast Aquifer System, *U. S. Geological Survey Scientific Investigations Report, 2004-5102, 111p.*
- Keese, K. E., B. R. Scanlon, and R. C. Reedy (2005), Assessing controls on diffuse groundwater recharge using unsaturated flow modeling, *Water Resour. Res., 41, W06010, doi:06010.01029/02004WR003841.*
- Keywood, M. D., A. R. Chivas, L. K. Fifield, R. G. Cresswell, and G. P. Ayers (1997), The accession of chloride to the western half of the Australian continent, *Australian Journal of Soil Research, 35(5), 1177-1189.*
- Larkin, T. J., and G. W. Bomar (1983), Climatic atlas of Texas *Rep. Publication LP-192, 151 p.,* Department of Water Resources, Austin, Texas.
- Loskot, C. L., W. M. Sandeen, and C. R. Follett (1982), Ground-water resources of Colorado, Lavaca, and Wharton Counties, Texas, *Texas Dept. of Water Resources Report 270, 240.*
- Noble, J. E., P. W. Bush, M. C. Kasmarek, and D. L. Barbie (1996), Estimated depth to the water table and estimated rate of recharge in outcrops of the Chicot and Evangeline aquifers near Houston, Texas, *U. S. Geological Survey Water Resources Investigations Report No 96-4018, 19 p.*
- Nolan, B. T., R. W. Healy, P. E. Taber, K. Perkins, K. J. Hitt, and D. M. Wolock (2007), Factors influencing ground-water recharge in the eastern United States, *Journal of Hydrology, 332(1-2), 187-205.*
- Nolan, B. T., K. J. Hitt, and B. C. Ruddy (2002), Probability of nitrate contamination of recently recharged groundwaters in the conterminous United States, *Env. Sci & Technol., 36(10), 2138-2145.*

- Proctor, C. V. J., T. E. Brown, N. B. Waechter, S. Aronow, and V. E. Barnes (1974), Sequin Sheet.
- Ryder, P. (1988), Hydrogeology and predevelopment flow in the Texas Gulf Coast Aquifer systems, 10.
- Ryder, P. D., and A. F. Ardis (1991), Hydrology of the Texas Gulf Coast aquifer systems, *Rep.*, U.S. Geological Survey Open-File Report 91-64, 147 p.
- Ryder, P. D., and A. F. Ardis (2002), Hydrology of the Texas Gulf Coast aquifer systems, *U.S. Geological Survey Professional Paper 1416-E*, 77 p.
- Saunders, G. P. (2006), Low Flow Gain-Loss Study of the Colorado River in Texas: , *Texas Water Development Board Report 365*, p. 293-297.
- Scanlon, B. R., J. P. Nicot, R. C. Reedy, J. A. Tachovsky, H. S. Nance, R. C. Smyth, K. E. Keese, R. E. Ashburn, and L. Christianson (2005), Evaluation of Arsenic Contamination in Texas, *The Univ. of Texas at Austin, Bureau of Economic Geology, final report prepared for Texas Commission on Environmental Quality, under umbrella contract no. 582-4-56385 and work order no. UT-08-5-70828*, 177 p., 167.
- Scanlon, B. R., R. W. Healy, and P. G. Cook (2002), Choosing appropriate techniques for quantifying groundwater recharge, *Hydrogeol. J.*, 10, 18-39.
- Scanlon, B. R., R. C. Reedy, and J. A. Tachovsky (2007), Semiarid unsaturated zone chloride profiles: Archives of past land use change impacts on water resources in the southern High Plains, United States, *Water Resour. Res.*, 43, W03437, doi:10.1029/2006WR005769.
- Scanlon, B. R., and R. S. Goldsmith (1997), Field study of spatial variability in unsaturated flow beneath and adjacent to playas, *Water Resour. Res.*, 33, 2239-2252.
- Scanlon, B. R., R. C. Reedy, and J. B. Gates (2010), Effects of irrigated agroecosystems: (1) Quantity of soil water and groundwater quantity in the Southern High Plains, Texas, *Water Resour. Res.*, 46, W09537, doi:10.1029/2009WR008427.
- Scanlon, B. R., R. C. Reedy, and K. F. Bronson (2008), Impacts of land use change on nitrogen cycling archived in semiarid unsaturated zone nitrate profiles, southern High Plains, Texas, *Env. Sci. & Tech.*, 42(20), 7566-7572.
- Senay, G. B., M. Budde, J. P. Verdin, and A. M. Melesse (2007), A coupled remote sensing and simplified surface energy balance approach to estimate actual evapotranspiration from irrigated fields, *Sensors*, 7(6), 979-1000.
- Senay, G. B., J. P. Verdin, R. Lietzow, and A. M. Melesse (2008), Global daily reference evapotranspiration modeling and evaluation, *Journal of the American Water Resources Association*, 44(4), 969-979.
- Shelby, C. A., S. Pieper, S. Aronow, and V. E. Barnes (1992), Beaumont Sheet.
- Slade, R. M. J., J. T. Bentley, and D. Michaud (2002), Results of streamflow gain-loss studies in Texas, with emphasis on gains from and losses to major and minor aquifers, Texas, 2000, *U.S. Geological Survey Open File Report 02-068*, 136 p.
- Toth, J. (1963), A theoretical analysis of groundwater flow in small drainage basins, *J. Geophys. Res.*, 68, 4795-4812.
- USDA (1995), Soil Survey Geographic Data Base, SSURGO, *Natural Resour. Cons. Svc.*, *USDA, Misc. Pub. 1527, variably paginated*.
- Wahl, K. L., and T. L. Wahl (1995), Determining the flow of Comal Springs at New Braunfels, Texas, *Texas Water '95, ASCE, Aug 16, 17, 1995, San Antonio, Texas*, 77-86.

Table 1. Monthly and annual reference ET (ET_0 , inches) at locations in and surrounding the Texas Gulf Coast region (TexasET Network, <http://texaset.tamu.edu>) for stated period of record (excluding Weslaco).

| <i>City</i> | <i>Jan</i> | <i>Feb</i> | <i>Mar</i> | <i>Apr</i> | <i>May</i> | <i>Jun</i> | <i>Jul</i> | <i>Aug</i> | <i>Sep</i> | <i>Oct</i> | <i>Nov</i> | <i>Dec</i> | <i>Annual</i> | <i>Yrs</i> |
|-----------------|------------|------------|------------|------------|------------|------------|------------|------------|------------|------------|------------|------------|---------------|------------|
| Austin | 2.3 | 2.7 | 4.3 | 5.3 | 6.4 | 7.2 | 7.2 | 7.3 | 5.6 | 4.4 | 2.7 | 2.2 | 57.5 | 70 |
| Brownsville | 2.7 | 3.0 | 4.5 | 5.2 | 6.0 | 6.3 | 6.7 | 6.7 | 5.2 | 4.3 | 3.0 | 2.6 | 56.2 | 79 |
| College Station | 2.2 | 2.7 | 4.2 | 5.2 | 6.3 | 6.9 | 7.1 | 6.9 | 5.6 | 4.3 | 2.8 | 2.2 | 56.3 | 47 |
| Corpus Christi | 2.4 | 3.0 | 4.3 | 5.2 | 6.0 | 6.4 | 6.7 | 6.7 | 5.2 | 4.3 | 3.0 | 2.6 | 55.7 | 52 |
| Galveston | 2.2 | 2.6 | 4.1 | 5.0 | 6.1 | 6.6 | 6.2 | 6.0 | 5.5 | 4.2 | 2.8 | 2.3 | 53.6 | 59 |
| Houston | 2.4 | 2.8 | 4.3 | 5.0 | 6.1 | 6.6 | 6.5 | 6.1 | 5.6 | 4.3 | 2.9 | 2.4 | 54.9 | 31 |
| Port Arthur | 2.3 | 2.6 | 4.0 | 5.1 | 6.1 | 6.6 | 5.8 | 5.6 | 5.5 | 4.2 | 2.8 | 2.2 | 52.7 | 53 |
| San Antonio | 2.4 | 2.9 | 4.4 | 5.5 | 6.5 | 7.0 | 7.3 | 7.0 | 5.6 | 4.4 | 2.9 | 2.4 | 58.2 | 54 |
| Victoria | 2.4 | 2.9 | 4.3 | 5.8 | 6.4 | 6.7 | 6.9 | 6.7 | 5.4 | 4.4 | 2.9 | 2.3 | 57.0 | 39 |
| Weslaco | 2.5 | 2.6 | 4.0 | 4.9 | 6.1 | 6.5 | 7.0 | 6.6 | 4.8 | 4.0 | 2.9 | 2.3 | 54.1 | - |

Table 2. Monthly and annual reference ET (ET_0 , inches) at locations in and surrounding the Texas Gulf Coast region (NSRDB) for the period 1991-2005.

| <i>Station</i> | <i>Jan</i> | <i>Feb</i> | <i>Mar</i> | <i>Apr</i> | <i>May</i> | <i>Jun</i> | <i>Jul</i> | <i>Aug</i> | <i>Sep</i> | <i>Oct</i> | <i>Nov</i> | <i>Dec</i> | <i>Annual</i> |
|----------------|------------|------------|------------|------------|------------|------------|------------|------------|------------|------------|------------|------------|---------------|
| Austin | 2.4 | 2.7 | 4.0 | 4.9 | 5.7 | 6.5 | 7.5 | 6.9 | 5.3 | 4.0 | 2.7 | 2.3 | 55.0 |
| Brownsville | 2.7 | 3.1 | 4.3 | 5.0 | 6.1 | 6.6 | 7.3 | 6.8 | 5.1 | 4.3 | 3.2 | 2.6 | 57.2 |
| Corpus Christi | 2.7 | 2.9 | 4.1 | 4.9 | 5.6 | 6.3 | 7.2 | 6.9 | 5.5 | 4.6 | 3.2 | 2.7 | 56.6 |
| Houston | 2.2 | 2.5 | 3.7 | 4.6 | 5.6 | 5.8 | 6.4 | 5.9 | 4.9 | 3.8 | 2.5 | 2.1 | 49.9 |
| Lufkin | 1.9 | 2.4 | 3.5 | 4.5 | 5.3 | 5.6 | 6.4 | 6.0 | 4.8 | 3.6 | 2.2 | 1.8 | 48.1 |
| Port Arthur | 2.0 | 2.3 | 3.5 | 4.4 | 5.3 | 5.6 | 5.9 | 5.5 | 4.8 | 3.8 | 2.5 | 2.1 | 47.8 |
| San Antonio | 2.5 | 2.8 | 4.1 | 5.1 | 5.9 | 6.7 | 7.6 | 7.1 | 5.6 | 4.2 | 2.9 | 2.5 | 57.1 |
| Victoria | 2.3 | 2.5 | 3.7 | 4.5 | 5.5 | 6.0 | 6.9 | 6.3 | 5.1 | 4.0 | 2.7 | 2.2 | 51.8 |

Table 3. Unsaturated zone borehole locations, dates drilled, land use setting, total borehole depth, and number of samples analyzed (total 308).

| <i>Borehole</i> | <i>Lat</i> | <i>Long</i> | <i>Date</i> | <i>Setting</i> | <i>Depth (ft)</i> | <i>Samples</i> |
|-----------------|------------|-------------|-------------|----------------|-------------------|----------------|
| Bee10-01 | 28.19002 | -97.76813 | 11/04/10 | Rainfed | 32.0 | 12 |
| Bee10-02 | 28.43468 | -97.84283 | 11/08/10 | Pasture | 44.0 | 15 |
| Col10-01 | 29.74026 | -96.75892 | 11/02/10 | Pasture | 28.4 | 11 |
| Dew10-01 | 29.29504 | -97.35400 | 11/11/10 | Pasture | 35.0 | 13 |
| Duv05-01 | 27.29339 | -98.31569 | 06/17/05 | Irrigated | 11.5 | 9 |
| Duv05-02 | 27.45808 | -98.71889 | 06/18/05 | Pasture | 10.0 | 8 |
| Duv05-03 | 27.79992 | -98.63011 | 06/21/05 | Pasture | 8.0 | 8 |
| Fay10-01 | 29.78278 | -97.00634 | 11/01/10 | Pasture | 30.0 | 12 |
| Fay10-02 | 29.72752 | -96.93236 | 11/01/10 | Pasture | 27.0 | 11 |
| Fay10-03 | 29.74825 | -96.76269 | 11/02/10 | Pasture | 11.5 | 6 |
| Fay10-04 | 29.75390 | -96.76389 | 11/02/10 | Pasture | 28.0 | 11 |
| Gol10-01 | 28.40507 | -97.37812 | 11/03/10 | Pasture | 36.5 | 13 |
| Gol10-02 | 28.84299 | -97.44082 | 11/03/10 | Pasture | 21.0 | 9 |
| Gol10-03 | 28.59273 | -97.51180 | 11/04/10 | Pasture | 15.5 | 8 |
| Hid05-01 | 26.56067 | -98.12419 | 06/19/05 | Pasture | 17.0 | 12 |
| Kar10-01 | 28.93886 | -97.79350 | 11/05/10 | Pasture | 20.4 | 9 |
| Kar10-02 | 28.93806 | -97.79307 | 11/05/10 | Pasture | 18.3 | 15 |
| Kar10-03 | 28.73305 | -97.74046 | 11/05/10 | Pasture | 47.5 | 12 |
| Ked05-01 | 26.75500 | -97.60483 | 06/18/05 | Forest | 18.0 | 13 |
| Lav10-01 | 29.23344 | -97.08854 | 11/10/10 | Pasture | 33.1 | 11 |
| Liv10-01 | 28.55307 | -98.12692 | 11/09/10 | Pasture | 29.0 | 12 |
| Liv10-02 | 28.29470 | -98.17455 | 11/09/10 | Pasture | 31.4 | 13 |
| Liv10-03 | 28.12194 | -97.99023 | 11/10/10 | Pasture | 36.7 | 23 |
| Nue05-01 | 27.67264 | -97.70756 | 06/16/05 | Rainfed | 24.0 | 9 |
| Sta05-01 | 26.70272 | -98.39742 | 06/20/05 | Pasture | 12.3 | 12 |
| Sta05-02 | 26.47456 | -98.74347 | 06/20/05 | Rainfed | 17.9 | 12 |
| Sta05-03 | 26.72083 | -98.52378 | 06/20/05 | Pasture | 18.0 | 12 |

Borehole: borehole ID designation, Lat, Long: latitude and longitude location (NAD83), Date: date borehole drilled, Setting: borehole land use setting, Depth: total borehole depth, Samples: number of depths analyzed for ionic concentrations.

Table 4. Groundwater well water level hydrograph analysis results. All wells are completed in the Chicot aquifer. Texts in parenthesis following county names indicate regional location (N, north; C, central). Values in parenthesis listed under BFI Rech heading indicate values for nearby basins.

| <i>Well ID</i> | <i>Depth (ft)</i> | <i>Well Rech. (in/yr)</i> | <i>Period (yr)</i> | <i>Start</i> | <i>End</i> | <i>County</i> | <i>High Cl:Br</i> | <i>CMB Rech. (in/yr)</i> | <i>BFI Rech (in/yr)</i> |
|----------------|-------------------|---------------------------|--------------------|--------------|------------|----------------|-------------------|--------------------------|-------------------------|
| 6045104 | 48 | 2.2 | 1.3 | 1940 | 1942 | Montgomery (N) | No | 1.0 | - |
| 6045107 | 21 | 4.8 | 1.6 | 1940 | 1942 | Montgomery (N) | No | 1.1 | - |
| 6045108 | 18 | 3.7 | 1.6 | 1940 | 1942 | Montgomery (N) | No | 1.1 | - |
| 6045409 | 34 | 2.3 | 2.6 | 1938 | 1941 | Montgomery (N) | No | 1.1 | - |
| 6045801 | 33 | 2.7 | 4.2 | 1931 | 1940 | Montgomery (N) | No | 1.3 | - |
| 6053503 | 21 | 0.8 | 7.0 | 1931 | 1947 | Montgomery (N) | No | 1.4 | 1.4 |
| 6053504 | 35 | 1.3 | 5.3 | 1931 | 1942 | Montgomery (N) | No | 1.4 | 1.4 |
| 6433921 | 24 | 2.1 | 30.6 | 1974 | 2008 | Galveston (N) | Yes | 0.6 | - |
| 6502311 | 32 | 5.7 | 2.8 | 1978 | 1981 | Harris (N) | No | 0.9 | 1.0 |
| 6512725 | 49 | 3.9 | 30.9 | 1974 | 2008 | Harris (N) | No | 1.3 | - |
| 6512818 | 47 | 1.2 | 2.5 | 1978 | 1981 | Harris (N) | No | 1.3 | - |
| 6512819 | 44 | 0.5 | 2.6 | 1978 | 1981 | Harris (N) | No | 1.3 | 2.0 |
| 6513838 | 36 | 2.5 | 4.5 | 1978 | 1983 | Harris (N) | No | 1.4 | 2.8 |
| 6515915 | 14 | 4.6 | 7.9 | 1974 | 1982 | Harris (N) | Yes | 1.8 | - |
| 6522333 | 44 | 3.6 | 7.9 | 1974 | 1982 | Harris (N) | Yes | 1.3 | 2.0 |
| 6523132 | 45 | 2.0 | 7.4 | 1974 | 1982 | Harris (N) | Yes | 1.3 | 2.0 |
| 6523319 | 34 | 2.7 | 32.5 | 1974 | 2008 | Harris (N) | Yes | 1.4 | 2.0 |
| 6531221 | 32 | 1.8 | 2.5 | 1978 | 1981 | Harris (N) | Yes | 1.3 | - |
| 6532631 | 24 | 2.0 | 31.3 | 1974 | 2008 | Harris (N) | Yes | 0.6 | - |
| 6541805 | 50 | 2.7 | 3.1 | 2005 | 2008 | Wharton (C) | No | 0.7 | (1.7) |
| 6548318 | 16 | 4.9 | 1.8 | 1979 | 1981 | Galveston (N) | Yes | 0.5 | - |
| 6548319 | 20 | 3.1 | 1.7 | 1979 | 1981 | Galveston (N) | Yes | 0.5 | - |
| 6634901 | 28 | 3.1 | 1.8 | 1970 | 1972 | Lavaca (C) | No | 0.5 | (1.4) |
| 6634902 | 30 | 2.4 | 1.8 | 1970 | 1972 | Lavaca (C) | No | 0.5 | (1.4) |
| 6634903 | 41 | 1.1 | 1.8 | 1970 | 1972 | Lavaca (C) | No | 0.5 | (1.4) |
| 6643703 | 31 | 3.3 | 1.8 | 1970 | 1972 | Lavaca (C) | No | 0.9 | 1.4 |
| 6643704 | 34 | 1.9 | 1.8 | 1970 | 1972 | Lavaca (C) | No | 0.9 | 1.4 |
| 6651703 | 45 | 2.6 | 1.8 | 1970 | 1972 | Jackson (C) | No | 0.7 | 1.4 |
| 6658603 | 29 | 5.0 | 1.8 | 1970 | 1972 | Jackson (C) | No | 0.6 | 1.0 |
| 6658604 | 41 | 1.1 | 1.8 | 1970 | 1972 | Jackson (C) | No | 0.6 | 1.0 |
| Median | 34 | 2.5 | 2.5 | - | - | - | - | 1.0 | 1.4 |

Well ID: state well ID number, *Depth*: well depth, *Well Rech*: well hydrograph analysis recharge rate, *Period*: total duration of hydrograph analysis period (may not be continuous, see text), *Start*, *End*: beginning and ending years of hydrograph analysis period, *County*: well location county name, *High Cl:Br*: whether well is located in the region of elevated Cl/Br ratios (Figure 15), *CMB Rech*: groundwater chloride mass balance recharge rate at the well location (Figure 17), *BFI Rech*: base flow index recharge rate for coincident or nearby drainage basin stream flow hydrograph analysis (Figure 26).

Table 5. Borehole sample analysis results summary. Concentrations represent depth-weighted average values below the root zone depth (~4-6 ft depth). Values are show as [mg per kg of dry soil] and [mg per L of soil water].

| <i>Borehole</i> | <i>Setting</i> | <i>WC</i> (g/g) | <i>Cl</i> (mg/kg) | <i>SO₄</i> (mg/kg) | <i>NO₃-N</i> (mg/kg) | <i>Cl</i> (mg/L) | <i>SO₄</i> (mg/L) | <i>NO₃-N</i> (mg/L) |
|-----------------|----------------|--------------------|----------------------|----------------------------------|------------------------------------|---------------------|---------------------------------|-----------------------------------|
| Bee10-01 | Rainfed | 0.12 | 540 | 460 | 4.8 | 5,300 | 3,500 | 31 |
| Bee10-02 | Pasture | 0.11 | 14 | 14 | 0.0 | 130 | 120 | 0.4 |
| Col10-01 | Pasture | 0.15 | 3.9 | 9.6 | 0.3 | 25 | 64 | 1.6 |
| Dew10-01 | Pasture | 0.09 | 7.9 | 54 | 0.0 | 90 | 660 | 0.6 |
| Duv05-01 | Irrigated | 0.12 | 130 | 48 | 0.1 | 1,100 | 390 | 0.7 |
| Duv05-02 | Pasture | 0.11 | 310 | 140 | 0.2 | 2,300 | 1,200 | 2.1 |
| Duv05-03 | Pasture | 0.06 | 32 | 29 | 15 | 560 | 490 | 280 |
| Fay10-01 | Pasture | 0.24 | 170 | 230 | 0.2 | 700 | 990 | 0.9 |
| Fay10-02 | Pasture | 0.22 | 210 | 120 | 0.2 | 960 | 550 | 1.0 |
| Fay10-03 | Pasture | 0.15 | 4.3 | 15 | 0.0 | 31 | 96 | 0.1 |
| Fay10-04 | Pasture | 0.18 | 6.5 | 15 | 0.1 | 36 | 95 | 0.8 |
| Gol10-01 | Pasture | 0.13 | 290 | 100 | 0.3 | 2,300 | 690 | 2.2 |
| Gol10-02 | Pasture | 0.15 | 27 | 20 | 0.5 | 190 | 180 | 2.7 |
| Gol10-03 | Pasture | 0.14 | 9.7 | 13 | 0.0 | 65 | 97 | 0.1 |
| Hid05-01 | Pasture | 0.08 | 230 | 1,300 | 16 | 2,400 | 15,300 | 160 |
| Kar10-01 | Pasture | 0.07 | 110 | 68 | 3.9 | 1,400 | 810 | 60 |
| Kar10-02 | Pasture | 0.10 | 0.7 | 11 | 0.0 | 7.3 | 110 | 0.2 |
| Kar10-03 | Pasture | 0.13 | 19 | 14 | 1.1 | 140 | 110 | 8.7 |
| Ken05-01 | Forest | 0.04 | 2.0 | 3.3 | 0.2 | 81 | 130 | 6.3 |
| Lav10-01 | Pasture | 0.13 | 1.5 | 4.8 | 0.3 | 12 | 37 | 2.4 |
| Liv10-01 | Pasture | 0.29 | 860 | 1,300 | 16 | 2,900 | 4,100 | 57 |
| Liv10-02 | Pasture | 0.19 | 1,200 | 330 | 0.8 | 6,400 | 1,700 | 5.5 |
| Liv10-03 | Pasture | 0.12 | 300 | 190 | 0.2 | 2,800 | 1,800 | 2.3 |
| Nue05-01 | Pasture | 0.21 | 2,200 | 1,200 | 7.1 | 10,200 | 5,600 | 32 |
| Sta05-01 | Rainfed | 0.05 | 6.2 | 9.8 | 0.3 | 86 | 150 | 6.2 |
| Sta05-02 | Pasture | 0.12 | 770 | 540 | 15 | 6,100 | 4,500 | 140 |
| Sta05-03 | Rainfed | 0.05 | 13 | 28 | 1.4 | 170 | 430 | 35 |

Borehole: borehole ID designation, *Setting*: borehole land use setting, *WC*: water content, *Cl*: chloride, *SO₄*: sulfate, *NO₃-N*: nitrate-N.

Table 6. Borehole chloride mass balance (CMB) percolation rates.

| <i>Borehole</i> | <i>Setting</i> | <i>Precip</i> (in/yr) | <i>Cl_P</i> (mg/L) | <i>CMB flux</i> (in/yr) | <i>% of Precip</i> | <i>Age</i> (yr) | <i>Depth</i> (ft) |
|-----------------|----------------|--------------------------|---------------------------------|----------------------------|--------------------|--------------------|----------------------|
| Bee10-01 | Rainfed | 32.1 | 1.64 | 0.02 | < 0.1 | 5,400 | 32.0 |
| Bee10-02 | Pasture | 31.5 | 1.42 | 0.63 | 2.0 | 470 | 44.0 |
| Col10-01 | Pasture | 40.9 | 0.92 | 3.73 | 9.1 | 60 | 28.4 |
| Dew10-01 | Pasture | 37.8 | 1.06 | 0.52 | 1.4 | 120 | 35.0 |
| Duv05-01 | Irrigated | 31.0 | 1.84 | 0.05 | 0.2 | 450 | 11.5 |
| Duv05-02 | Pasture | 25.5 | 1.54 | 0.12 | 0.5 | 910 | 10.0 |
| Duv05-03 | Pasture | 24.1 | 1.42 | 0.07 | 0.3 | 75 | 8.0 |
| Fay10-01 | Pasture | 39.6 | 0.90 | 0.06 | 0.1 | 2,300 | 30.0 |
| Fay10-02 | Pasture | 40.1 | 0.92 | 0.04 | 0.1 | 2,200 | 27.0 |
| Fay10-03 | Pasture | 40.8 | 0.92 | 6.75 | 16.5 | 27 | 11.5 |
| Fay10-04 | Pasture | 40.8 | 0.92 | 2.52 | 6.2 | 87 | 28.0 |
| Gol10-01 | Pasture | 36.6 | 1.74 | 0.03 | 0.1 | 2,800 | 36.5 |
| Gol10-02 | Pasture | 35.4 | 1.30 | 0.36 | 1.0 | 180 | 21.0 |
| Gol10-03 | Pasture | 34.8 | 1.46 | 2.00 | 5.7 | 50 | 15.5 |
| Hid05-01 | Pasture | 25.8 | 2.26 | 0.16 | 0.6 | 1,100 | 17.0 |
| Kar10-01 | Pasture | 30.6 | 1.26 | 0.03 | 0.1 | 1,300 | 20.4 |
| Kar10-02 | Pasture | 30.6 | 1.26 | 5.65 | 18.5 | 9 | 18.3 |
| Kar10-03 | Pasture | 31.7 | 1.34 | 0.35 | 1.1 | 230 | 47.5 |
| Ken05-01 | Forest | 24.3 | 4.84 | 4.91 | 20.2 | 5 | 18.0 |
| Lav10-01 | Pasture | 40.7 | 1.10 | 4.02 | 9.9 | 21 | 33.1 |
| Liv10-01 | Pasture | 26.8 | 1.42 | 0.02 | 0.1 | 11,400 | 29.0 |
| Liv10-02 | Pasture | 27.8 | 1.46 | 0.01 | < 0.1 | 12,900 | 31.4 |
| Liv10-03 | Pasture | 30.4 | 1.54 | 0.02 | 0.1 | 3,900 | 36.7 |
| Nue05-01 | Pasture | 23.3 | 2.32 | 0.01 | < 0.1 | 12,300 | 24.0 |
| Sta05-01 | Rainfed | 23.7 | 1.90 | 1.41 | 6.0 | 27 | 12.3 |
| Sta05-02 | Pasture | 23.2 | 1.72 | 0.02 | 0.1 | 5,000 | 17.9 |
| Sta05-03 | Rainfed | 21.7 | 1.78 | 0.73 | 3.4 | 71 | 18.0 |

Borehole: borehole ID designation, *Setting*: borehole land use setting, *Precip*: mean annual precipitation depth (1971-2000, PRISM), *Cl_P*: chloride concentration in bulk precipitation at borehole location (Figure 9), *CMB flux*: chloride mass balance percolation rate, *% of Precip*: CMB flux expressed as a percentage of mean annual precipitation, *Age*: CMB age of soil pore water at borehole total depth, *Depth*: borehole total depth.

Table 7. Recharge estimates and variability based on baseflow separation analysis of stream gauge hydrographs for gages located in the Gulf Coast aquifer system compared with chloride mass balance (CMB) recharge rates in corresponding drainage basins. Baseflow values represent temporal statistical values while CMB values represent spatial statistical values.

| <i>Gage</i> | <i>Period</i> | <i>Years</i> | <i>Area</i> | <i>Baseflow (in/yr)</i> | | | | <i>CMB (in/yr)</i> | | | |
|-------------|---------------|--------------|-------------|-------------------------|------------|------------|------------|--------------------|------------|------------|------------|
| | | | | <i>Mean</i> | <i>Std</i> | <i>Min</i> | <i>Max</i> | <i>Mean</i> | <i>Std</i> | <i>Min</i> | <i>Max</i> |
| 8029500 | 1952-2009 | 58 | 128 | 6.07 | 2.22 | 2.71 | 11.89 | 3.56 | 0.98 | 1.73 | 7.05 |
| 8030000 | 1952-1983 | 31 | 69 | 0.75 | 0.53 | 0.05 | 2.11 | 3.01 | 0.59 | 1.89 | 4.41 |
| 8031000 | 1952-2009 | 42 | 83 | 1.70 | 1.40 | 0.21 | 6.25 | 1.82 | 0.98 | 0.59 | 4.33 |
| 8041500 | 1924-2009 | 74 | 860 | 5.31 | 2.56 | 1.58 | 11.98 | 3.18 | 1.32 | 0.47 | 6.61 |
| 8041700 | 1967-2009 | 43 | 336 | 3.03 | 1.93 | 0.65 | 8.77 | 1.16 | 0.78 | 0.20 | 3.74 |
| 8066200 | 1963-2009 | 47 | 141 | 1.21 | 0.74 | 0.16 | 3.28 | 0.60 | 0.14 | 0.35 | 0.98 |
| 8066300 | 1965-2009 | 44 | 152 | 4.23 | 1.99 | 0.89 | 9.49 | 2.21 | 0.70 | 0.87 | 3.23 |
| 8067500 | 1971-2009 | 29 | 65 | 1.04 | 0.57 | 0.22 | 2.71 | 0.94 | 0.47 | 0.28 | 2.01 |
| 8068500 | 1939-2009 | 71 | 409 | 1.36 | 0.71 | 0.24 | 3.69 | 0.86 | 0.15 | 0.51 | 1.34 |
| 8068720 | 1975-2009 | 32 | 110 | 0.37 | 0.52 | 0.00 | 2.36 | 0.94 | 0.09 | 0.71 | 1.14 |
| 8068740 | 1975-2009 | 35 | 131 | 0.47 | 0.49 | 0.02 | 1.85 | 0.94 | 0.09 | 0.71 | 1.14 |
| 8068800 | 1982-2009 | 19 | 214 | 0.53 | 0.55 | 0.09 | 1.85 | 0.90 | 0.09 | 0.75 | 1.14 |
| 8069000 | 1944-2009 | 66 | 285 | 0.95 | 0.79 | 0.01 | 3.25 | 0.89 | 0.09 | 0.67 | 1.14 |
| 8070200 | 1984-2009 | 26 | 388 | 2.92 | 0.96 | 1.46 | 4.61 | 1.03 | 0.46 | 0.43 | 2.20 |
| 8070500 | 1944-2009 | 66 | 105 | 3.42 | 1.29 | 1.42 | 6.55 | 1.39 | 0.43 | 0.55 | 2.09 |
| 8071000 | 1943-2009 | 45 | 117 | 2.93 | 1.60 | 1.00 | 7.15 | 2.03 | 0.27 | 1.42 | 2.64 |
| 8071280 | 1984-2009 | 23 | 218 | 0.88 | 0.62 | 0.13 | 2.72 | 1.39 | 0.28 | 0.51 | 2.05 |
| 8072300 | 1977-2009 | 33 | 63 | 0.97 | 0.53 | 0.28 | 2.32 | 0.79 | 0.11 | 0.63 | 0.94 |
| 8072730 | 1977-2009 | 33 | 22 | 0.70 | 0.80 | 0.06 | 3.49 | 0.91 | 0.07 | 0.83 | 1.02 |
| 8074250 | 1964-2004 | 17 | 11 | 2.45 | 0.85 | 0.70 | 3.56 | 1.04 | 0.04 | 0.98 | 1.10 |
| 8074500 | 1936-2009 | 74 | 86 | 2.82 | 2.28 | 0.10 | 7.76 | 0.99 | 0.14 | 0.83 | 1.42 |
| 8074800 | 1964-2004 | 17 | 13 | 2.12 | 1.79 | 0.03 | 4.96 | 1.21 | 0.12 | 1.02 | 1.38 |
| 8075000 | 1936-2009 | 74 | 95 | 7.13 | 6.25 | 0.13 | 16.93 | 1.29 | 0.20 | 0.98 | 1.65 |
| 8075400 | 1964-2009 | 40 | 20 | 6.04 | 2.03 | 2.33 | 9.42 | 0.99 | 0.16 | 0.75 | 1.22 |
| 8075500 | 1952-1995 | 43 | 63 | 5.66 | 3.36 | 0.69 | 12.18 | 0.91 | 0.19 | 0.51 | 1.26 |
| 8075730 | 1971-2009 | 39 | 7 | 2.03 | 1.09 | 0.59 | 4.70 | 1.01 | 0.09 | 0.91 | 1.14 |
| 8075770 | 1964-2009 | 46 | 16 | 4.43 | 1.12 | 1.58 | 6.49 | 1.52 | 0.29 | 1.14 | 2.05 |
| 8076000 | 1952-2009 | 58 | 69 | 3.17 | 2.52 | 0.02 | 8.60 | 1.09 | 0.26 | 0.83 | 1.81 |
| 8076500 | 1952-2009 | 50 | 29 | 3.02 | 1.92 | 0.13 | 6.18 | 1.13 | 0.21 | 0.91 | 1.61 |
| 8077000 | 1944-1993 | 41 | 39 | 1.21 | 0.71 | 0.15 | 3.40 | 0.79 | 0.11 | 0.59 | 1.10 |
| 8078000 | 1959-2009 | 51 | 88 | 2.97 | 0.86 | 1.29 | 4.81 | 0.58 | 0.17 | 0.31 | 0.94 |

Gage: USGS stream gage ID number, *Period*: period of unregulated stream flow analyzed, *Years*: number of years of baseflow analyzed, *Area*: basin area in square miles, *Mean*: mean recharge value, *Std*: interannual standard deviation, *Min*: minimum recharge value, *Max*: maximum recharge value, *Med*: median recharge value.

Table 8. Recharge estimates and variability based on baseflow separation analysis of stream gauge hydrographs for gages located in the Gulf Coast aquifer system compared with chloride mass balance (CMB) recharge rates in corresponding drainage basins. Baseflow values represent temporal statistical values while CMB values represent spatial statistical values.

| <i>Gage</i> | <i>Period</i> | <i>Years</i> | <i>Area</i> | <i>Baseflow (in/yr)</i> | | | | <i>CMB (in/yr)</i> | | | |
|-------------|---------------|--------------|-------------|-------------------------|------------|------------|------------|--------------------|------------|------------|------------|
| | | | | <i>Mean</i> | <i>Std</i> | <i>Min</i> | <i>Max</i> | <i>Mean</i> | <i>Std</i> | <i>Min</i> | <i>Max</i> |
| 8116400 | 1958-2009 | 23 | 9 | 1.37 | 1.99 | 0.15 | 9.38 | 0.79 | 0.03 | 0.75 | 0.83 |
| 8111700 | 1963-1992 | 29 | 377 | 1.16 | 0.75 | 0.13 | 3.08 | 0.65 | 0.32 | 0.28 | 1.73 |
| 8115000 | 1947-1996 | 49 | 48 | 0.30 | 0.20 | 0.02 | 0.82 | 0.87 | 0.12 | 0.67 | 1.06 |
| 8115500 | 1947-2053 | 6 | 24 | 0.14 | 0.18 | 0.00 | 0.49 | 0.69 | 0.04 | 0.63 | 0.79 |
| 8117500 | 1954-2009 | 55 | 722 | 1.69 | 1.14 | 0.13 | 7.23 | 0.84 | 0.30 | 0.28 | 1.77 |
| 8160800 | 1962-2009 | 47 | 17 | 0.69 | 0.46 | 0.07 | 2.14 | 0.53 | 0.10 | 0.39 | 0.75 |
| 8162600 | 1970-2009 | 39 | 158 | 1.38 | 0.46 | 0.64 | 2.52 | 0.70 | 0.12 | 0.47 | 1.06 |
| 8163500 | 1939-1991 | 52 | 107 | 0.64 | 0.49 | 0.05 | 2.05 | 0.30 | 0.06 | 0.20 | 0.43 |
| 8164000 | 1938-2009 | 53 | 707 | 0.96 | 0.72 | 0.03 | 2.91 | 0.37 | 0.12 | 0.12 | 0.83 |
| 8164300 | 1961-2009 | 48 | 332 | 0.90 | 0.54 | 0.13 | 2.16 | 0.41 | 0.12 | 0.20 | 0.75 |
| 8164370 | 1996-2000 | 4 | 105 | 1.17 | 0.13 | 1.02 | 1.26 | 0.60 | 0.15 | 0.28 | 0.87 |
| 8164390 | 1996-2009 | 4 | 28 | 1.36 | 0.68 | 0.60 | 1.94 | 0.59 | 0.14 | 0.28 | 0.87 |
| 8164450 | 1977-2009 | 32 | 301 | 0.63 | 0.53 | 0.08 | 2.04 | 0.42 | 0.15 | 0.16 | 0.83 |
| 8164503 | 1977-1998 | 21 | 168 | 0.95 | 0.51 | 0.19 | 2.21 | 0.42 | 0.15 | 0.20 | 0.98 |
| 8164504 | 1996-2009 | 13 | 53 | 0.45 | 0.27 | 0.27 | 0.76 | 0.60 | 0.15 | 0.31 | 0.91 |
| 8164600 | 1970-2009 | 39 | 90 | 0.52 | 0.39 | 0.01 | 1.84 | 0.61 | 0.07 | 0.47 | 0.75 |
| 8164800 | 1970-2009 | 39 | 98 | 0.19 | 0.20 | 0.01 | 1.04 | 0.37 | 0.11 | 0.20 | 0.55 |
| 8176550 | 1984-1988 | 4 | 168 | 0.56 | 0.26 | 0.33 | 0.92 | 0.32 | 0.11 | 0.16 | 0.63 |
| 8176900 | 1978-1995 | 5 | 189 | 0.37 | 0.37 | 0.02 | 0.97 | 0.55 | 0.20 | 0.12 | 1.18 |
| 8177300 | 1978-1990 | 12 | 28 | 0.18 | 0.11 | 0.02 | 0.34 | 0.52 | 0.13 | 0.31 | 0.83 |
| 8189200 | 1970-2009 | 39 | 62 | 0.60 | 0.78 | 0.00 | 2.62 | 0.35 | 0.11 | 0.24 | 0.55 |
| 8189300 | 1962-1976 | 14 | 203 | 0.02 | 0.02 | 0.00 | 0.08 | 0.17 | 0.09 | 0.04 | 0.39 |
| 8189500 | 1939-2009 | 47 | 495 | 0.47 | 0.36 | 0.03 | 1.26 | 0.20 | 0.06 | 0.08 | 0.35 |
| 8189700 | 1964-2009 | 45 | 243 | 0.19 | 0.11 | 0.02 | 0.44 | 0.21 | 0.06 | 0.12 | 0.35 |
| 8189800 | 1970-1990 | 20 | 134 | 0.06 | 0.10 | 0.00 | 0.42 | 0.16 | 0.06 | 0.08 | 0.31 |
| 8210400 | 1972-1988 | 16 | 156 | 0.00 | 0.00 | 0.00 | 0.00 | 0.07 | 0.03 | 0.04 | 0.12 |
| 8211520 | 1972-2009 | 37 | 74 | 0.37 | 0.12 | 0.23 | 0.68 | 0.16 | 0.05 | 0.08 | 0.24 |
| 8212400 | 1967-1984 | 17 | 484 | 0.00 | 0.00 | 0.00 | 0.01 | 0.10 | 0.04 | 0.04 | 0.28 |

Gage: USGS stream gage ID number, *Period*: period of unregulated stream flow analyzed, *Years*: number of years of baseflow analyzed, *Area*: basin area in square miles, *Mean*: mean recharge value, *Std*: interannual standard deviation, *Min*: minimum recharge value, *Max*: maximum recharge value, *Med*: median recharge value.

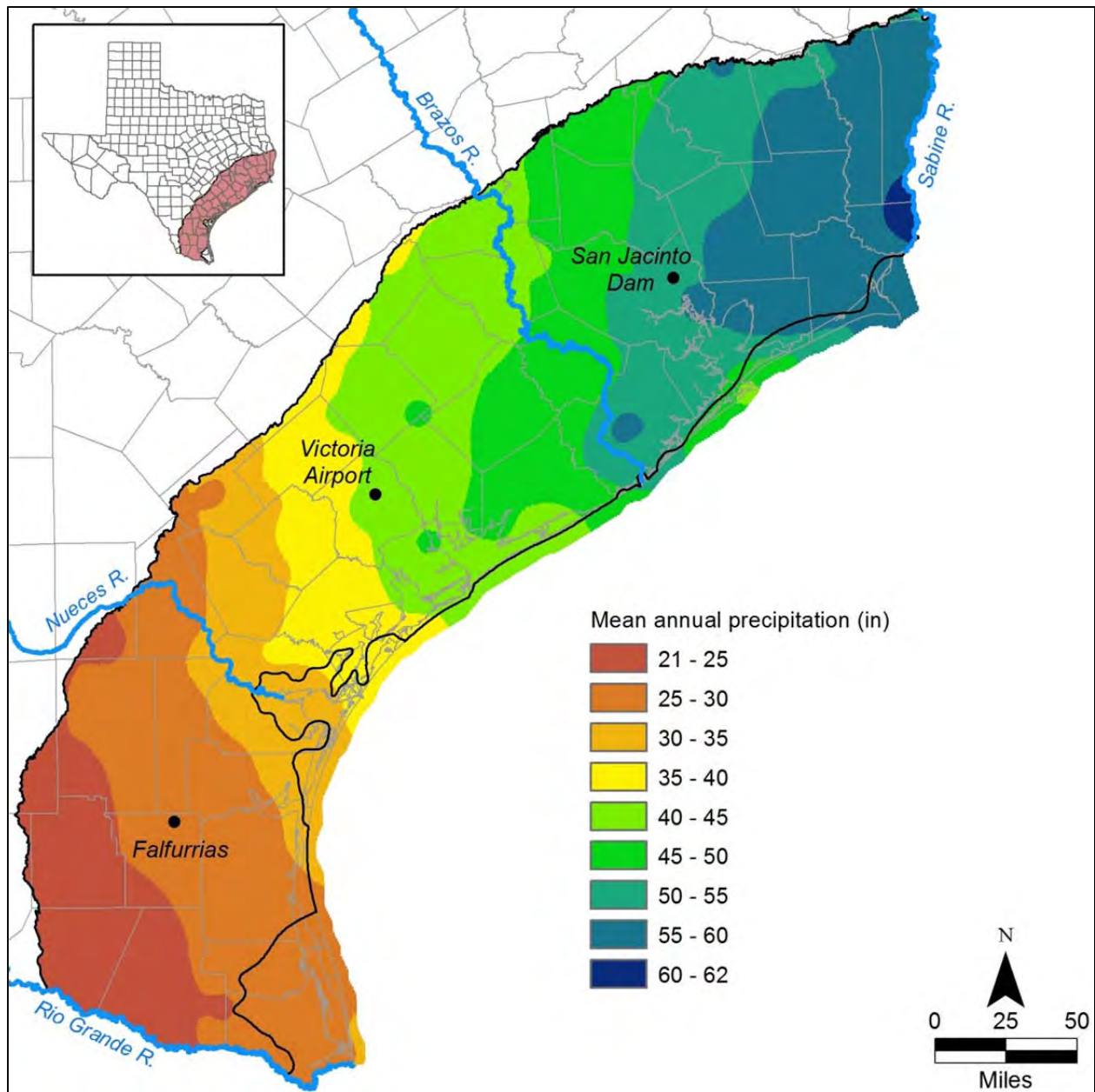


Figure 1. Mean annual precipitation in the Texas Gulf Coast region (1971 – 2000; PRISM www.prism.oregonstate.edu). Points represent locations of stations shown in Figure 2. Black lines represent extent of the Gulf Coast aquifer system study area regions bounded by the Rio Grande and Nueces Rivers (southern region), the Nueces and Brazos Rivers (central region) and the Brazos and Sabine Rivers (northern region).

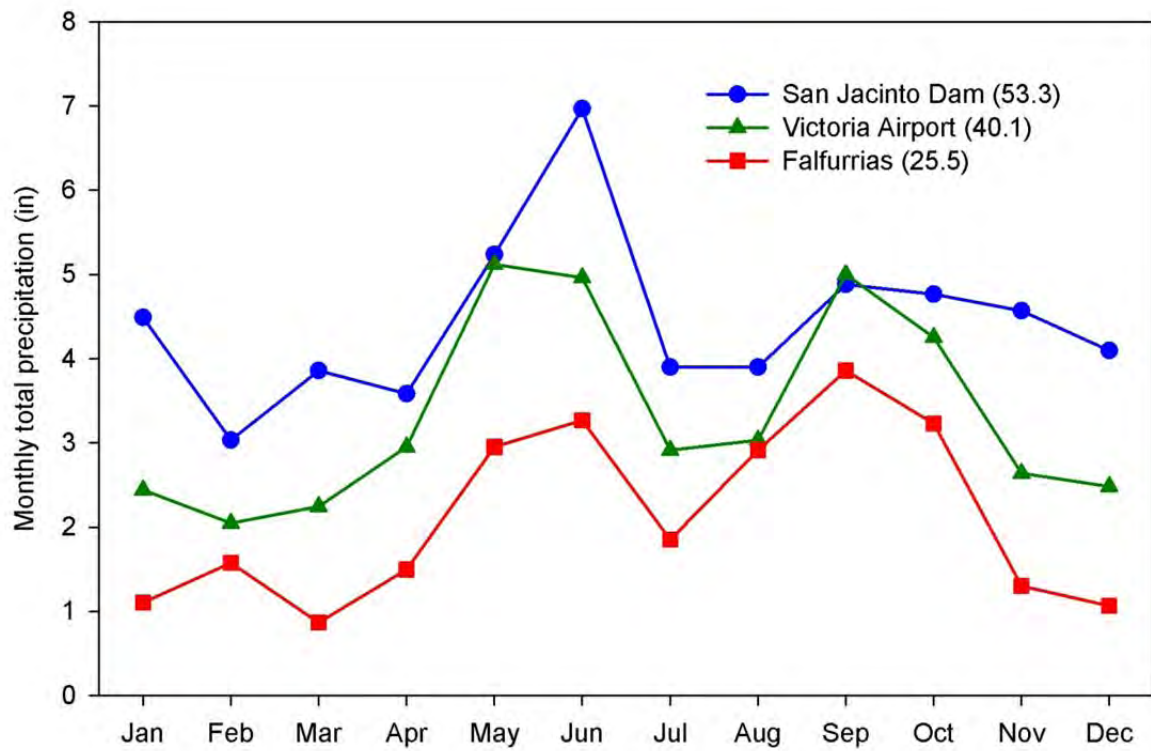


Figure 2. Distribution of mean monthly total precipitation for selected stations in the Texas Gulf Coast region (Figure 1). (1971 – 2000; PRISM www.prism.oregonstate.edu). Values shown in parenthesis represent mean total annual precipitation for each station.

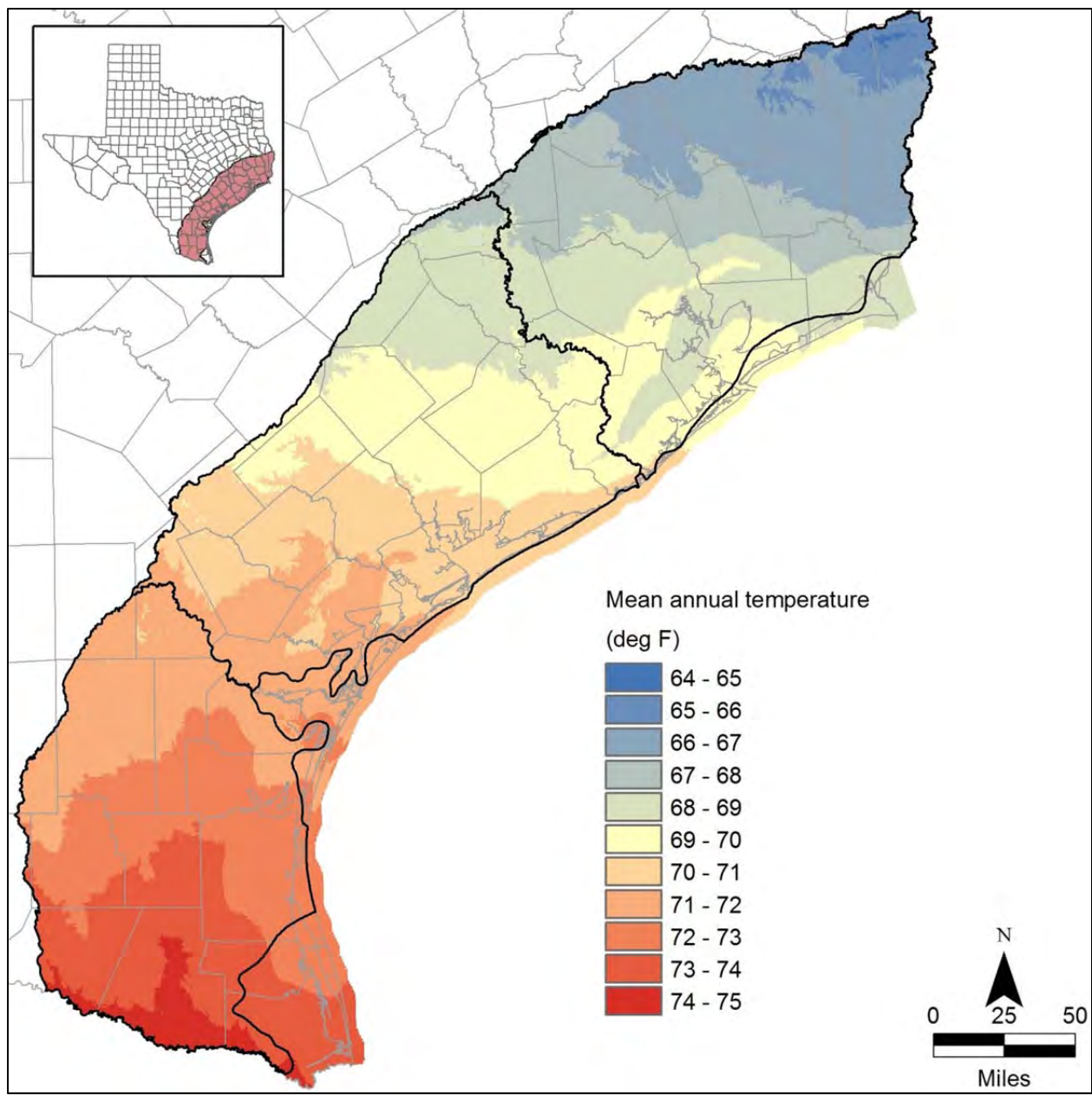


Figure 3. Mean annual temperature in the Texas Gulf Coast region (1971 – 2000; PRISM www.prism.oregonstate.edu). Black lines represent extent of the Gulf Coast aquifer system study area subdivided into southern, central, and northern regions.

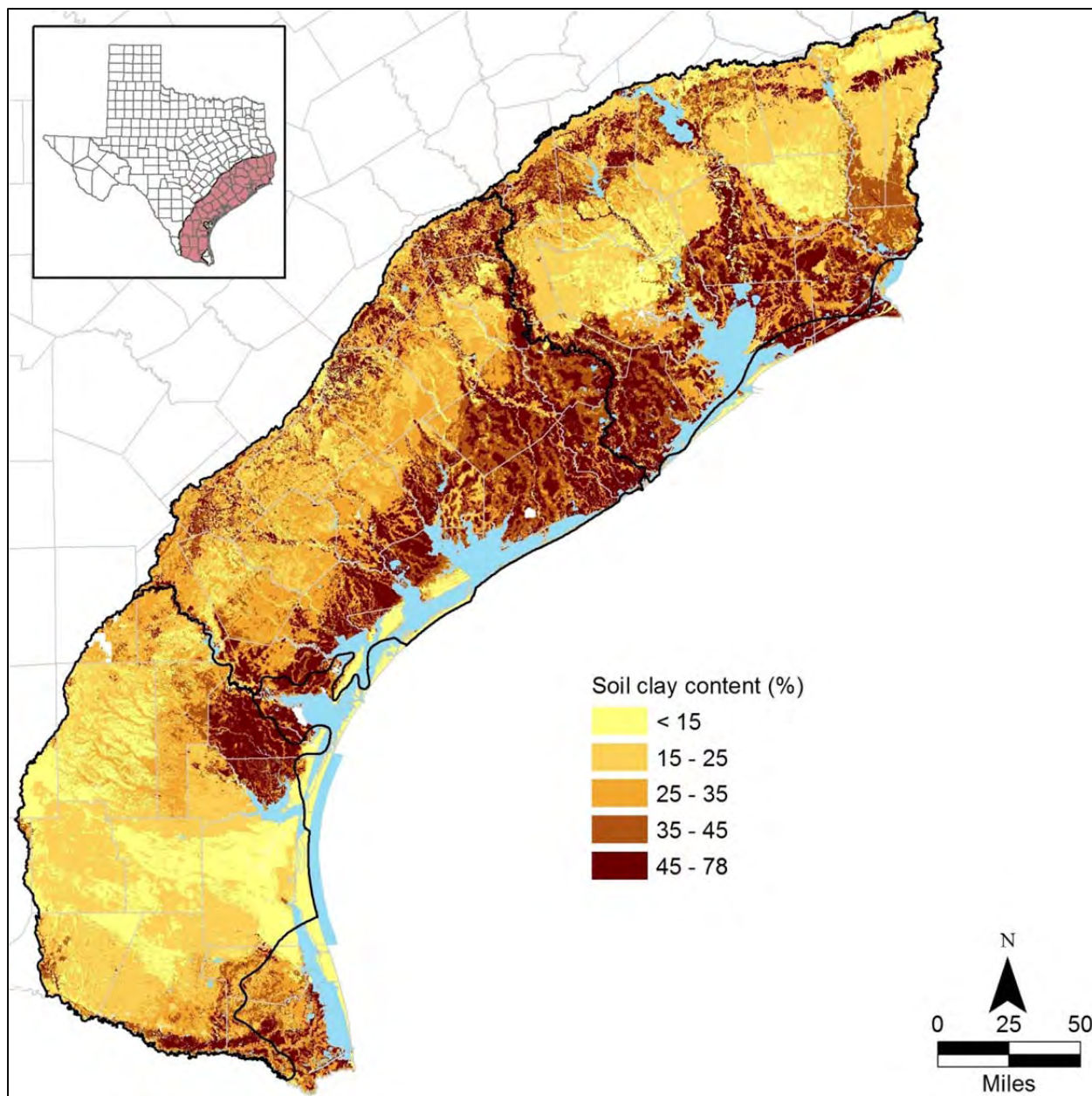


Figure 4. Distribution of soil clay content in the Texas Gulf Coast region based on SSURGO (USDA, 1995). Black lines represent extent of the Gulf Coast aquifer system study area subdivided into southern, central, and northern regions. Blue regions represent water-covered areas defined in the SSURGO database.

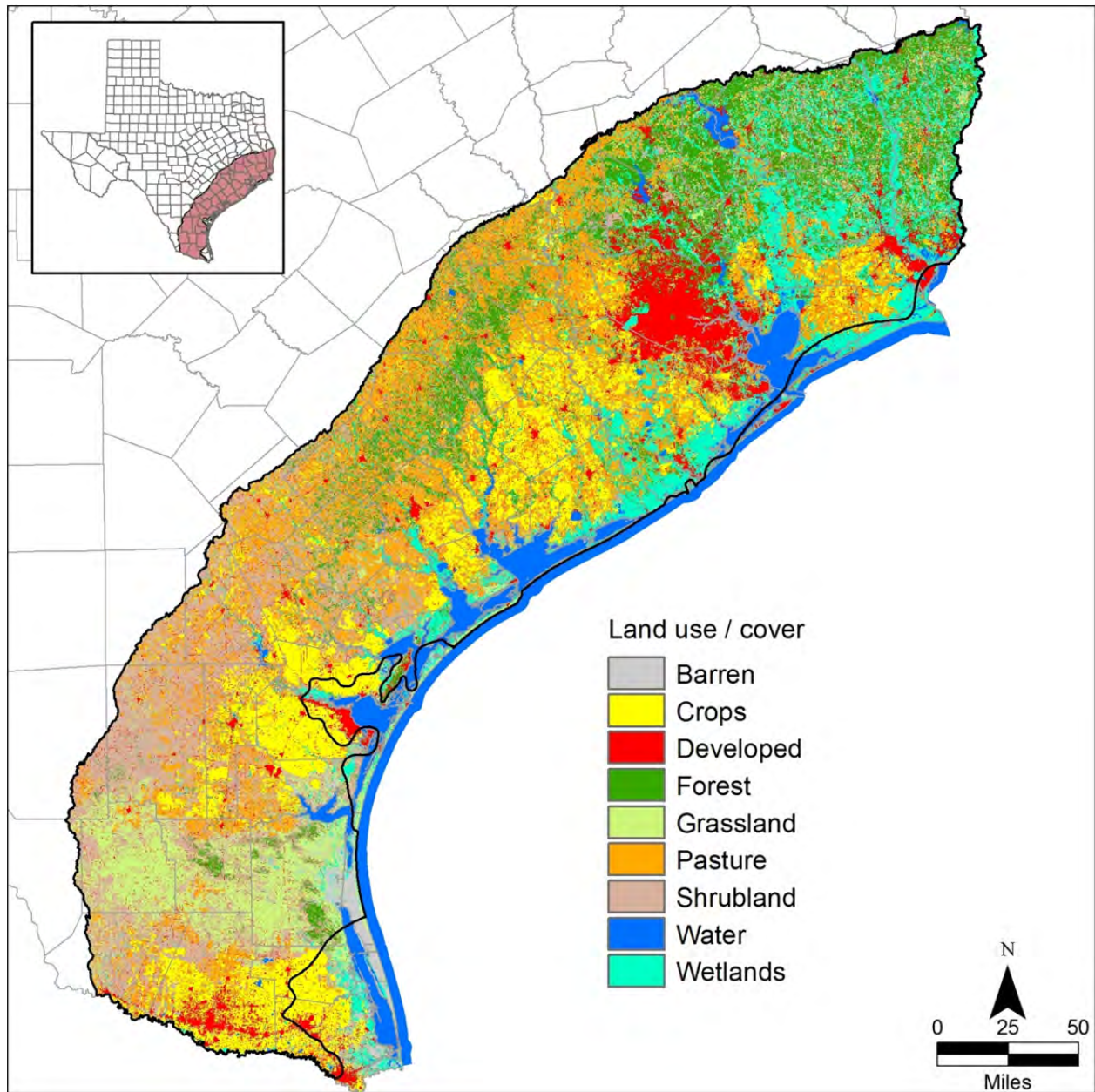


Figure 5. Distribution of land use / cover in the Texas Gulf Coast region based on National Land Cover Database (NLCD, 2001). Black lines represent extent of the Gulf Coast aquifer system study area subdivided into southern, central, and northern regions.

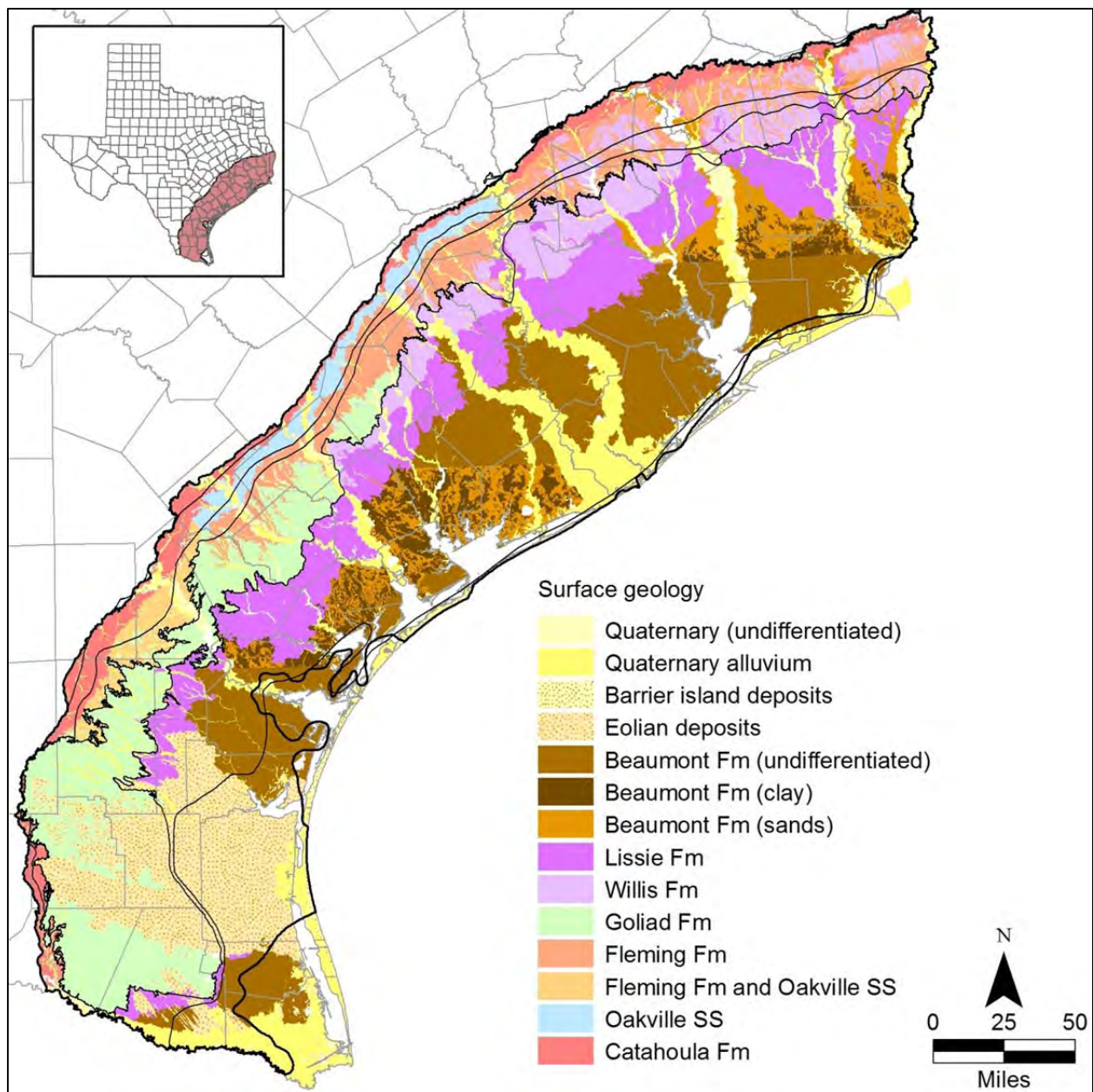


Figure 6. Surface geology map of the Texas Gulf Coast region (Geologic Atlas of Texas, Bureau of Economic Geology, 2002). Wide black lines represent the extent of the Gulf Coast aquifer. Narrow black lines represent the outcrop areas of the Jasper, Evangeline, and Chicot aquifers. SS: sandstone, Fm: formation.

| System | Series | Stratigraphic Units | | Groundwater Sources | Hydrogeologic Units |
|---------------------|-------------|------------------------------------|--------------------------------|---|-----------------------------|
| | | | | Baker and Dale (1961) | Baker (1979) |
| Quaternary | Holocene | Alluvium | | Lower Rio Grande Groundwater Reservoir | Chicot aquifer |
| | Pleistocene | Beaumont Clay | | *Mercedes-Sebastian Groundwater Reservoir | |
| | | Lissie Formation | Montgomery Formation | *Linn-Faysville Groundwater Reservoir | |
| | | | Bentley Formation | | |
| | | Willis Sand | | | |
| Tertiary | Pliocene | Goliad Sand | | *Linn-Faysville Groundwater Reservoir | Evangeline aquifer |
| | Miocene | Fleming Formation/ Lagarto Clay | | Oakville Sandstone | Burkeville Confining System |
| | | Oakville Sandstone | | | |
| | | Oakville Sandstone | | | |
| | Oligocene | 1 Catahoula tuff or sandstone | 2 Upper part of Catahoula tuff | | Catahoula Confining System |
| 2 Anahuac Formation | | | | | |
| 2 Frio Formation | | | | | |
| 1 Frio Clay | | 2 Vicksburg Group equivalent | | | |

1 = outcrop

2 = subsurface

* includes the Lower Rio Grande Groundwater Reservoir

Figure 7. Stratigraphic and hydrostratigraphic classification of the Gulf Coast aquifer in south Texas (after Baker and Dale, 1961; Baker, 1979).

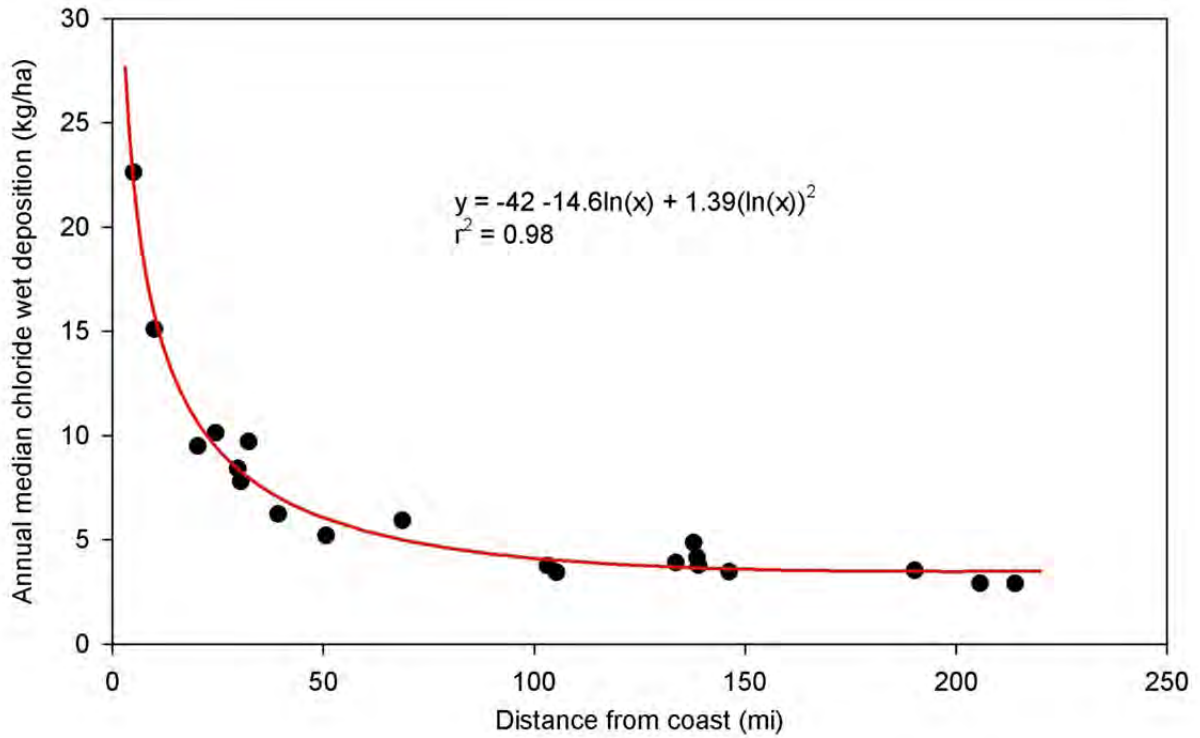


Figure 8. Relationship between annual median chloride wet deposition and distance from the US Gulf of Mexico coastline based for monitoring stations of the National Atmospheric Deposition Program (NADP).

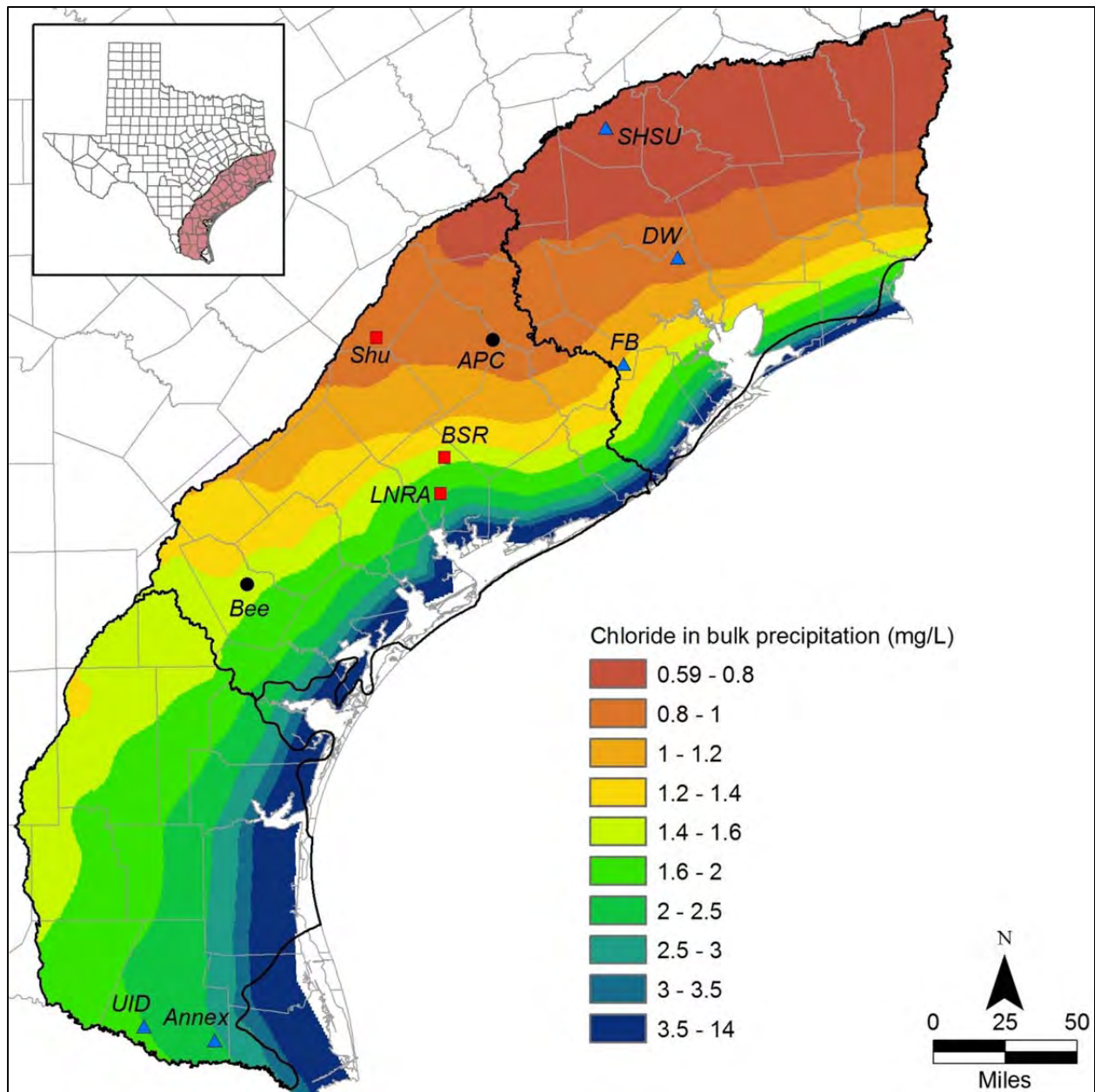


Figure 9. Estimated distribution of mean annual chloride concentrations in bulk precipitation in the study area based on mass deposition (Figure 8, equation 8) and the distribution of mean annual precipitation (Figure 1). Wet chloride deposition from NADP was multiplied by two to account for dry deposition. Points represent locations of open (bulk) precipitation collectors at the NADP sites (circles), and at sites hosted by the Lavaca-Navidad River Authority (LNRA, squares) and by the TexasET Network (Texas A&M University, triangles).

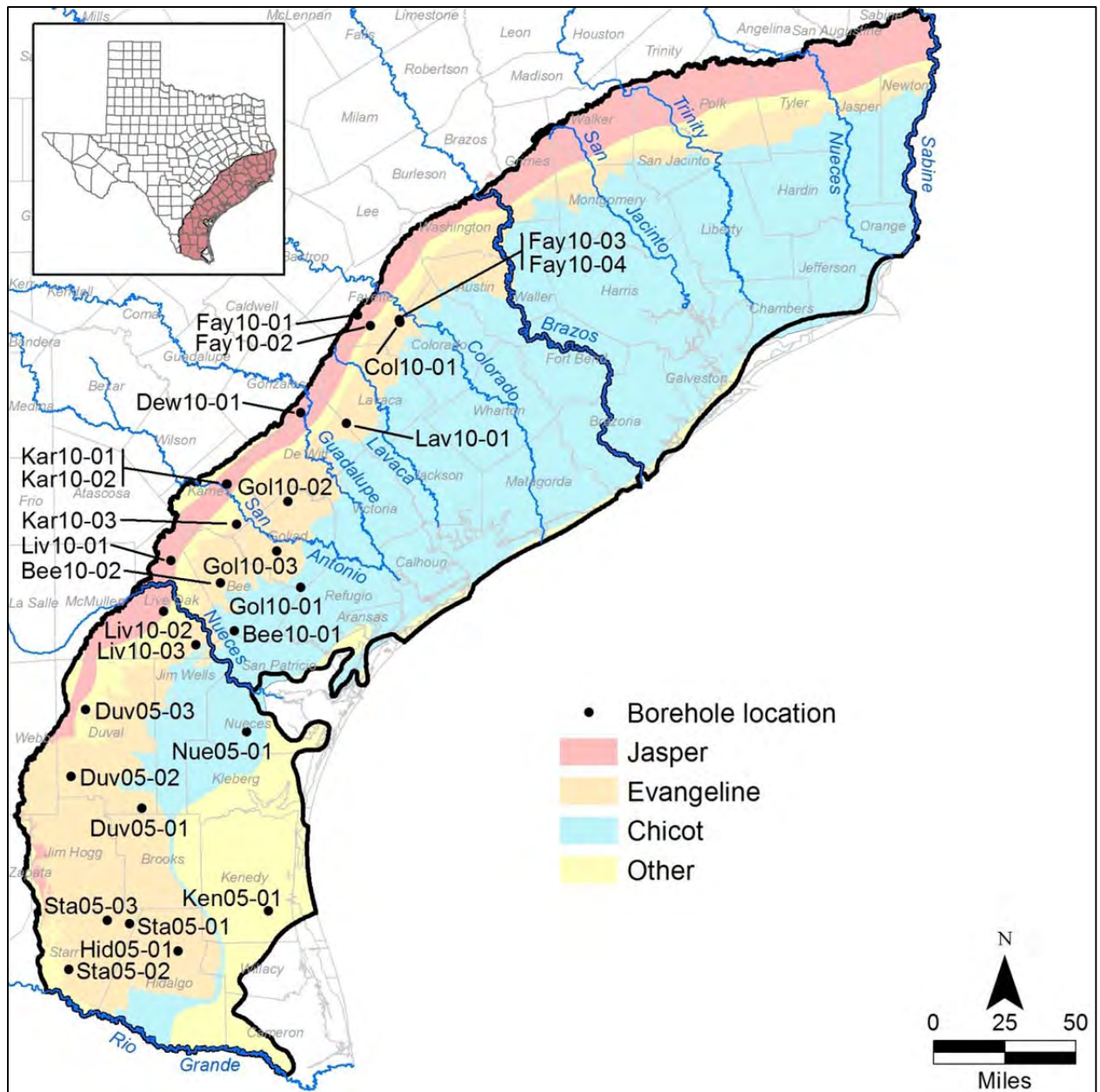


Figure 10. Location of 27 boreholes drilled for unsaturated zone sampling. Borehole names include first three letters of county names. Major rivers and county names are also shown for reference. Black lines represent extent of the Gulf Coast aquifer system study area subdivided into southern, central, and northern regions.

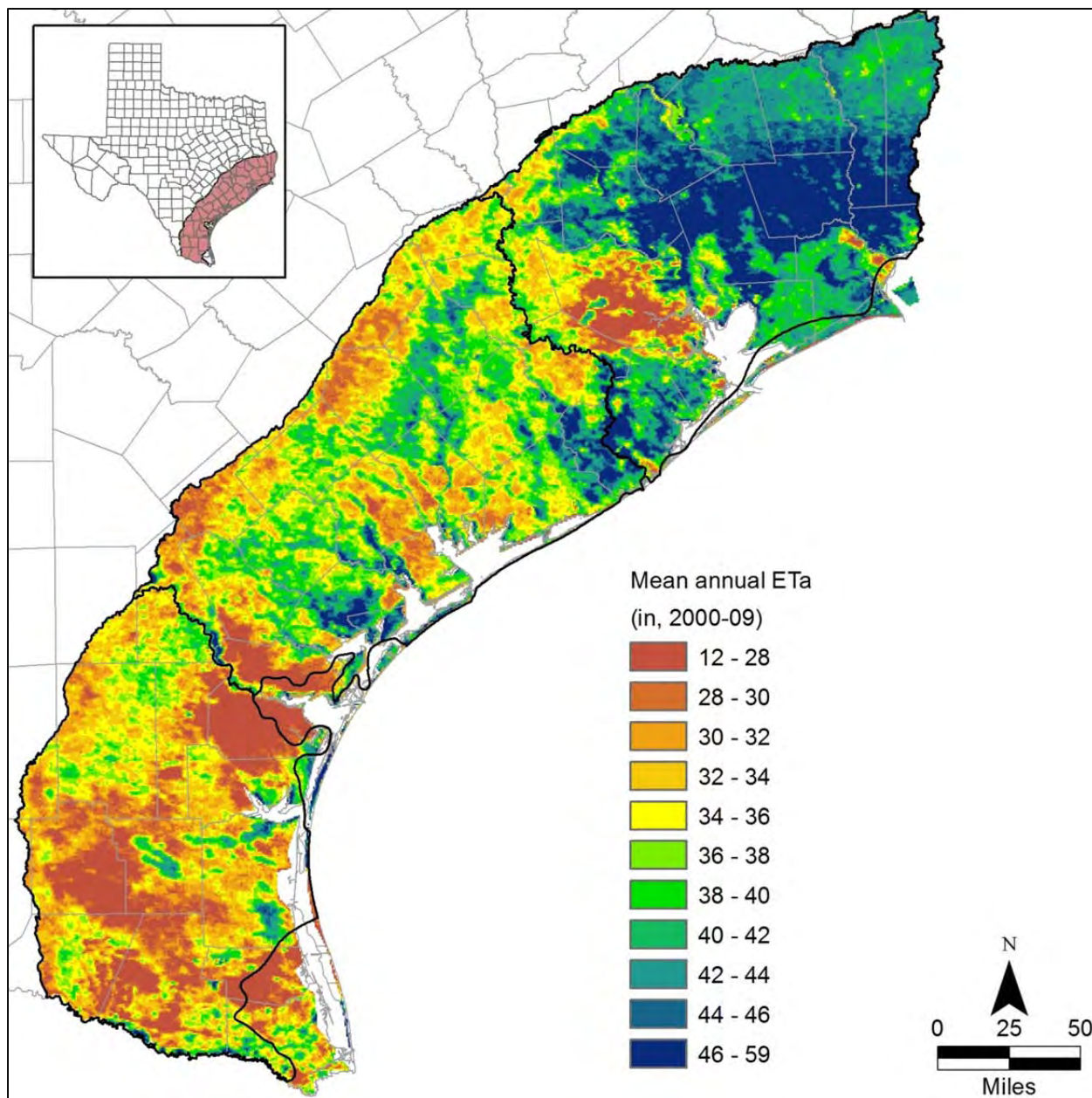


Figure 11. Mean annual actual ET (ETa) in the Texas Gulf Coast region for the period 2000-2009 based on MODIS satellite imagery. Black lines represent extent of the Gulf Coast aquifer system study area subdivided into southern, central, and northern regions.

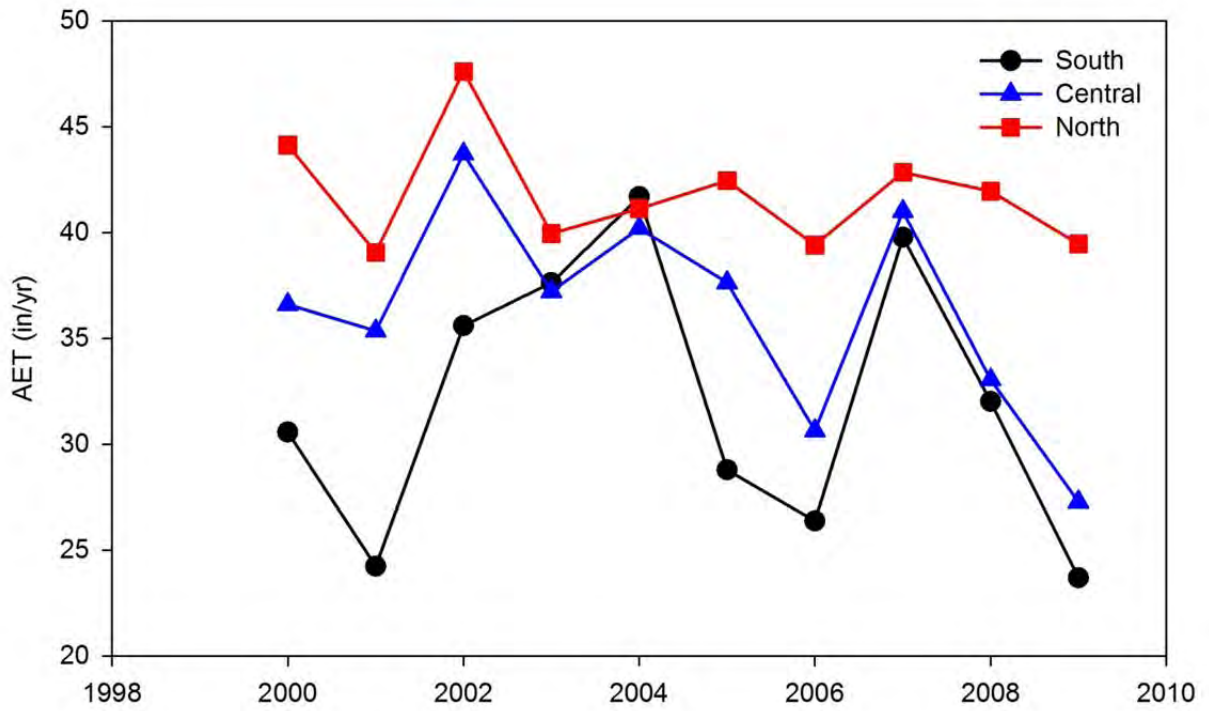


Figure 12. Annual actual ET (AET) in the south, central, and north regions of the Texas Gulf Coast region for the period 2000-2009.

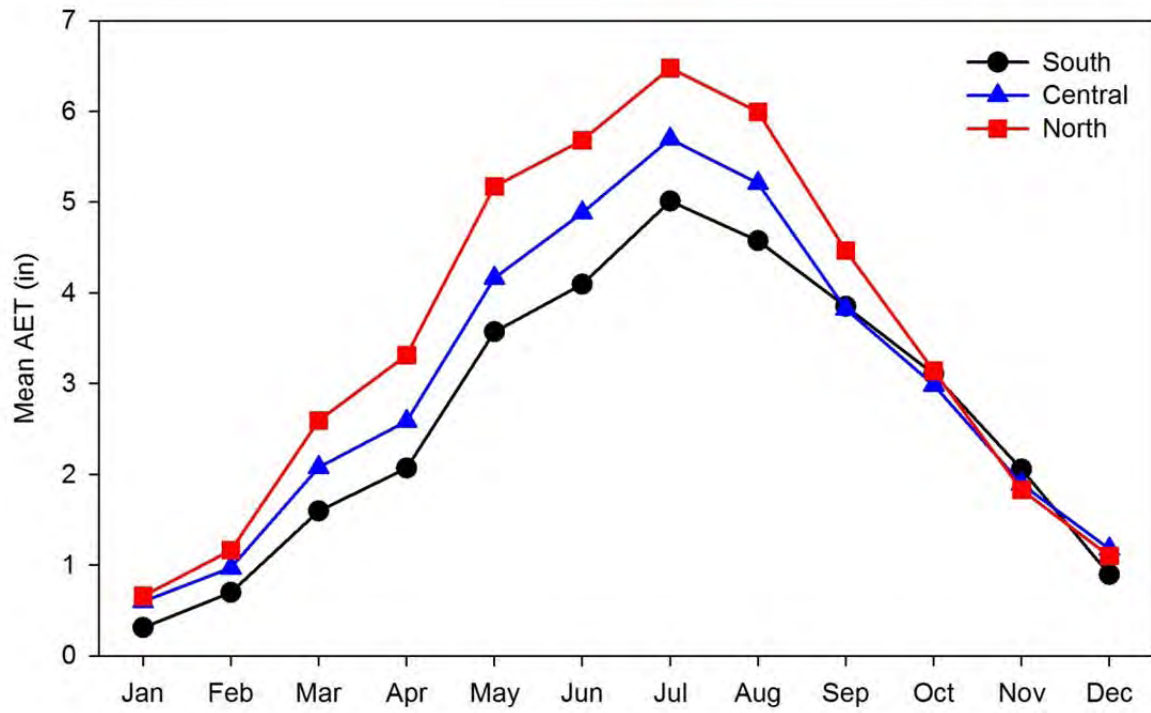


Figure 13. Mean monthly actual ET (AET) in the south, central, and north regions of the Texas Gulf Coast region for the period 2000-2009.

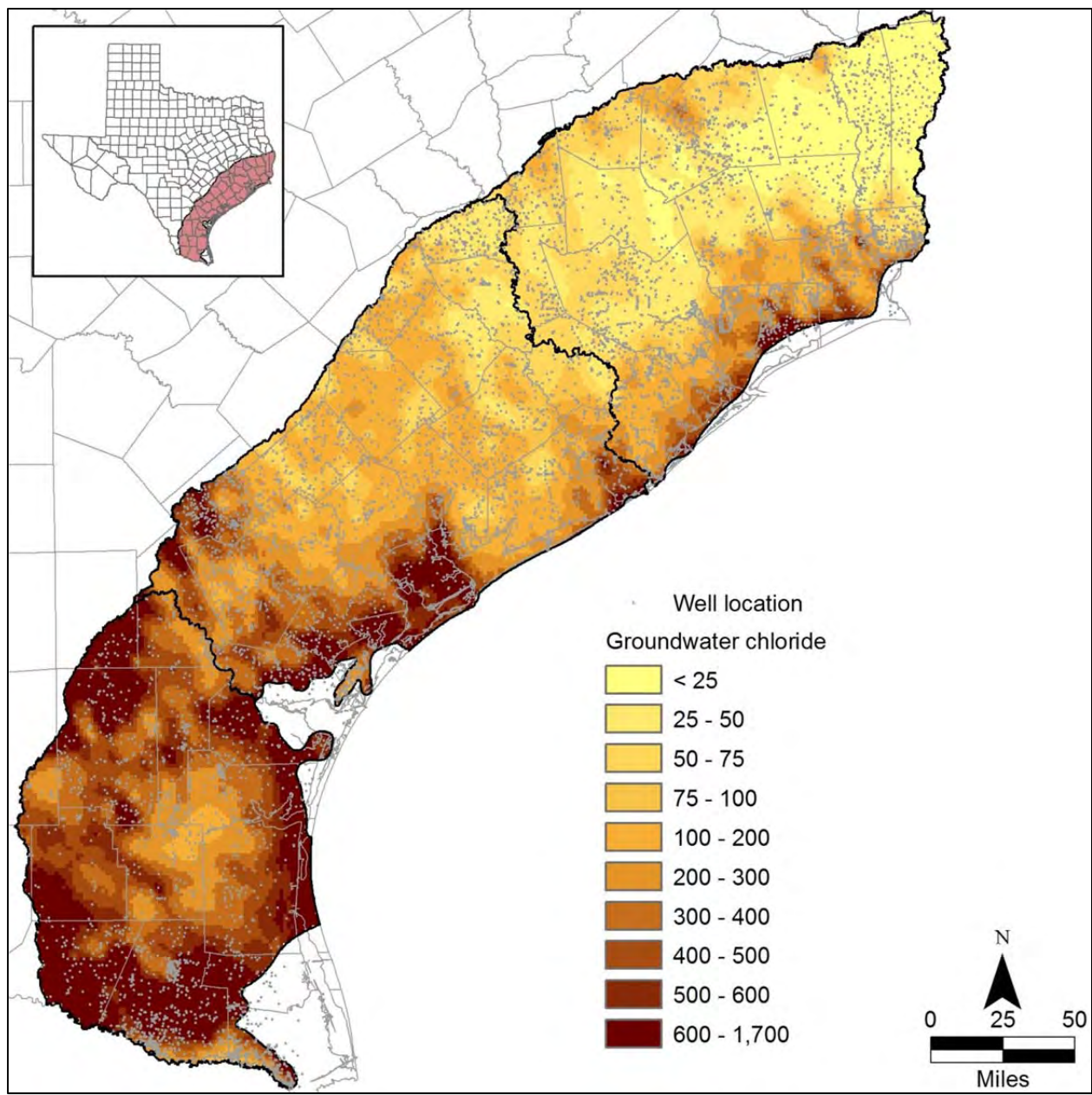


Figure 14. Distribution of groundwater chloride concentrations in the Gulf Coast aquifer based on samples from 8,721 wells. Black lines represent extent of the Gulf Coast aquifer system study area subdivided into southern, central, and northern regions.

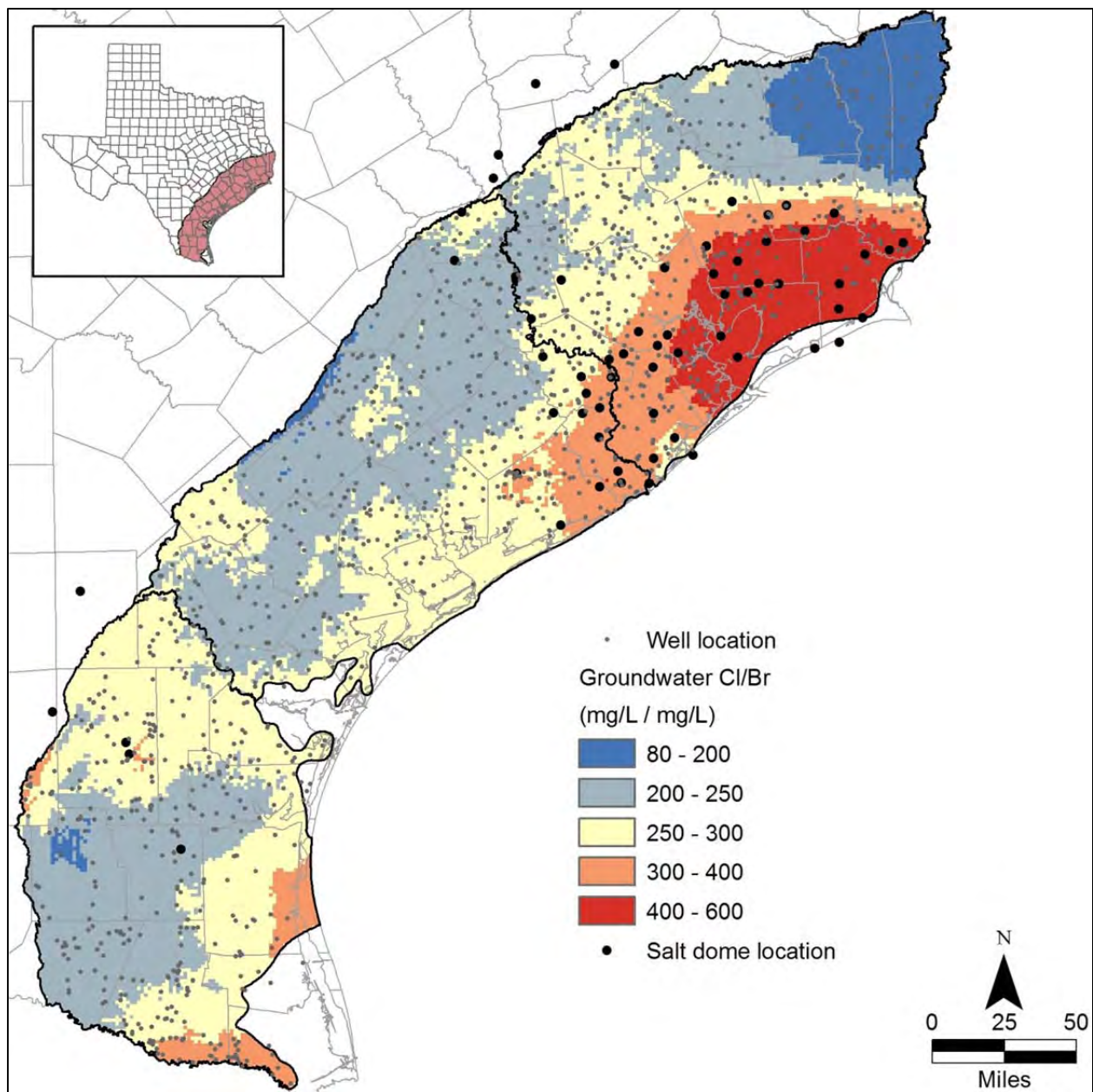


Figure 15. Distribution of groundwater Cl/Br concentration mass ratios in the Gulf Coast aquifer based on samples from 1,339 wells. Black lines represent extent of the Gulf Coast aquifer system study area subdivided into southern, central, and northern regions.

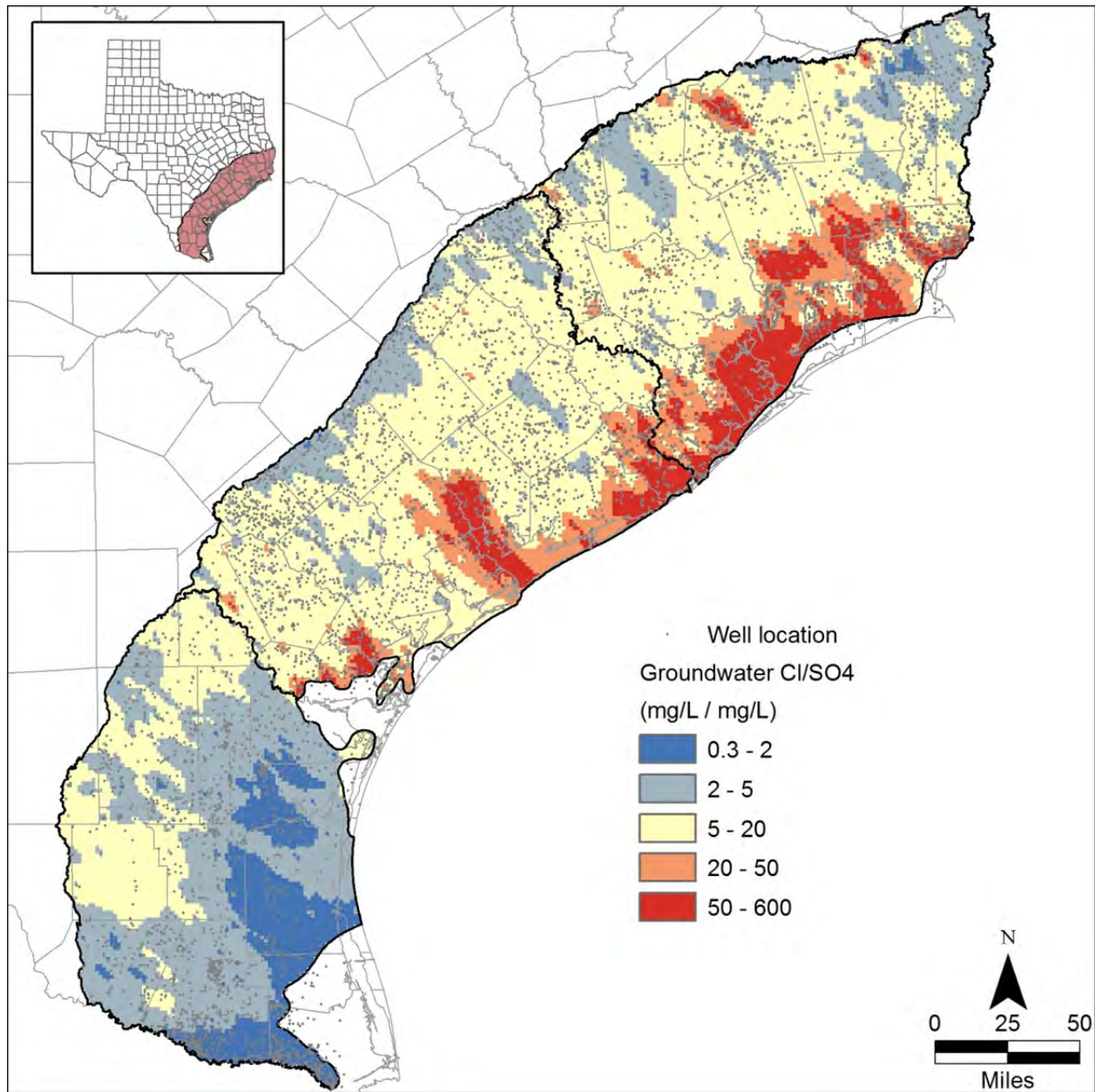


Figure 16. Distribution of groundwater Cl/SO₄ concentration mass ratios in the Gulf Coast aquifer based on samples from 8,086 wells. Black lines represent extent of the Gulf Coast aquifer system study area subdivided into southern, central, and northern regions.

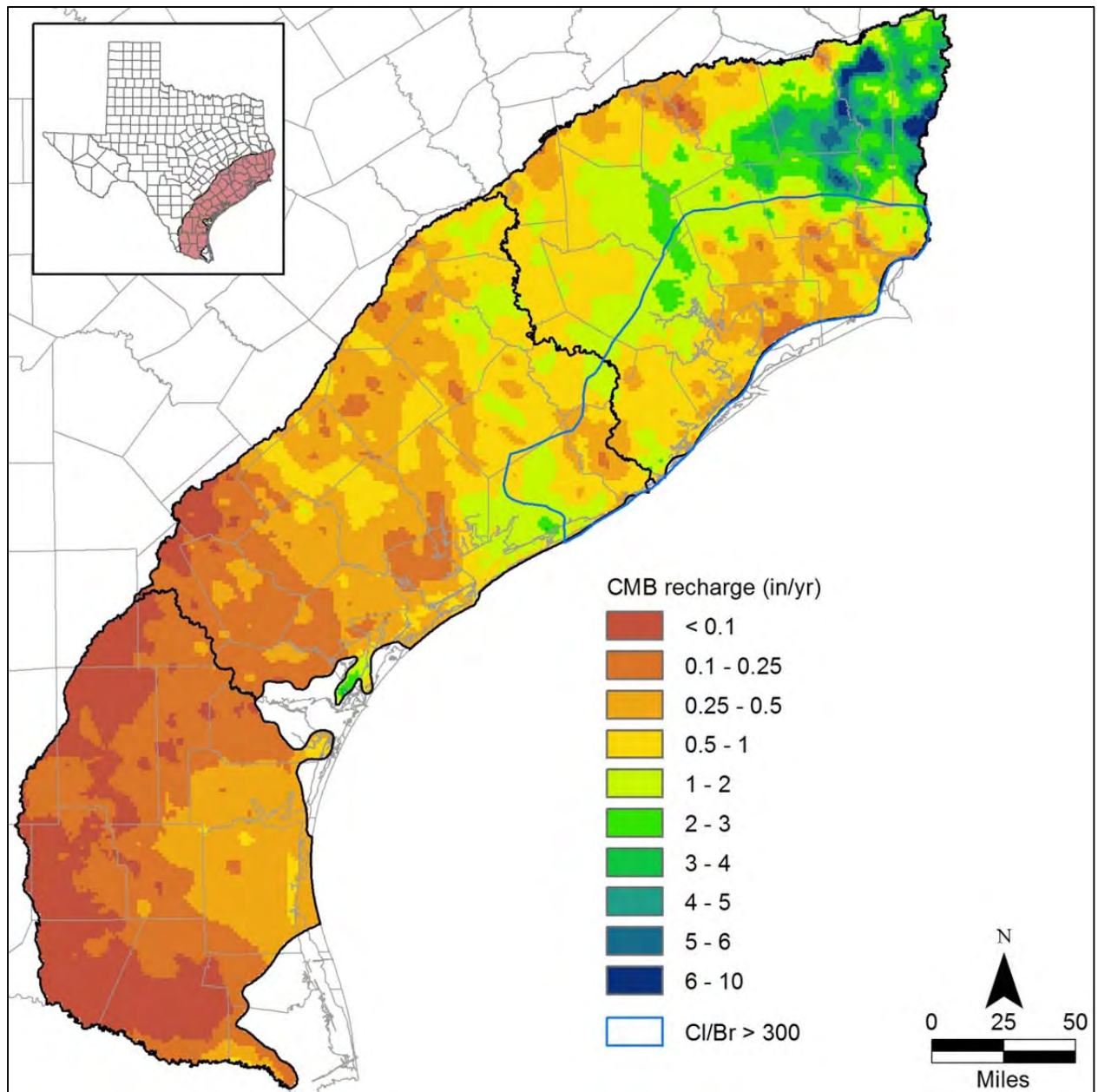


Figure 17. Distribution of groundwater chloride mass balance (CMB) recharge rates based on groundwater chloride concentrations (Figure 14) and chloride concentration in bulk precipitation (Figure 9) in the Gulf Coast aquifer system. Blue line delineates northern region where $Cl/Br > 300$ (Figure 15). Black lines represent extent of the Gulf Coast aquifer system study area subdivided into southern, central, and northern regions.

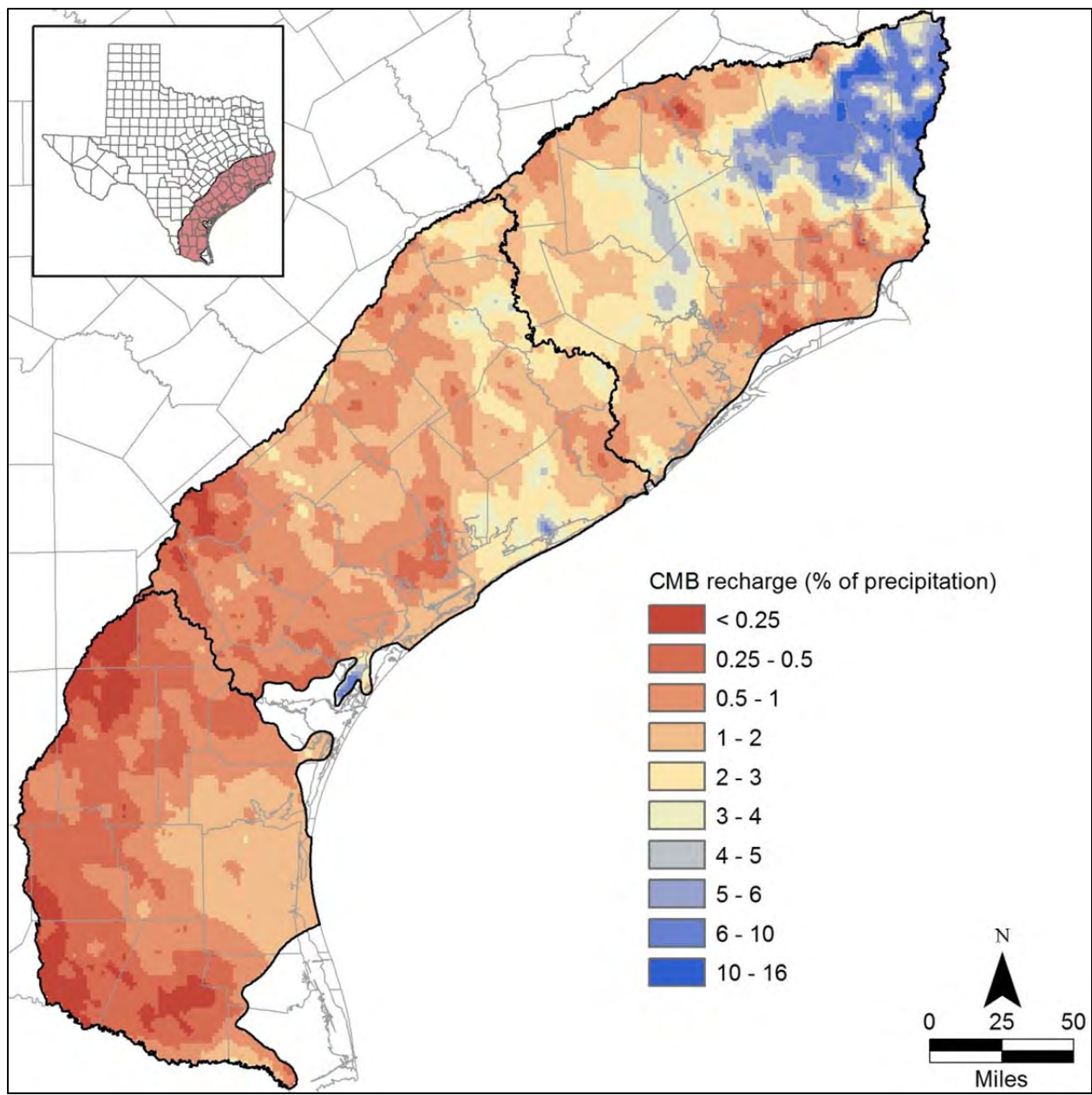


Figure 18. Distribution of groundwater chloride mass balance (CMB) recharge rates expressed as a percentage of annual average precipitation (Figure 1) in the Gulf Coast aquifer system. Black lines represent extent of the Gulf Coast aquifer system study area subdivided into southern, central, and northern regions.

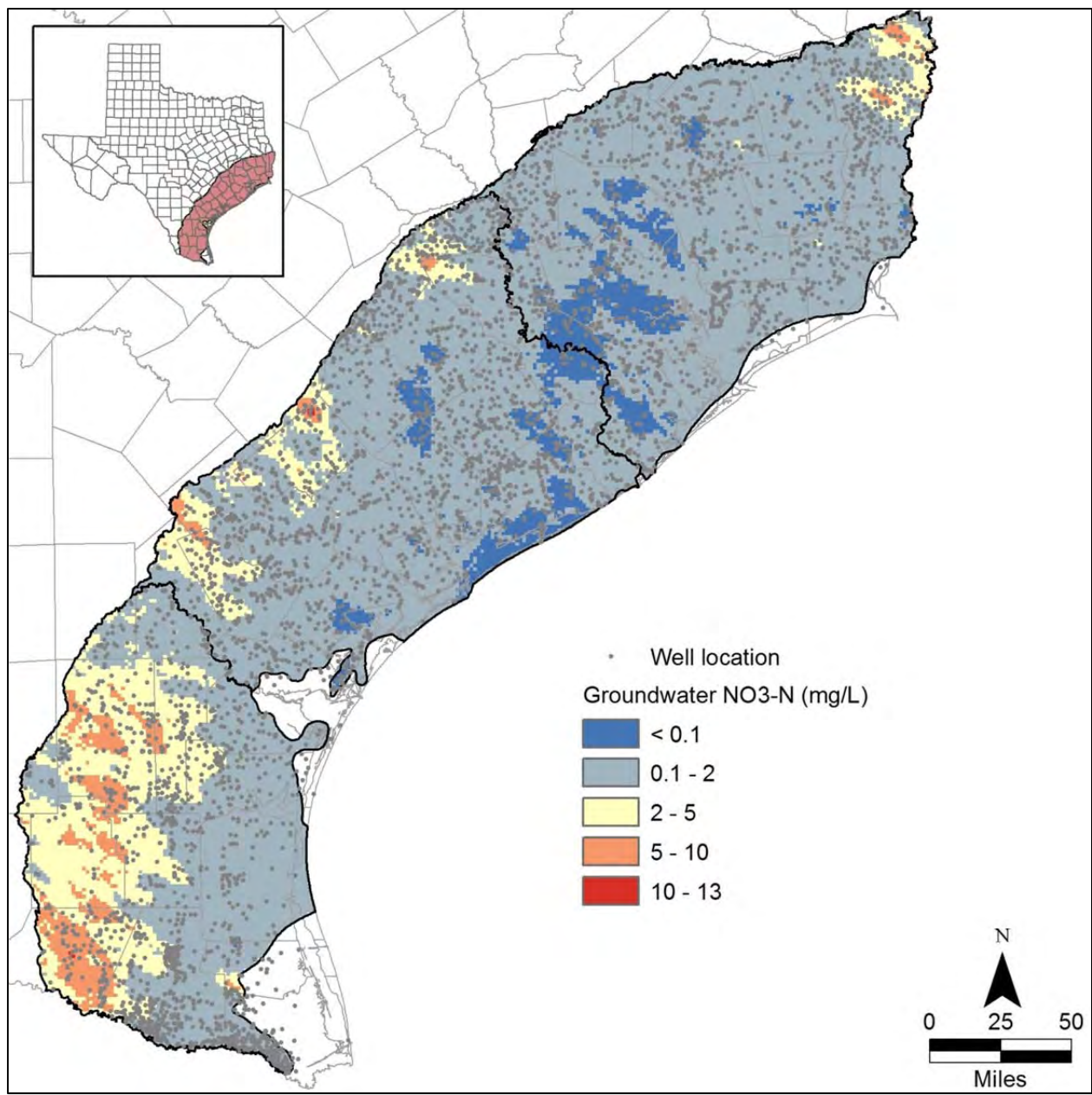


Figure 19. Distribution of groundwater nitrate-N (NO₃-N) concentrations in the Gulf Coast aquifer system based on samples from 3,887 wells. Black lines represent extent of the Gulf Coast aquifer system study area subdivided into southern, central, and northern regions.

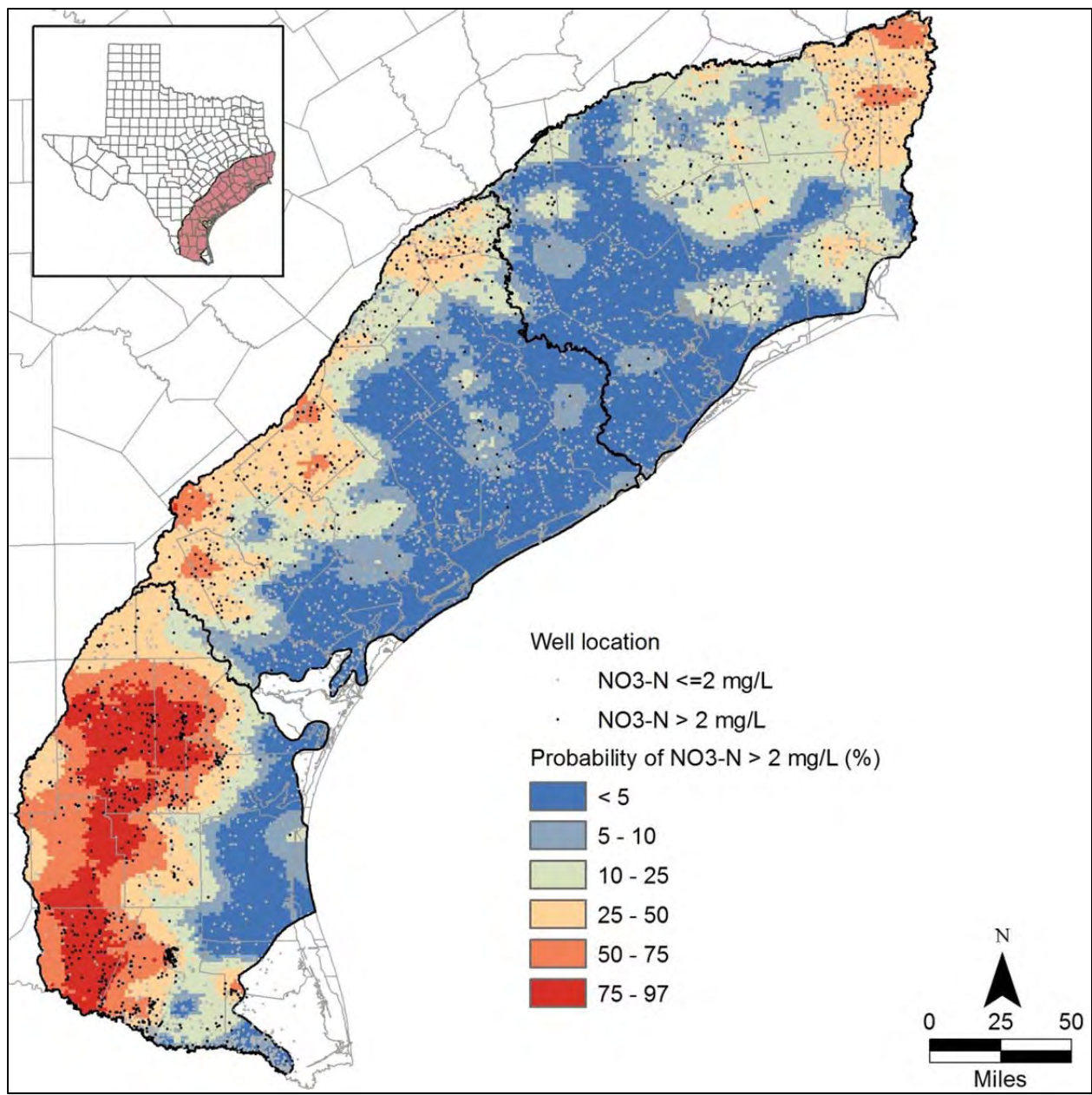


Figure 20. Probability of groundwater NO₃-N concentrations exceeding the nominal background concentration of 2 mg/L in the Gulf Coast aquifer system based on samples from 5,787 wells (includes all well locations shown in Figure 19 and an additional 1,900 locations having sample analyses below a detection limit of 2 mg/L). Black lines represent extent of the Gulf Coast aquifer system study area subdivided into southern, central, and northern regions.

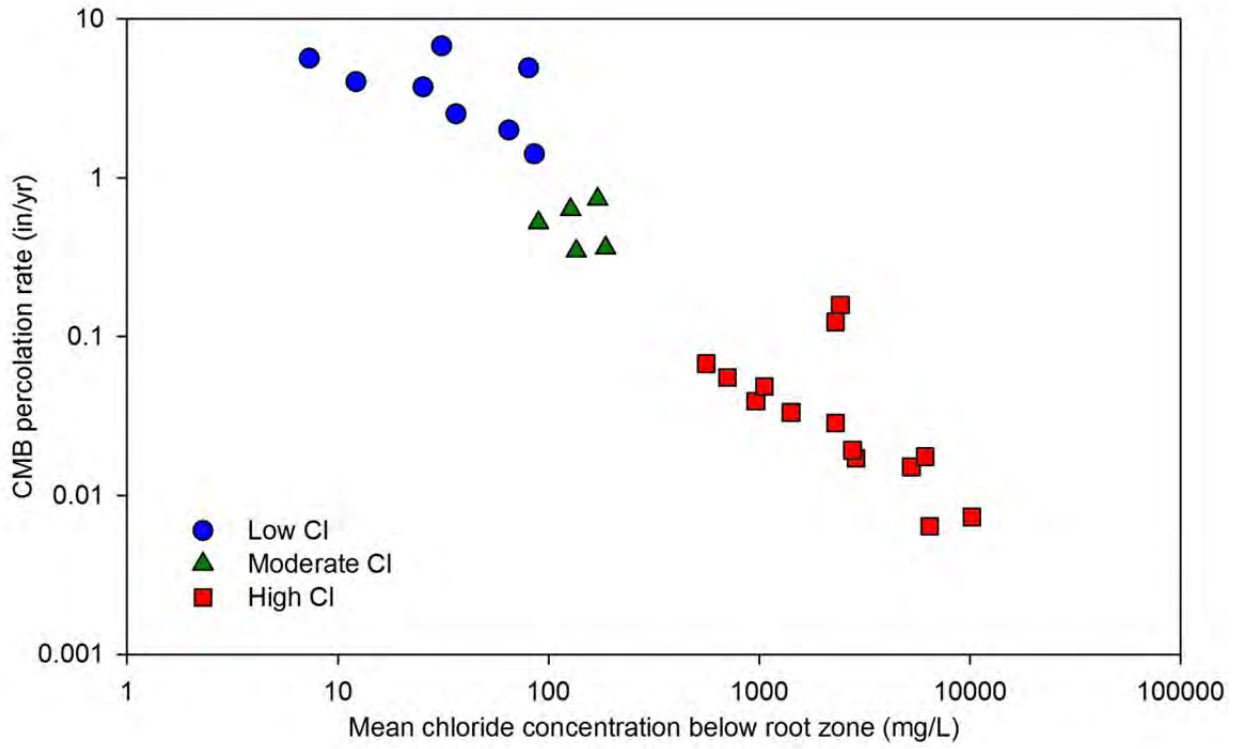


Figure 21. Relationship between unsaturated mean chloride concentrations below the root zone and resulting calculated chloride mass balance (CMB) percolation rate.

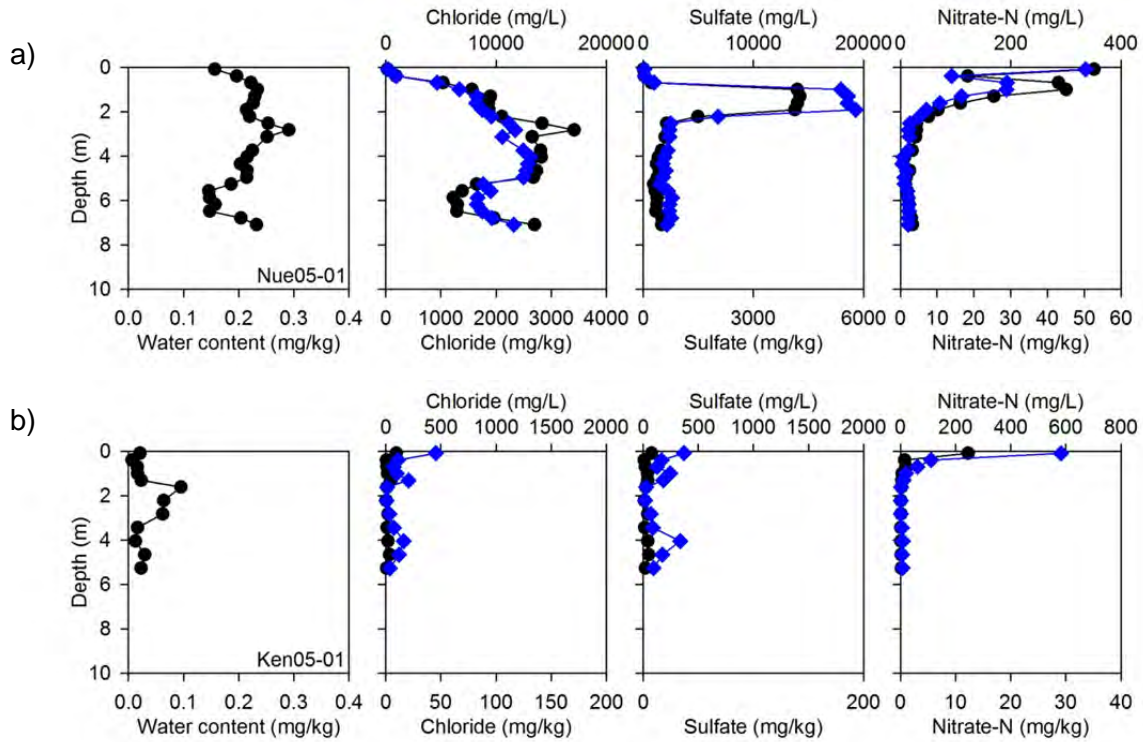


Figure 22. Unsaturated zone profiles of water content and chloride, sulfate, and nitrate-N concentrations for two boreholes located in the coastal area of the southern region in a) cultivated and b) coastal forest settings. Circle symbols represent mg/L values and diamond symbols represent mg/kg values. Borehole locations shown in Figure 10.

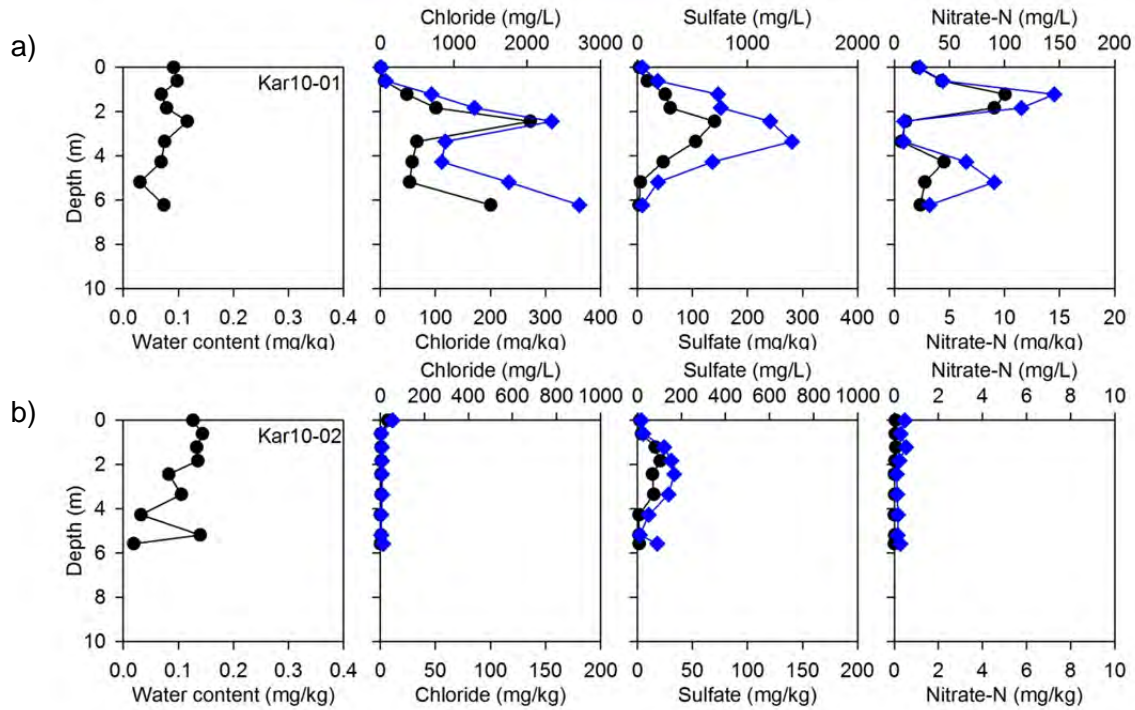


Figure 23. Unsaturated zone profiles of water content and chloride, sulfate, and nitrate-N concentrations for two boreholes located near the southern inland margin of the central region in a) pastureland and b) previously cultivated pastureland settings. The two boreholes are separated by ~300 ft and have similar texture profiles. Circle symbols represent mg/L values and diamond symbols represent mg/kg values. Borehole locations shown in Figure 10.

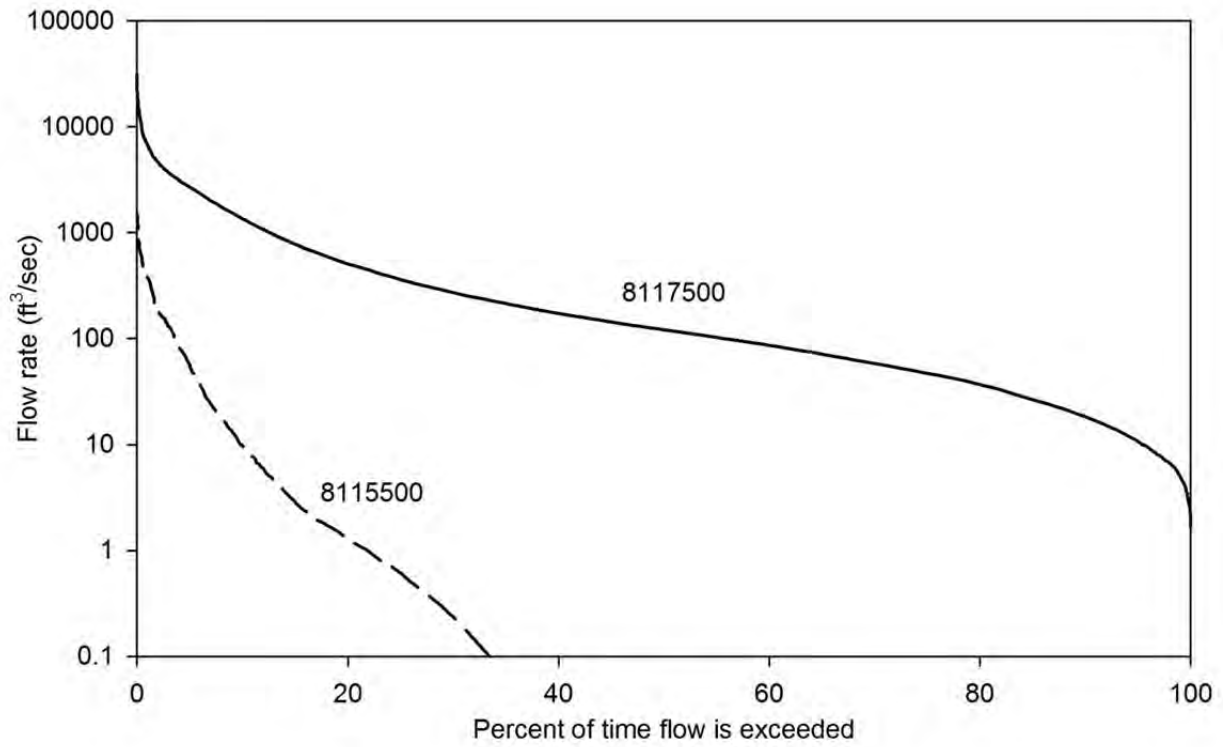


Figure 24. Example flow duration curves for two gauging stations in the study area (Figure 26). The solid line represents perennial flow conditions, with flow occurring at all times. The dashed line represents intermittent flow conditions, with flow occurring about 35% of the time.

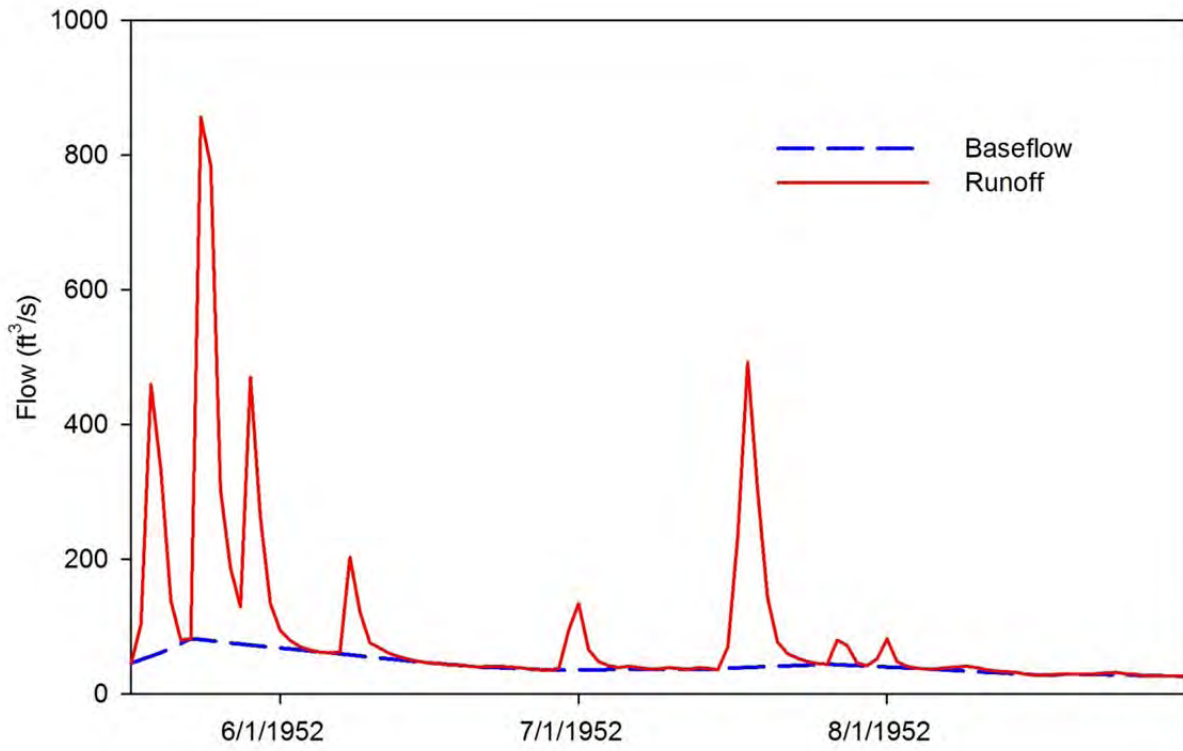


Figure 25. Baseflow separation performed with BFI on USGS Gage No. 8029500 (Figure 26).

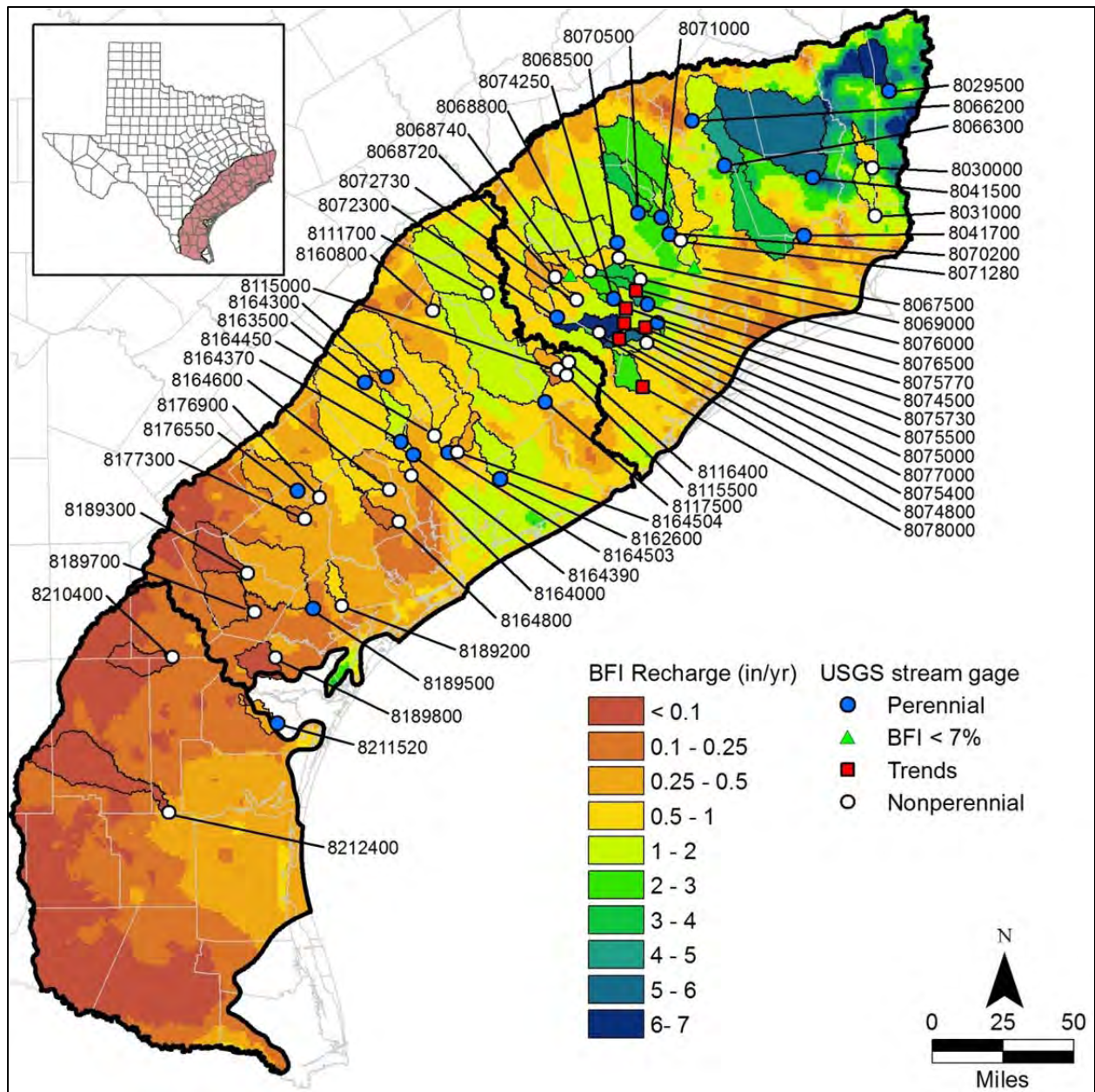


Figure 26. Distribution of streamflow hydrograph separation recharge rates based on the BFI analysis and USGS stream gage station locations and identification numbers. Recharge distribution based on the groundwater CMB results (Figure 17) is shown for reference. Relationship between BFI and CMB recharge rates shown in Figure 27.

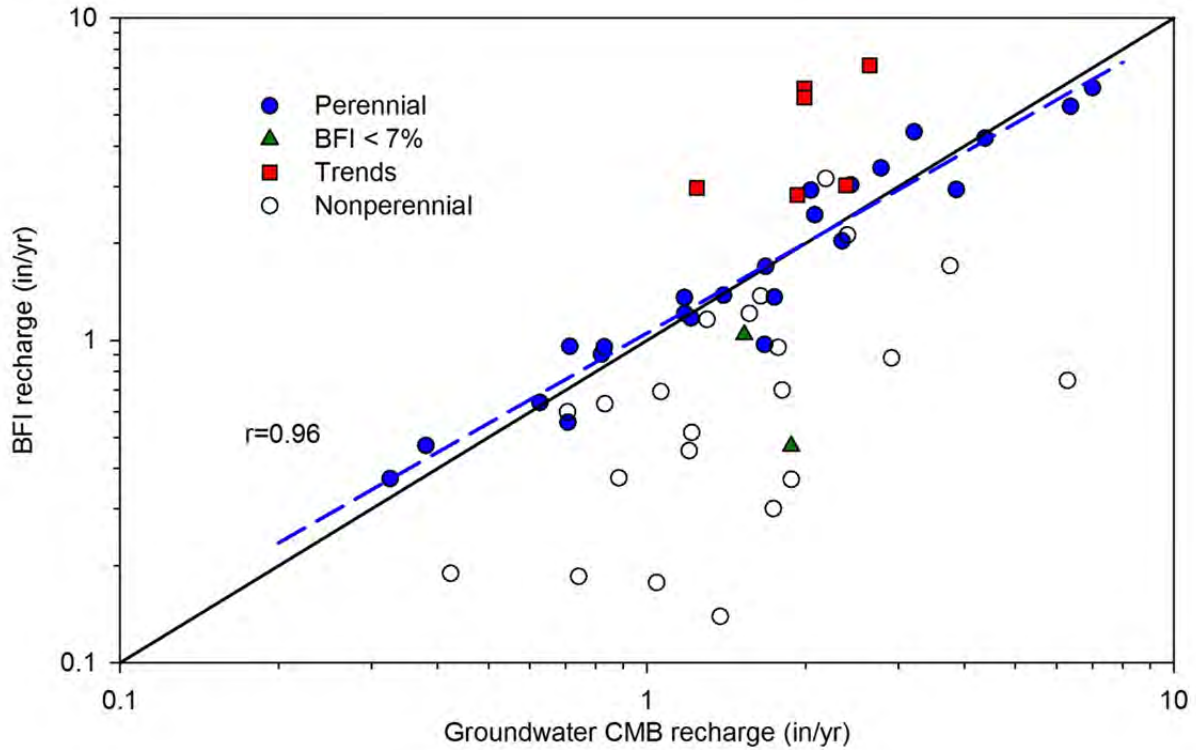


Figure 27. Relationship between CMB recharge and BFI recharge. Symbols match those shown in Figure 26. Solid line represents the 1:1 ratio, dashed line represents a power law regression for perennial stream basin areas only (blue filled circle symbols) and does not include data from the remaining three categories.

ATTACHMENT I
DRAFT REPORT COMMENTS
TWDB CONTRACT 0904831001

"Estimation of Groundwater Recharge to the Gulf Coast Aquifer in Texas, USA"
draft report and deliverables for TWDB Contract No. 0904831001

The draft report was interesting and informative. However, the electronic GIS database appeared corrupted and staff was unable to review the data and therefore unable to ascertain the relevance of applying the recharge information to future modeling efforts and adherence to the requirements set forth in the contract Exhibit B, Section 3.0 Deliverables. Please re-submit the geodatabase in a format compatible with ESRI ArcGIS version 9.x or 10.x, including appropriate and sufficient metadata and a method of applying this data to the modeling efforts for the Gulf Coast Aquifer region.

While several approaches were reviewed and analyzed, it is unclear how this information can be applied for modeling purposes. The discussion on page 24 that compares the results of the various methods needs expansion. Please provide some specific details of how to use the results of this study spatially and temporally to improve groundwater flow models of the area. We recognize that there will be adjustments to recharge during model calibration. However, it would be advantageous to gain your perspective on how to use these results as a starting point and how to incorporate uncertainty of your results into the calibration process. For example, please clarify if Figure 18 (Chloride Mass Balance) shown as percent of precipitation can be used as a starting point to apply annual precipitation (PRISM data) for model calibration and how the other approaches can then be used to set bounds.

Report comments.

1. Please seal final report with appropriate geoscientist(s) seal(s) as required by Texas state law.
Reply: Seal(s) will be affixed to final report copies.
2. Please clarify location of US Geological Survey office for Gabriel Senay as Sioux Falls, South Dakota or Boise, Idaho and update text appropriately.
Reply: Location changes to Sioux Falls, South Dakota.
3. Please update all figures throughout the report showing the study area with a north arrow and scale.
Reply: A north arrow and scale bar have been added to all relevant figures.
4. Introduction, page 3, 5 and 4 lines from bottom of page: Please clarify citation of (Halford, 2000) and either update References with associated reference or change text to (Halford and Mayer, 2000).
Reply: Citation text changed.
5. Geology, page 5, 5 lines from bottom of page: Please clarify citation of Galloway (2000) and either update References with associated documentation or change text to Galloway et al. (2000).
Reply: Citation text changed.
6. Oakville Sandstone/Fleming Formations, page 6-7: please clarify citation of Baker (1986) and update References with associated documentation.
Reply: References updated.
7. Recharge Rates from Previous Studies, page 9, 4 lines from top of page: please clarify citation of (Johnston, 1999) and either update References with associated documentation or change text to (Johnston, 1997).
Reply: Citation text changed.

8. Recharge Rates from Previous Studies, page 9, second paragraph: please clarify citation of (Hay, 1999) and update References with associated documentation.
Reply: References updated.
9. Recharge Rates from Previous Studies, page 9, third paragraph: please clarify citations of Ryder and Ardis (2002) and Dutton and Richter (1990) and update References with associated documentation.
Reply: References updated.
10. Recharge Rates from Previous Studies, page 9, third paragraph: Please remove last sentence. Recharge should only be applied to the uppermost model layer representing the outcrop. Flow down dip has other terminology.
Reply. Sentence removed.
11. Recharge Rates from Previous Studies, page 9, fourth paragraph: please clarify citation of Chowdhury and Mace, 2007 either update References with associated documentation or change text to Chowdhury and Mace, 2003.
Reply: Citation text changed.
12. Actual Evapotranspiration, page 12, 5 lines from the top of the page: please clarify citation of (Allen et al., 2005) and either update References with associated documentation or change text to (Allen and Tasumi, 2005).
Reply: Citation text changed.
13. Figure 14, page 50: please update figure 14 with location of the 8,721-groundwater chloride sample locations or include an inset showing the sampling distribution to see if there is any bias in the dataset.
Reply: Groundwater well sample locations added to map.
14. Figure 15, page 51: please update figure 15 with the sampling locations of the 1,339-groundwater Cl/Br concentration mass ratios or include an inset showing the sampling distribution to see if there is any bias in the dataset.
Reply: Groundwater well sample locations added to map.
15. Figure 16, page 52: please update figure 16 with the sampling locations of the 8,086-groundwater Cl/SO₄ concentration mass ratios or include an inset showing the sampling distribution to see if there is any bias in the dataset.
Reply: Groundwater well sample locations added to map.
16. Figure 17, page 53: Caption references Figure 12, please clarify if this should be Figure 14.
Reply: Caption reference changed.
17. Figure 19, page 55: please update Figure 19 with the sampling locations of the 3,887-groundwater nitrate-N (NO₃-N) concentrations or include an inset showing the sampling distribution to see if there is any bias in the dataset.
Reply: Groundwater well sample locations added to map.
18. Figure 20, page 56: please update figure 19 with the sampling locations of the 7,687 – groundwater nitrate-N (NO₃-N) concentrations or include an inset showing the sampling distribution to see if there is any bias in the dataset.
Reply: Groundwater well sample locations added to map.
19. Figure 21, page 57: please include in the caption or in a legend the significance of the three symbols used in the graph.
Reply: Legend added to graph.
20. Figures 10, 22, 23, and Appendix 1: please be consistent in the figures with labeling and referencing boreholes. For example, Figure 22 cites boreholes Nue05-01 and Ken05-01, while Figure 10 includes Nue-I and Ken-I.
Reply: All relevant figures and tables now have consistent borehole reference labels.

21. Figures 24, 25, Appendix 3 and Appendix 4, pages 60-61, A3-2 to A3-16, and A4-2 to A4-12: please include inset showing location of the gauging stations cited in the graphs and/or clearly label station numbers in Figure 26 and cross reference.

Reply: All station numbers added to Figure 26 and cross references added to relevant figure captions.

APPENDIX 1
Unsaturated Zone Borehole Profiles

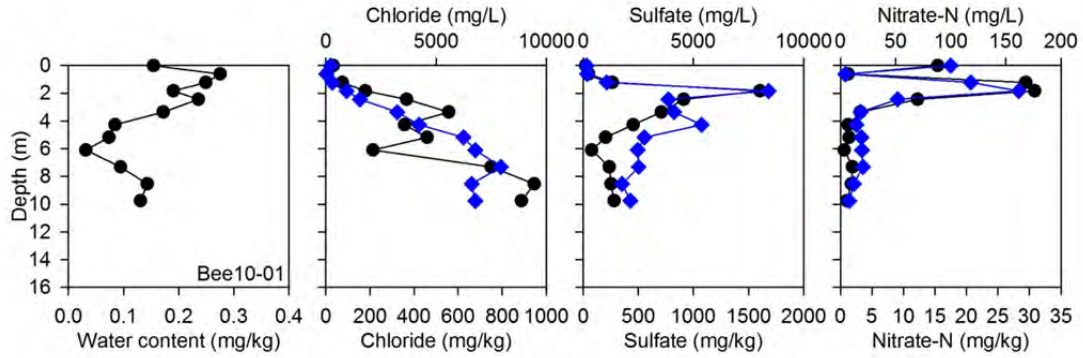


Figure A1-1. Unsaturated zone borehole Bee10-01 profile results (mg/kg circles, mg/L diamonds).

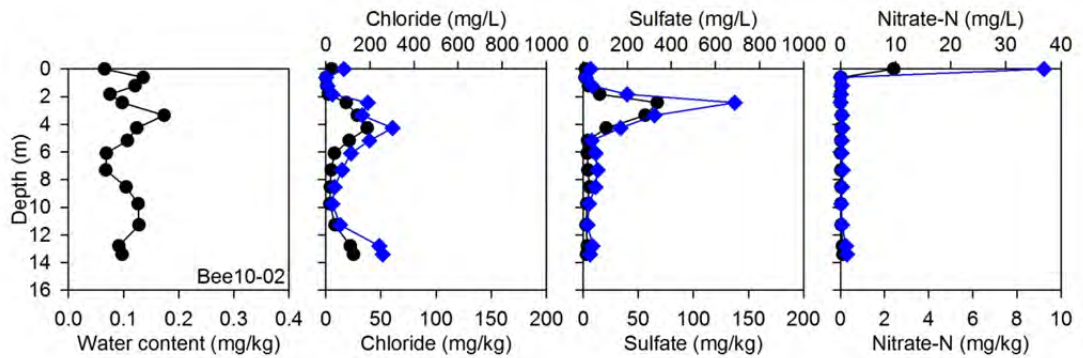


Figure A1-2. Unsaturated zone borehole Bee10-02 profile results (mg/kg circles, mg/L diamonds).

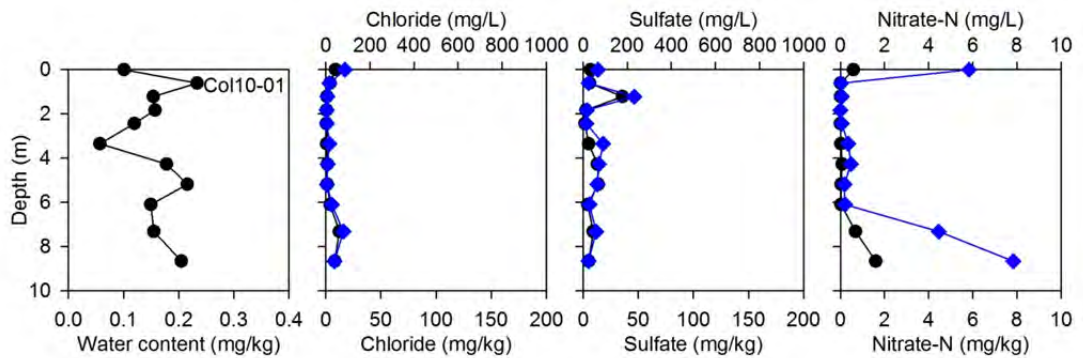


Figure A1-3. Unsaturated zone borehole Col10-01 profile results (mg/kg circles, mg/L diamonds).

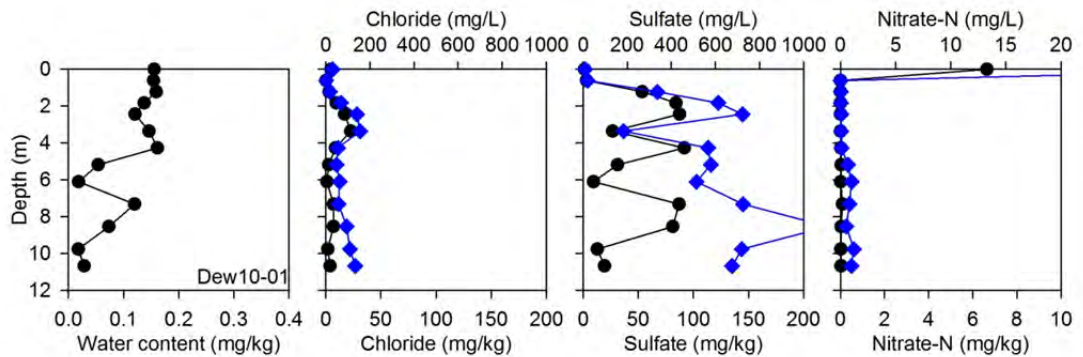


Figure A1-4. Unsaturated zone borehole Dew10-01 profile results (mg/kg circles, mg/L diamonds).

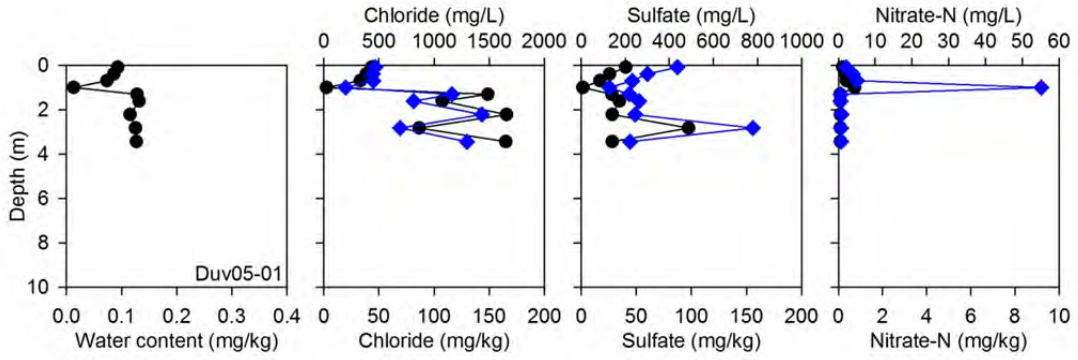


Figure A1-5. Unsaturated zone borehole Duv05-01 profile results (mg/kg circles, mg/L diamonds).

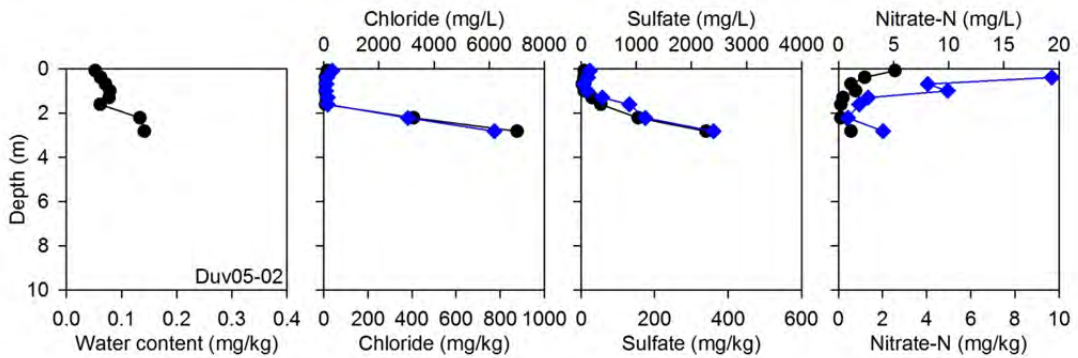


Figure A1-6. Unsaturated zone borehole Duv05-02 profile results (mg/kg circles, mg/L diamonds).

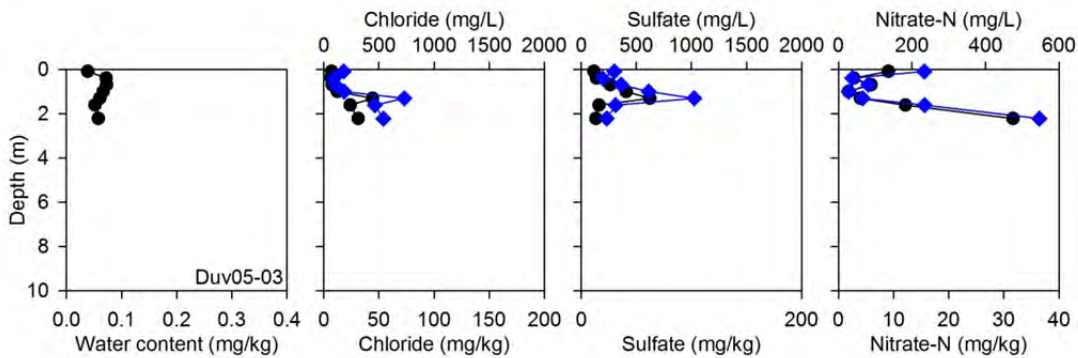


Figure A1-7. Unsaturated zone borehole Duv05-03 profile results (mg/kg circles, mg/L diamonds).

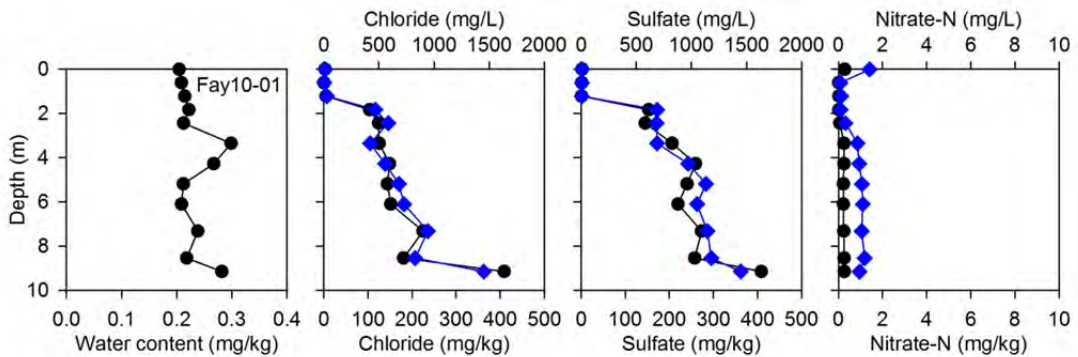


Figure A1-8. Unsaturated zone borehole Fay10-01 profile results (mg/kg circles, mg/L diamonds).

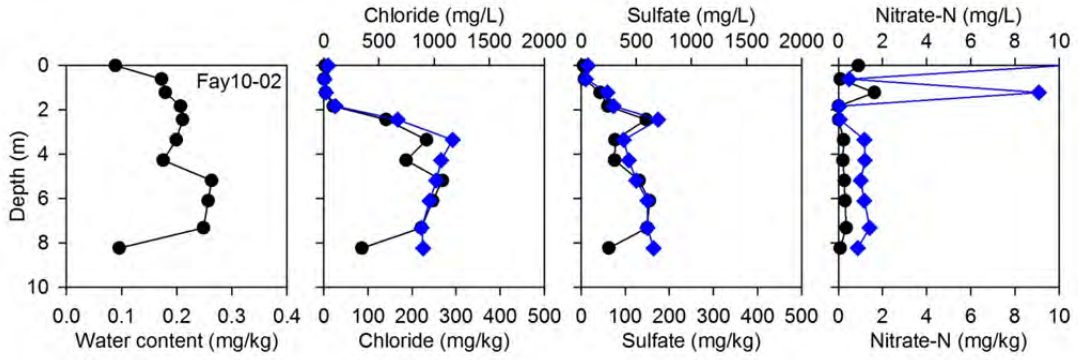


Figure A1-9. Unsaturated zone borehole Fay10-02 profile results (mg/kg circles, mg/L diamonds).

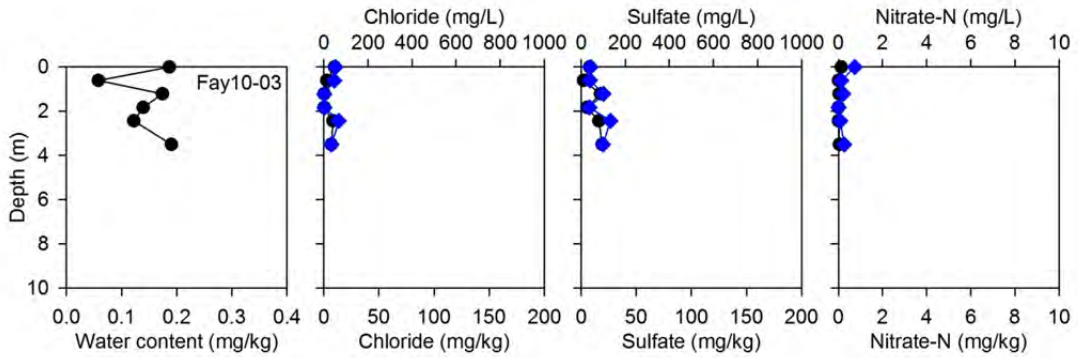


Figure A1-10. Unsaturated zone borehole Fay10-03 profile results (mg/kg circles, mg/L diamonds).

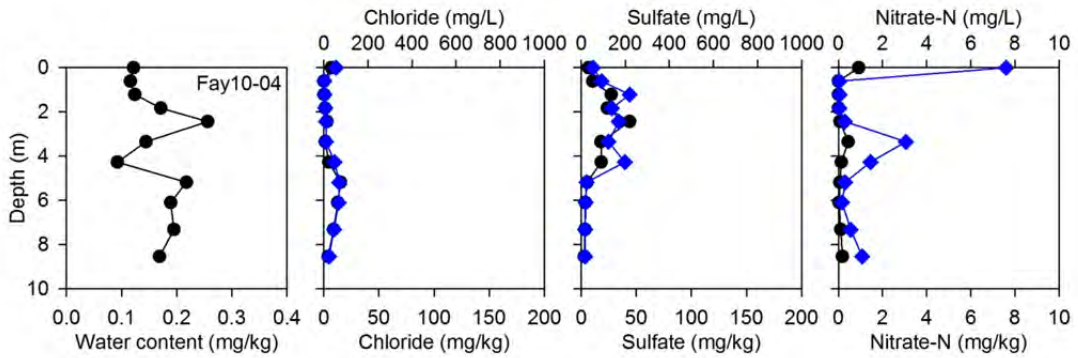


Figure A1-11. Unsaturated zone borehole Fay10-04 profile results (mg/kg circles, mg/L diamonds).

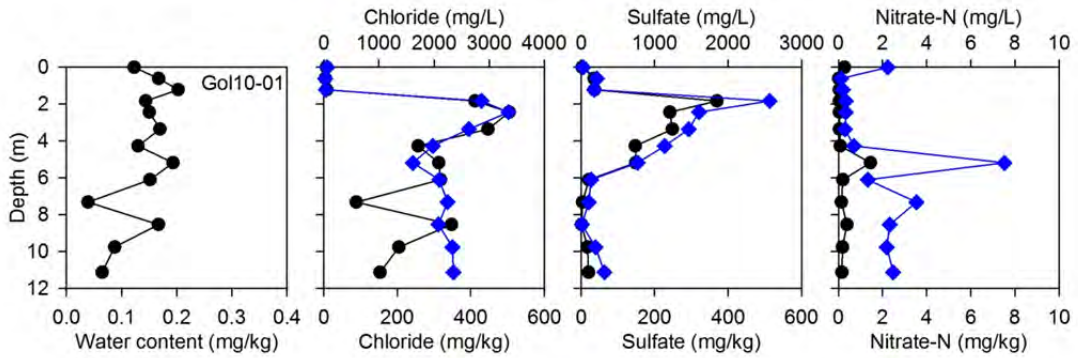


Figure A1-12. Unsaturated zone borehole Gol10-01 profile results (mg/kg circles, mg/L diamonds).

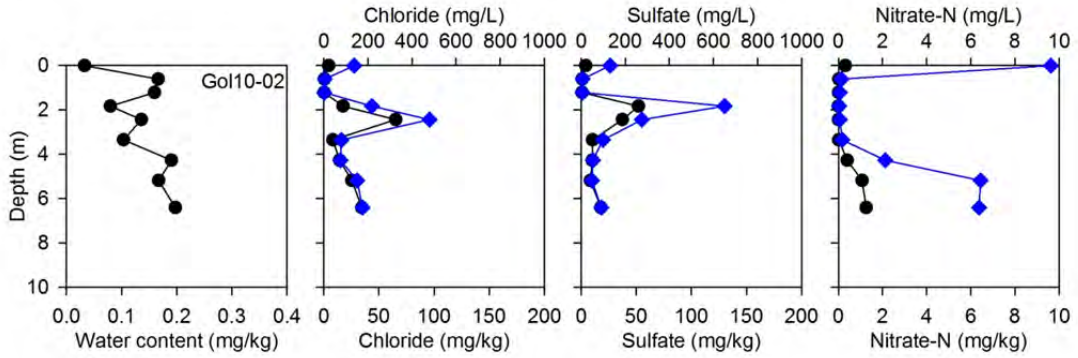


Figure A1-13. Unsaturated zone borehole Gol10-02 profile results (mg/kg circles, mg/L diamonds).

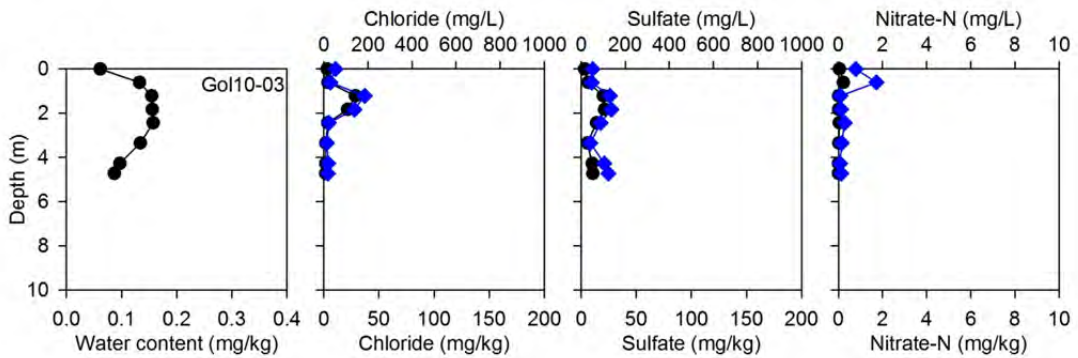


Figure A1-14. Unsaturated zone borehole Gol10-03 profile results (mg/kg circles, mg/L diamonds).

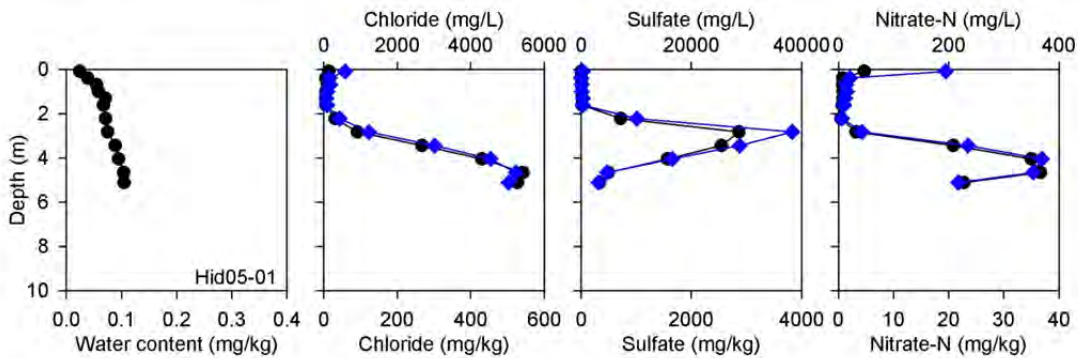


Figure A1-15. Unsaturated zone borehole Hid05-01 profile results (mg/kg circles, mg/L diamonds).

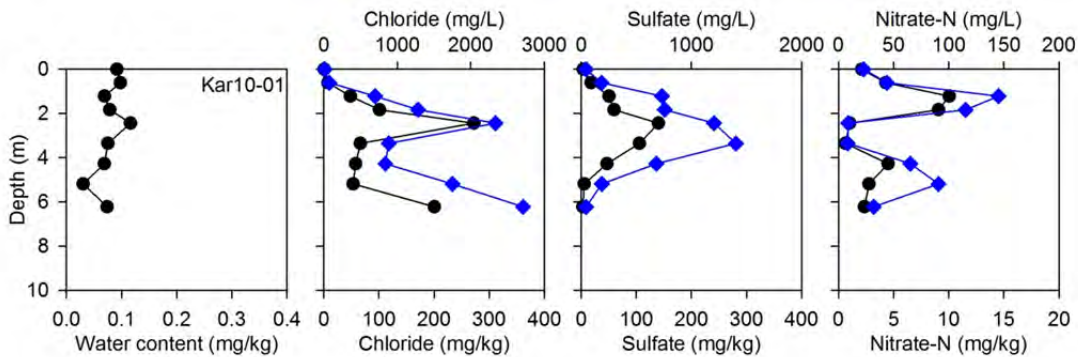


Figure A1-16. Unsaturated zone borehole Kar10-01 profile results (mg/kg circles, mg/L diamonds).

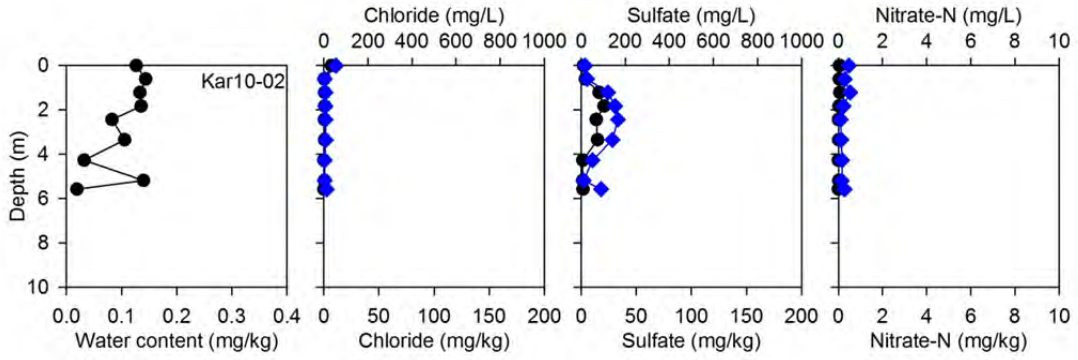


Figure A1-17. Unsaturation zone borehole Kar10-02 profile results (mg/kg circles, mg/L diamonds).

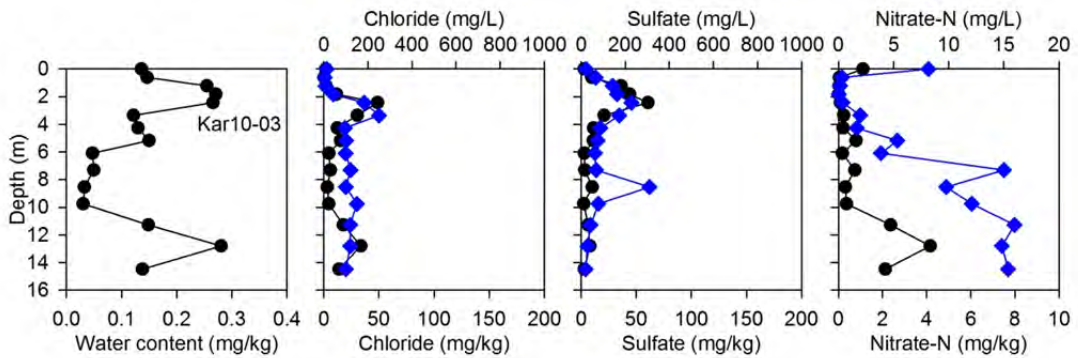


Figure A1-18. Unsaturation zone borehole Kar10-03 profile results (mg/kg circles, mg/L diamonds).

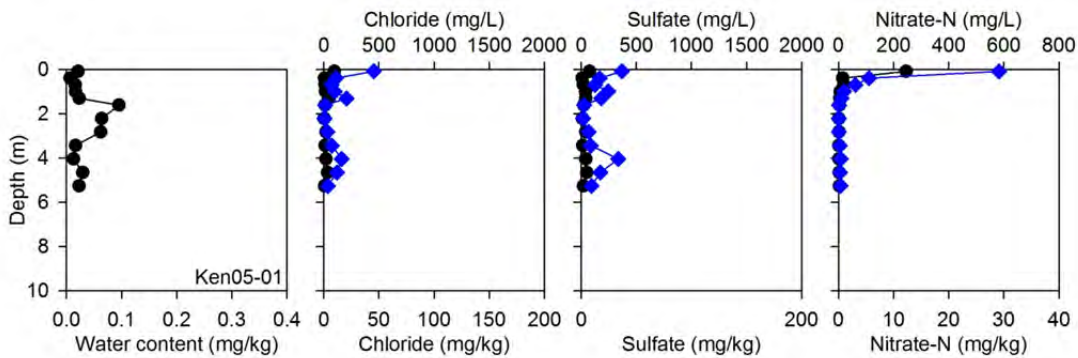


Figure A1-19. Unsaturation zone borehole Ken05-01 profile results (mg/kg circles, mg/L diamonds).

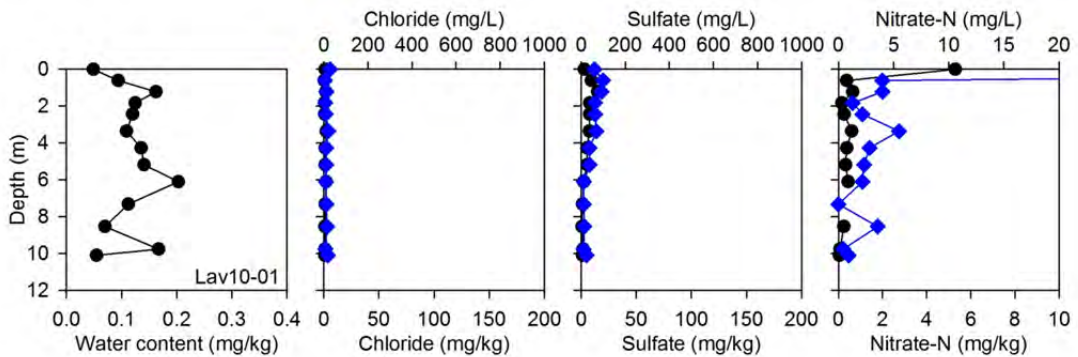


Figure A1-20. Unsaturation zone borehole Lav10-01 profile results (mg/kg circles, mg/L diamonds).

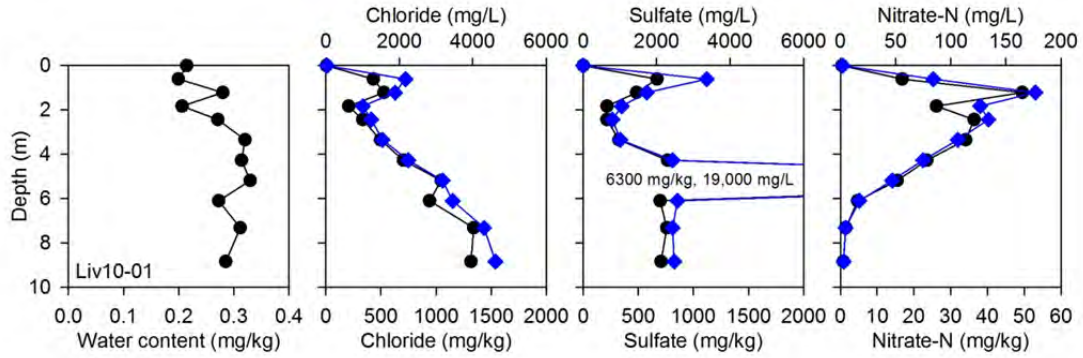


Figure A1-21. Unsaturated zone borehole Liv10-01 profile results (mg/kg circles, mg/L diamonds).

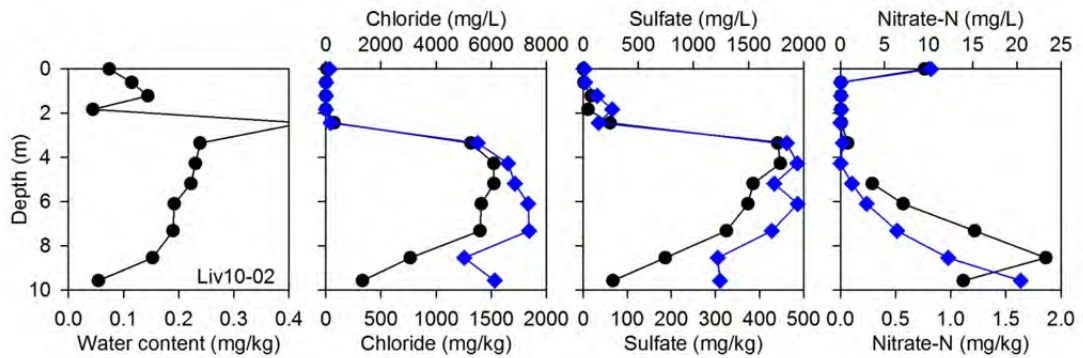


Figure A1-22. Unsaturated zone borehole Liv10-02 profile results (mg/kg circles, mg/L diamonds).

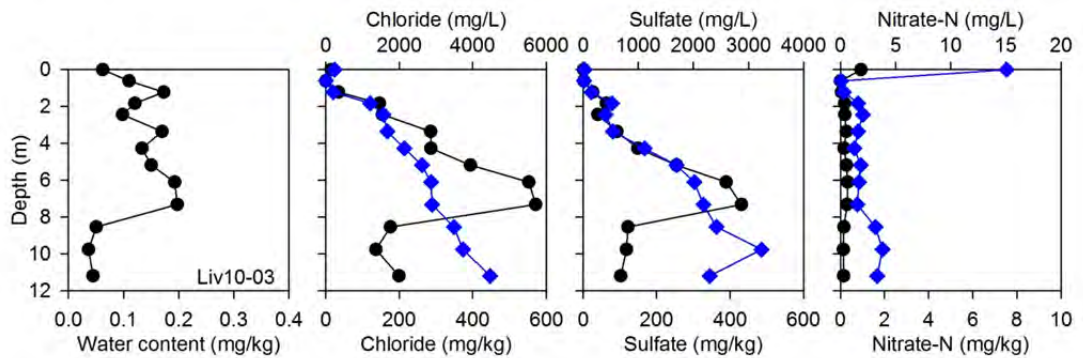


Figure A1-23. Unsaturated zone borehole Liv10-03 profile results (mg/kg circles, mg/L diamonds).

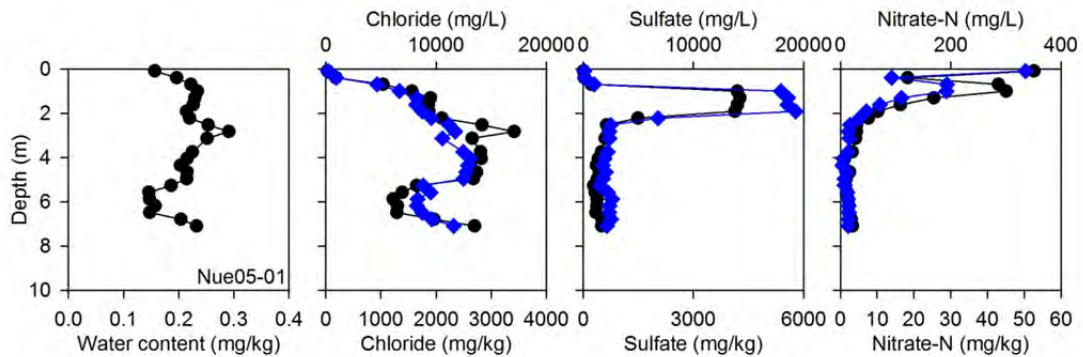


Figure A1-24. Unsaturated zone borehole Nue05-01 profile results (mg/kg circles, mg/L diamonds).

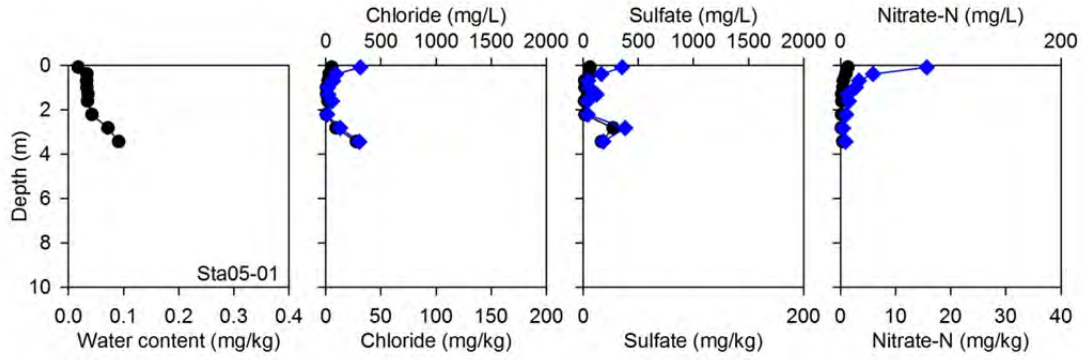


Figure A1-25. Unsaturation zone borehole Sta05-01 profile results (mg/kg circles, mg/L diamonds).

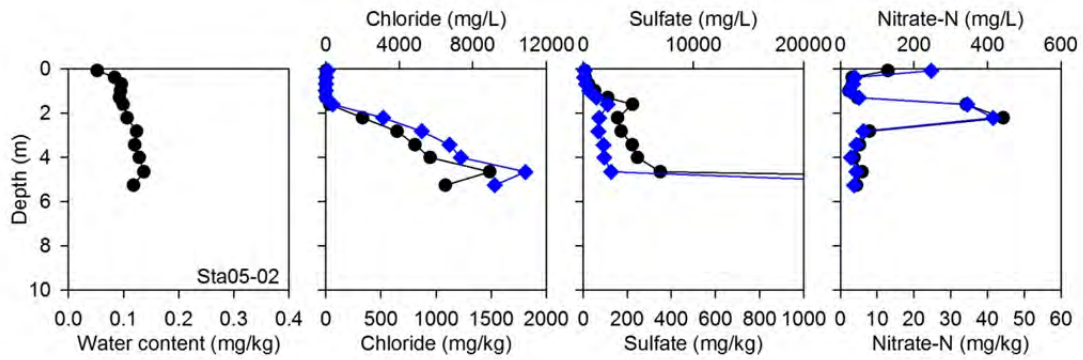


Figure A1-26. Unsaturation zone borehole Sta05-02 profile results (mg/kg circles, mg/L diamonds).

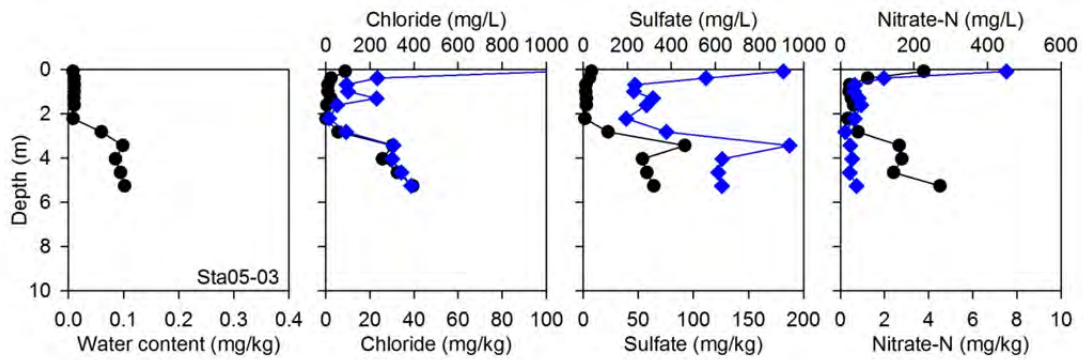


Figure A1-27. Unsaturation zone borehole Sta05-03 profile results (mg/kg circles, mg/L diamonds).

Table A1-1. Unsaturated zone borehole sample analysis results for gravimetric water content (WC), chloride (Cl), sulfate (SO₄), nitrate-N (NO₃-N), and soil texture. Gravimetric water content is expressed as [g water per g soil]. Values for Cl, SO₄, and NO₃-N are expressed both as soil concentrations [mg ion per kg soil] and as soil water concentrations [mg ion per L soil pore water].

| Borehole | Depth (ft) | WC (g/g) | Soil (mg/kg) | | | Water (mg/L) | | | Texture (%) | | |
|----------|------------|----------|--------------|-----------------|--------------------|--------------|-----------------|--------------------|-------------|------|------|
| | | | Cl | SO ₄ | NO ₃ -N | Cl | SO ₄ | NO ₃ -N | Sand | Silt | Clay |
| Fay10-01 | 0.0 | 0.20 | 3.1 | 2.4 | 0.3 | 14.9 | 11.5 | 1.4 | | | |
| Fay10-01 | 2.0 | 0.21 | 1.0 | 1.7 | 0.0 | 4.8 | 8.2 | 0.1 | | | |
| Fay10-01 | 4.0 | 0.21 | 5.8 | 1.3 | 0.0 | 27.1 | 6.2 | 0.1 | | | |
| Fay10-01 | 6.0 | 0.22 | 104.3 | 153.5 | 0.0 | 469.0 | 690.3 | 0.1 | | | |
| Fay10-01 | 8.0 | 0.21 | 124.4 | 145.6 | 0.1 | 584.8 | 684.2 | 0.3 | | | |
| Fay10-01 | 11.0 | 0.30 | 125.7 | 206.4 | 0.3 | 420.7 | 690.9 | 0.9 | | | |
| Fay10-01 | 14.0 | 0.27 | 149.3 | 259.6 | 0.3 | 558.6 | 971.2 | 1.0 | | | |
| Fay10-01 | 17.0 | 0.21 | 144.3 | 240.4 | 0.2 | 680.9 | 1134.0 | 1.2 | | | |
| Fay10-01 | 20.0 | 0.21 | 152.1 | 219.7 | 0.3 | 728.2 | 1052.0 | 1.2 | | | |
| Fay10-01 | 24.0 | 0.24 | 225.3 | 273.1 | 0.3 | 945.1 | 1145.4 | 1.1 | | | |
| Fay10-01 | 28.0 | 0.22 | 181.1 | 257.7 | 0.2 | 829.7 | 1180.6 | 1.1 | | | |
| Fay10-01 | 30.0 | 0.28 | 409.2 | 408.8 | 0.3 | 1451.2 | 1450.0 | 1.0 | | | |
| Fay10-02 | 0.0 | 0.09 | 3.6 | 5.5 | 0.9 | 40.4 | 61.4 | 10.2 | 63.5 | 16.9 | 19.6 |
| Fay10-02 | 2.0 | 0.17 | 1.2 | 7.7 | 0.1 | 7.2 | 44.5 | 0.5 | 55.8 | 17.1 | 27.1 |
| Fay10-02 | 4.0 | 0.18 | 4.1 | 43.2 | 1.6 | 22.6 | 240.5 | 9.1 | 48.0 | 22.5 | 29.5 |
| Fay10-02 | 6.0 | 0.21 | 21.9 | 60.9 | 0.0 | 105.9 | 294.1 | 0.0 | 36.2 | 25.8 | 38.0 |
| Fay10-02 | 8.0 | 0.21 | 141.4 | 147.5 | 0.0 | 670.4 | 699.4 | 0.1 | 27.1 | 27.7 | 45.2 |
| Fay10-02 | 11.0 | 0.20 | 233.0 | 77.3 | 0.3 | 1168.4 | 387.5 | 1.3 | 40.1 | 23.2 | 36.7 |
| Fay10-02 | 14.0 | 0.18 | 186.9 | 76.3 | 0.2 | 1064.4 | 434.5 | 1.3 | 38.3 | 21.6 | 40.1 |
| Fay10-02 | 17.0 | 0.26 | 269.0 | 131.7 | 0.3 | 1021.5 | 500.2 | 1.0 | 7.1 | 24.9 | 68.0 |
| Fay10-02 | 20.0 | 0.26 | 246.9 | 155.3 | 0.3 | 960.4 | 604.0 | 1.2 | 21.7 | 19.3 | 59.0 |
| Fay10-02 | 24.0 | 0.25 | 221.1 | 149.9 | 0.4 | 888.6 | 602.7 | 1.5 | 82.9 | 10.5 | 6.6 |
| Fay10-02 | 27.0 | 0.10 | 86.5 | 63.0 | 0.1 | 902.5 | 657.5 | 0.9 | | | |
| Fay10-03 | 0.0 | 0.19 | 9.9 | 8.0 | 0.1 | 52.9 | 42.7 | 0.7 | | | |
| Fay10-03 | 2.0 | 0.06 | 2.8 | 2.4 | 0.0 | 48.3 | 41.2 | 0.1 | | | |
| Fay10-03 | 4.0 | 0.17 | 0.4 | 17.7 | 0.0 | 2.3 | 101.7 | 0.2 | | | |
| Fay10-03 | 6.0 | 0.14 | 0.5 | 5.4 | 0.0 | 3.4 | 38.6 | 0.0 | | | |
| Fay10-03 | 8.0 | 0.12 | 8.4 | 16.1 | 0.0 | 69.1 | 132.2 | 0.1 | | | |
| Fay10-03 | 11.5 | 0.19 | 6.9 | 19.1 | 0.1 | 36.0 | 100.3 | 0.3 | | | |
| Fay10-04 | 0.0 | 0.12 | 6.8 | 6.7 | 0.9 | 56.1 | 54.9 | 7.6 | 56.0 | 14.0 | 30.0 |
| Fay10-04 | 2.0 | 0.12 | 0.3 | 10.8 | 0.0 | 2.2 | 92.8 | 0.0 | 47.2 | 27.5 | 25.3 |
| Fay10-04 | 4.0 | 0.12 | 0.4 | 27.5 | 0.0 | 3.6 | 221.3 | 0.1 | 19.8 | 55.4 | 24.8 |
| Fay10-04 | 6.0 | 0.17 | 1.2 | 23.9 | 0.0 | 7.1 | 139.6 | 0.1 | 53.8 | 31.3 | 14.9 |
| Fay10-04 | 8.0 | 0.26 | 2.8 | 44.0 | 0.1 | 10.9 | 171.5 | 0.3 | 81.7 | 11.7 | 6.6 |
| Fay10-04 | 11.0 | 0.14 | 1.5 | 18.0 | 0.4 | 10.6 | 124.9 | 3.1 | 49.2 | 23.8 | 27.0 |
| Fay10-04 | 14.0 | 0.09 | 4.6 | 18.4 | 0.1 | 49.5 | 198.3 | 1.5 | 80.3 | 11.8 | 7.9 |
| Fay10-04 | 17.0 | 0.22 | 15.3 | 5.5 | 0.1 | 70.2 | 25.1 | 0.3 | 80.3 | 11.4 | 8.2 |

| Borehole | Depth (ft) | WC (g/g) | Soil (mg/kg) | | | Water (mg/L) | | | Texture (%) | | |
|----------|------------|----------|--------------|-----------------|--------------------|--------------|-----------------|--------------------|-------------|------|------|
| | | | Cl | SO ₄ | NO ₃ -N | Cl | SO ₄ | NO ₃ -N | Sand | Silt | Clay |
| Fay10-04 | 20.0 | 0.19 | 12.8 | 3.9 | 0.0 | 67.5 | 20.5 | 0.2 | 85.4 | 9.6 | 5.0 |
| Fay10-04 | 24.0 | 0.20 | 9.1 | 3.7 | 0.1 | 46.4 | 18.8 | 0.6 | | | |
| Fay10-04 | 28.0 | 0.17 | 4.1 | 3.0 | 0.2 | 24.0 | 18.0 | 1.1 | 81.6 | 8.0 | 10.4 |
| Col10-01 | 0.0 | 0.10 | 8.9 | 6.7 | 0.6 | 88.0 | 66.8 | 5.9 | 49.5 | 6.2 | 44.3 |
| Col10-01 | 2.0 | 0.23 | 3.9 | 5.9 | 0.0 | 16.9 | 25.3 | 0.0 | 54.9 | 7.1 | 38.0 |
| Col10-01 | 4.0 | 0.15 | 1.1 | 35.8 | 0.0 | 7.0 | 232.1 | 0.1 | 70.1 | 5.3 | 24.6 |
| Col10-01 | 6.0 | 0.16 | 0.7 | 2.7 | 0.0 | 4.4 | 17.0 | 0.1 | 76.5 | 13.1 | 10.4 |
| Col10-01 | 8.0 | 0.12 | 0.6 | 1.8 | 0.0 | 5.4 | 15.4 | 0.0 | 62.2 | 26.3 | 11.5 |
| Col10-01 | 11.0 | 0.06 | 0.9 | 5.2 | 0.0 | 16.1 | 90.1 | 0.3 | 45.9 | 24.1 | 30.0 |
| Col10-01 | 14.0 | 0.18 | 1.5 | 13.1 | 0.1 | 8.5 | 73.3 | 0.5 | | | |
| Col10-01 | 17.0 | 0.22 | 1.2 | 13.8 | 0.0 | 5.6 | 64.1 | 0.2 | 75.2 | 15.3 | 9.5 |
| Col10-01 | 20.0 | 0.15 | 4.1 | 4.3 | 0.0 | 27.3 | 28.8 | 0.2 | 80.3 | 15.0 | 4.7 |
| Col10-01 | 24.0 | 0.16 | 12.4 | 9.3 | 0.7 | 79.8 | 60.0 | 4.5 | 8.9 | 33.1 | 58.1 |
| Col10-01 | 28.4 | 0.20 | 8.2 | 5.2 | 1.6 | 39.8 | 25.3 | 7.8 | 64.6 | 15.5 | 19.9 |
| Gol10-01 | 0.0 | 0.12 | 7.5 | 3.5 | 0.3 | 60.6 | 28.5 | 2.2 | | | |
| Gol10-01 | 2.0 | 0.17 | 4.6 | 35.9 | 0.0 | 27.3 | 214.5 | 0.1 | | | |
| Gol10-01 | 4.0 | 0.20 | 8.2 | 36.7 | 0.0 | 40.4 | 180.8 | 0.2 | | | |
| Gol10-01 | 6.0 | 0.14 | 411.7 | 369.6 | 0.0 | 2859.9 | 2567.9 | 0.3 | | | |
| Gol10-01 | 8.0 | 0.15 | 504.4 | 241.7 | 0.0 | 3352.2 | 1606.6 | 0.3 | | | |
| Gol10-01 | 11.0 | 0.17 | 446.9 | 248.8 | 0.1 | 2632.3 | 1465.3 | 0.3 | | | |
| Gol10-01 | 14.0 | 0.13 | 257.0 | 147.9 | 0.1 | 1977.9 | 1138.7 | 0.7 | | | |
| Gol10-01 | 17.0 | 0.19 | 312.9 | 148.6 | 1.5 | 1618.6 | 768.6 | 7.5 | | | |
| Gol10-01 | 20.0 | 0.15 | 317.8 | 20.9 | 0.2 | 2094.7 | 137.7 | 1.3 | | | |
| Gol10-01 | 24.0 | 0.04 | 88.5 | 4.1 | 0.1 | 2247.9 | 105.4 | 3.6 | | | |
| Gol10-01 | 28.0 | 0.17 | 347.9 | 1.7 | 0.4 | 2081.6 | 10.1 | 2.3 | | | |
| Gol10-01 | 32.0 | 0.09 | 204.7 | 17.3 | 0.2 | 2335.3 | 196.8 | 2.2 | | | |
| Gol10-01 | 36.5 | 0.07 | 153.3 | 20.7 | 0.2 | 2356.2 | 318.7 | 2.5 | | | |
| Gol10-02 | 0.0 | 0.03 | 4.5 | 4.3 | 0.3 | 138.0 | 131.2 | 9.6 | | | |
| Gol10-02 | 2.0 | 0.17 | 0.8 | 1.1 | 0.0 | 4.7 | 6.7 | 0.1 | | | |
| Gol10-02 | 4.0 | 0.16 | 0.4 | 1.0 | 0.0 | 2.7 | 6.4 | 0.1 | | | |
| Gol10-02 | 6.0 | 0.08 | 17.5 | 52.1 | 0.0 | 218.8 | 651.1 | 0.1 | | | |
| Gol10-02 | 8.0 | 0.14 | 65.2 | 37.6 | 0.0 | 479.4 | 276.3 | 0.1 | | | |
| Gol10-02 | 11.0 | 0.10 | 8.3 | 10.4 | 0.0 | 80.3 | 100.6 | 0.2 | | | |
| Gol10-02 | 14.0 | 0.19 | 14.5 | 10.2 | 0.4 | 76.0 | 53.7 | 2.1 | | | |
| Gol10-02 | 17.0 | 0.17 | 25.6 | 8.4 | 1.1 | 152.7 | 50.3 | 6.5 | | | |
| Gol10-02 | 21.0 | 0.20 | 34.7 | 18.0 | 1.3 | 175.2 | 91.1 | 6.4 | | | |
| Gol10-03 | 0.0 | 0.06 | 3.3 | 3.3 | 0.0 | 53.2 | 52.8 | 0.8 | | | |
| Gol10-03 | 2.0 | 0.13 | 4.0 | 6.4 | 0.2 | 30.0 | 48.5 | 1.7 | | | |
| Gol10-03 | 4.0 | 0.15 | 28.8 | 20.1 | 0.0 | 185.9 | 130.2 | 0.1 | | | |
| Gol10-03 | 6.0 | 0.16 | 21.6 | 21.4 | 0.0 | 138.7 | 137.7 | 0.1 | | | |
| Gol10-03 | 8.0 | 0.16 | 3.7 | 14.1 | 0.0 | 23.6 | 89.6 | 0.3 | | | |

| Borehole | Depth (ft) | WC (g/g) | Soil (mg/kg) | | | Water (mg/L) | | | Texture (%) | | |
|----------|------------|----------|--------------|-----------------|--------------------|--------------|-----------------|--------------------|-------------|------|------|
| | | | Cl | SO ₄ | NO ₃ -N | Cl | SO ₄ | NO ₃ -N | Sand | Silt | Clay |
| Gol10-03 | 11.0 | 0.13 | 1.9 | 5.7 | 0.0 | 14.2 | 42.5 | 0.2 | | | |
| Gol10-03 | 14.0 | 0.10 | 2.0 | 10.2 | 0.0 | 20.3 | 105.2 | 0.1 | | | |
| Gol10-03 | 15.5 | 0.09 | 1.7 | 10.8 | 0.0 | 19.9 | 123.4 | 0.1 | | | |
| Kar10-01 | 0.0 | 0.09 | 0.9 | 4.2 | 2.1 | 10.2 | 46.0 | 23.2 | 59.4 | 23.8 | 16.7 |
| Kar10-01 | 2.0 | 0.10 | 7.8 | 18.3 | 4.3 | 79.4 | 186.6 | 44.1 | 43.1 | 39.1 | 17.9 |
| Kar10-01 | 4.0 | 0.07 | 48.5 | 50.9 | 10.1 | 700.3 | 734.0 | 145.2 | 41.0 | 45.2 | 13.8 |
| Kar10-01 | 6.0 | 0.08 | 101.3 | 59.8 | 9.1 | 1285.4 | 758.9 | 115.4 | 60.7 | 29.3 | 10.0 |
| Kar10-01 | 8.0 | 0.12 | 272.4 | 140.4 | 1.0 | 2339.7 | 1205.8 | 8.8 | 78.7 | 16.5 | 4.8 |
| Kar10-01 | 11.0 | 0.08 | 66.6 | 106.0 | 0.6 | 883.0 | 1404.0 | 8.6 | 70.8 | 20.8 | 8.4 |
| Kar10-01 | 14.0 | 0.07 | 58.0 | 47.1 | 4.5 | 839.7 | 682.7 | 65.3 | 88.9 | 7.0 | 4.1 |
| Kar10-01 | 17.0 | 0.03 | 53.5 | 5.8 | 2.8 | 1749.7 | 188.8 | 90.9 | 52.2 | 35.2 | 12.6 |
| Kar10-01 | 20.4 | 0.07 | 200.7 | 3.4 | 2.4 | 2712.1 | 45.7 | 32.0 | 74.8 | 10.7 | 14.5 |
| Kar10-02 | 0.0 | 0.13 | 7.0 | 2.3 | 0.1 | 55.0 | 18.0 | 0.5 | 60.7 | 21.8 | 17.5 |
| Kar10-02 | 2.0 | 0.14 | 0.6 | 3.9 | 0.0 | 4.2 | 27.3 | 0.3 | 47.5 | 31.6 | 20.8 |
| Kar10-02 | 4.0 | 0.13 | 1.0 | 16.3 | 0.1 | 7.1 | 122.0 | 0.5 | 59.4 | 30.4 | 10.2 |
| Kar10-02 | 6.0 | 0.14 | 1.0 | 20.9 | 0.0 | 7.7 | 154.1 | 0.2 | 83.8 | 11.7 | 4.4 |
| Kar10-02 | 8.0 | 0.08 | 0.7 | 13.8 | 0.0 | 8.5 | 167.4 | 0.1 | 86.3 | 10.9 | 2.9 |
| Kar10-02 | 11.0 | 0.11 | 0.9 | 15.0 | 0.0 | 8.7 | 142.1 | 0.1 | 77.4 | 17.3 | 5.4 |
| Kar10-02 | 14.0 | 0.03 | 0.2 | 1.7 | 0.0 | 5.1 | 51.4 | 0.1 | 67.2 | 20.9 | 11.8 |
| Kar10-02 | 17.0 | 0.14 | 0.7 | 1.7 | 0.0 | 5.0 | 12.2 | 0.2 | 82.5 | 12.2 | 5.4 |
| Kar10-02 | 18.3 | 0.02 | 0.3 | 1.7 | 0.0 | 13.9 | 90.9 | 0.2 | 52.9 | 12.1 | 35.0 |
| Kar10-03 | 0.0 | 0.14 | 1.9 | 3.0 | 1.1 | 14.1 | 22.1 | 8.2 | | | |
| Kar10-03 | 2.0 | 0.15 | 0.5 | 9.8 | 0.1 | 3.6 | 66.5 | 0.3 | | | |
| Kar10-03 | 4.0 | 0.25 | 2.0 | 36.4 | 0.0 | 8.0 | 142.9 | 0.1 | | | |
| Kar10-03 | 6.0 | 0.27 | 11.7 | 44.1 | 0.0 | 43.3 | 162.7 | 0.1 | | | |
| Kar10-03 | 8.0 | 0.27 | 48.9 | 60.7 | 0.1 | 183.7 | 228.3 | 0.4 | | | |
| Kar10-03 | 11.0 | 0.12 | 30.5 | 21.0 | 0.2 | 250.8 | 172.8 | 2.0 | | | |
| Kar10-03 | 14.0 | 0.13 | 12.4 | 11.4 | 0.2 | 95.3 | 88.0 | 1.6 | | | |
| Kar10-03 | 17.0 | 0.15 | 15.3 | 11.1 | 0.8 | 102.2 | 74.2 | 5.4 | | | |
| Kar10-03 | 20.0 | 0.05 | 4.7 | 3.0 | 0.2 | 100.0 | 62.9 | 3.9 | | | |
| Kar10-03 | 24.0 | 0.05 | 6.1 | 3.4 | 0.7 | 121.5 | 67.7 | 15.0 | | | |
| Kar10-03 | 28.0 | 0.03 | 3.3 | 10.2 | 0.3 | 101.3 | 310.8 | 9.8 | | | |
| Kar10-03 | 32.0 | 0.03 | 4.6 | 2.4 | 0.4 | 150.5 | 78.8 | 12.2 | | | |
| Kar10-03 | 37.0 | 0.15 | 17.8 | 6.5 | 2.4 | 119.5 | 43.7 | 16.0 | | | |
| Kar10-03 | 42.0 | 0.28 | 33.7 | 8.1 | 4.2 | 120.1 | 28.7 | 14.8 | | | |
| Kar10-03 | 47.5 | 0.14 | 13.9 | 2.9 | 2.1 | 100.9 | 21.4 | 15.4 | | | |
| Bee10-01 | 0.0 | 0.15 | 34.1 | 24.3 | 15.5 | 220.5 | 157.1 | 100.1 | 48.7 | 12.1 | 39.2 |
| Bee10-01 | 2.0 | 0.28 | 7.7 | 51.0 | 1.2 | 27.9 | 185.3 | 4.5 | 39.2 | 14.4 | 46.4 |
| Bee10-01 | 4.0 | 0.25 | 74.9 | 266.6 | 29.4 | 300.7 | 1070.4 | 118.2 | 49.1 | 11.7 | 39.2 |
| Bee10-01 | 6.0 | 0.19 | 179.7 | 1605.0 | 30.8 | 942.6 | 8419.4 | 161.7 | 42.6 | 16.9 | 40.5 |
| Bee10-01 | 8.0 | 0.24 | 367.3 | 913.3 | 12.2 | 1557.3 | 3872.2 | 51.9 | 82.5 | 5.0 | 12.5 |

| Borehole | Depth (ft) | WC (g/g) | Soil (mg/kg) | | | Water (mg/L) | | | Texture (%) | | |
|----------|------------|----------|--------------|-----------------|--------------------|--------------|-----------------|--------------------|-------------|------|------|
| | | | Cl | SO ₄ | NO ₃ -N | Cl | SO ₄ | NO ₃ -N | Sand | Silt | Clay |
| Bee10-01 | 11.0 | 0.17 | 557.8 | 710.2 | 3.2 | 3240.5 | 4125.9 | 18.5 | 91.3 | 4.2 | 4.4 |
| Bee10-01 | 14.0 | 0.08 | 358.0 | 454.7 | 1.2 | 4231.1 | 5374.9 | 14.6 | | | |
| Bee10-01 | 17.0 | 0.07 | 459.8 | 205.2 | 1.4 | 6245.5 | 2787.9 | 18.9 | 85.0 | 6.2 | 8.8 |
| Bee10-01 | 20.0 | 0.03 | 214.0 | 78.1 | 0.6 | 6783.4 | 2476.8 | 19.7 | 42.7 | 32.0 | 25.3 |
| Bee10-01 | 24.0 | 0.09 | 750.4 | 238.5 | 1.9 | 7948.2 | 2525.7 | 20.3 | 30.2 | 44.3 | 25.6 |
| Bee10-01 | 28.0 | 0.14 | 945.9 | 253.9 | 1.7 | 6613.2 | 1774.9 | 12.2 | 82.5 | 10.5 | 7.0 |
| Bee10-01 | 32.0 | 0.13 | 887.5 | 281.3 | 1.1 | 6784.6 | 2150.6 | 8.0 | 69.7 | 8.3 | 22.0 |
| Bee10-02 | 0.0 | 0.07 | 5.5 | 2.2 | 2.4 | 83.2 | 33.5 | 36.9 | 63.3 | 12.6 | 24.1 |
| Bee10-02 | 2.0 | 0.14 | 0.4 | 1.8 | 0.0 | 2.8 | 13.0 | 0.1 | 55.8 | 31.3 | 12.9 |
| Bee10-02 | 4.0 | 0.12 | 1.0 | 5.0 | 0.0 | 8.5 | 41.4 | 0.3 | 58.1 | 27.5 | 14.3 |
| Bee10-02 | 6.0 | 0.08 | 2.3 | 15.1 | 0.0 | 30.1 | 199.8 | 0.1 | 57.9 | 35.7 | 6.4 |
| Bee10-02 | 8.0 | 0.10 | 18.7 | 67.3 | 0.0 | 191.0 | 688.4 | 0.0 | 44.2 | 50.7 | 5.2 |
| Bee10-02 | 11.0 | 0.17 | 28.7 | 56.3 | 0.1 | 165.0 | 324.2 | 0.3 | 78.7 | 18.5 | 2.8 |
| Bee10-02 | 14.0 | 0.12 | 37.7 | 21.0 | 0.0 | 303.3 | 169.4 | 0.4 | 78.7 | 16.0 | 5.4 |
| Bee10-02 | 17.0 | 0.11 | 21.2 | 4.2 | 0.0 | 198.5 | 39.2 | 0.3 | | | |
| Bee10-02 | 20.0 | 0.07 | 7.9 | 3.9 | 0.0 | 114.6 | 57.1 | 0.2 | 72.3 | 12.8 | 14.9 |
| Bee10-02 | 24.0 | 0.07 | 5.0 | 4.4 | 0.0 | 73.8 | 65.3 | 0.5 | 73.6 | 11.2 | 15.2 |
| Bee10-02 | 28.0 | 0.10 | 4.2 | 5.9 | 0.0 | 40.2 | 56.5 | 0.3 | | | |
| Bee10-02 | 32.0 | 0.13 | 3.8 | 3.4 | 0.0 | 30.2 | 27.2 | 0.2 | 76.1 | 18.0 | 5.9 |
| Bee10-02 | 37.0 | 0.13 | 8.5 | 2.7 | 0.0 | 66.0 | 21.2 | 0.3 | 26.6 | 26.6 | 46.8 |
| Bee10-02 | 42.0 | 0.09 | 22.3 | 4.0 | 0.1 | 243.0 | 43.6 | 1.0 | 27.9 | 29.0 | 43.1 |
| Bee10-02 | 44.0 | 0.10 | 25.2 | 3.1 | 0.1 | 258.6 | 32.0 | 1.2 | | | |
| Liv10-01 | 0.0 | 0.21 | 7.9 | 1.6 | 0.4 | 36.8 | 7.3 | 2.1 | 82.8 | 15.0 | 2.2 |
| Liv10-01 | 2.0 | 0.20 | 432.7 | 671.2 | 16.8 | 2169.0 | 3365.1 | 84.3 | 65.5 | 29.7 | 4.8 |
| Liv10-01 | 4.0 | 0.28 | 528.1 | 486.4 | 49.5 | 1885.8 | 1736.6 | 176.7 | 65.8 | 29.7 | 4.5 |
| Liv10-01 | 6.0 | 0.21 | 208.4 | 217.5 | 26.2 | 1010.9 | 1054.7 | 126.8 | 30.8 | 43.0 | 26.2 |
| Liv10-01 | 8.0 | 0.27 | 335.8 | 217.0 | 36.4 | 1239.5 | 801.0 | 134.3 | 6.2 | 40.9 | 52.8 |
| Liv10-01 | 11.0 | 0.32 | 496.8 | 326.1 | 34.1 | 1550.7 | 1017.9 | 106.4 | | | |
| Liv10-01 | 14.0 | 0.31 | 705.2 | 767.1 | 23.5 | 2246.3 | 2443.4 | 75.0 | 8.8 | 38.2 | 52.9 |
| Liv10-01 | 17.0 | 0.33 | 1047.0 | 6315.8 | 15.5 | 3176.6 | 19161.2 | 46.9 | | | |
| Liv10-01 | 20.0 | 0.27 | 941.7 | 699.9 | 4.7 | 3454.8 | 2567.7 | 17.3 | 91.7 | 4.5 | 3.8 |
| Liv10-01 | 24.0 | 0.31 | 1342.1 | 759.4 | 1.5 | 4308.7 | 2438.0 | 4.7 | | | |
| Liv10-01 | 29.0 | 0.29 | 1317.5 | 707.0 | 0.8 | 4616.4 | 2477.1 | 2.9 | 92.9 | 2.4 | 4.7 |
| Liv10-02 | 0.0 | 0.07 | 10.8 | 1.1 | 0.8 | 144.8 | 15.1 | 10.3 | | | |
| Liv10-02 | 2.0 | 0.11 | 1.5 | 2.3 | 0.0 | 12.8 | 19.6 | 0.0 | | | |
| Liv10-02 | 4.0 | 0.14 | 0.8 | 18.6 | 0.0 | 5.5 | 128.7 | 0.0 | | | |
| Liv10-02 | 6.0 | 0.04 | 0.4 | 11.6 | 0.0 | 8.8 | 262.8 | 0.1 | | | |
| Liv10-02 | 8.0 | 0.43 | 76.2 | 61.2 | 0.0 | 179.3 | 143.9 | 0.0 | | | |
| Liv10-02 | 11.0 | 0.24 | 1316.4 | 441.5 | 0.1 | 5510.8 | 1848.3 | 0.3 | | | |
| Liv10-02 | 14.0 | 0.23 | 1524.7 | 447.5 | 0.2 | 6616.9 | 1942.2 | 0.7 | | | |
| Liv10-02 | 17.0 | 0.22 | 1525.7 | 385.6 | 0.3 | 6863.4 | 1734.6 | 1.3 | | | |

| Borehole | Depth (ft) | WC (g/g) | Soil (mg/kg) | | | Water (mg/L) | | | Texture (%) | | |
|----------|------------|----------|--------------|-----------------|--------------------|--------------|-----------------|--------------------|-------------|------|------|
| | | | Cl | SO ₄ | NO ₃ -N | Cl | SO ₄ | NO ₃ -N | Sand | Silt | Clay |
| Liv10-02 | 20.0 | 0.19 | 1411.9 | 374.0 | 0.6 | 7346.3 | 1945.7 | 3.0 | | | |
| Liv10-02 | 24.0 | 0.19 | 1399.4 | 325.1 | 1.2 | 7375.6 | 1713.2 | 6.4 | | | |
| Liv10-02 | 28.0 | 0.15 | 767.0 | 186.4 | 1.9 | 5025.4 | 1221.0 | 12.2 | | | |
| Liv10-02 | 31.4 | 0.05 | 334.3 | 67.7 | 1.1 | 6129.2 | 1241.9 | 20.3 | | | |
| Liv10-03 | 0.0 | 0.06 | 15.0 | 1.8 | 0.9 | 240.6 | 28.6 | 15.0 | 67.7 | 2.2 | 30.1 |
| Liv10-03 | 2.0 | 0.11 | 0.6 | 2.0 | 0.0 | 5.5 | 18.2 | 0.1 | 82.8 | 4.3 | 12.9 |
| Liv10-03 | 4.0 | 0.17 | 35.1 | 26.5 | 0.1 | 202.7 | 153.4 | 0.3 | 85.3 | 4.2 | 10.4 |
| Liv10-03 | 6.0 | 0.12 | 146.3 | 63.4 | 0.2 | 1213.3 | 525.5 | 1.6 | 71.4 | 4.8 | 23.8 |
| Liv10-03 | 8.0 | 0.10 | 154.1 | 40.2 | 0.2 | 1569.6 | 409.0 | 2.1 | 68.8 | 4.0 | 27.2 |
| Liv10-03 | 11.0 | 0.17 | 285.4 | 92.2 | 0.3 | 1679.8 | 542.7 | 1.6 | 65.0 | 8.7 | 26.3 |
| Liv10-03 | 14.0 | 0.13 | 286.4 | 148.9 | 0.2 | 2143.8 | 1114.3 | 1.2 | | | |
| Liv10-03 | 17.0 | 0.15 | 393.6 | 254.2 | 0.3 | 2618.7 | 1691.1 | 1.8 | 68.8 | 22.6 | 8.6 |
| Liv10-03 | 20.0 | 0.19 | 552.5 | 389.2 | 0.3 | 2862.1 | 2016.4 | 1.8 | | | |
| Liv10-03 | 24.0 | 0.20 | 571.4 | 430.9 | 0.3 | 2893.2 | 2181.6 | 1.5 | 94.1 | 2.4 | 3.4 |
| Liv10-03 | 28.0 | 0.05 | 176.1 | 122.3 | 0.2 | 3484.9 | 2420.5 | 3.0 | 94.2 | 1.1 | 4.7 |
| Liv10-03 | 32.0 | 0.04 | 136.5 | 118.3 | 0.1 | 3732.3 | 3235.2 | 4.1 | | | |
| Liv10-03 | 36.7 | 0.04 | 199.6 | 102.6 | 0.1 | 4475.8 | 2300.9 | 3.2 | 60.1 | 4.8 | 35.1 |
| Lav10-01 | 0.0 | 0.05 | 1.4 | 2.9 | 5.3 | 28.4 | 60.2 | 108.6 | 71.3 | 1.5 | 27.2 |
| Lav10-01 | 2.0 | 0.09 | 0.6 | 9.4 | 0.4 | 5.9 | 100.0 | 4.0 | 66.4 | 2.7 | 30.9 |
| Lav10-01 | 4.0 | 0.16 | 1.9 | 15.2 | 0.6 | 11.8 | 93.6 | 4.0 | 84.1 | 1.3 | 14.7 |
| Lav10-01 | 6.0 | 0.13 | 0.9 | 7.9 | 0.2 | 7.2 | 62.8 | 1.3 | 80.3 | 2.5 | 17.2 |
| Lav10-01 | 8.0 | 0.12 | 1.0 | 7.8 | 0.3 | 8.7 | 64.6 | 2.2 | 82.8 | 1.3 | 15.9 |
| Lav10-01 | 11.0 | 0.11 | 2.3 | 7.6 | 0.6 | 21.4 | 69.4 | 5.5 | 74.7 | 13.6 | 11.7 |
| Lav10-01 | 14.0 | 0.14 | 1.5 | 5.3 | 0.4 | 10.7 | 39.3 | 2.8 | 90.4 | 3.7 | 5.9 |
| Lav10-01 | 17.0 | 0.14 | 1.5 | 5.5 | 0.3 | 10.4 | 39.3 | 2.3 | 36.9 | 38.5 | 24.6 |
| Lav10-01 | 20.0 | 0.20 | 2.1 | 2.4 | 0.4 | 10.5 | 12.1 | 2.2 | 10.1 | 19.9 | 70.1 |
| Lav10-01 | 24.0 | 0.11 | 1.4 | 1.5 | 0.3 | 12.6 | 13.0 | 2.9 | | | |
| Lav10-01 | 28.0 | 0.07 | 1.1 | 1.1 | 0.2 | 15.7 | 15.2 | 3.6 | 38.1 | 37.8 | 24.1 |
| Lav10-01 | 32.0 | 0.17 | 1.3 | 2.0 | 0.1 | 7.7 | 11.8 | 0.5 | 70.5 | 24.5 | 5.1 |
| Lav10-01 | 33.1 | 0.05 | 1.0 | 1.4 | 0.1 | 18.8 | 25.3 | 0.9 | | | |
| Dew10-01 | 0.0 | 0.16 | 4.9 | 1.4 | 6.6 | 31.3 | 8.7 | 42.7 | | | |
| Dew10-01 | 2.0 | 0.15 | 0.3 | 3.2 | 0.0 | 1.8 | 20.8 | 0.0 | | | |
| Dew10-01 | 4.0 | 0.16 | 3.2 | 53.6 | 0.0 | 19.9 | 336.8 | 0.1 | | | |
| Dew10-01 | 6.0 | 0.14 | 9.5 | 84.3 | 0.0 | 69.2 | 613.2 | 0.1 | | | |
| Dew10-01 | 8.0 | 0.12 | 17.1 | 87.6 | 0.0 | 141.4 | 723.7 | 0.1 | | | |
| Dew10-01 | 11.0 | 0.15 | 22.8 | 26.8 | 0.0 | 155.9 | 183.5 | 0.1 | | | |
| Dew10-01 | 14.0 | 0.16 | 8.9 | 91.8 | 0.0 | 54.8 | 567.8 | 0.1 | | | |
| Dew10-01 | 17.0 | 0.05 | 2.7 | 31.3 | 0.0 | 49.4 | 578.7 | 0.7 | | | |
| Dew10-01 | 20.0 | 0.02 | 1.2 | 9.6 | 0.0 | 62.7 | 514.8 | 1.1 | | | |
| Dew10-01 | 24.0 | 0.12 | 7.0 | 87.1 | 0.1 | 58.6 | 725.9 | 0.8 | | | |
| Dew10-01 | 28.0 | 0.07 | 7.0 | 81.5 | 0.0 | 94.7 | 1107.9 | 0.6 | | | |

| Borehole | Depth (ft) | WC (g/g) | Soil (mg/kg) | | | Water (mg/L) | | | Texture (%) | | |
|----------|------------|----------|--------------|-----------------|--------------------|--------------|-----------------|--------------------|-------------|------|------|
| | | | Cl | SO ₄ | NO ₃ -N | Cl | SO ₄ | NO ₃ -N | Sand | Silt | Clay |
| Dew10-01 | 32.0 | 0.02 | 2.0 | 13.0 | 0.0 | 109.5 | 719.7 | 1.3 | | | |
| Dew10-01 | 35.0 | 0.03 | 3.9 | 19.5 | 0.0 | 134.6 | 676.7 | 1.1 | | | |
| Duv05-01 | 0.25 | 0.09 | 43.6 | 40.7 | 0.2 | 467.9 | 436.8 | 2.1 | 54.9 | 5.9 | 39.3 |
| Duv05-01 | 1.25 | 0.09 | 38.5 | 25.9 | 0.3 | 447.7 | 301.3 | 3.9 | | | |
| Duv05-01 | 2.25 | 0.07 | 33.3 | 17.2 | 0.4 | 450.4 | 232.2 | 5.0 | 76.5 | 5.6 | 17.9 |
| Duv05-01 | 3.25 | 0.09 | 2.6 | 1.7 | 0.7 | 29.4 | 19.0 | 8.2 | 89.4 | 1.2 | 9.4 |
| Duv05-01 | 4.25 | 0.13 | 148.9 | 28.0 | 0.1 | 1162.1 | 218.4 | 0.6 | 64.9 | 4.9 | 30.2 |
| Duv05-01 | 5.25 | 0.13 | 107.5 | 34.8 | 0.1 | 815.9 | 263.9 | 0.7 | | | |
| Duv05-01 | 7.25 | 0.12 | 165.9 | 28.4 | 0.1 | 1434.3 | 245.4 | 0.9 | 67.8 | 4.6 | 27.7 |
| Duv05-01 | 9.25 | 0.13 | 86.6 | 97.6 | 0.1 | 691.0 | 778.2 | 0.8 | | | |
| Duv05-01 | 11.25 | 0.13 | 165.1 | 28.3 | 0.1 | 1299.1 | 222.5 | 0.8 | 62.6 | 14.8 | 22.6 |
| Duv05-02 | 0.25 | 0.05 | 16.7 | 8.5 | 2.6 | 318.6 | 161.5 | 49.0 | 69.0 | 14.6 | 16.4 |
| Duv05-02 | 1.25 | 0.06 | 7.5 | 7.8 | 1.2 | 120.7 | 125.6 | 19.4 | | | |
| Duv05-02 | 2.25 | 0.07 | 7.5 | 3.5 | 0.6 | 105.7 | 48.9 | 8.1 | 61.3 | 13.5 | 25.2 |
| Duv05-02 | 3.25 | 0.08 | 6.9 | 8.7 | 0.8 | 87.9 | 110.8 | 9.9 | | | |
| Duv05-02 | 4.25 | 0.08 | 11.5 | 29.8 | 0.2 | 147.9 | 385.0 | 2.7 | 48.5 | 20.6 | 30.9 |
| Duv05-02 | 5.25 | 0.06 | 8.6 | 53.6 | 0.1 | 139.5 | 873.3 | 1.9 | 48.2 | 21.3 | 30.5 |
| Duv05-02 | 7.25 | 0.13 | 407.8 | 155.4 | 0.1 | 3055.0 | 1164.5 | 0.9 | 20.1 | 48.2 | 31.8 |
| Duv05-02 | 9.25 | 0.14 | 876.8 | 340.1 | 0.6 | 6193.0 | 2402.1 | 4.1 | 26.6 | 40.9 | 32.6 |
| Duv05-03 | 0.25 | 0.04 | 7.1 | 11.7 | 9.1 | 182.0 | 300.5 | 233.7 | | | |
| Duv05-03 | 1.25 | 0.07 | 6.7 | 14.1 | 2.8 | 93.2 | 195.4 | 38.5 | | | |
| Duv05-03 | 2.25 | 0.07 | 7.7 | 26.5 | 5.9 | 105.2 | 363.7 | 81.3 | | | |
| Duv05-03 | 3.25 | 0.07 | 12.3 | 41.0 | 1.9 | 184.1 | 613.6 | 27.8 | | | |
| Duv05-03 | 4.25 | 0.06 | 44.4 | 62.4 | 4.0 | 730.0 | 1026.0 | 65.7 | | | |
| Duv05-03 | 5.25 | 0.05 | 24.1 | 16.3 | 12.2 | 463.4 | 314.1 | 234.1 | | | |
| Duv05-03 | 7.25 | 0.06 | 31.3 | 13.5 | 31.7 | 540.1 | 232.8 | 547.0 | | | |
| Hid05-01 | 0.25 | 0.02 | 14.1 | 7.7 | 4.7 | 582.7 | 320.6 | 194.7 | 84.4 | 6.2 | 9.4 |
| Hid05-01 | 1.25 | 0.04 | 6.1 | 2.7 | 0.8 | 156.6 | 68.8 | 21.0 | | | |
| Hid05-01 | 2.25 | 0.05 | 9.8 | 8.2 | 0.8 | 180.5 | 151.2 | 14.7 | 70.4 | 7.7 | 21.9 |
| Hid05-01 | 3.25 | 0.06 | 5.7 | 8.4 | 0.9 | 98.1 | 144.0 | 15.2 | | | |
| Hid05-01 | 4.25 | 0.07 | 5.3 | 22.7 | 0.8 | 74.4 | 321.1 | 11.8 | | | |
| Hid05-01 | 5.25 | 0.07 | 6.3 | 17.5 | 0.7 | 93.2 | 259.6 | 10.4 | 66.4 | 8.4 | 25.1 |
| Hid05-01 | 7.25 | 0.07 | 31.2 | 721.8 | 0.5 | 438.4 | 10149.5 | 6.9 | | | |
| Hid05-01 | 9.25 | 0.07 | 91.9 | 2862.7 | 3.2 | 1228.4 | 38277.0 | 43.1 | 58.8 | 14.4 | 26.7 |
| Hid05-01 | 11.25 | 0.09 | 267.2 | 2549.1 | 20.8 | 3014.4 | 28752.0 | 235.1 | | | |
| Hid05-01 | 13.25 | 0.09 | 430.1 | 1570.5 | 35.0 | 4533.9 | 16557.8 | 369.1 | 53.5 | 20.7 | 25.8 |
| Hid05-01 | 15.25 | 0.10 | 542.0 | 493.9 | 36.7 | 5220.2 | 4756.9 | 353.1 | | | |
| Hid05-01 | 16.75 | 0.10 | 526.9 | 333.9 | 22.8 | 5029.7 | 3187.7 | 217.2 | 53.7 | 19.2 | 27.1 |
| Nue05-01 | 0.25 | 0.16 | 33.4 | 17.0 | 52.7 | 213.3 | 108.3 | 336.1 | 19.5 | 32.0 | 48.5 |
| Nue05-01 | 1.25 | 0.20 | 184.7 | 33.2 | 18.3 | 940.6 | 169.2 | 93.4 | | | |
| Nue05-01 | 2.25 | 0.22 | 1039.0 | 224.9 | 43.0 | 4673.1 | 1011.5 | 193.4 | 20.2 | 22.8 | 56.9 |

| Borehole | Depth (ft) | WC (g/g) | Soil (mg/kg) | | | Water (mg/L) | | | Texture (%) | | |
|----------|------------|----------|--------------|-----------------|--------------------|--------------|-----------------|--------------------|-------------|------|------|
| | | | Cl | SO ₄ | NO ₃ -N | Cl | SO ₄ | NO ₃ -N | Sand | Silt | Clay |
| Nue05-01 | 3.25 | 0.23 | 1564.6 | 4196.8 | 45.1 | 6685.7 | 17933.5 | 192.7 | | | |
| Nue05-01 | 4.25 | 0.23 | 1898.7 | 4267.6 | 25.4 | 8274.7 | 18598.9 | 110.9 | 18.2 | 37.4 | 44.3 |
| Nue05-01 | 5.25 | 0.23 | 1862.0 | 4202.5 | 16.3 | 8220.2 | 18552.8 | 72.1 | | | |
| Nue05-01 | 6.25 | 0.21 | 1872.3 | 4135.4 | 10.2 | 8734.3 | 19291.5 | 47.6 | 26.6 | 47.3 | 26.1 |
| Nue05-01 | 7.25 | 0.22 | 2108.5 | 1494.2 | 7.6 | 9584.9 | 6792.5 | 34.7 | | | |
| Nue05-01 | 8.25 | 0.25 | 2836.7 | 641.5 | 4.4 | 11186.0 | 2529.8 | 17.4 | | | |
| Nue05-01 | 9.25 | 0.29 | 3418.4 | 693.9 | 4.4 | 11739.8 | 2383.1 | 15.1 | 10.5 | 22.3 | 67.2 |
| Nue05-01 | 10.25 | 0.25 | 2658.1 | 601.3 | 4.1 | 10568.5 | 2390.7 | 16.4 | 14.4 | 22.8 | 62.9 |
| Nue05-01 | 12.25 | 0.22 | 2809.6 | 505.2 | 3.2 | 12489.8 | 2245.9 | 14.2 | | | |
| Nue05-01 | 13.25 | 0.22 | 2822.9 | 416.9 | 1.2 | 13111.7 | 1936.6 | 5.5 | 20.9 | 25.7 | 53.4 |
| Nue05-01 | 14.25 | 0.20 | 2621.1 | 364.7 | 0.7 | 12896.9 | 1794.6 | 3.6 | | | |
| Nue05-01 | 15.25 | 0.22 | 2737.8 | 443.5 | 2.5 | 12721.1 | 2060.7 | 11.6 | 20.2 | 25.6 | 54.2 |
| Nue05-01 | 16.25 | 0.21 | 2678.3 | 388.0 | 1.6 | 12483.5 | 1808.6 | 7.5 | | | |
| Nue05-01 | 17.25 | 0.19 | 1649.8 | 289.1 | 1.4 | 8863.6 | 1553.0 | 7.5 | 26.9 | 26.5 | 46.6 |
| Nue05-01 | 18.25 | 0.15 | 1388.4 | 329.2 | 1.9 | 9513.5 | 2256.0 | 12.7 | | | |
| Nue05-01 | 19.25 | 0.15 | 1225.7 | 387.6 | 2.1 | 8321.6 | 2631.8 | 14.1 | 42.6 | 28.1 | 29.2 |
| Nue05-01 | 20.25 | 0.16 | 1301.0 | 378.8 | 2.3 | 8277.7 | 2410.2 | 14.8 | | | |
| Nue05-01 | 21.25 | 0.15 | 1293.1 | 348.5 | 2.3 | 8758.9 | 2360.7 | 15.6 | 45.7 | 26.7 | 27.6 |
| Nue05-01 | 22.25 | 0.20 | 1964.1 | 518.2 | 3.0 | 9619.1 | 2537.8 | 14.7 | | | |
| Nue05-01 | 23.25 | 0.23 | 2699.9 | 509.0 | 3.3 | 11622.5 | 2191.0 | 14.3 | 10.5 | 22.9 | 66.6 |
| Sta05-01 | 0.25 | 0.02 | 5.6 | 6.3 | 1.4 | 315.0 | 353.9 | 78.3 | 84.5 | 2.4 | 13.1 |
| Sta05-01 | 1.25 | 0.03 | 3.2 | 5.6 | 1.0 | 93.5 | 165.8 | 29.7 | | | |
| Sta05-01 | 2.25 | 0.03 | 2.2 | 1.6 | 0.6 | 67.3 | 47.7 | 16.8 | 81.9 | 3.7 | 14.4 |
| Sta05-01 | 3.25 | 0.03 | 0.7 | 1.8 | 0.5 | 21.5 | 54.8 | 14.1 | | | |
| Sta05-01 | 4.25 | 0.04 | 0.9 | 4.4 | 0.2 | 24.8 | 122.7 | 6.8 | 83.2 | 4.6 | 12.2 |
| Sta05-01 | 5.25 | 0.03 | 2.1 | 1.4 | 0.3 | 59.3 | 40.5 | 7.7 | | | |
| Sta05-01 | 7.25 | 0.04 | 0.6 | 1.8 | 0.2 | 14.2 | 43.0 | 5.2 | 81.9 | 4.6 | 13.5 |
| Sta05-01 | 9.25 | 0.07 | 9.4 | 27.3 | 0.2 | 130.4 | 380.7 | 2.5 | | | |
| Sta05-01 | 11.25 | 0.09 | 27.8 | 16.7 | 0.4 | 304.6 | 182.7 | 4.7 | 78.0 | 14.4 | 7.6 |
| Sta05-02 | 0.25 | 0.05 | 5.6 | 8.2 | 13.0 | 106.4 | 156.9 | 247.5 | 57.9 | 25.5 | 16.6 |
| Sta05-02 | 1.25 | 0.08 | 2.0 | 9.9 | 3.3 | 23.6 | 118.0 | 38.9 | | | |
| Sta05-02 | 2.25 | 0.10 | 0.5 | 24.8 | 3.4 | 5.5 | 257.7 | 34.9 | 43.9 | 23.8 | 32.2 |
| Sta05-02 | 3.25 | 0.09 | 0.4 | 52.7 | 2.3 | 4.2 | 557.9 | 24.8 | | | |
| Sta05-02 | 4.25 | 0.09 | 1.6 | 112.2 | 4.7 | 17.6 | 1210.8 | 50.5 | 35.6 | 29.2 | 35.2 |
| Sta05-02 | 5.25 | 0.10 | 37.2 | 224.0 | 34.3 | 374.2 | 2253.8 | 344.9 | | | |
| Sta05-02 | 7.25 | 0.11 | 334.0 | 156.7 | 44.3 | 3132.8 | 1469.8 | 415.6 | 37.8 | 27.1 | 35.2 |
| Sta05-02 | 9.25 | 0.12 | 647.3 | 172.8 | 7.9 | 5220.8 | 1393.6 | 63.6 | | | |
| Sta05-02 | 11.25 | 0.12 | 810.3 | 223.1 | 5.2 | 6731.6 | 1853.5 | 43.2 | 29.4 | 32.8 | 37.7 |
| Sta05-02 | 13.125 | 0.13 | 947.1 | 247.3 | 3.8 | 7362.0 | 1922.1 | 29.2 | | | |
| Sta05-02 | 15.25 | 0.14 | 1487.5 | 350.2 | 5.9 | 10864.3 | 2557.6 | 43.0 | | | |
| Sta05-02 | 17.25 | 0.12 | 1086.4 | 4098.2 | 4.4 | 9194.4 | 34682.2 | 37.4 | 66.2 | 25.8 | 7.9 |

| Borehole | Depth (ft) | WC (g/g) | Soil (mg/kg) | | | Water (mg/L) | | | Texture (%) | | |
|----------|------------|----------|--------------|-----------------|--------------------|--------------|-----------------|--------------------|-------------|------|------|
| | | | Cl | SO ₄ | NO ₃ -N | Cl | SO ₄ | NO ₃ -N | Sand | Silt | Clay |
| Sta05-03 | 0.25 | 0.01 | 8.8 | 7.6 | 3.8 | 1055.4 | 908.6 | 451.3 | 88.2 | 2.4 | 9.4 |
| Sta05-03 | 1.25 | 0.01 | 2.5 | 5.9 | 1.2 | 233.6 | 557.4 | 118.4 | | | |
| Sta05-03 | 2.25 | 0.01 | 1.0 | 2.6 | 0.4 | 94.4 | 236.3 | 39.3 | 92.5 | <0.1 | 7.5 |
| Sta05-03 | 3.25 | 0.01 | 1.1 | 2.4 | 0.4 | 100.7 | 230.4 | 37.6 | | | |
| Sta05-03 | 4.25 | 0.01 | 2.3 | 3.2 | 0.5 | 230.0 | 316.1 | 49.8 | 90.1 | 2.4 | 7.5 |
| Sta05-03 | 5.25 | 0.01 | 0.5 | 3.0 | 0.6 | 51.1 | 287.9 | 57.1 | | | |
| Sta05-03 | 7.25 | 0.01 | 0.1 | 1.7 | 0.3 | 15.9 | 196.0 | 38.9 | 95.0 | <0.1 | 5.0 |
| Sta05-03 | 9.25 | 0.06 | 5.6 | 22.7 | 0.8 | 93.2 | 378.8 | 13.5 | | | |
| Sta05-03 | 11.25 | 0.10 | 30.4 | 92.3 | 2.7 | 307.9 | 935.4 | 27.0 | 77.5 | 2.5 | 20.0 |
| Sta05-03 | 13.25 | 0.09 | 25.8 | 54.0 | 2.8 | 301.3 | 630.7 | 32.6 | 82.6 | 2.4 | 15.0 |
| Sta05-03 | 15.25 | 0.09 | 32.5 | 58.0 | 2.4 | 343.8 | 613.7 | 25.6 | | | |
| Sta05-03 | 17.25 | 0.10 | 39.5 | 64.2 | 4.5 | 387.5 | 629.8 | 44.3 | 65.8 | 15.9 | 18.2 |

APPENDIX 2
Previous Baseflow Studies

RECHARGE ESTIMATES FROM EXISTING REPORTS

Previous recharge studies are presented in this section. The first study was completed as part of the LCRA-SAWS Water Project (LSWP). In this project, the results for a low flow study by the LCRA (Saunders, 2006) and an analysis using hydrograph separation were given. The previous LCRA low flow study used streamflow measurements that were recorded in November 1999. The hydrograph separation analysis used unregulated stream gage data along with the hydrograph separation code Base Flow Index (Wahl & Wahl, 1995) in order to make long term estimates for baseflow.

The second recharge study that this section will review was conducted on the Brazos River by the United States Geological Survey (USGS) (Turco, East, & Milburn, 2007). This study looked at low flow measurements collected during March and August of 2006 in order to determine gaining and losing stretches along this river.

The final report presented in this section was completed by the USGS (Slade and others, 2002). This report, unlike the previous reports, summarized previous Gain-Loss studies in Texas instead of presenting new data.

In addition to these reports, two other reports were reviewed but not summarized in this section. A study that was conducted by the USGS for the San Antonio River (Lizarraga & Ockerman, 2010) was reviewed to see if any additional baseflow data could be garnered. This study used the watershed hydrology and water quality simulation program Hydrological Simulation Program-FORTRAN (HSPF) in order to simulate groundwater recharge in the San Antonio River. In this report there was no data presented for recharge to streams. Instead values are given for recharge to the aquifer (the portion of rainfall that reaches deep inactive groundwater storage). The second study is Wolock (2003), where estimates of recharge were made for the entire United States. The authors used the hydrograph-separation code BFI to estimate the ratio of baseflow to runoff (the ratio is called the baseflow index) at hundreds of gages nationwide. They then interpolated the baseflow indices between gages by assuming the point value was applicable at the center of the contributing subwatershed. After creating a grid of baseflow indices, they multiplied that grid by a nationwide average runoff grid (data from 1951-1980) to estimate an average recharge. The reasons the results of the Wolock (2003) study are not summarized in the current work are twofold: 1) the authors did not consider whether gages were regulated or unregulated when estimating the baseflow index, which could cause significant local error, especially in the Gulf Coast region where many gages are regulated, 2) the interpolation method they used created many obvious artifacts in the index grid.

A2.1 LSWP RECHARGE ESTIMATES-LOW FLOW

The Lower Colorado River Authority (LCRA) completed a low flow study on the Colorado River from Austin to Bay City (Saunders, 2006). This study was performed by conducting a water balance using historical data during the first half of Water Year 2000. The results of this analysis can be seen in Table A2-1. The results presented in the study were calculated as a volume of water per unit time (e.g. cfs and acre-ft/yr). Areal recharge was estimated by dividing the calculated gain by the drainage area. These estimates are included in Table A2-1.

1 . Figure A2-1 shows the drainage areas along with their corresponding recharge rate in inches per year.

Table A2-1 Recharge rates in the Colorado River basin. (Adapted from Saunders, 2006)

| <i>Reach</i> | <i>Description</i> | <i>Length (mi)</i> | <i>Area (acre)</i> | <i>Formation</i> | <i>Aquifer (TWDB)</i> | <i>Median adjusted gain/loss</i> | | | |
|--------------|--------------------|------------------------|------------------------|-----------------------------|------------------------------|----------------------------------|--------------|----------------|-----------------|
| | | | | | | <i>(cfs)</i> | <i>(AFY)</i> | <i>(in/yr)</i> | <i>(AFY/mi)</i> |
| #4 | LaGrange-Columbus | 40.9 | 377,171 | Catahoula, Oakville, Goliad | Catahoula-Jasper, Evangeline | 81 | 58,680 | 1.87 | 1,630 |
| #5 | Columbus-Wharton | 68.5 | 232,573 | Goliad, Willis, Lissie | Evangeline, Chicot | 10 | 7,244 | 0.37 | 177 |
| #6 | Wharton-Bay City | 34.1 | 165,817 | Lissie, Beaumont | Chicot | 98 | 70,996 | 5.14 | 1,036 |
| Total Gain: | | | | | | 189 | 136,920 | 2.12 | 954 |

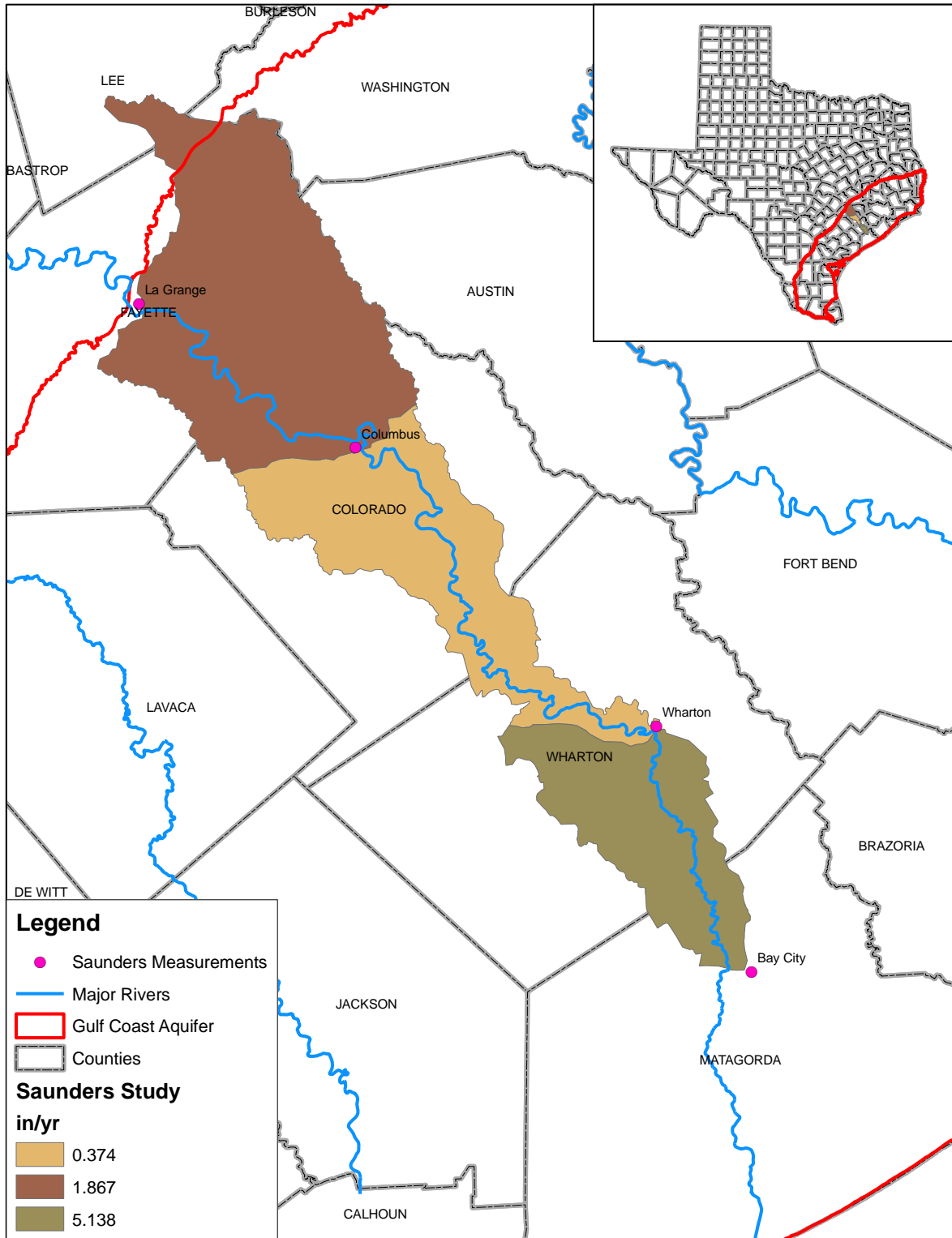


Figure A2-1. Recharge rates in the Colorado River Basin. (Adapted from Saunders, 2006)

A2.2 LSWP RECHARGE ESTIMATES-HYDROGRAPH SEPARATION

In addition to the LCRA low-flow study, the LSWP work also included hydrograph separation studies with estimates of shallow recharge (Young, Kelley, Budge, & Deeds, 2007). The results for selected gages that were least affected by external factors (as determined by the authors of the original study) and were within the Gulf Coast Aquifer are presented below in Table A2-2. **Error! Reference source not found.** shows the locations of the drainage areas where these recharge estimates were calculated.

Hydrograph separation was accomplished for each watershed with the code Base Flow Index (BFI) (Wahl & Wahl, 1995). When diversions were reported in the watershed, the baseflow calculated by hydrograph separation was increased by adding a portion of the reported diversion amount. This portion was calculated by determining the percentage of time that the river was flowing due to baseflow and not surface runoff. This percentage was then multiplied by the reported diversions and added to the baseflow calculated by hydrograph separation. The results of this calculation are presented under the column labeled “Baseflow (AFY)” in Table A2-2. Shallow areal recharge was then estimated by dividing by the reported incremental drainage area.

Table A2-2. LSWP recharge estimates from hydrograph separation analysis (Young et al., 2007).

| <i>Basin or Subbasin</i> | <i>Gage</i> | <i>Description</i> | <i>Area (mi²)</i> | <i>Baseflow (AFY)</i> | <i>Flux (in/yr)</i> |
|--------------------------|-------------|---------------------------------------|------------------------------|-----------------------|---------------------|
| Lavaca W | 8164000 | Lavaca River near Edna, TX | 817 | 41,220 | 0.95 |
| Lavaca E | 8164500 | Navidad River near Ganado, TX | 1062 | 50,616 | 0.89 |
| Lavaca E | 8164503 | West Mustang Creek near Ganado, TX | 178 | 8,543 | 0.90 |
| Lavaca E | 8164504 | East Mustang Creek near Louise, TX | 91 | 936 | 0.19 |
| Lavaca - Guadalupe | 8164600 | Garcitas Creek near Inez, TX | 92 | 2,369 | 0.48 |
| Lavaca - Guadalupe | 8164800 | Placedo Creek near Placedo, TX | 68 | 925 | 0.26 |
| Colorado - Lavaca | 8162600 | Tres Palacios River near Midfield, TX | 145 | 12,159 | 1.57 |
| Brazos - Colorado E | 8117500 | San Bernard River near Boling, TX | 727 | 75,529 | 1.95 |

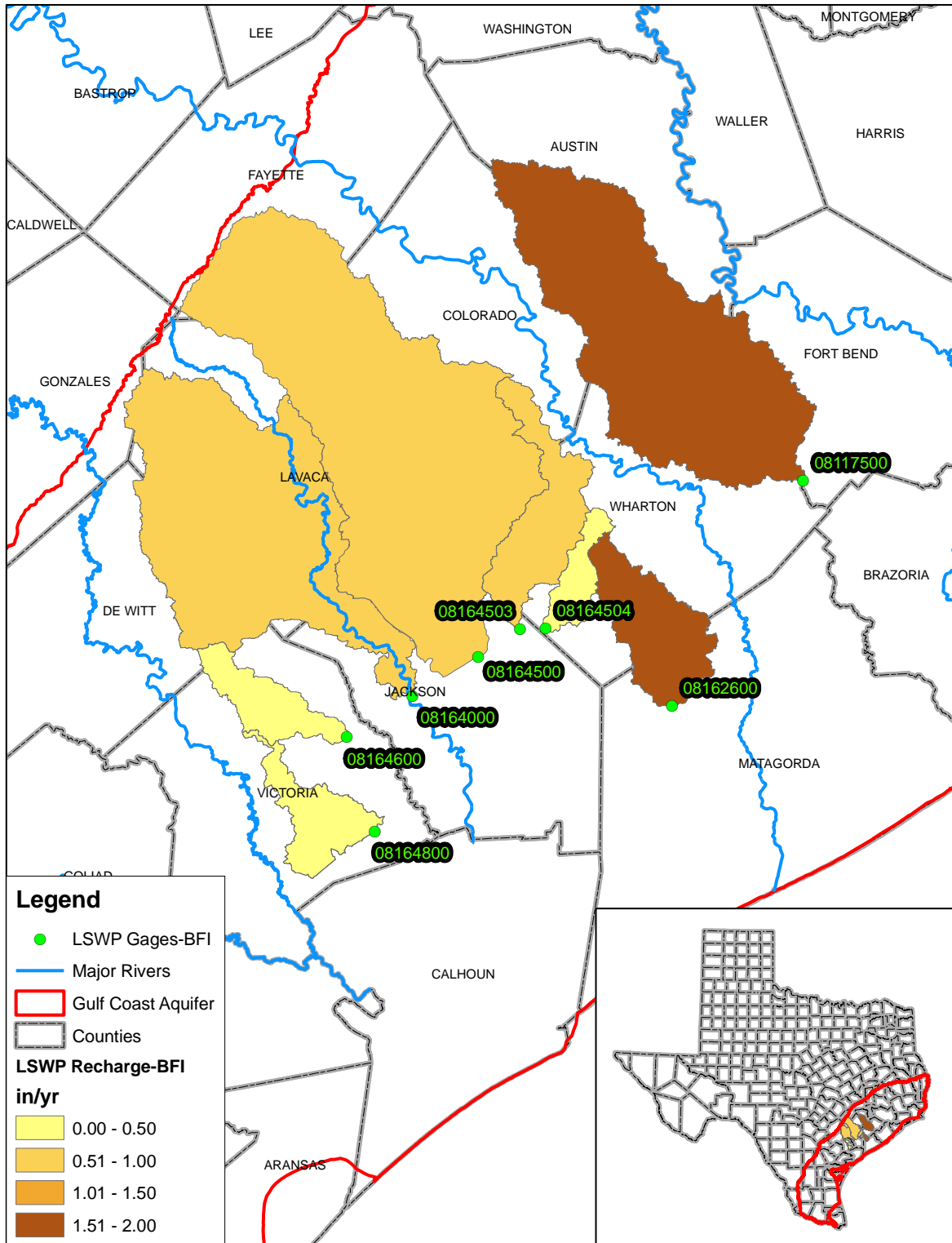


Figure A2-2. LSWP recharge estimates from hydrograph separation analysis.

A2.3 USGS RECHARGE ESTIMATES-BRAZOS RIVER

In March and August of 2006 the United States Geological Survey (USGS) conducted streamflow measurements along the Brazos River in an attempt to determine streamflow gains and losses (Turco, East, & Milburn, 2007). According to this report, the gain/loss in a river segment was calculated by taking a mass balance whereby the downstream flow rate was subtracted from the upstream flow rate and any additional inflows measured between the sites. However, the gain/loss was not reported as valid if the potential error in measured stream flow rate was greater than the calculated gain/loss. In order to calculate the measurements errors, the analyst rates the measurement as: excellent, good, fair, or poor. Each of these ratings has an associated percent range which the measurement could be within. The USGS then summed these errors for the downstream and upstream measurements in order to determine the potential error.

Unfortunately, only one of the estimates (B20, August 2006) for areas intersecting the Gulf Coast aquifer was considered valid according to the error analysis, and this estimate appears erroneously high (677.62 inches per year). We present a summary of the results, but do not recommend any of them be considered reliable. Table A2-3 and Table A2-4 show the results of the March and August measurements for the areas located within the Gulf Coast Aquifer. These tables have been adapted from the original report to include the recharge as a flux in inch/yr along with the sub-drainage area between the measurement locations. The recharge areas with the calculated flux are also presented in Figure A2-3 and Figure A2-4.

Table A2-3. March 2006 recharge calculated from USGS Scientific investigations report 2007-5286.

| Gage # | Site | Description | Lat | Long | Area (mi ²) | Gain (ft ³ /s) | Rech (in/yr) | Valid ¹ |
|-----------------|------|--|--------|---------|-------------------------|---------------------------|--------------|--------------------|
| 302230096175000 | B18 | Brazos River near FM 1955 near Clay, Tex. | 30.375 | -96.297 | 11.89 | -5 | -5.71 | No |
| 302200096152900 | B19 | Brazos River at Rogers Plantation near Millican Tex. | 30.367 | -96.258 | 8.17 | 94 | 156.2 | No |
| 302342096110400 | B20 | Brazos River near FM 159 near Millican Tex. | 30.395 | -96.184 | 4.75 | -118 | -337.4 | No |
| 302134096091800 | B21 | Brazos River at SH 105 near Washington Tex. | 30.359 | -96.155 | 21.8 | -19 | -11.83 | No |
| 301927096085300 | B22 | Brazos River below Navasota River near Washington Tex. | 30.324 | -96.148 | 84.07 | 38 | 6.14 | No |
| 301713096050000 | B23 | Brazos River at Old River Road near Courtney Tex. | 30.287 | -96.083 | 86.71 | 28 | 4.38 | No |
| 301313096071200 | B24 | Brazos River near FM 2726 near Courtney Tex. | 30.220 | -96.120 | 38.45 | 75 | 26.48 | No |
| 301014096092700 | B25 | Brazos River near FM 1736 near Hempstead Tex. | 30.171 | -96.158 | 235.96 | -152 | -8.74 | No |
| 8111500 | B26 | Brazos River near Hempstead Tex. | 30.129 | -96.188 | 56.6 | 77.2 | 18.52 | No |
| 300217096063400 | B27 | Brazos River at SH 159 near Hempstead Tex. | 30.038 | -96.109 | 10.98 | 19 | 23.5 | No |
| 300024096050500 | B28 | Brazos River near FM 1887 near Hempstead Tex. | 30.007 | -96.085 | 13.53 | 24.6 | 24.69 | No |
| 295431096064800 | B29 | Brazos River at FM 529 near Burleigh Tex. | 29.909 | -96.113 | 100.16 | -35.8 | -4.85 | No |
| 294830096054400 | B30 | Brazos River at FM 1458 at San Felipe Tex. | 29.808 | -96.096 | 16.2 | 167 | 139.97 | No |
| 294617096021200 | B31 | Brazos River at IH010 near Brookshire Tex. | 29.771 | -96.037 | 92.49 | -40 | -5.87 | No |
| 294017096011400 | B32 | Brazos River at FM 1093 at Simonton Tex. | 29.671 | -96.021 | 17.03 | -80 | -63.78 | No |
| 293820095583200 | B33 | Brazos River at FM 1489 near Simonton Tex. | 29.639 | -95.976 | 47.46 | -139 | -39.76 | No |
| 293621095521300 | B34 | Brazos River at CR near FM 359 near Rosenberg Tex. | 29.606 | -95.870 | 17.98 | 56 | 42.29 | No |
| 293403095483700 | B35 | Brazos River at FM 723 near Rosenberg Tex. | 29.568 | -95.810 | 25.78 | -59 | -31.06 | No |
| 8114000 | B36 | Brazos River at Richmond Tex. | 29.582 | -95.758 | | | | |

¹ Recharge is valid if potential error in measurement is less than the absolute value of the calculated gain/loss.

Table A2-4. August 2006 recharge calculated from USGS Scientific investigations report 2007-5286

| Gage # | Site | Description | Lat | Long | Area (mi ²) | Gain (ft ³ /s) | Rech (in/yr) | Valid ¹ |
|-----------------|------|--|---------|----------|-------------------------|---------------------------|--------------|--------------------|
| 302230096175000 | B18 | Brazos River near FM 1955 near Clay, Tex. | 30.3750 | -96.2972 | 11.89 | 14 | 15.98 | No |
| 302200096152900 | B19 | Brazos River at Rogers Plantation near Millican Tex. | 30.3667 | -96.2581 | 8.17 | 138 | 229.31 | No |
| 302342096110400 | B20 | Brazos River near FM 159 near Millican Tex. | 30.3950 | -96.1844 | 4.75 | -237 | - | Yes |
| 302134096091800 | B21 | Brazos River at SH 105 near Washington Tex. | 30.3594 | -96.1550 | 21.80 | -24 | -14.94 | No |
| 301927096085300 | B22 | Brazos River below Navasota River near Washington Tex. | 30.3242 | -96.1481 | 84.07 | 97 | 15.66 | No |
| 301713096050000 | B23 | Brazos River at Old River Road near Courtney Tex. | 30.2869 | -96.0833 | 86.71 | 36 | 5.64 | No |
| 301313096071200 | B24 | Brazos River near FM 2726 near Courtney Tex. | 30.2203 | -96.1200 | 38.45 | -7 | -2.47 | No |
| 301014096092700 | B25 | Brazos River near FM 1736 near Hempstead Tex. | 30.1706 | -96.1575 | 235.96 | -11 | -0.63 | No |
| 08111500 | B26 | Brazos River near Hempstead Tex. | 30.1289 | -96.1875 | 56.60 | 66 | 15.83 | No |
| 300217096063400 | B27 | Brazos River at SH 159 near Hempstead Tex. | 30.0381 | -96.1094 | 10.98 | -12 | -14.84 | No |
| 300024096050500 | B28 | Brazos River near FM 1887 near Hempstead Tex. | 30.0067 | -96.0847 | 13.53 | 36.6 | 36.73 | No |
| 295431096064800 | B29 | Brazos River at FM 529 near Burleigh Tex. | 29.9086 | -96.1133 | 100.16 | -21.8 | -2.95 | No |
| 294830096054400 | B30 | Brazos River at FM 1458 at San Felipe Tex. | 29.8083 | -96.0956 | 16.20 | 1 | 0.84 | No |
| 294617096021200 | B31 | Brazos River at IHû10 near Brookshire Tex. | 29.7714 | -96.0367 | 92.49 | -70 | -10.27 | No |
| 294017096011400 | B32 | Brazos River at FM 1093 at Simonton Tex. | 29.6714 | -96.0206 | 17.03 | 56 | 44.65 | No |
| 293820095583200 | B33 | Brazos River at FM 1489 near Simonton Tex. | 29.6389 | -95.9756 | 65.44 | -35 | -7.26 | No |
| 293403095483700 | B35 | Brazos River at FM 723 near Rosenberg Tex. | 29.5675 | -95.8103 | 25.78 | -103 | -54.23 | No |
| 08114000 | B36 | Brazos River at Richmond Tex. | 29.5822 | -95.7575 | | | | |

¹ Recharge is valid if potential error in measurement is less than the absolute value of the calculated gain/loss.

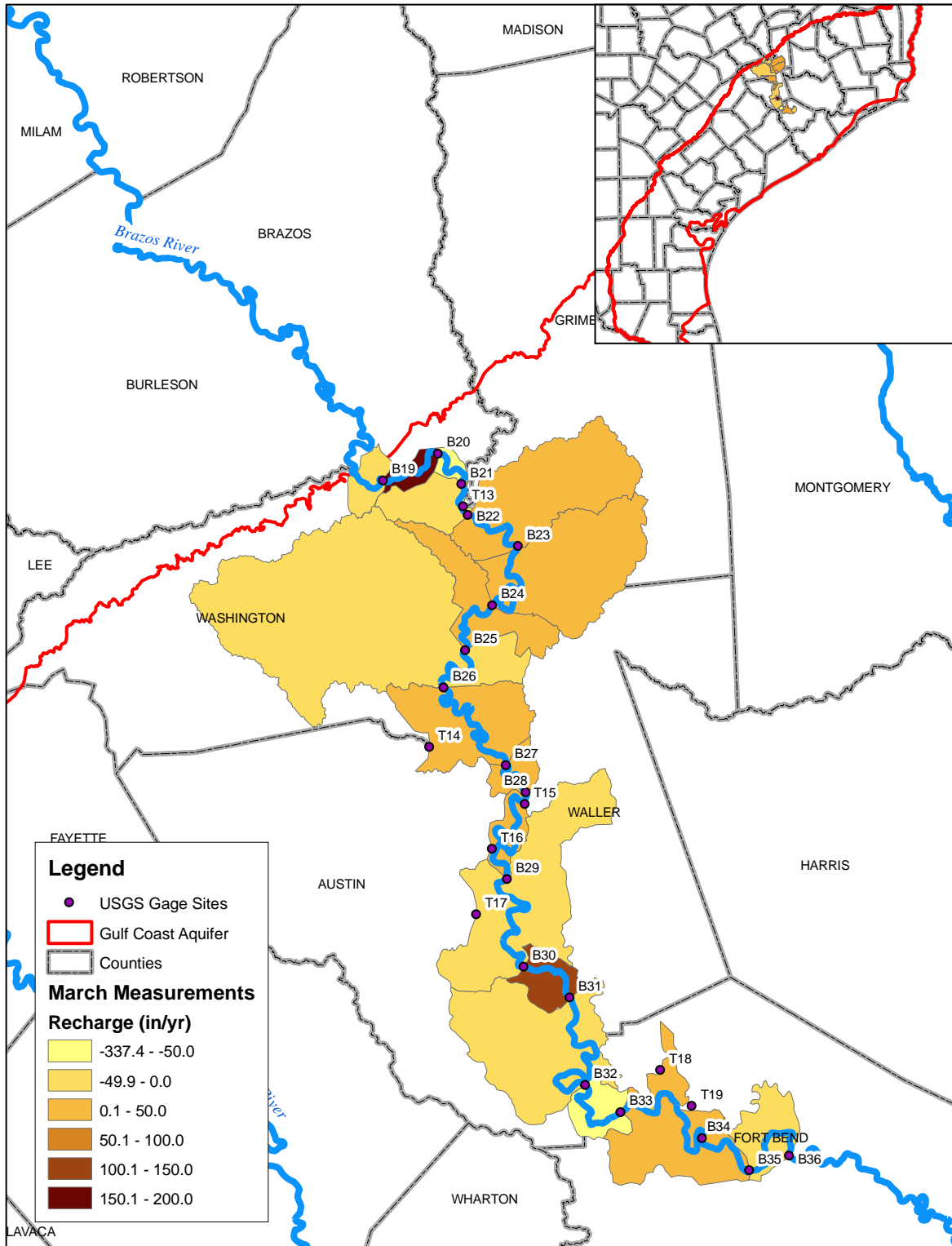


Figure A2-3. March 2006 recharge calculated from SUGS Scientific investigations report 2007-5286.

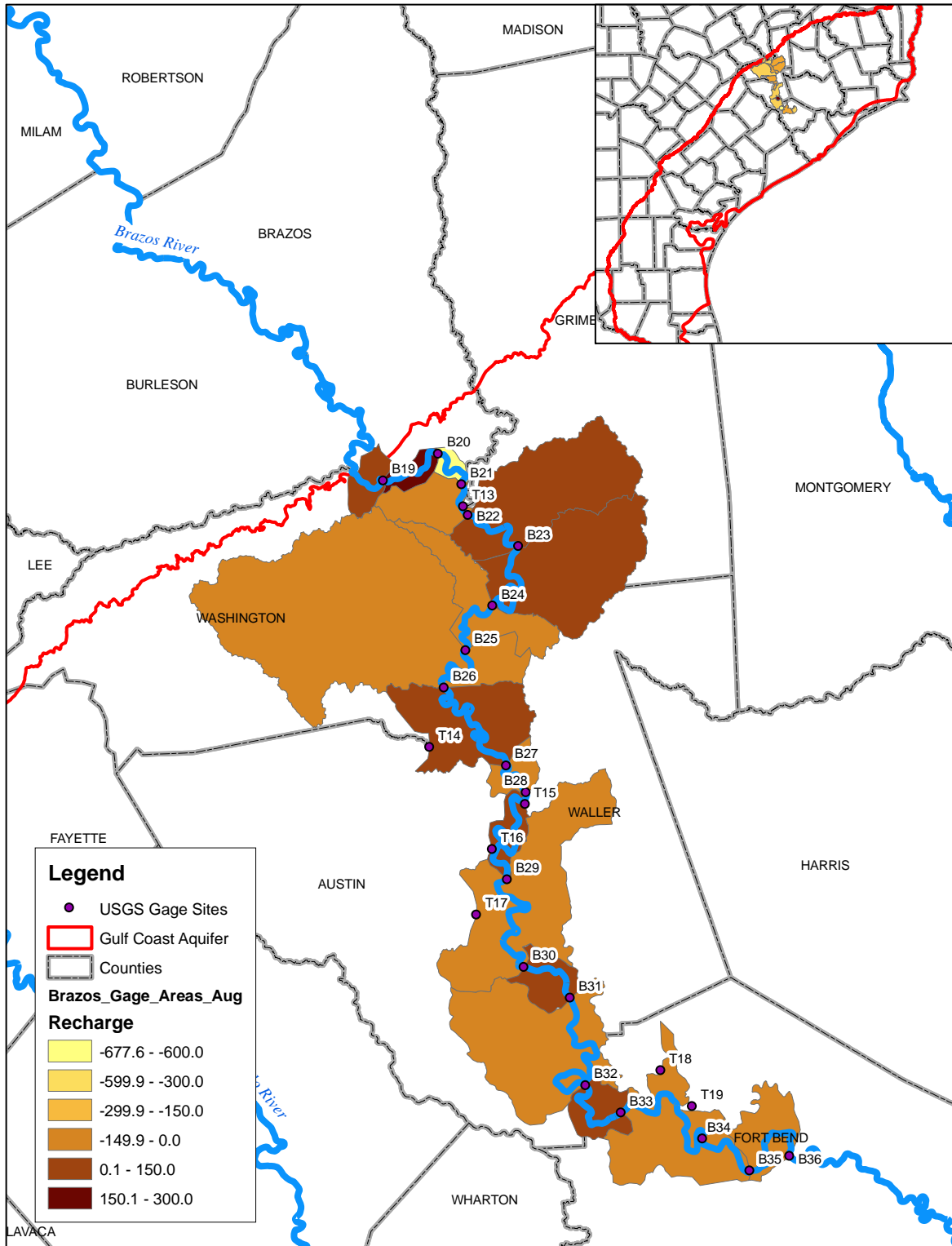


Figure A2-4. August 2006 recharge calculated from USGS Scientific investigations report 2007-5286.

A2.4 USGS RECHARGE ESTIMATES-SLADE ET AL.

The USGS in cooperation with the Texas Water Development Board (TWDB) published Results of Streamflow Gain-Loss Studies in Texas, With Emphasis on Gains From and Losses to Major and Minor Aquifers by Slade et al. (2002) This report lists the results of 366 gain-loss studies conducted by calculating a mass-balance from low flow stream measurements, return flows, withdrawals, and evapotranspiration. Four studies from this report, which are located in the Gulf Coast Aquifer, are presented in this section. The total gain (expressed in cfs) for each reach was taken from the report and the watershed for each reach delineated by using the gage location of each measurement along with ArcGIS Spatial Analyst tools. The gain was then computed in inch/year by dividing by the calculated watershed area and converting units. The results of this analysis are presented below in Table A2-5 and Figure A2-5.

Table A2-5. Gains reported by Slade et al. (2002) for areas within the Gulf Coast Aquifer.

| Study # | Area (acre) | Gain (ft ³ /s) | Gain (inch/year) |
|---------|-------------|---------------------------|------------------|
| 54 | 909,427 | 204.4 | 1.95 |
| 135 | 458,417 | 15.8 | 0.30 |
| 138 | 158,464 | 10.2 | 0.56 |
| 142 | 263,653 | 2.6 | 0.08 |

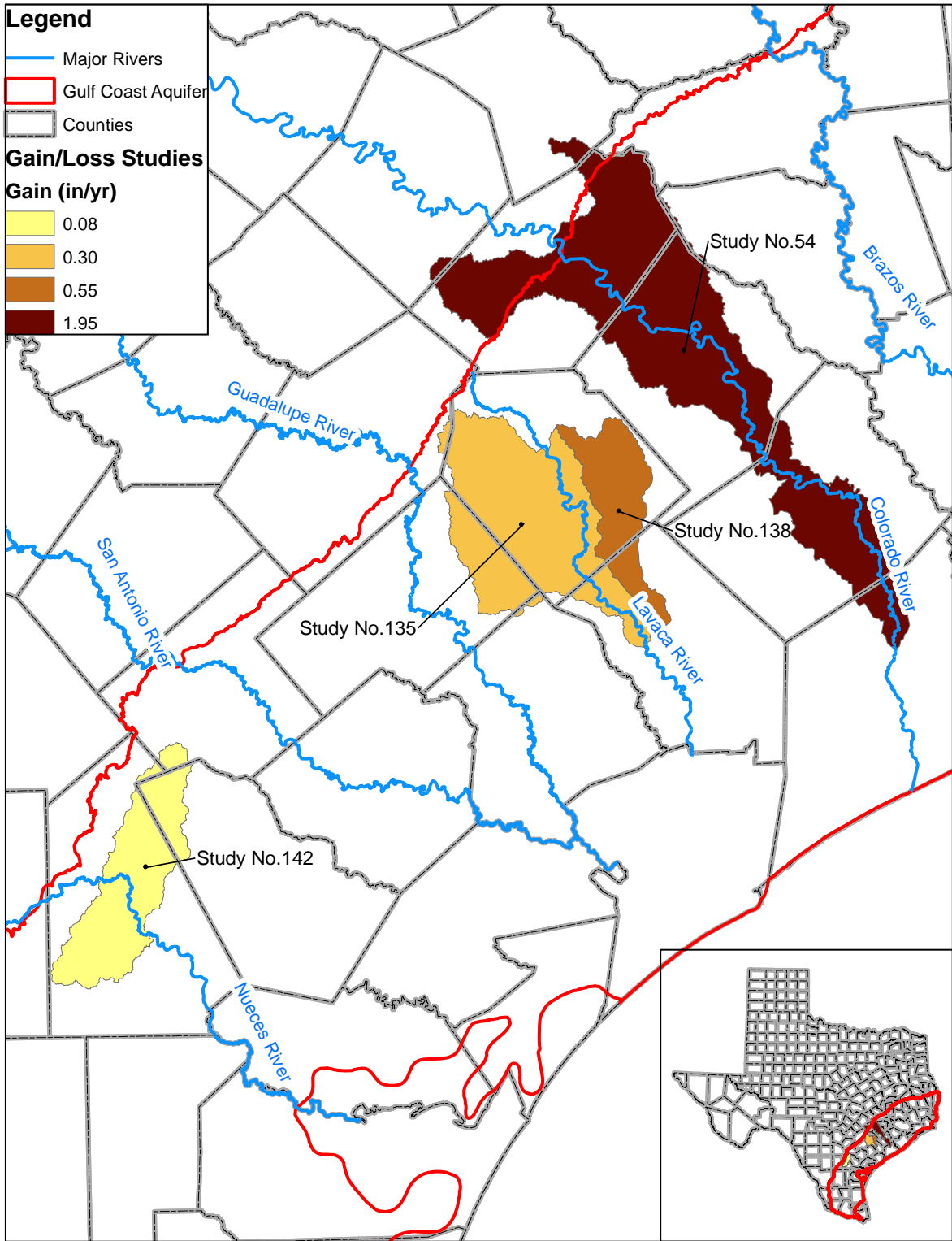
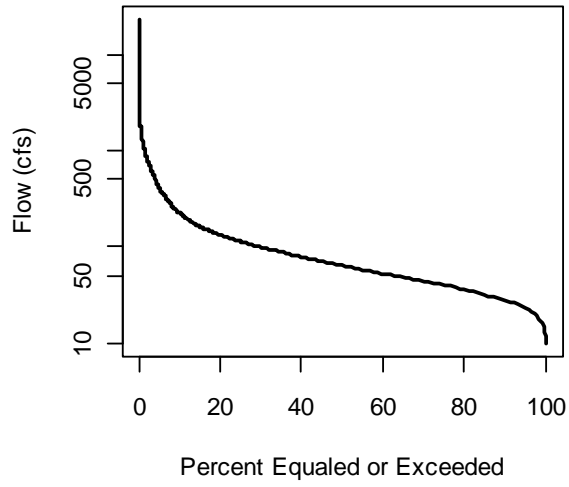


Figure A2-5. Location of studies reported by Slade et al. (2002) within the Gulf Coast Aquifer.

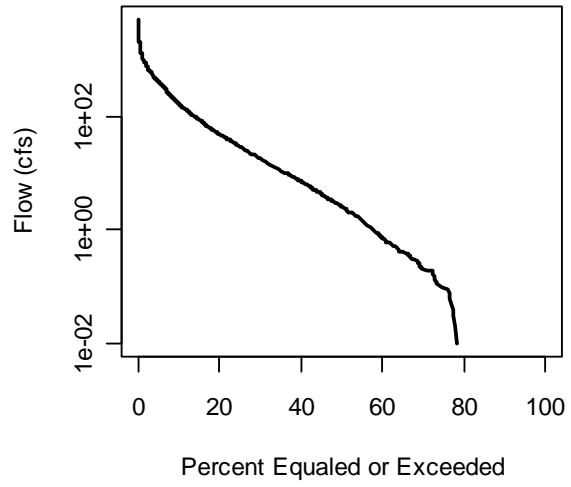
APPENDIX 3
Flow Duration Curves

Locations of the following USGS gage stations shown in Figure 26.

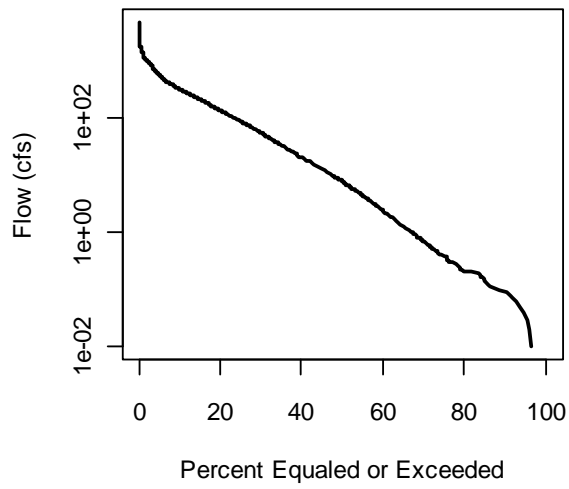
8029500



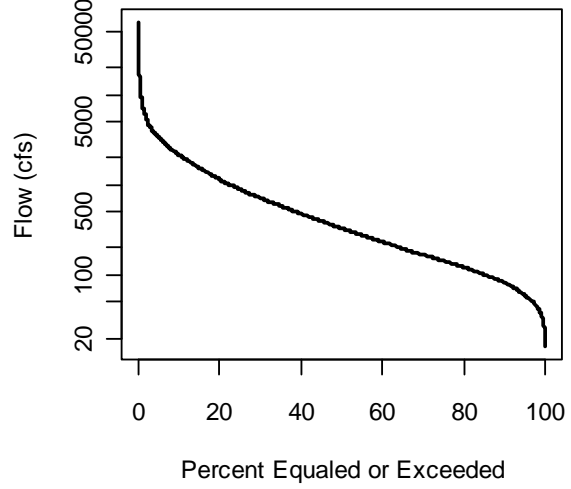
8030000



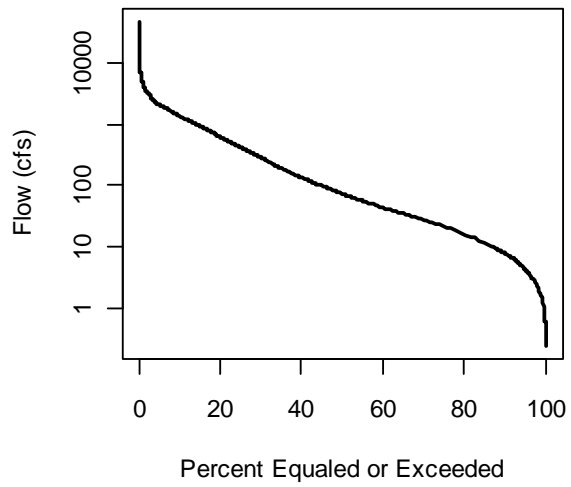
8031000



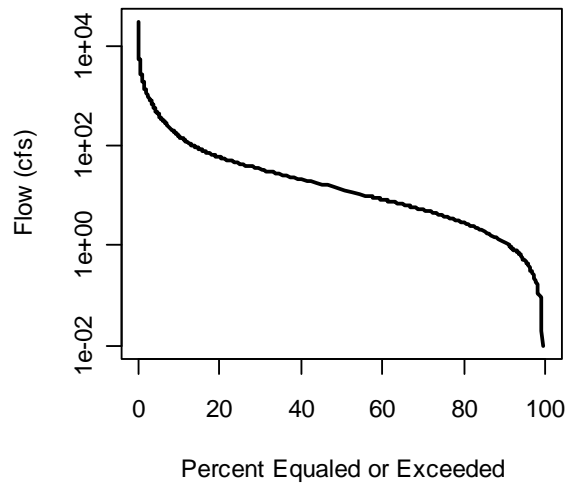
8041500



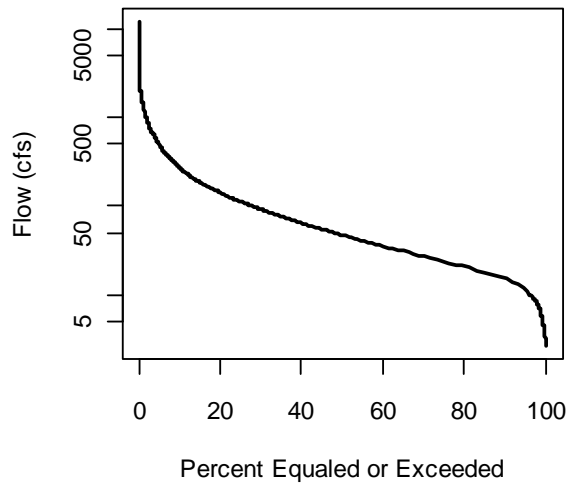
8041700



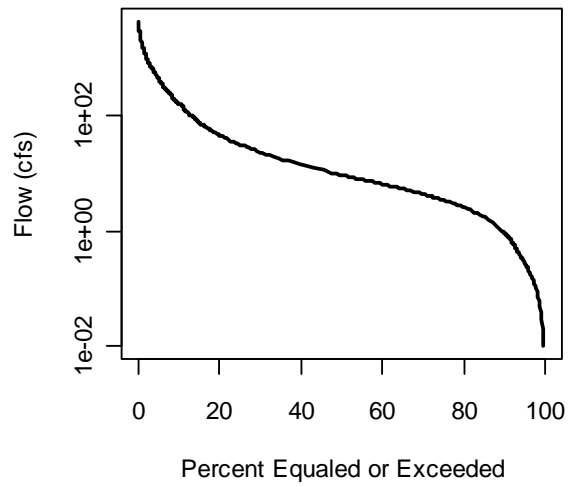
8066200



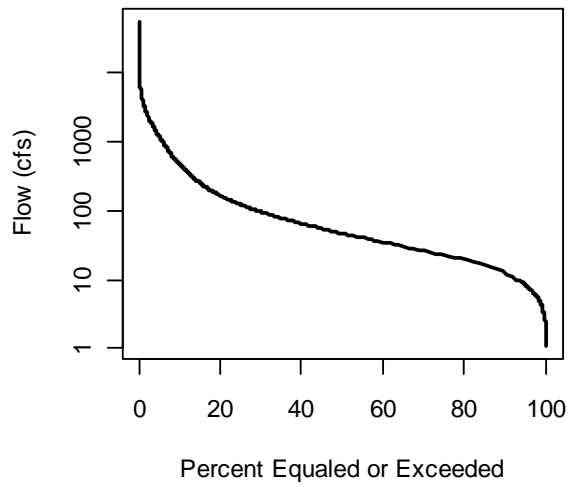
8066300



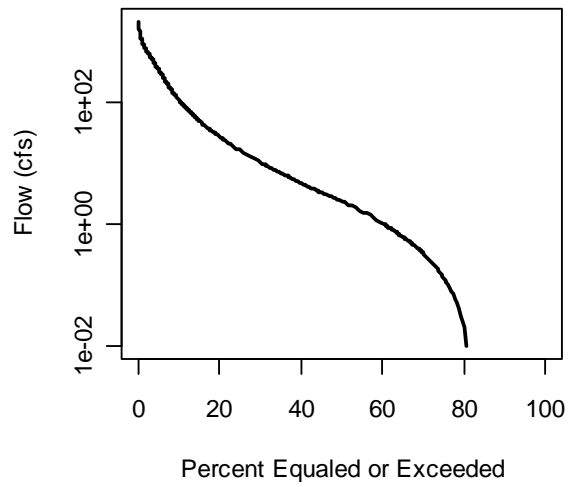
8067500



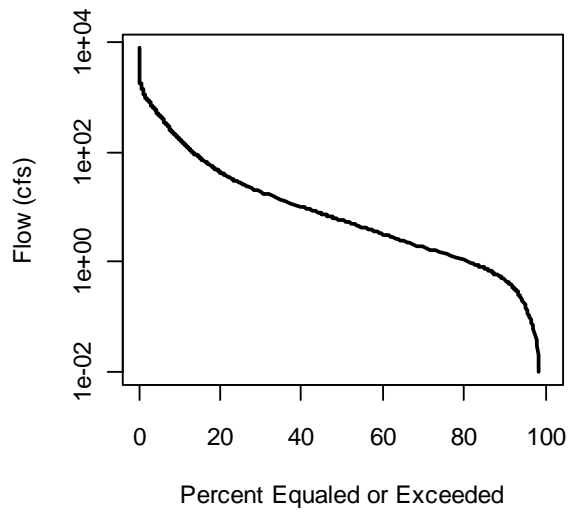
8068500



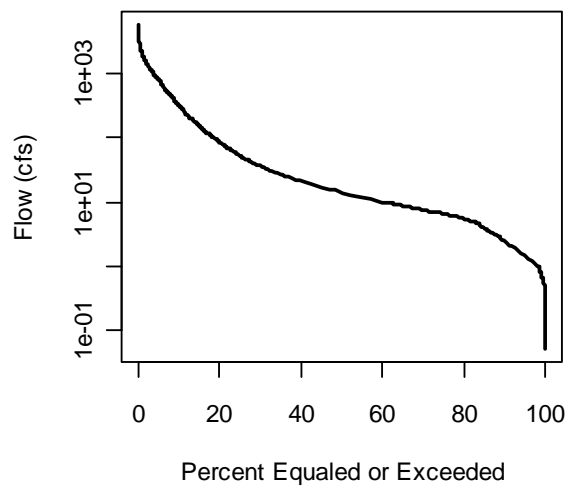
8068720



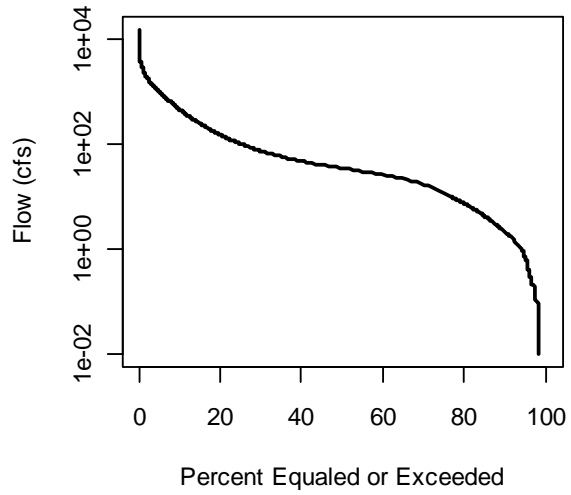
8068740



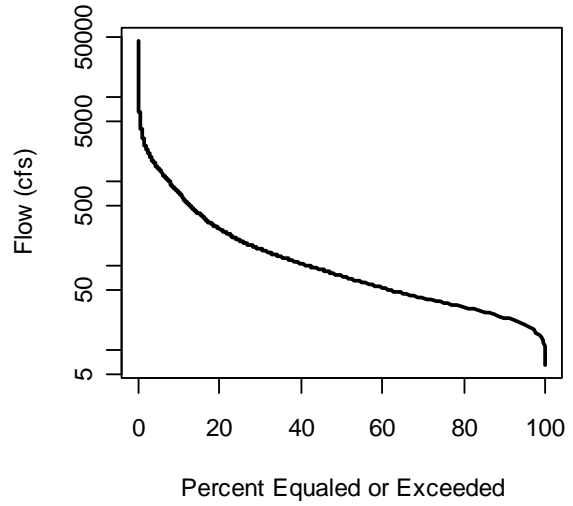
8068800



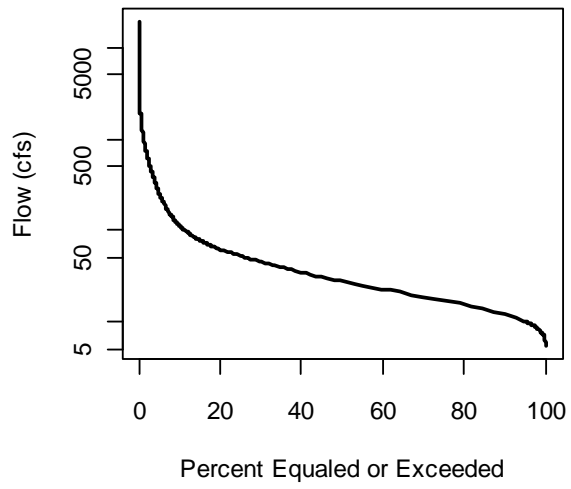
8069000



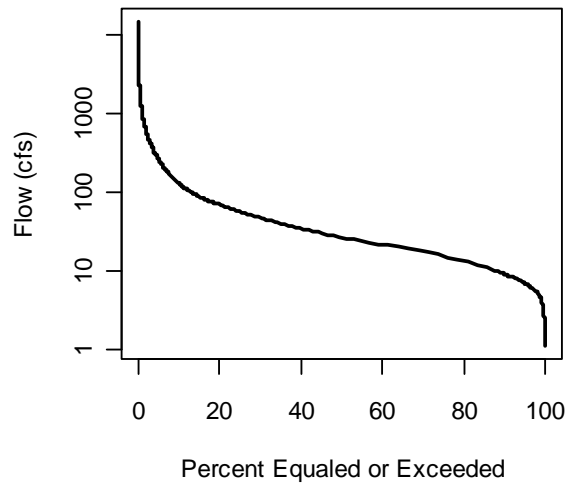
8070200



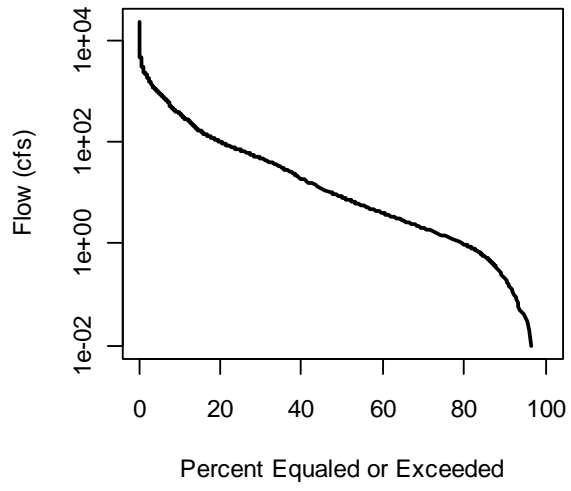
8070500



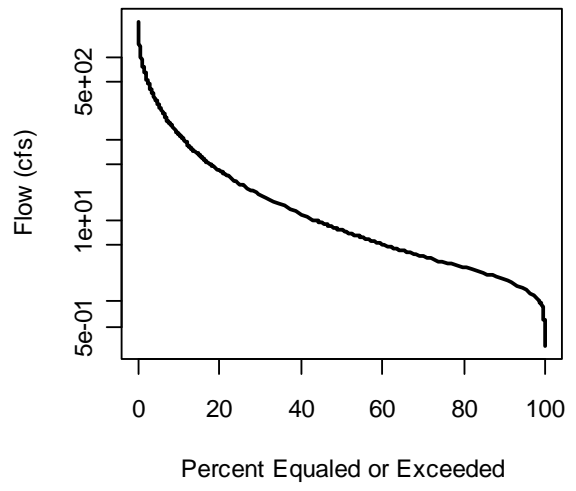
8071000



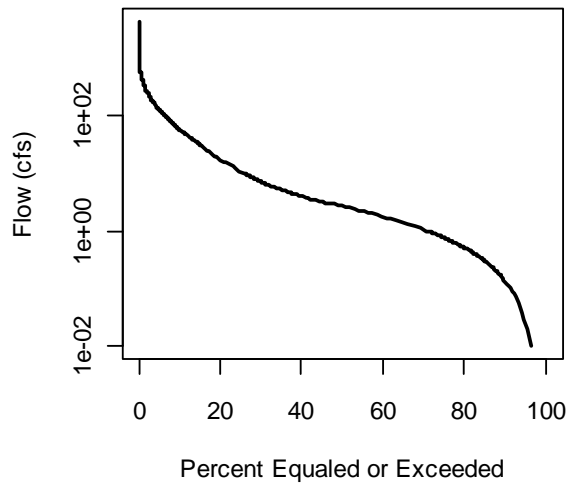
8071280



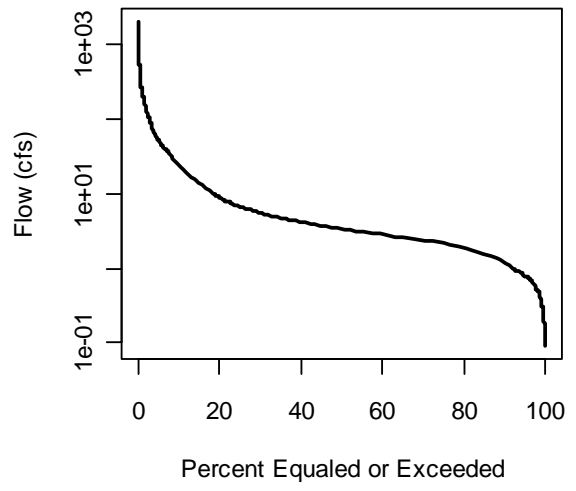
8072300



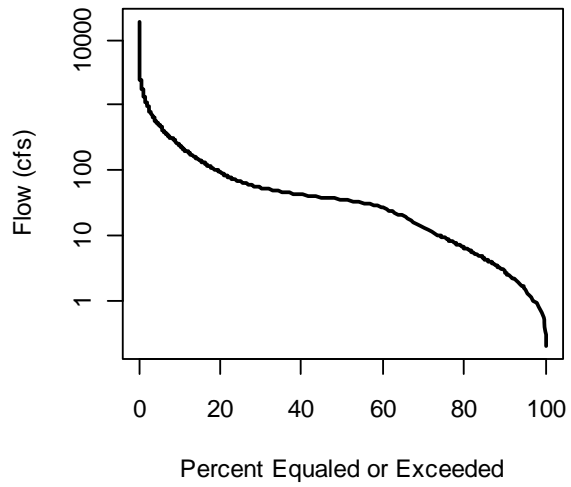
8072730



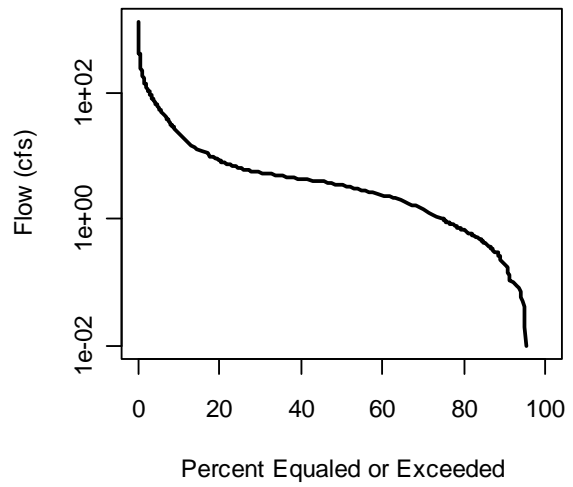
8074250



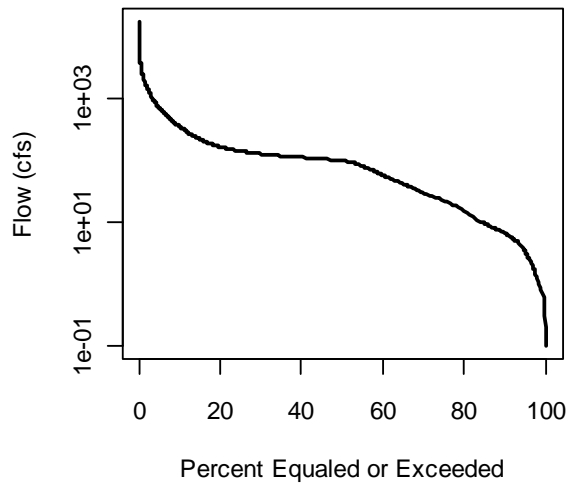
8074500



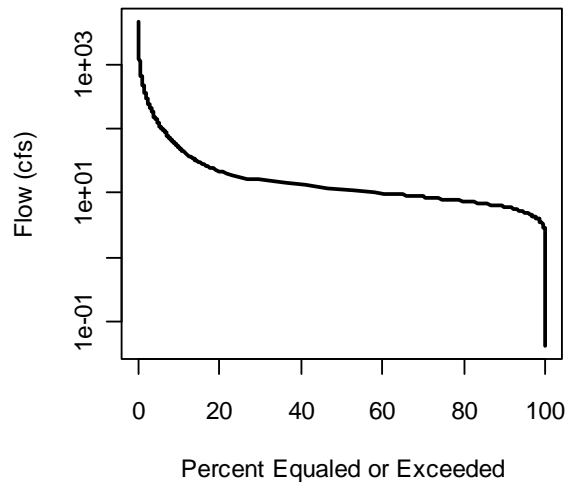
8074800



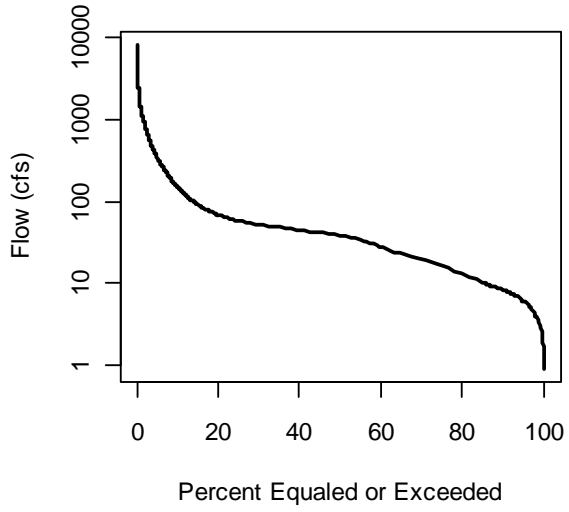
8075000



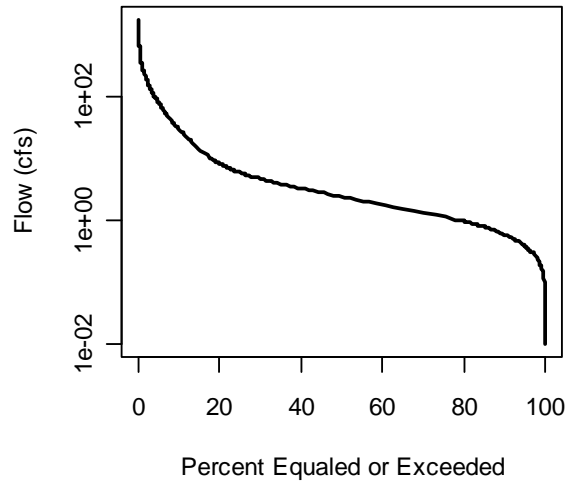
8075400



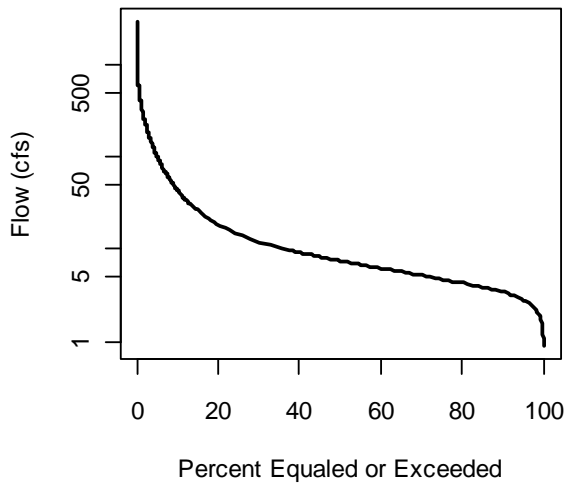
8075500



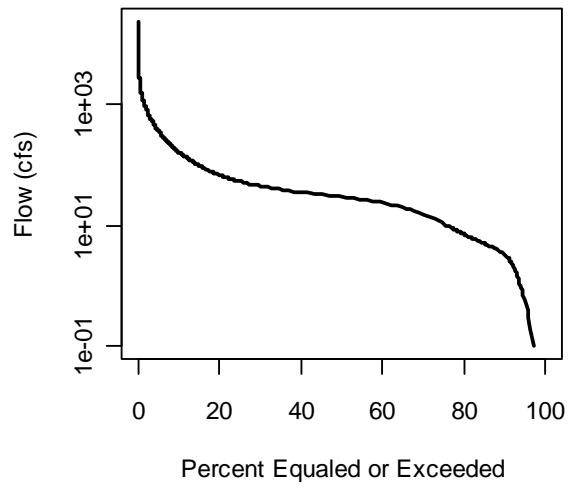
8075730



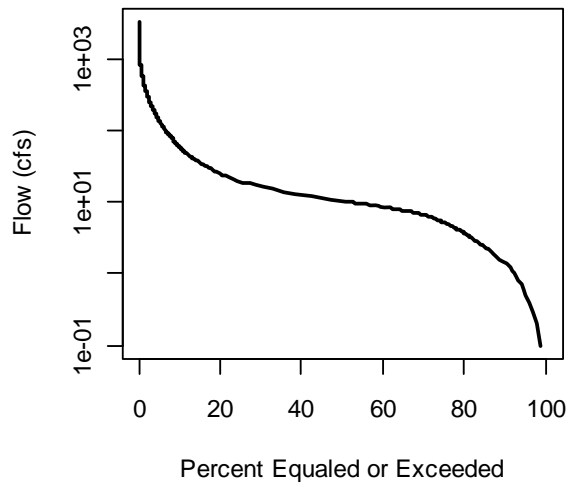
8075770



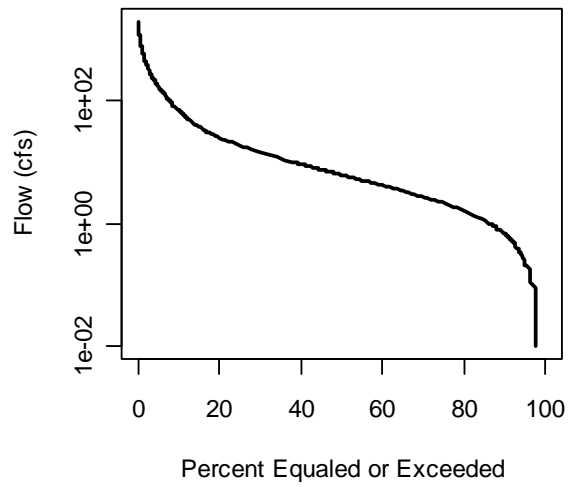
8076000



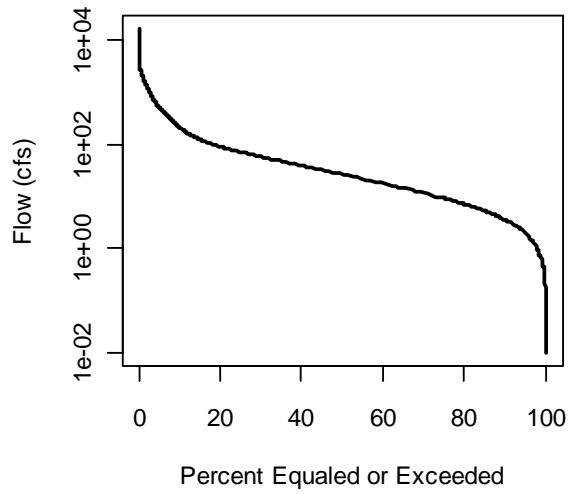
8076500



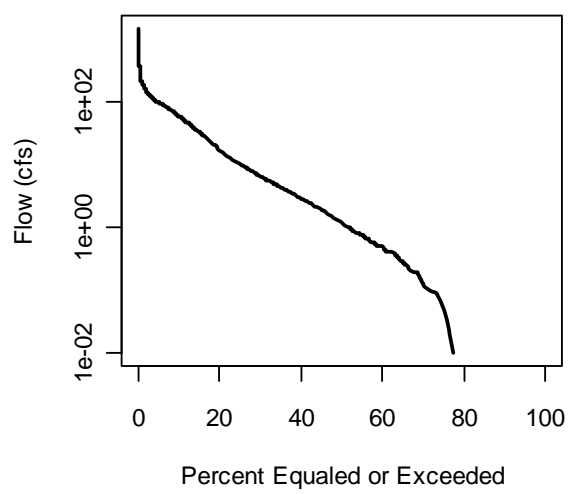
8077000



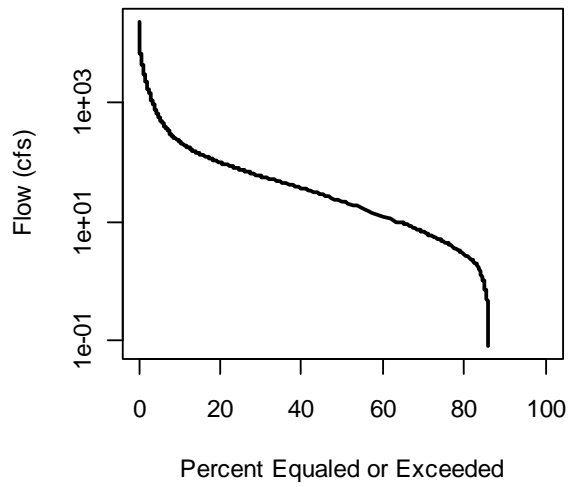
8078000



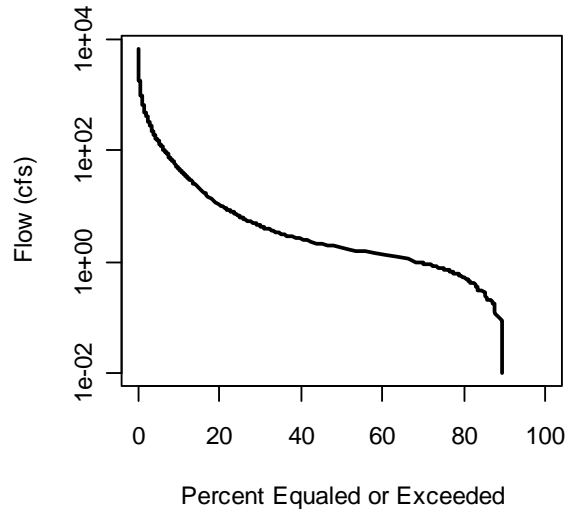
8116400



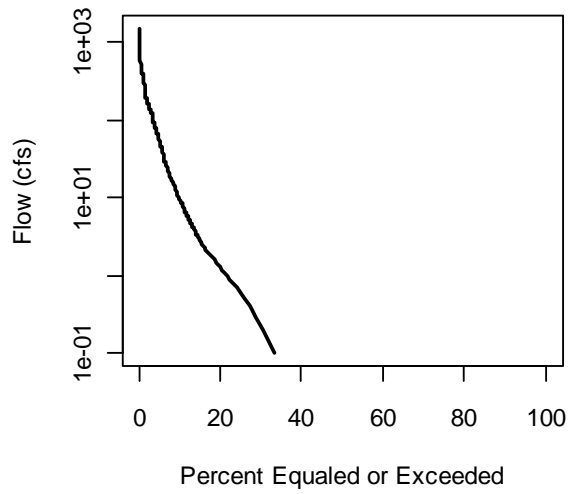
8111700



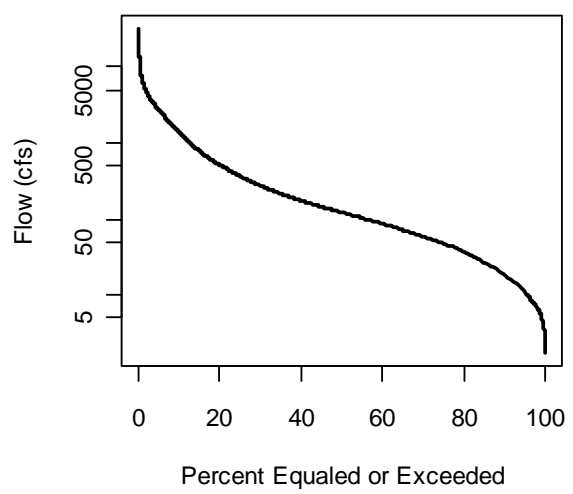
8115000



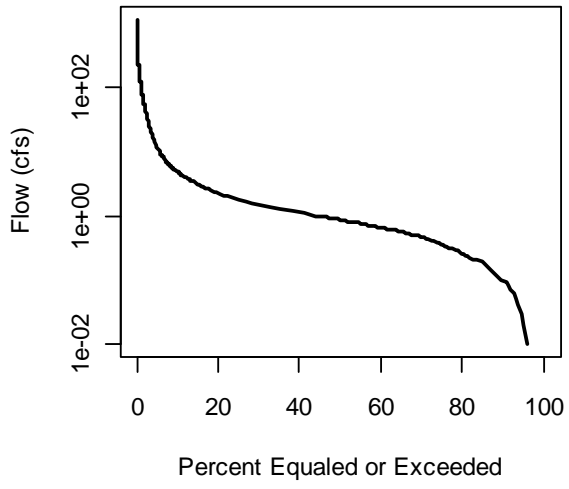
8115500



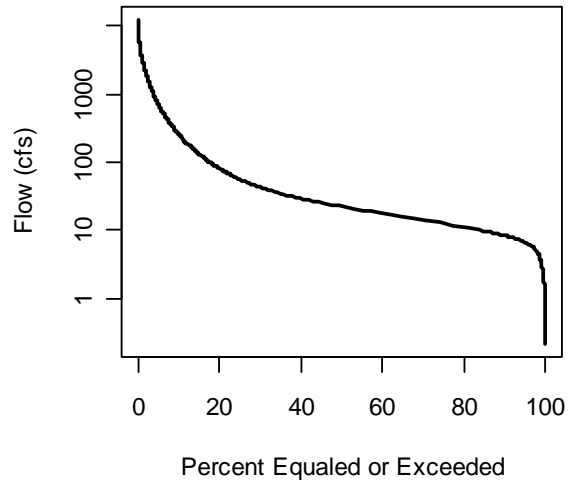
8117500



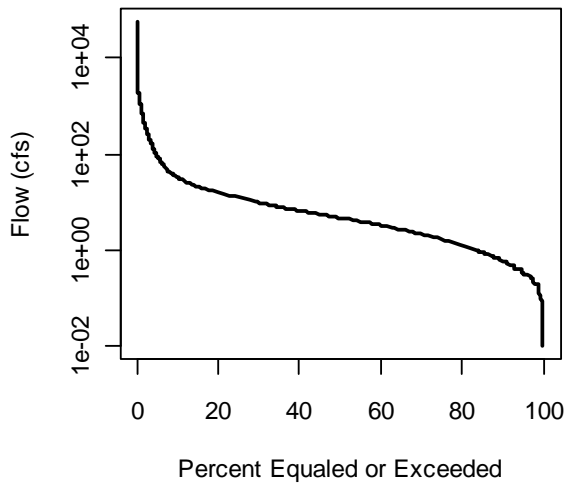
8160800



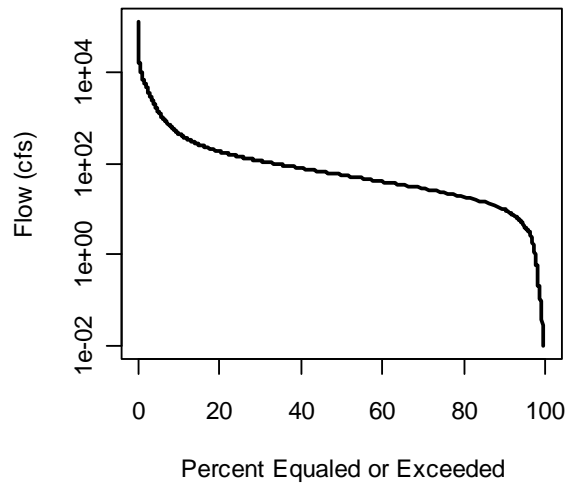
8162600



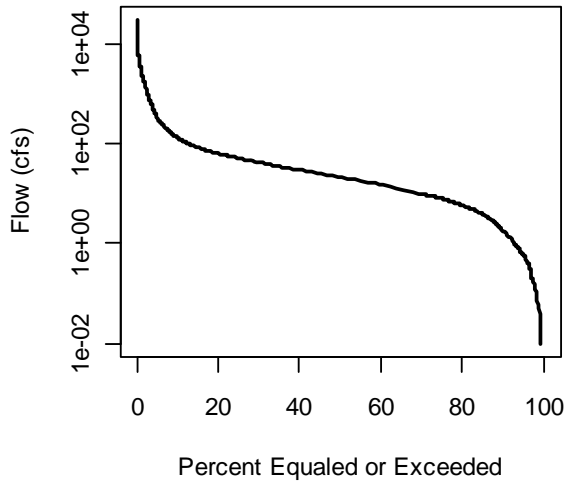
8163500



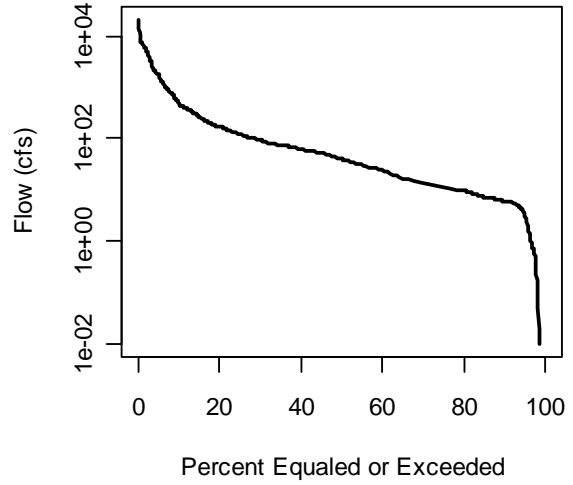
8164000



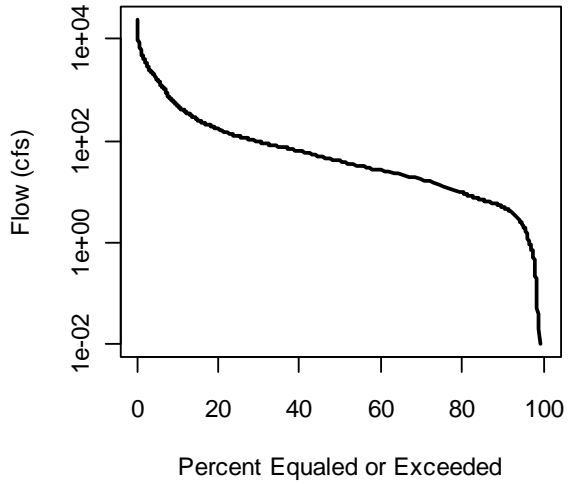
8164300



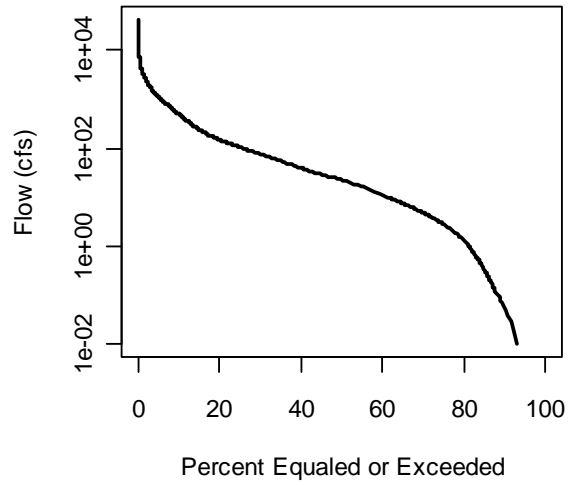
8164370



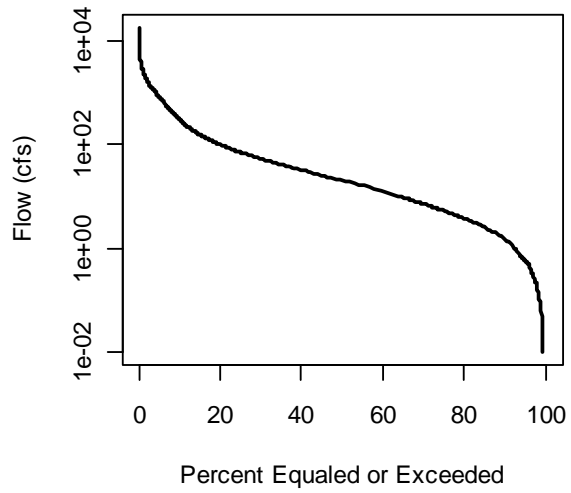
8164390



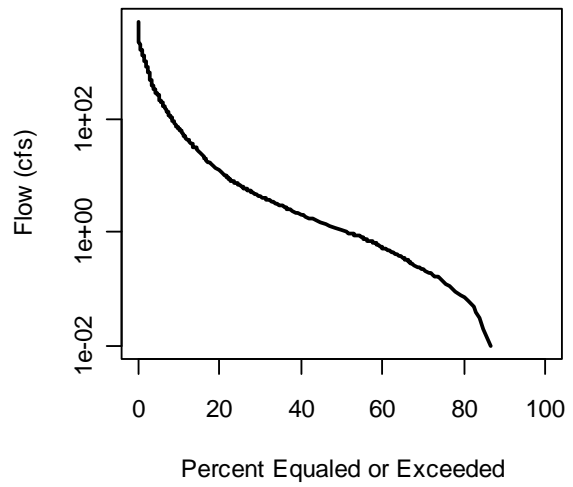
8164450



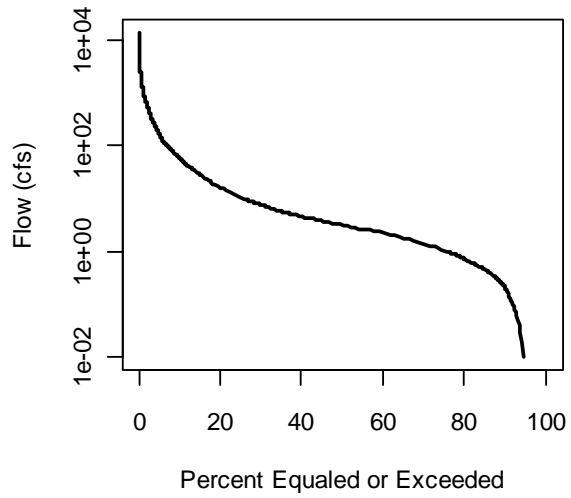
8164503



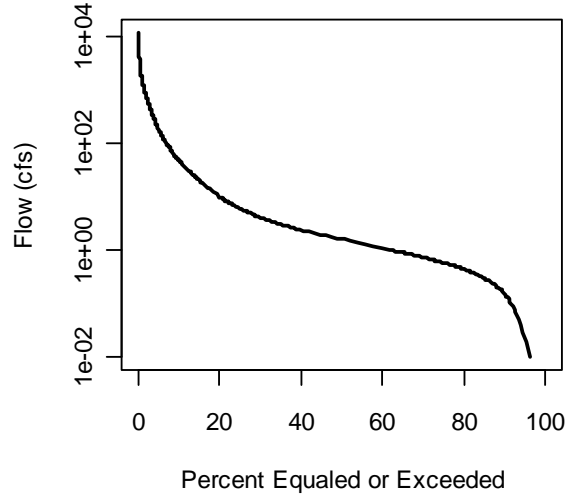
8164504



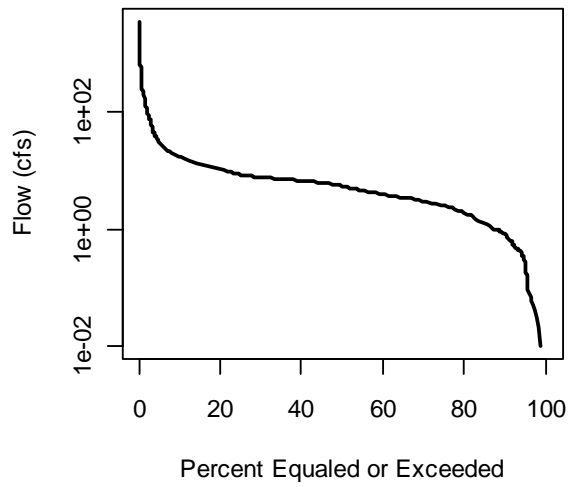
8164600



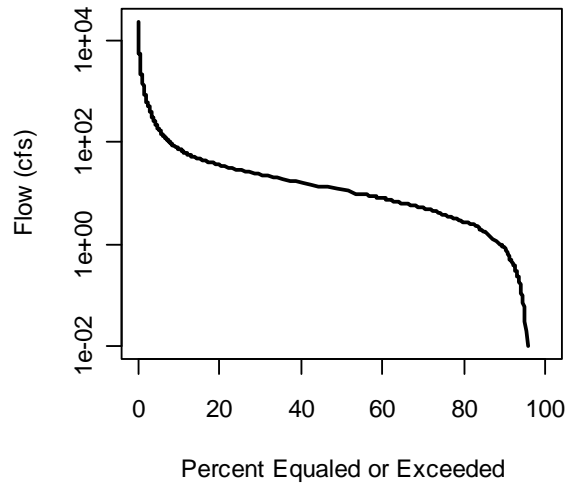
8164800



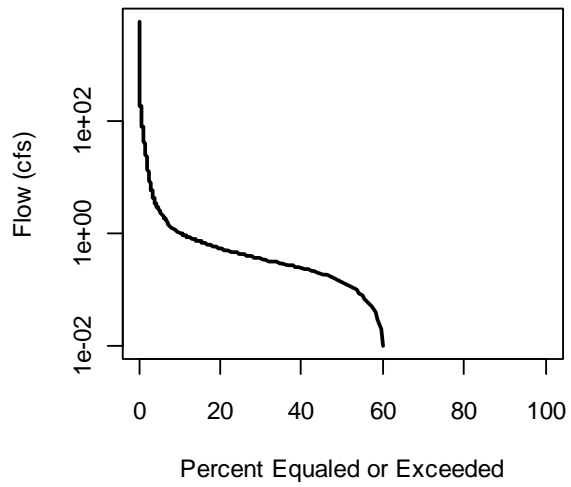
8176550



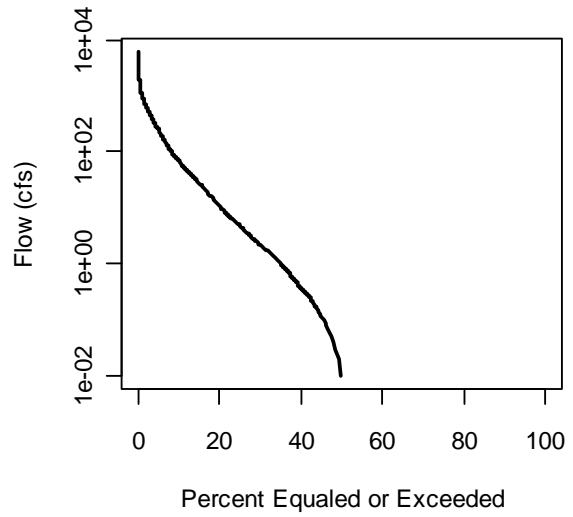
8176900



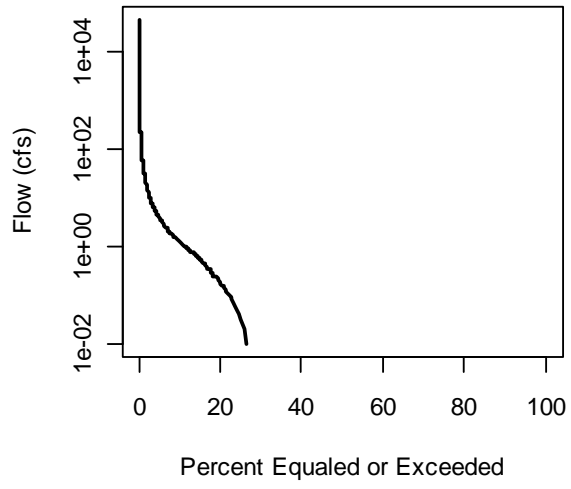
8177300



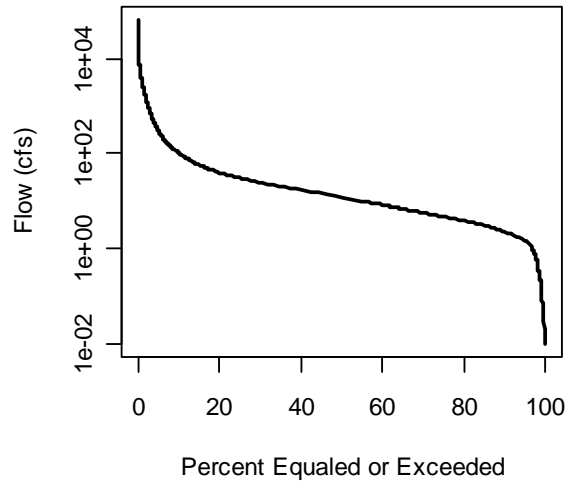
8189200



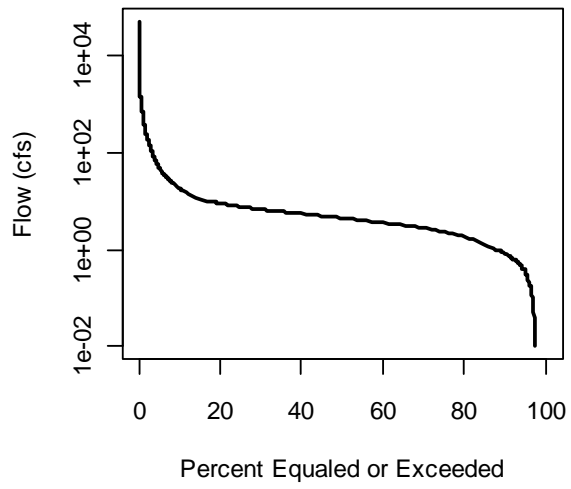
8189300



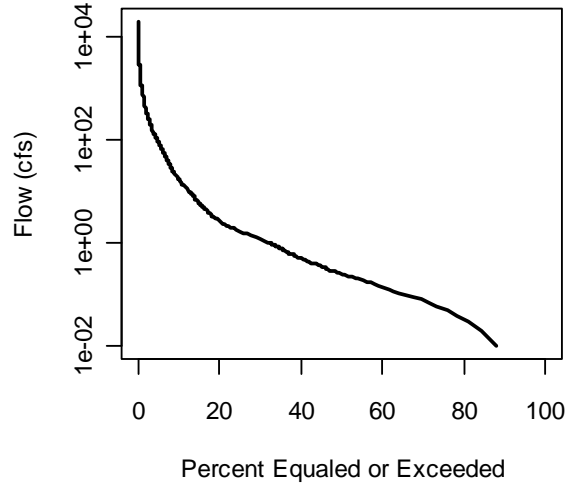
8189500



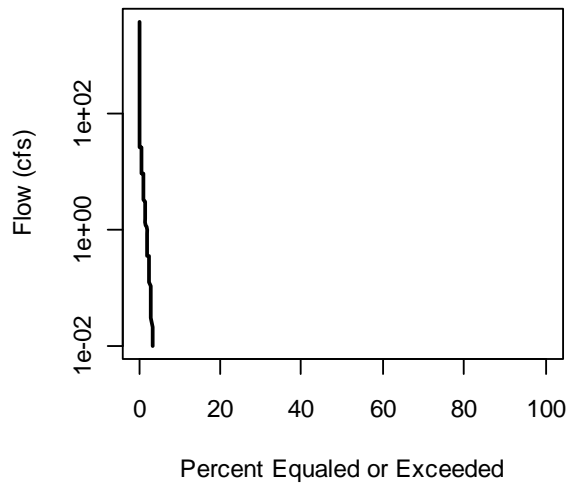
8189700



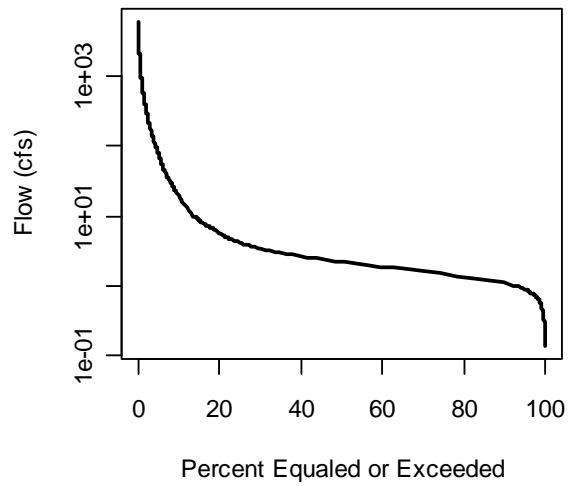
8189800



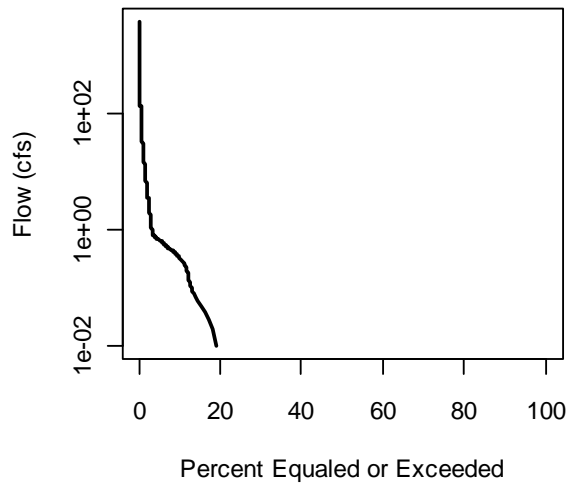
8210400



8211520



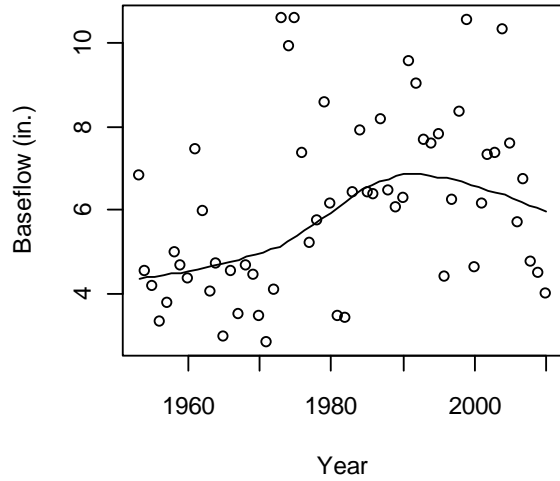
8212400



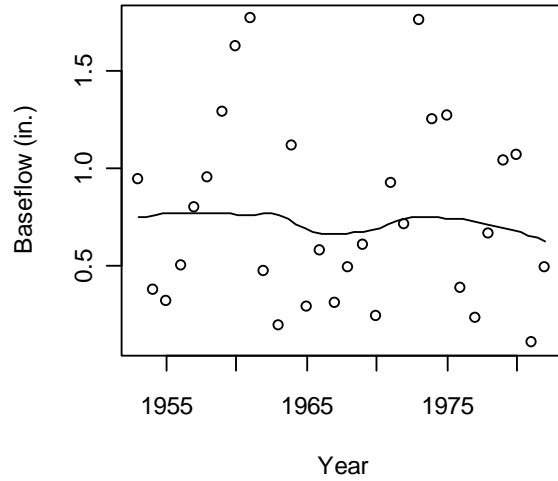
APPENDIX 4
Baseflow Trends

Locations of the following USGS gage stations shown in Figure 26.

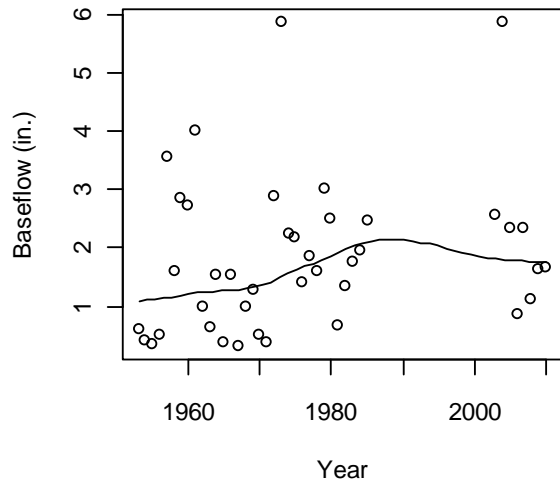
8029500



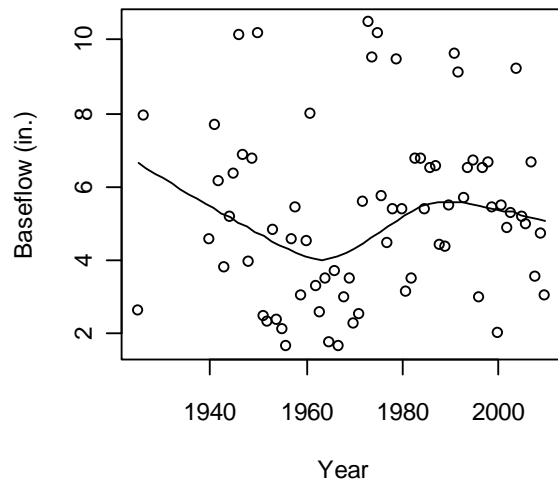
8030000



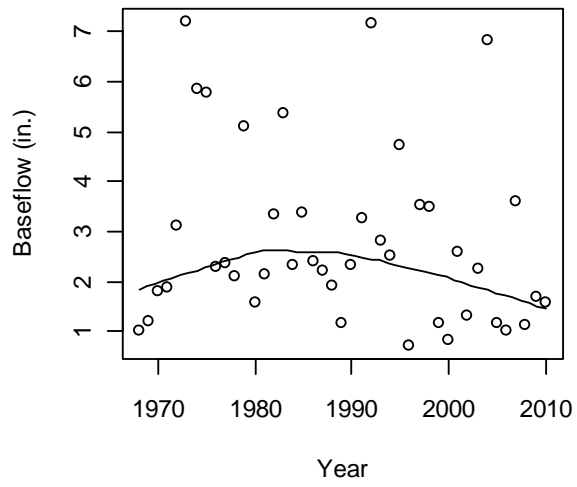
8031000



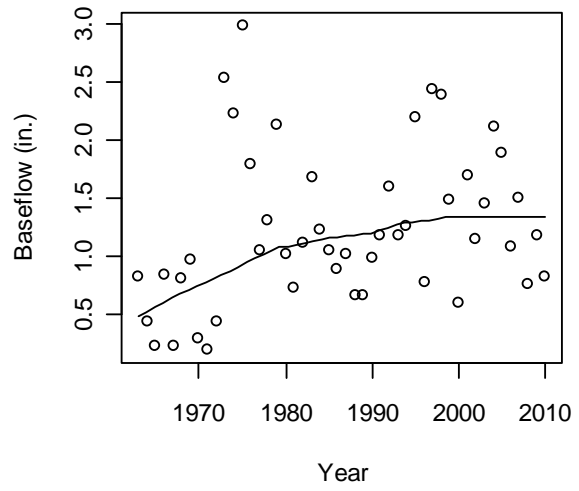
8041500



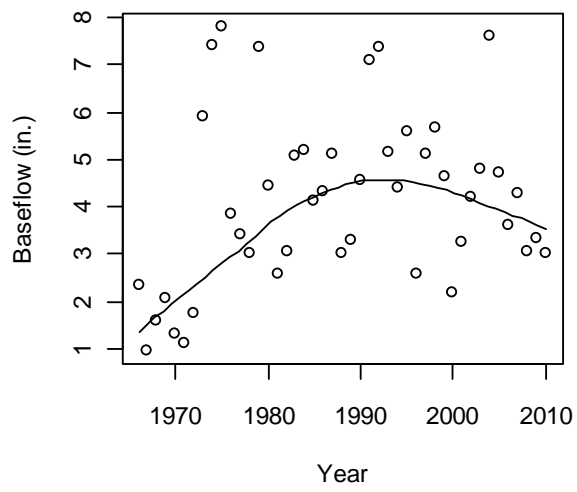
8041700



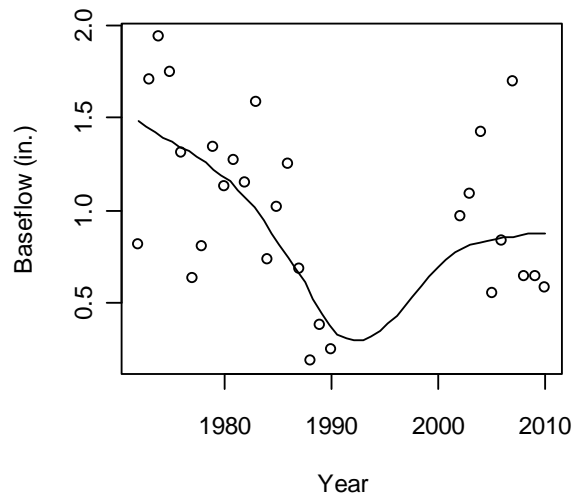
8066200



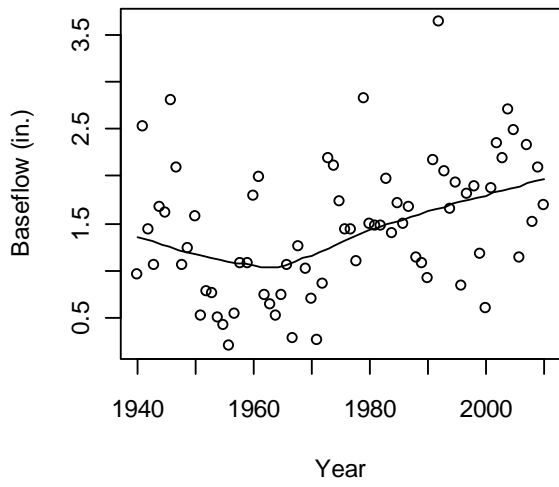
8066300



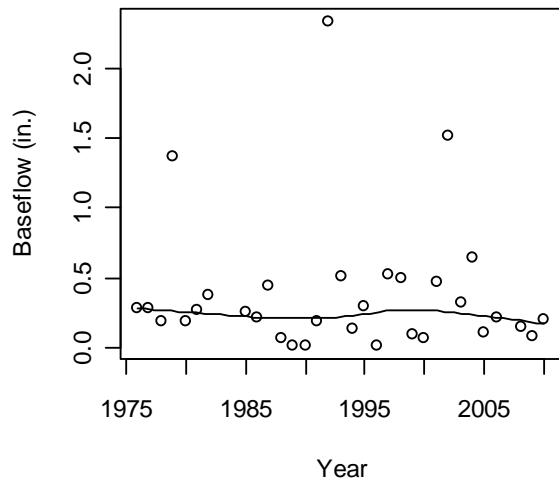
8067500



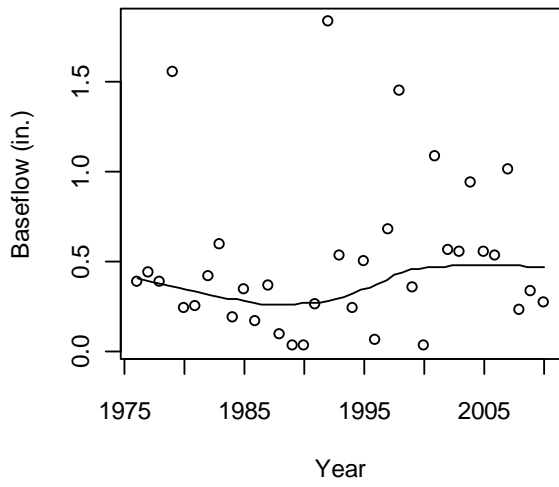
8068500



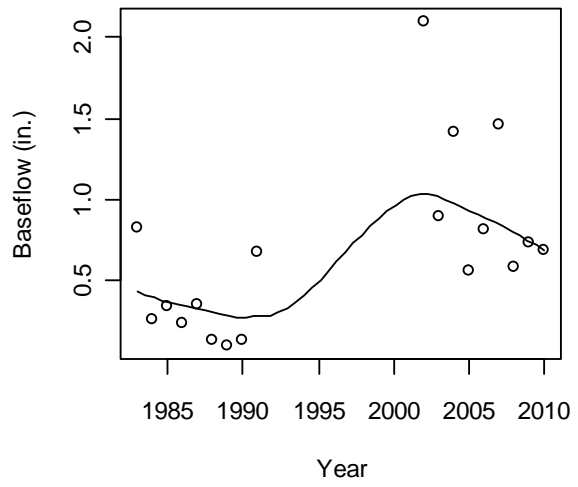
8068720



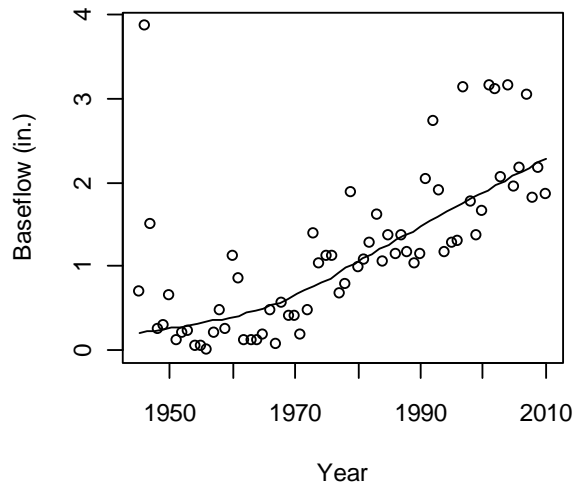
8068740



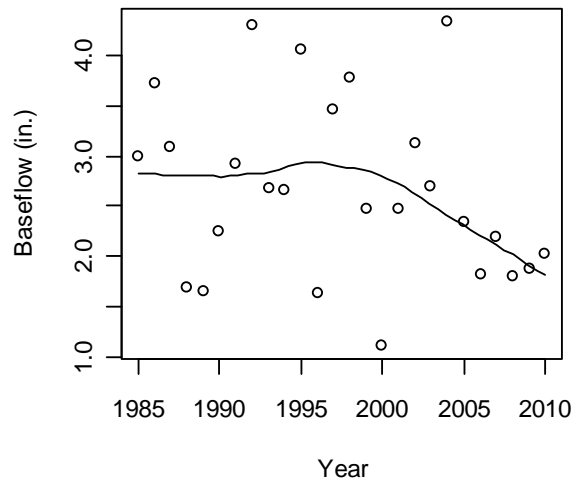
8068800



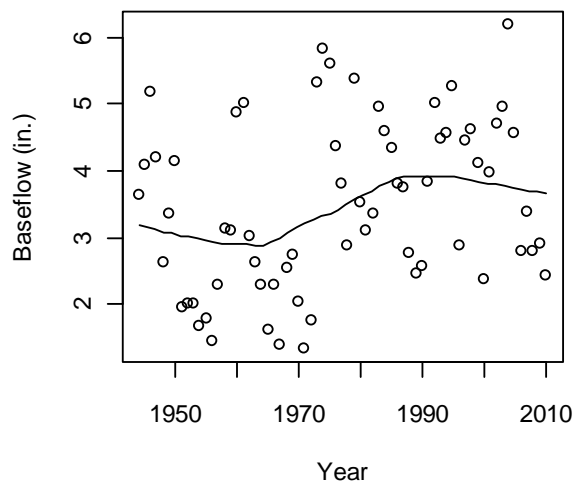
8069000



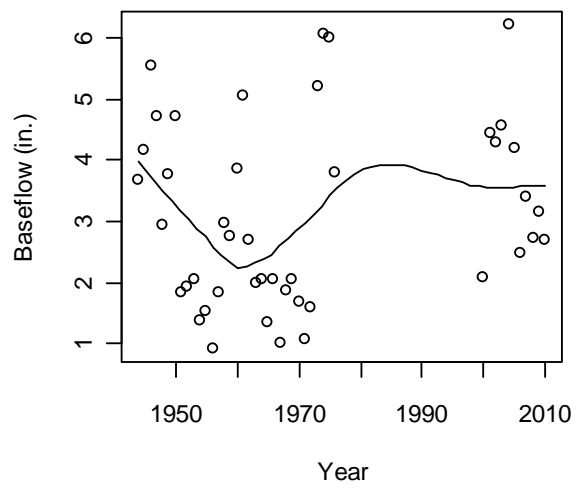
8070200



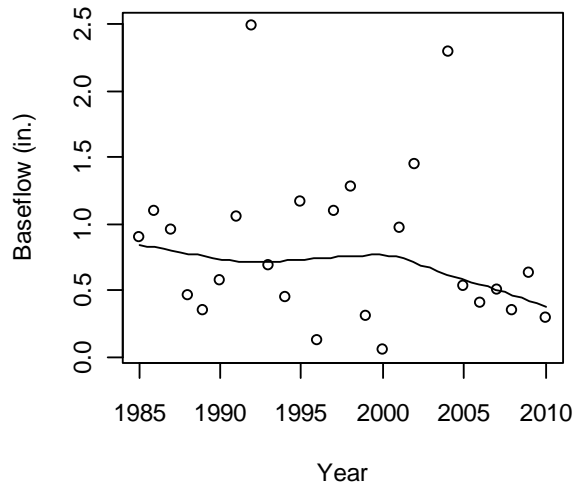
8070500



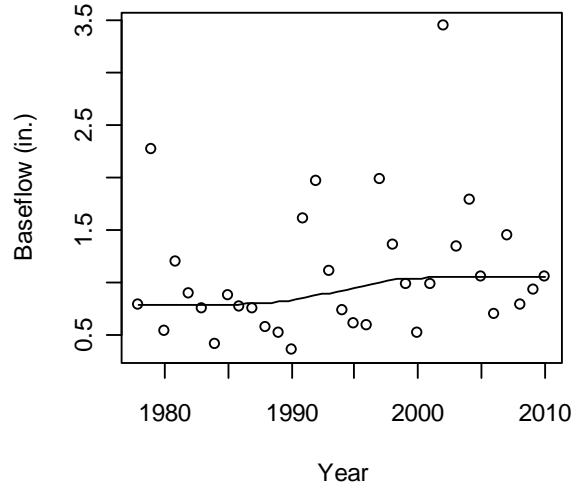
8071000



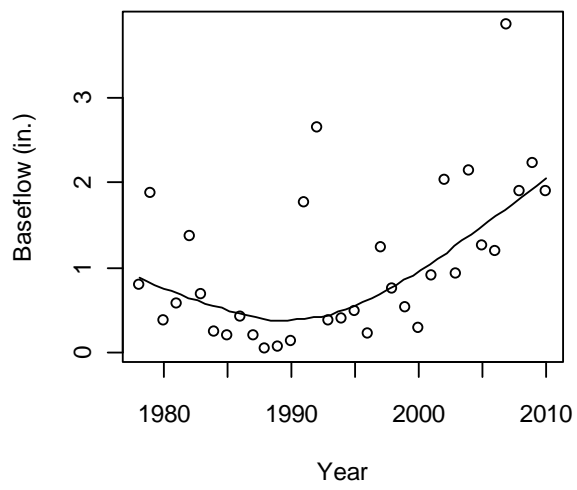
8071280



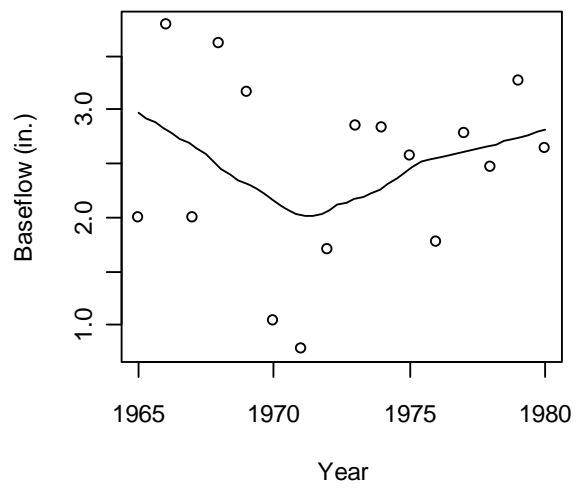
8072300



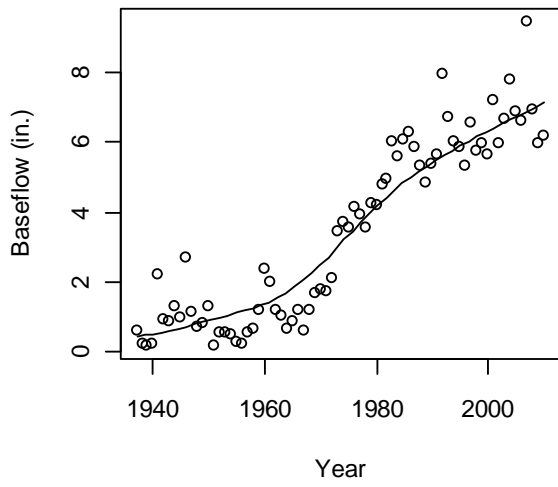
8072730



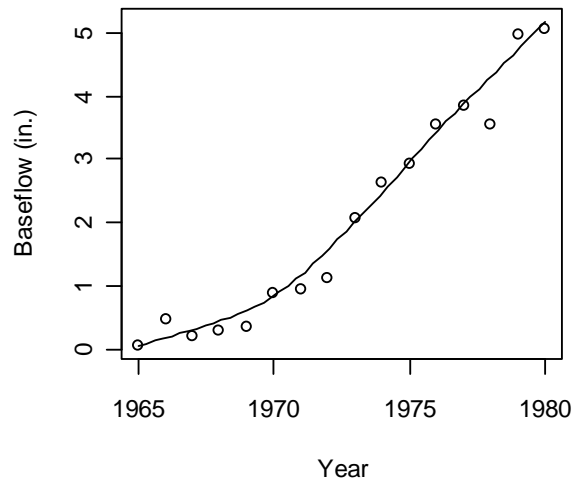
8074250



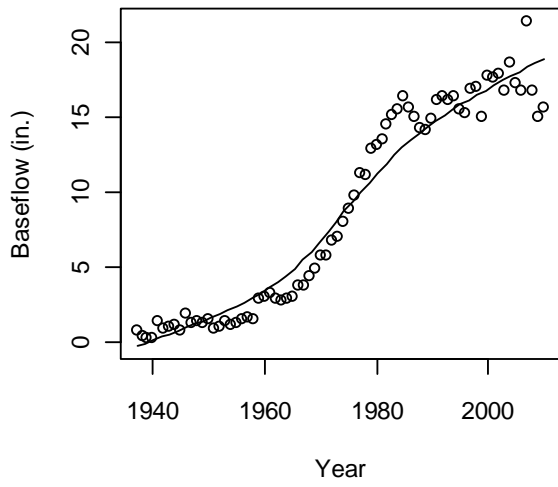
8074500



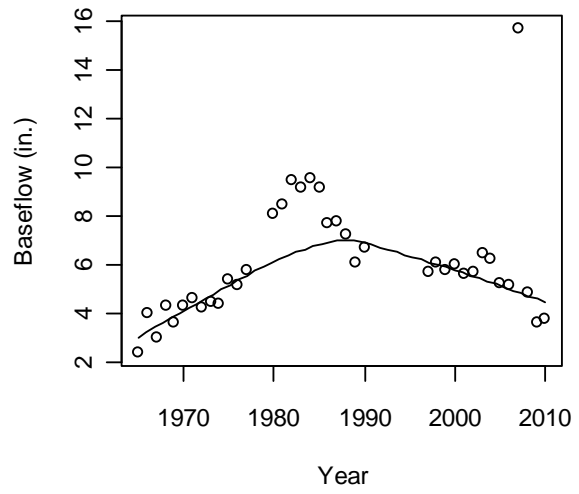
8074800



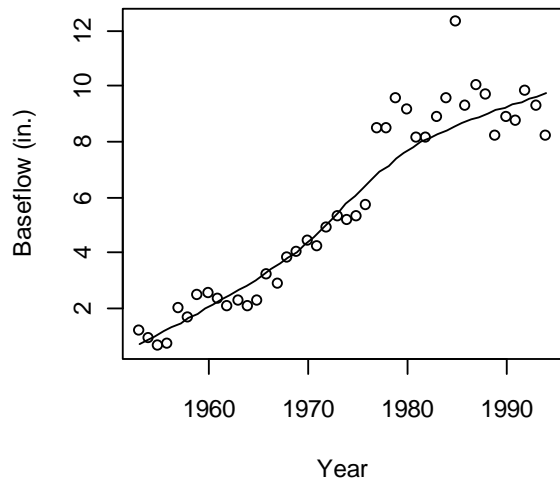
8075000



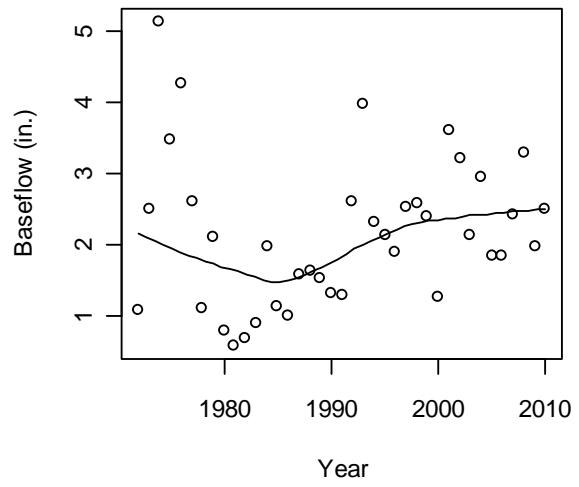
8075400



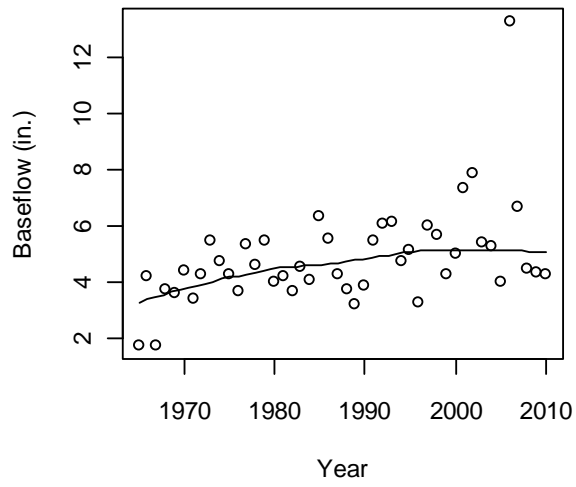
8075500



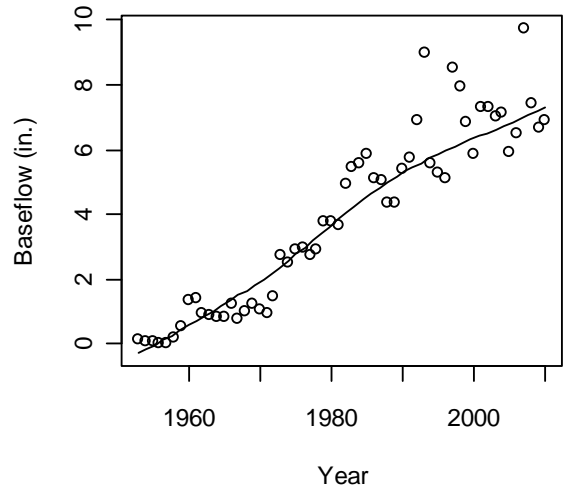
8075730



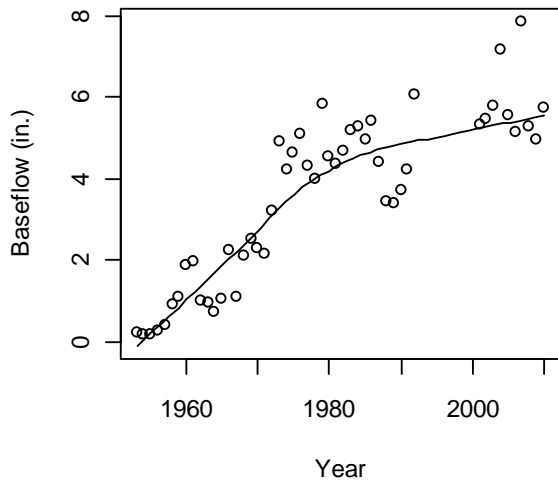
8075770



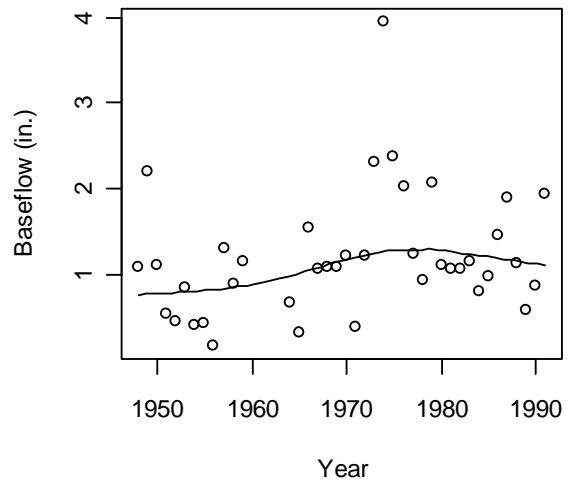
8076000



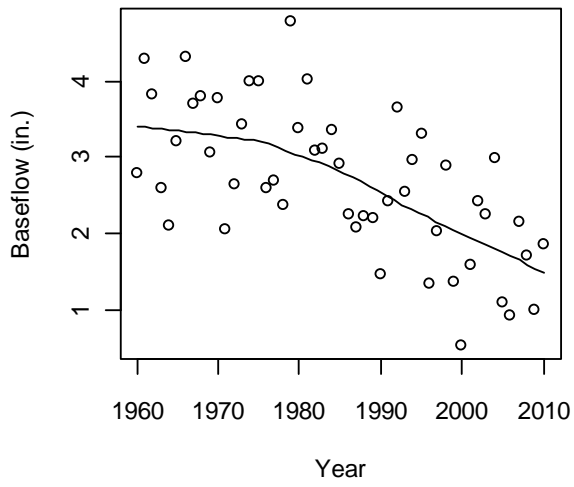
8076500



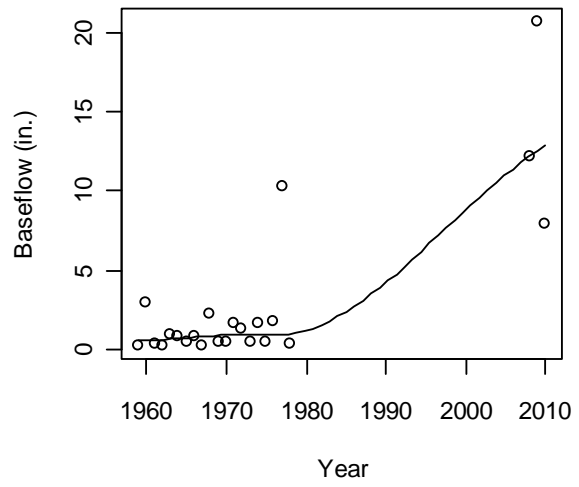
8077000



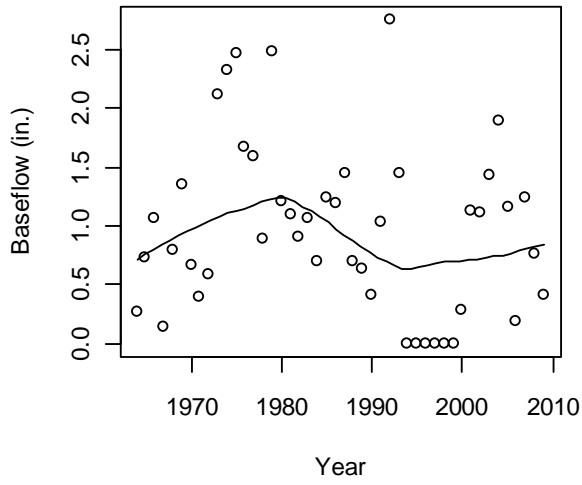
8078000



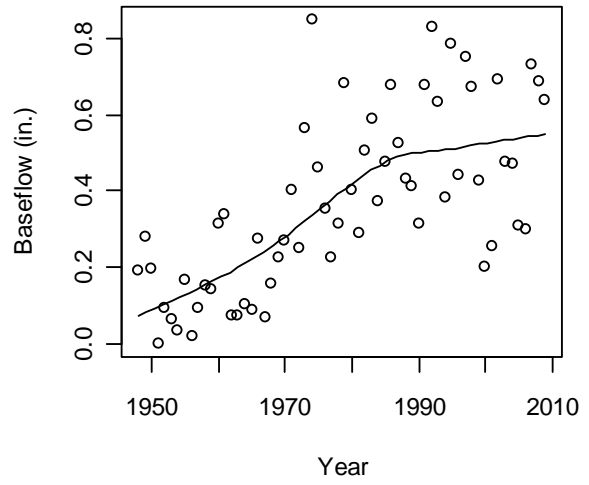
8116400



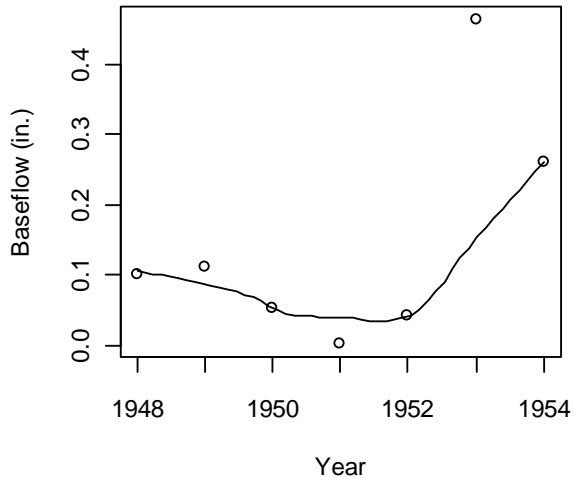
8111700



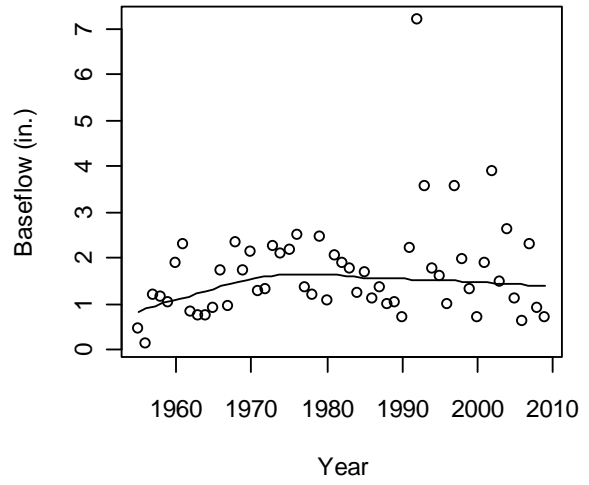
8115000



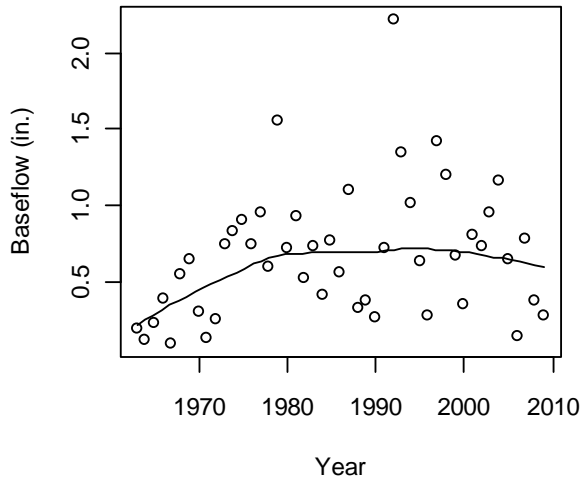
8115500



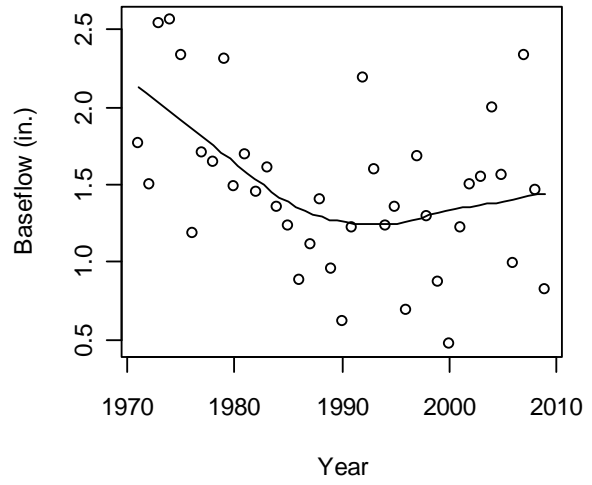
8117500



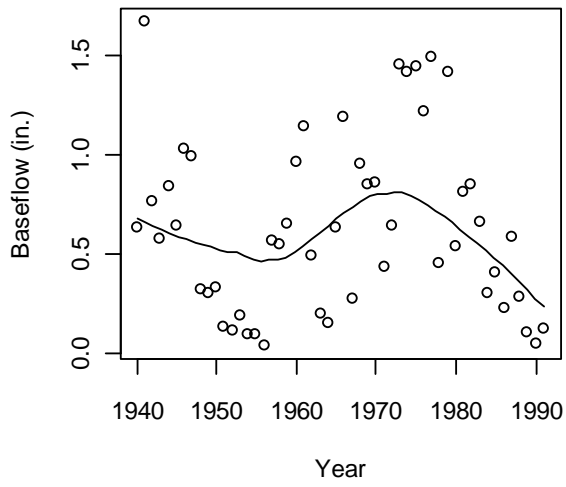
8160800



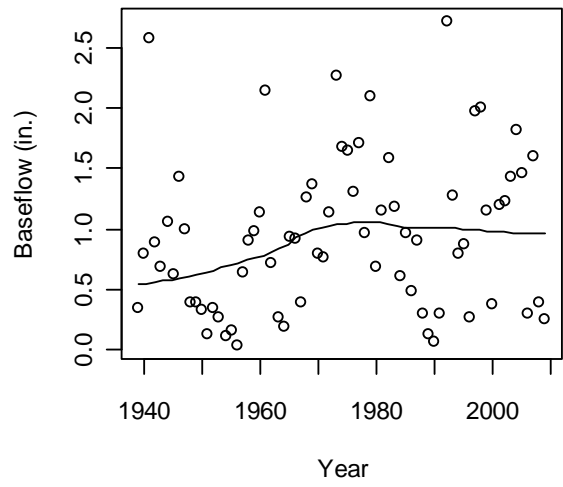
8162600



8163500



8164000



8164300

